RISK ASSESSMENT OF BUILDING INVENTORIES EXPOSED TO LARGE SCALE NATURAL HAZARDS

A Dissertation
Presented to
The Academic Faculty

by

Soravit Vitoontus

In Partial Fulfillment
of the Requirements for the Degree
Doctor of Philosophy in the
School of Civil and Environmental Engineering

Georgia Institute of Technology
May 2012

RISK ASSESSMENT OF BUILDING INVENTORIES EXPOSED TO LARGE SCALE NATURAL HAZARDS

Approved by:

Dr. Bruce R. Ellingwood, Advisor
School of Civil and Environmental Engineering
Georgia Institute of Technology

Dr. Abdul-Hamid Zureick
School of Civil and Environmental Engineering
Georgia Institute of Technology

Dr. Barry Goodno
School of Civil and Environmental Engineering
Georgia Institute of Technology

Dr. David Goldsman
School of Industrial and Systems Engineering
Georgia Institute of Technology

Dr. Kenneth M. Will
School of Civil and Environmental Engineering
Georgia Institute of Technology

Date Approved: March 29, 2012

Dedicated to my parents Somsak and Tasanee,
and my brother Saravut

ACKNOWLEDGEMENTS

I wish to express my sincere gratitude to Dr. Bruce R. Ellingwood for his encouragement, enthusiasm, and patience during my entire Ph.D. level. I would like to appreciate him for providing not only insight in all aspects of this research but also valuable feedback and recommendation on this dissertation. I consider myself to extremely fortunate to be his advisee and to have an opportunity to work with him.

I would like to thank him and my thesis committee - Dr. David Goldsman, Dr. Barry Goodno, Dr. Kenneth M. Will, and Dr. Abdul-Hamid Zureick- for their review and guidance. I also would like to thank all entire faculty members whom I have studied with during master's and doctorate degrees at Georgia Institute of Technology.

My gratitude also goes to my colleague in Structural Engineering Mechanics and Material program and all friends for their valuable suggestions, encouragement, and true friendship: especially to Dr. Naiyu Wang, Dr. Guoqing Xu, Eun Jeong Cha, Mustafa Can Kara, Dr. Saroch Boonsiripant, Dr. Kanoknart Leelarcharoen, Chanin Ruangtaveekoon, Seksan Laitrakun, and Pisit Jarumaneeroj.

Lastly, I would like to thank my parents and brother for their unconditional support and encouragement to pursue master's and doctorate degrees at Georgia Institute of Technology. I am deeply grateful to my girlfriend, Rumpapit Russameewongjan, for her support, understanding, and patience over last three years.

TABLE OF CONTENTS

LIST OF TABLES

LIST OF FIGURES

SUMMARY

Earthquakes, among the most devastating and unpredictable of natural hazards that affect civil infrastructure, have the potential for causing numerous casualties and significant economic losses over large areas. For example, the Mw 7.9 Sichuan, China Earthquake in 2008 caused at least 69,000 deaths, collapses of over 5 million buildings, and damage to more than 21 million buildings. While the Mw 8.8 Chile Earthquake in 2010 caused at least 500 deaths, at least 380,000 buildings were damaged or destroyed by the earthquake and tsunami that followed. The total estimated economic losses for the Sichuan and Chile earthquakes were $86 and $30 billion, respectively. Every region that has the potential for great earthquakes should have an integrated plan for aseismic design and risk mitigation. As part of this plan, methods are required for estimating the vulnerability of building inventories and for forecasting the casualties and economic losses for future events. This dissertation advances the state of the art in vulnerability assessment by proposing methods that take correlation in seismic demand, building damages and losses to structural systems and nonstructural components into account.

Risk to distributed building inventories exposed to earthquake hazards is generally determined using one of two basic approaches: scenario earthquake risk assessment (SERA) and probabilistic seismic risk assessment (PSRA). The latter approach is required if the probable maximum loss (PML) decision metric, which often is used for underwriting purposes in the insurance industry, is to be estimated. The uncertainty of the SERA and PSRA, and in the estimate of the PML for building inventories, is dependent on correlation in building losses within the inventory, which is

caused by spatial correlations in ground motion (demand), building response and damage. Previous studies that neglect these correlations underestimate the uncertainty in losses. Moreover, while correlation in demand has been considered in a few studies, response and damage correlations due to common building practices and occupancy characteristics have yet to be investigated.

This study proposes a new model for estimating correlations in response and damage for structural and nonstructural components within a building, and for structural and structural damage of building inventories. The total building inventory loss for a SERA, probabilities of loss exceedence (risk curves) for PSRA, and the PML decision metric are determined and the effect of correlations in demand and damage is included in the analyses. Since estimates of losses for a large building inventory requires numerous computational and numerical efforts, a sampling technique is developed that provides sufficiently accurate estimates. The sensitivity of the total structural loss and the combination of nonstructural and structural losses due to parameters that were assumed in modeling spatial correlation is investigated, and the role of epistemic uncertainty in the total structural losses and PML are examined. It is concluded that estimates of losses to building inventories made under the common assumption that the individual losses can be treated as statistically independent may underestimate the PML by a factor of range from 1.7 to 3.0, depending on which structural and nonstructural elements are included in the assessment.

CHAPTER 1

INTRODUCTION

1.1 Statement of the Problem

Earthquakes are among the natural hazards with the potential for causing deaths, injuries and significant direct and indirect economic losses over large areas. For example, more than 69,000 people were killed and approximately $146.5 billion was spent to rebuild areas damaged by the 2008 Sichuan earthquake.[1] The 1994 Northridge earthquake caused 72 deaths, injured at least 7,000 people, and resulted in an estimated $20 billion in damages occurred.[2] Setting aside the enormous human costs of such natural disasters, the direct economic losses stem mainly from damage or collapse of buildings and failures of other civil infrastructure systems, while indirect losses result mainly from loss of business opportunity during the period of reconstruction following the disaster.

In order to understand and forecast the risk to a large area (e.g., an urban community) from such natural hazards with large geographic footprints, the uncertainties in repair and reconstruction costs of building portfolios and civil infrastructure systems must be thoroughly understood. Appropriate community risk mitigation strategies also must reflect the uncertainty in the loss to a community; this uncertainty, in turn, depends on the stochastic variability in the demand from the occurrence of the hazardous event over the affected area at both spatial and temporal scales, the number of structures and

[1] http://earthquake.usgs.gov/eqcenter/eqinthenews/2008/us2008ryan/#summary
[2] http://earthquake.usgs.gov/regional/states/events/1994_01_17.php

their locations, and their susceptibility to damage if the hazardous event occurs. When hazardous events occur over wide areas, the spatial correlations in intensity (demand) and damage are significant factors in the overall risk assessment that supports risk mitigation strategies and must be properly taken into account.

Large earthquakes pose a significant threat to many densely populated urban areas in much of the United States and in many other countries. The assessment of risk to civil infrastructure from earthquake hazards is a major part of modern disaster planning (Zimmerman, 2001). Methods for assessing risk to individual buildings and other structures subjected to seismic hazards have greatly improved during the past decade and are reasonably mature (Chang and Shinozuka, 1996; Elms, 1997; Faber and Stewart, 2003; Wen and Ellingwood, 2005). However, the regions impacted by large earthquakes may cover more than one county or city, and may include inventories of buildings with different occupancies and types of construction, and other distributed infrastructure systems. In such cases, the risk analysis and assessment is far more complex. Only a few studies to date have investigated risk to distributed civil infrastructure in a systematic fashion (Kiremidjian *et al.*, 2007; Lee and Kiremidjian, 2007; Straub *et al.*, 2008; Bensi *et al.*, 2009).

Structural engineers usually confine their attention to individual projects for which they have design responsibility. Governments, community or city planners, and insurance underwriters, on the other hand, are concerned with safety of inventories of buildings with different occupancy characteristics and other civil infrastructure systems. Public decision-makers frequently consider only short-term costs due to construction, maintenance costs and immediate economic benefits to the community served. However,

they seldom consider the future benefits of such projects over their service lives; nor do they consider the costs due to repair and reconstruction of such facilities following a natural disaster. One reason may be lack of knowledge to determine these costs. Another may be that elected public officials with responsibility for decisions may have little motivation to think beyond their terms of office (Corotis, 2009). Moreover, the type of structure and its location in a hazardous region must be known to determine the risk accurately. While the types and locations of key infrastructure facilities at the present time may be known, they may only be determined in a general sense (e.g., through local zoning laws or development plans) over an extended risk assessment horizon for a community that is under development. In such a community, new public development projects may be constructed during a risk assessment horizon which may extend for decades. Neglecting such factors and uncertainties will lead to an erroneous assessment of risk of building inventories to the community.

The assessment of risk to building inventories or other distributed infrastructure systems requires the aggregation of risks to individual buildings or facilities. Supporting data to support a risk assessment is likely to be available for individual facilities, since facilities normally are insured individually rather than collectively; these data must be aggregated to assess loss to the inventory. For instance, if monetary loss is considered as the decision variable or loss metric, the overall risk to the inventory is:

$$L_T = \sum_{i=1}^{N} L_i \tag{1-1}$$

in which L_i = loss to facility i, N = number of facilities at risk, and L_T = total loss. Since the demand on each facility is random, as is facility performance under a given demand

(fragility), the individual facility losses are random, as is L_T. The mean and variance of L_T are:

$$\mathrm{E}[L_T] = \sum_{i=1}^{N} \mathrm{E}[L_i] \tag{1-2}$$

$$\mathrm{Var}[L_T] = \sum_{i=1}^{N} \mathrm{Var}[L_i] + \sum_{\substack{i=1 \\ i \neq j}}^{N} \sum_{j=1}^{N} \rho_{L_i, L_j} \cdot \mathrm{SD}[L_i] \cdot SD[L_j] \tag{1-3}$$

where E[-], SD[-], and Var[-] are the expected values, standard deviations, and variances, respectively; and $\rho_{Li,Lj}$ represents the correlations in loss of buildings *i* and structure *j*. The probability distribution of L_T is required to determine the probable maximum loss, or PML. This distribution generally is unknown.[1] The PML is generally taken as that value of the distribution with a small probability of being exceeded in a given year. In the insurance industry, this probability is on the order of 0.001 – 0.004 (Woo, 2002; Grossi and Kunreuther, 2005).

Sources of this correlation in damage and loss include the spatial correlation of seismic intensity over the felt area resulting from large earthquakes and common occupancies, construction technology and building code enforcement. The result is correlation in earthquake-related structural damage within spatially distributed building inventories. This correlation should be considered in any attempt to aggregate risk to a building inventory from existing information on individual buildings. The correlation is almost certain to be positive because of the underlying nature of a single large-area hazardous event, common design and construction practices, and infrastructure response. Equation (1-3) shows that if this correlation is ignored, Var[L_T] will be underestimated.

[1]The form of Eq (1-1) suggests that if the correlations are weak, L_T will be approximately normal for large N (by the Central Limit Theorem).

Figure 1-1 also illustrates that if the correlation is neglected, the PML will be underestimated. Nevertheless, most previous research on loss estimation for building portfolios (Trendafiloski *et al.*, 2009; Ploeger *et al.*, 2010) has ignored correlation in damages and in losses between buildings. Only a few studies have considered such correlations; those studies have focused on large bridges (Lee and Kiremidjian, 2007), where the number in an affected region is relatively small and the analysis of correlation effects can be managed numerically.

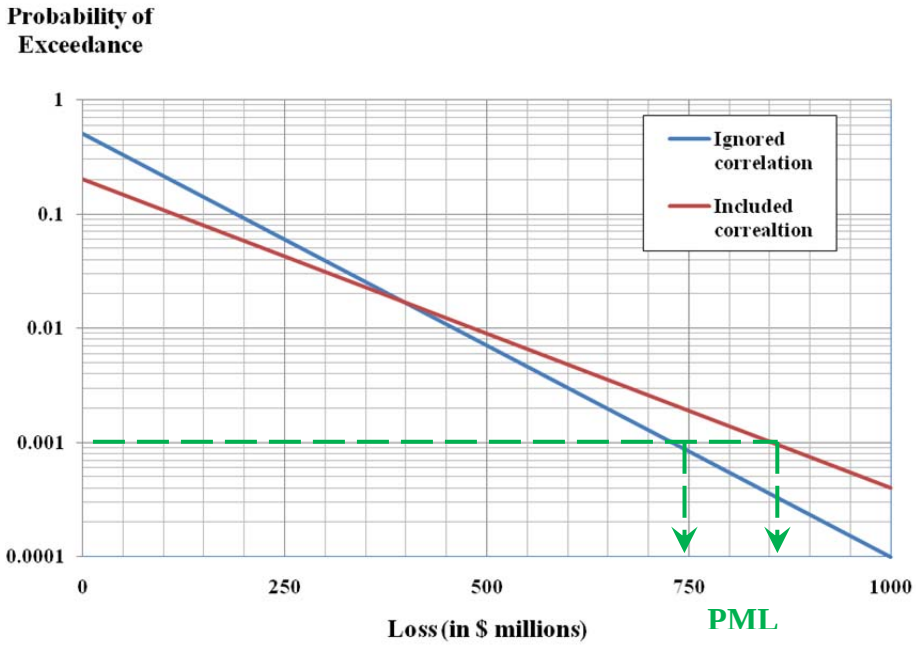

Figure 1-1 Probability of exceedence curves.

Thus, a fundamental research challenge is to establish stochastic field models that capture the spatial correlation in building losses distributed over a community (or larger) – scale region as an integral part of a regional risk or loss assessment. At the most fundamental level, these models must properly reflect the spatial correlation in intensity (or demand) resulting from the large-scale hazardous event, as well as buildings and

infrastructure response and damage patterns resulting from those demands. Loss estimation methodologies that take this correlation structure in to account once developed, would lead to more accurate estimates of probable maximum losses and thus would provide improved tools for public decision-makers and insurance underwriters. At the present, such spatial correlation models are in a rudimentary state of development (Woo, 1997).

1.2 Research Objectives and Scope

The research herein will develop stochastic models for incorporation in a risk assessment framework for use by decision-makers confronted by hazards from large earthquakes with the potential to cause disruption over large regions (on the community or county scale). Such models will address the effect of spatial correlation in ground motion intensity on probabilistic measures of demand, damage and loss to buildings distributed within extended regions subjected to a common earthquake. While the stochastic modeling process is completely general, this dissertation will focus on building damage due to earthquakes in order to take advantage of damage and loss data from other studies.

To achieve the goals and objectives of this dissertation, the following research tasks will be conducted:

- Review and critically appraise current practices in risk assessment of individual facilities and spatially distributed buildings and civil infrastructure systems;
- Investigate hazard demands due to ground shaking and develop models of seismic intensity correlations between building occupancy classes;

- Synthesize fragilities that describe building performance under strong ground motions statistically from previous research and develop damage correlation models (models of common-cause failures) for buildings reflecting common sitting, code and code enforcement, and construction practices;
- Develop an efficient loss assessment methodology to evaluate mean, variance and exceedence probabilities for loss metrics related to repair and replacement cost ratio;
- Assess uncertainty and sensitivity of correlation parameters that affect the loss matrices; and
- Summarize the main attributes of improved risk reduction and risk mitigation strategies that take this spatial correlation in demand and in damage into account, and recommend guidelines for improvements to risk-informed decision-making.

1.3 Organization of Dissertation

This dissertation has eight chapters. Chapter 2 reviews and critiques existing methodologies that are used to assess risks to individual facilities and civil infrastructure systems. In Chapter 3, fundamental tools for modeling seismic demand and building response are introduced. Chapter 4 introduces an analytical model to evaluate structural losses to building inventories due to a scenario earthquake event. Chapter 5 demonstrates the application of the model utilizing Monte Carlo simulation to scenario earthquake analysis, probabilistic seismic hazard analysis, and decision metrics. In Chapter 6, a method to aggregate nonstructural and structural losses which includes correlation between them is introduced. Chapter 7 examines the uncertainty and sensitivity of the

estimated risks to parameters that are necessary to define the stochastic field models and building damage assessment. This sensitivity analysis can be used to guide the collection and analysis of additional supporting data. Chapter 8 summarizes major conclusions, applications and recommendations for future study.

CHAPTER 2

SEISMIC RISK ASSESSMENT OF BUILDING INVENTORIES

In the past 30 years, seismic risk assessment of buildings and other civil infrastructure, such as bridges, utility systems, offshore structures, etc, has advanced on many fronts. Uncertainties in demands on individual facilities and their ability to withstand such demands have been investigated widely. Several transportation infrastructure systems in the Western United States have been investigated recently and various methodologies have been used to analyze their performance (Lee and Kiremidjian, 2007; Straub *et al.*, 2008; Jayaram, 2010; Jayaram and Baker, 2010). In contrast, few studies of distributed infrastructure systems in the Eastern United States have been completed (Duenas-Osorio, 2005; Adachi, 2007). Research in the use of geographic information systems (GIS) in evaluating seismic risk to building inventories has been attempted with mixed success (Chen *et al.*, 1998; Kircher *et al.*, 2006; Kappos *et al.*, 2007; Trendafiloski *et al.*, 2009).

In this section, a review of previous research in areas that form the building blocks of risk assessment of building inventories in this dissertation is conducted in two parts: risk assessment of individual facilities, and risk assessment of distributed buildings and civil infrastructure systems.

2.1 Review of Previous Work

2.1.1 Risk Assessment of Individual Facilities

Risk assessment and risk-informed design for individual facilities are at a reasonably advanced state of development. To design new facilities to withstand natural hazards or to evaluate robustness of existing facilities, there are four levels at which engineers can approach the task of facility safety assessment (Melchers, 1999). Level 1 is comparable to what currently is specified in codes and standards, i.e. *ASCE7-10*, ANSI/AISC 360-10 or *ACI318-11*. The safety requirements generally take the form of prescriptive provisions and safety checking equations that contain nominal loads and strengths and safety elements (safety factors). These safety factors may be computed using methods derived from modern structural reliability theory [so-called level 2 and level 3 methods (Melchers, 1999)]. Certain special facilities in which the consequences of failure extend far beyond the individual facility sometimes receive further detailed study, including a qualitative risk analysis or a more quantified fragility or fully-coupled probabilistic risk analysis (PRA).

The fourth level of structural safety assessment involves decision methods based on minimum expected cost, cost/benefit analysis, or maximum utility, which are facility-dependent and depend on the risk perception and tolerance of the facility stakeholders (e.g. Chang and Shinozuka, 1996; Kanda and Shah, 1997; Wen and Kang, 2001; ATC-58, 2011). Chang and Shinozuka (1996) proposed that bridges in high-seismic regions should be assessed on a minimum expected life-cycle cost basis because earthquake damage-related costs, which seldom were anticipated by the owner or government, were approximately twice the costs that typically were budgeted for bridge repair. Such life-

cycle costs, which account for the effect of extreme environmental hazards, are not reflected in building code requirements. Note that the expected service life of a typical building or bridge structure is usually on the order of 50 to 100 years, while the term of office of an elected public official is much less. As a result, decision-makers in the public sector may choose a design and construction alternative that has the most immediate short-term benefit (Corotis, 2009).

Seismic vulnerability/fragility modeling is an essential part of seismic risk assessment of individual buildings and other infrastructure. The fragility defines the probability of failure to meet a performance objective as a function of seismic demand, often expressed in terms of peak ground acceleration (PGA), peak ground velocity (PGV), or spectral displacement (S_d) (Lee and Rosowsky, 2006; Ellingwood *et al.*, 2007; Padgett, 2007; Park *et al.*, 2009). Fragility curves for each structural type (i.e. wood light frame, steel frame, reinforced concrete frame, or unreinforced masonry) are developed in four steps. First, damage measures and performance levels are identified by relating structural response levels (e.g, interstory drift, floor acceleration) to damage states (i.e., slight/extensive/complete, or immediate-occupancy/life-safety/collapse-prevention). Second, ground motions are characterized using ensembles of natural or synthetic uniform hazard ground motions. The third step involves the estimation of aleatory and epistemic uncertainties associated with both seismic demand and building capacity. Finally, the fragility curves are determined from the information in step 1 to 3.

To perform a seismic loss assessment using these models, the repair and replacement costs, which depend on damage state, must be determined. While the damage state is estimated from the type of structure and construction technology, the

available cost data depends on building occupancy. Most researchers usually cease their study of fragility/vulnerability functions at the point where losses are calculated, and leave the loss calculation to risk estimation software because the cost data is difficult to assess and may contain high uncertainty.

It should be noted that fragility functions are always developed independently for each facility. To the best of the writer's knowledge, no existing research on seismic fragility modeling has considered the joint damage state probabilities for two (or more) buildings. As will be shown subsequently, such joint probabilities are a necessary ingredient in risk assessment of building inventories where stochastic dependence among building damage states is required.

The aforementioned methodologies to assess risk of new or existing facilities do not consider the relation of one facility to other nearby facilities or the role of such facilities in an integrated civil infrastructure system. For individual facilities such as buildings, bridges, offshore structures, nuclear plants, etc., there is no need to consider spatial correlation in demand or on performance of other nearby facilities when risk is evaluated and a spectrum of decision alternatives are considered. However, such considerations can be important when assessing risk to a community due to natural hazards with large geographic footprints. For example, consider the cost of earthquake insurance in single-family residences in a modern urban area. The insurer must set premiums for homeowners in the area. These premiums can be computed from probability of losses exceeding an acceptable limit, which is related to the general cost of doing business and the profit needed to attract and hold shareholders. This acceptable limit is affected by the variance in the total loss (Grossi and Kunreuther, 2005). If spatial

correlation in demand and capacity is ignored, the premium will be inexpensive but the likelihood of unacceptable losses will be underestimated. If a strong earthquake were to occur subsequently, the insurer may be driven into bankruptcy. Similarly, when transportation networks or utility systems in a city or region are assessed, these inter-relations and statistical correlations in their performance when subjected to a common extreme event must be taken into account. In the latter case, public resources may be inadequate to cover the loss from a natural disaster. Regardless of whether the loss is to the private or public sector, failure to take these dependencies into account invariably will result in an underestimate of risk, as described in Chapter 1. The risk assessment of distributed civil infrastructure systems, summarized in the next section, is intended to deal with this situation.

2.1.2 Risk Assessment of Spatially Distributed Buildings and Civil Infrastructure Systems

Risk assessment of distributed civil infrastructure systems must begin with an evaluation of each facility in the system, but then move toward including the effect of statistical correlation in demand and response between nearby facilities as well as functional dependencies (cause-and-effect) between the facilities. For example, if the probability of failure of a transportation network consisting of many bridges due to earthquake is the decision metric, its assessment must begin by calculating the probabilities of failure of each bridge. In the subsequent system performance analysis, correlations in behavior between each bridge subjected to the same earthquake must be taken into account. Similarly, the loss to each building has to be determined before the loss to an inventory of buildings can be estimated.

For example, suppose that two buildings in the same area that were designed according to the same building code are subjected to an earthquake. To aggregate losses of individual buildings to assess inventory loss, correlations in seismic demand and structural performance among individual buildings must be considered. These correlations are difficult to evaluate exactly since there are many uncertainties affecting the earthquake scenarios and buildings, such as uncertainties in attenuation (intra-event), in earthquake sources (inter-event), and structural damage correlations. The correlation in performance of bridges, which are large discrete systems and widely separated, is likely to be lower than correlation in performance of distributed buildings and other civil infrastructure which are more densely situated.

Among the factors leading to correlations in seismic demand, building response and damage, and losses are:

- An earthquake event that places demands on a large inventory of buildings;
- Common regional geology or local soil conditions;
- Common building construction materials, material properties, or structural types;
- Common building codes, specifications and design procedures and local building regulatory practices;
- Common design/construction practices.

Methods for assessing risk to buildings distributed over a large area have been investigated previously (Shinozuka *et al.*, 1997; Chen *et al.*, 1998; He, 2006; Kircher *et al.*, 2006; Kappos *et al.*, 2007; Cardona *et al.*, 2008; Goda and Hong, 2008; Trendafiloski

et al., 2009; Ploeger *et al.*, 2010), but have some limitations that the current research will attempt to address. Wesson *et al.* (2009) developed a method to compute directly the probability distribution and probability of exceedence of earthquake loss to a portfolio. Their model included only correlation in the ground motion intensity. The study of Trendafiloski *et al.* (2009) developed a risk model for Bucharest, Romania, utilizing QLARM, a software platform designed to estimate earthquake losses on a global scale with a focus on developing countries[1], for cities in developing countries that have limited information due to earthquake. Cities are represented as one point for cases where only summary data for the entire city are available, while they are modeled discretely when data for each district/county in the city are available. Ploeger *et al.* (2010) utilized HAZUS-MH to estimate seismic loss to downtown Ottawa, Canada. Since HAZUS-MH does not include the effect of correlations in either demand or performance between pairs of buildings in an urban area, the variance in loss of their analysis cannot be computed. With the exception of the work of Goda and Hong (2008), which will be discussed in the following paragraph, none of the above studies consider the role of correlations in demand and in performance of buildings in estimating losses to building portfolios.

Risk assessment of bridges and other distributed infrastructure systems has also been considered in recent research (Adachi, 2007; Kiremidjian *et al.*, 2007; Lee and Kiremidjian, 2007; Straub *et al.*, 2008; Bensi *et al.*, 2009). One of the common challenges in these studies has been to determine the spatial correlation of seismic intensity or demand between each site. It has been common to assume that the correlation structure in demand can be modeled as a spatially homogeneous and isotropic

[1]http://qlarm.ethz.ch/

stochastic field. For example, Adachi (2007) used the spatial correlation of peak ground acceleration or peak ground velocity between two facilities, which can be expressed as:

$$R_{LL}\left(\left\|r_{ij}\right\|\right)=\exp\left(-\frac{\left\|r_{ij}\right\|}{r_o}\right) \tag{2-1}$$

where R_{LL} is the auto-correlation in intensity between site i and site j, r_{ij} is the distance between site i and site j, and r_0 is the correlation distance. Lee and Kiremidjian (2007) derived the distance-dependent ground motion correlation between two sites from the variance of intra-event, σ^2_s, earthquake, σ^2_e, and residual errors, σ^2_r, in the form:

$$\rho_{i,j}=\frac{\sigma_e^2+\sigma_s^2\cdot\exp\left[-\left(r_{ij}/r_0\right)^2\right]}{\sigma_e^2+\sigma_s^2+\sigma_r^2} \tag{2-2}$$

The contribution of each component of variance was assumed to be $\sigma^2_e = \sigma^2_s = 0.40(\sigma^2_{Total})$ and $\sigma^2_r = 0.20(\sigma^2_{Total})$, in which σ^2_{Total} = total variability in ground motion attenuation. Lee and Kiremidjian (2007) stated that the contributions of σ^2_e and σ^2_s in total variance are larger than that of σ^2_r because the earthquake and local site effect are known (physical) contributors to spatial ground motion correlation.

An alternative spatial correlation model for bridges in a network was introduced by Straub *et al.* (2008):

$$\rho(i,j)=\frac{\sigma^2+\tau^2\rho_r(i,j)}{\sigma^2+\tau^2} \tag{2-3}$$

where σ^2 and τ^2 is the variance of inter-event and intra-event errors, and $\rho_r(i,j)$ is the correlation between pairs of intra-event errors.

Goda and Hong (2008) proposed the following correlation coefficient for ground motion intensity between pairs of buildings in Vancouver, Canada:

$$\rho(T_{n1},T_{n2},\Delta_{12}) = \frac{\rho_1(T_{n1},T_{n2})\left[\sigma_1(T_{n1})\sigma_1(T_{n2}) + \rho_2(\max(T_{n1},T_{n2}),\Delta_{12})\sigma_2(T_{n1})\sigma_2(T_{n2})\right]}{\sigma_\varepsilon(T_{n1})\sigma_\varepsilon(T_{n2})} \tag{2-4}$$

where T_{n1} and T_{n2} are the natural vibration periods of SDOF systems at two sites; terms ρ_1 and ρ_2 are functions defined in Goda and Hong (2008); and $\sigma_1(T_n)$, $\sigma_2(T_n)$, and $\sigma_\varepsilon(T_n)$ are the standard deviation of inter-event, intra-event, and total variability, respectively. Note that ρ_1 is a function of T_{n1} and T_{n2}, and ρ_2 is a function of distance between two buildings. Assuming that $\sigma_1(T_n)$ and $\sigma_2(T_n)$ are independent of period and are equal to σ_1 and σ_2, respectively, and the inter-event and intra-event variability are statistically independent, Eq (2-4) becomes:

$$\rho(T_{n1},T_{n2},\Delta_{12}) = \frac{\rho_1\sigma_1^2 + \rho_1\rho_2\sigma_2^2}{\sigma_1^2 + \sigma_2^2} \tag{2-5}$$

There are common terms in Eqs (2-2), (2-3), and (2-5) defining inter-event variability (σ_e, σ, and σ_1) and intra-event variability (σ_s, τ, and σ_2). A slight difference between Eq (2-2) and the others is that it incorporates the residual error, σ^2_r. All multiplicative terms $exp[-(\rho_{ij}/\rho_o)^2]$, $\rho_r(i,j)$, and ρ_2 of intra-event variability in Eq (2-2), (2-3), and (2-5)are functions of distance between two sites but are independent of direction (i.e., the stochastic field is assumed to be isotropic).

The aforementioned studies of buildings and bridges (Lee and Kiremidjian, 2007; Goda and Hong, 2008; Straub *et al.*, 2008) indicated that neglecting the ground motion correlation could cause the decision metric, such as probability of failure or the variance

of the total repair cost, to be underestimated. However, only Lee and Kiremidjian's study of bridges in a transportation network accounted for damage correlation between facilities. Note that although correlation in damage is considered in the study of Lee and Kiremidjian, there are still no experimental or mathematical models to estimate the correlation. This represents a source of epistemic uncertainty, which arises from inefficient model or databases. The epistemic uncertainty can be reduced by investing in additional data or by using a better correlation model to improve the accuracy of the estimation.

2.2 Critical Appraisal and Pending Research Issues

A review of the existing literature, summarized in the previous section, identified a numbers of deficiencies and limitations in current approaches to risk assessment of distributed civil infrastructure systems. Among the issues identified in this review, the following appear to be particularly significant:

- Only a limited number of research studies have considered the inter-dependence among components of civil infrastructure systems and pairs of buildings. While some of these studies have accounted for the ground motion correlation (Goda and Hong, 2008; Straub *et al.*, 2008; Wesson *et al.*, 2009), the structural damage correlations are rarely considered. As a result, the loss metrics such as probability of failure, repair cost, and life-cycle cost may be underestimated.
- Second-order parameters, such as the variance, standard deviation and coefficient of variation of the loss, are rarely determined (Lee and Kiremidjian, 2007; Cardona *et al.*, 2008; Goda and Hong, 2008; Wesson *et al.*, 2009). These parameters convey a sense of the quality of the estimate of expected loss, high-

quality estimates being associated with low variance. These estimators require knowledge of the correlation in losses which, as noted previously, has not been determined in most studies. Having them available would make the loss estimate more functional for the decision makers. Furthermore, the parameters that go into the loss estimates have both aleatory and epistemic components, the latter being associated with modeling uncertainties and limited data. Both sources of uncertainty should be taken into account to allow for differences in risk aversion among decision-makers (Cha and Ellingwood, 2011). The neglect of this uncertainty may lead to underestimation of the probable maximum loss (PML), a common decision metric for insurance underwriting.

- Software tools, such as HAZUS-MH and QLARM, for estimating seismic loss to buildings portfolios usually compute loss at centroid of studied census tracts, and use the result to represent losses of the whole tract. It is more realistic to estimate losses from spatially distributed buildings rather than from the centroids of the building tracts; at least, the error in this approximation should be assessed quantitatively. In addition, these software tools cannot estimate second-order parameters because earthquake variability, such as inter- and intra-event variability, and correlations in demand and performance are neglected.
- Existing studies mainly have considered discrete large facilities or bridges in transportation networks (Lee and Kiremidjian, 2007). In such cases, the correlation structure is manageable computationally because the facilities are fixed in location and relatively small in number. However, for distributed buildings, computation associated with analyzing correlation is formidable and

expensive because distributed buildings in neighborhood consist of large numbers and their locations are randomly distributed.

In the following chapter, quantitative tools for addressing the above approximations and deficiencies will be developed.

CHAPTER 3

CHARACTERIZING SEISMIC DEMAND AND BUILDING RESPONSE

Seismic demands and building response must be identified and quantified to estimate the risk to building inventories resulting from seismic hazards. Moreover, since an earthquake affects buildings and facilities over a region, the correlation in seismic demand on separate facilities and in building performance in response to those demands should be taken into account.

This chapter summarizes fundamental methods for characterizing the seismic hazard that will be utilized in later sections to determine seismic demand, building response and damage. Earthquake demand on building inventories requires knowledge of earthquake source, ground motion attenuation, local soil amplification, and spatial ground motion correlation. Two methods of seismic hazard analysis are presented: scenario earthquake analysis (SEA) and probabilistic seismic hazard analysis (PSHA). Building response to seismic demand, including response of individual and distributed buildings and structure-to-structure correlation, also are described.

3.1 Seismic Hazard Analysis

The spectrum of the earthquake ground motion at a site is represented by the contributions of earthquake source (*E*), propagation path (*P*), site response (*G*), and instrument or type of motion (*I*) (Boore, 2003; Campbell, 2003):

$$Y\left(M_0, R, f\right) = E\left(M_0, f\right) \cdot P\left(R, f\right) \cdot G\left(f\right) \cdot I\left(f\right) \tag{3-1}$$

where M_0 is the seismic moment related to the moment magnitude, f is the frequency, and R is the distance from the source to the site. This equation represents the basis for determining seismic intensity and demand at individual building sites as well as the stochastic dependence of intensity and demand among buildings in the inventory.

3.1.1 Earthquake Source

Earthquake sources are identified from geologic and tectonic evidence or from historical seismicity (Kramer, 1996). In *scenario seismic hazard analysis*, the epicenter and magnitude level are selected for the earthquake that is believed to produce the most significant ground motion at the site. In *probabilistic seismic hazard analysis*, all earthquake sources and their recurrence rates are considered, leading a relationship between magnitude and the number of earthquakes that will exceed those magnitudes. The mean annual recurrence rate λ_m of exceedence of earthquake magnitude m, is computed from the Gutenberg-Richter law (Kramer, 1996):

$$\begin{aligned} \lambda_m &= 10^{a-b\cdot m} \\ &= \exp\left(\alpha - \beta \cdot m\right) \end{aligned} \tag{3-2}$$

where 10^a is the mean annual number of earthquakes with magnitudes greater than or equal to zero and b describes the relative likelihood of earthquakes of different magnitudes, $\alpha = \ln(10)\cdot a$, and $\beta = \ln(10)\cdot b$. Eq (3-2) implies that earthquake magnitudes have an exponential distribution. Small earthquakes which cause insignificant damage [those with magnitudes less than 4 to 5 (Srbulov, 2008)] are usually disregarded, as are sources are believed incapable of generating earthquakes above a certain magnitude.

Thus, the mean annual rate of exceedence of earthquake magnitude is expressed as (Kramer, 1996):

$$\lambda_m = \nu \cdot \frac{\exp\left[-\beta \cdot \left(m - m_o\right)\right] - \exp\left[-\beta \cdot \left(m_{\max} - m_o\right)\right]}{1 - \exp\left[-\beta \cdot \left(m_{\max} - m_o\right)\right]} \quad m_o \le m \le m_{\max} \tag{3-3}$$

where $\nu = \exp\left(\alpha - \beta \cdot m_o\right)$, m_o is the lower threshold magnitude (4.0 to 5.0), and m_{max} is the maximum magnitude. According to the U.S. Geological Survey, the maximum moment magnitude recorded for in the CEUS is 7.7[1]. The probability density function of magnitude, derived from the Gutenberg-Richter law with upper and lower bounds, is expressed as:

$$f_M\left(m\right) = \frac{\beta \cdot \exp\left[-\beta \cdot \left(m - m_o\right)\right]}{1 - \exp\left[-\beta \cdot \left(m_{\max} - m_o\right)\right]} \tag{3-4}$$

3.1.2 Ground Motion Attenuation

Ground motion attenuation from source to site is described by an equation estimating the median or mean of the seismic intensity measure [e.g. peak ground acceleration (PGA) or spectral acceleration (S_a)] as a function of the magnitude of the earthquake and the distance from the epicenter to the site. In addition, some attenuation relations may include type of faulting or local site conditions (Campbell, 2003; Atkinson and Boore, 2006). The aleatory uncertainty related to these attenuations is one of the major sources of uncertainty in seismic risk assessment of buildings and building inventories. Some attenuation relations for estimating ground motion intensity in the eastern North America are, as described below.

[1]http://earthquake.usgs.gov/earthquakes/states/10_largest_us.php

Campbell (2003) developed a ground motion attenuation relation for hard-rock sites in eastern North America (ENA) by using empirical ground motion relations developed for western North America (WNA). The relation for spectral acceleration (S_a) is:

$$\begin{aligned}\ln\left(S_a\right) &= c_1 + c_2 \cdot M_w + c_3 \cdot \left(8.5 - M_w\right)^2 \\ &\quad + c_4 \cdot \ln R + \left(c_5 + c_6 \cdot M_w\right) \cdot R + f\end{aligned} \tag{3-5}$$

where

$$f = \begin{cases} 0 & ; R \le 70km \\ c_7 \cdot \left[\ln\left(\dfrac{R}{70}\right)\right] & ; 70km < R \le 130km \\ c_7 \cdot \left[\ln\left(\dfrac{R}{70}\right)\right] + c_8 \cdot \left[\ln\left(\dfrac{R}{130}\right)\right] & ; R > 130km \end{cases}$$

The (logarithmic) standard deviation of the residual, $\sigma_{ln(Sa)}$, describing the aleatory uncertainty in the ground-motion intensity, is expressed by:

$$\sigma_{\ln(PSA)} = \begin{cases} c_{11} + c_{12} \cdot M_w & ; M_w < 7.16 \\ c_{13} & ; M_w \ge 7.16 \end{cases} \tag{3-6}$$

in which coefficients c_1 through c_{13} depend on period, and are listed in Table 6 in Campbell's paper (2003).

Atkinson and Boore (1995) proposed a ground motion attenuation relationship from an empirically based stochastic ground-motion model based on Eq (3-1). The S_a on a hard-rock site is expressed by:

$$\begin{aligned}\log_{10}\left(S_a\right) = &\; c_1 + c_2 \cdot (M_w - 6) + c_3 \cdot (M_w - 6)^2 \\ &- \log_{10}(R) - c_4 \cdot R\end{aligned} \tag{3-7}$$

where the period-dependent coefficients c_1 through c_4 are listed in Atkinson and Boore's paper (1995).

The $\log_{10}$-standard deviation (aleatory uncertainty) for this attenuation relation is 0.32. Subsequently, Atkinson and Boore (2006) improved their 1995 equations by incorporating more recent seismological data obtained from eastern North America (ENA). From this later study, the S_a for a hard-rock site was estimated by:

$$\begin{aligned}\log_{10}\left(S_a\right) = \; & c_1 + c_2 \cdot M_w + c_3 \cdot M_w^2 + \left(c_4 + c\ M_w\right) \cdot f_1 \\ & + \left(c_6 + c_7 M_w\right) \cdot f_2 + \left(c_8 + c_9 M_w\right) \cdot f_0 \\ & - c_{10} \cdot R\end{aligned} \tag{3-8}$$

where $f_0 = \max[\log_{10}(10/R),0)]$; $f_1 = \min[\log_{10}(R),\log_{10}(70)]$; $f_2 = \max[\log_{10}(R/140),0]$; and the coefficients c_1 through c_{10} are listed in Table 6 in paper of Atkinson and Boore (2006). The $\log_{10}$-standard deviation for this attenuation relation is 0.30.

The aforementioned ground-motion attenuation equations for S_a (at fundamental period, $T_1 = 0.3$ s) on a hard-rock site when M_w equals 7.0 and the epicentral distance is 50 km are compared in Figure 3-1. Each attenuation relation predicts the median value of S_a ($T_1 = 0.3$ sec) at specific distances. The aleatory uncertainty is provided along with the attenuation equations, as noted above. The epistemic uncertainty, which is associated with lack of knowledge and imperfect models of real–world phenomena, is represented by the differences among the attenuation relationships. A sensitivity analysis involving epistemic uncertainties in these ground motion models will be presented in Chapter 7.

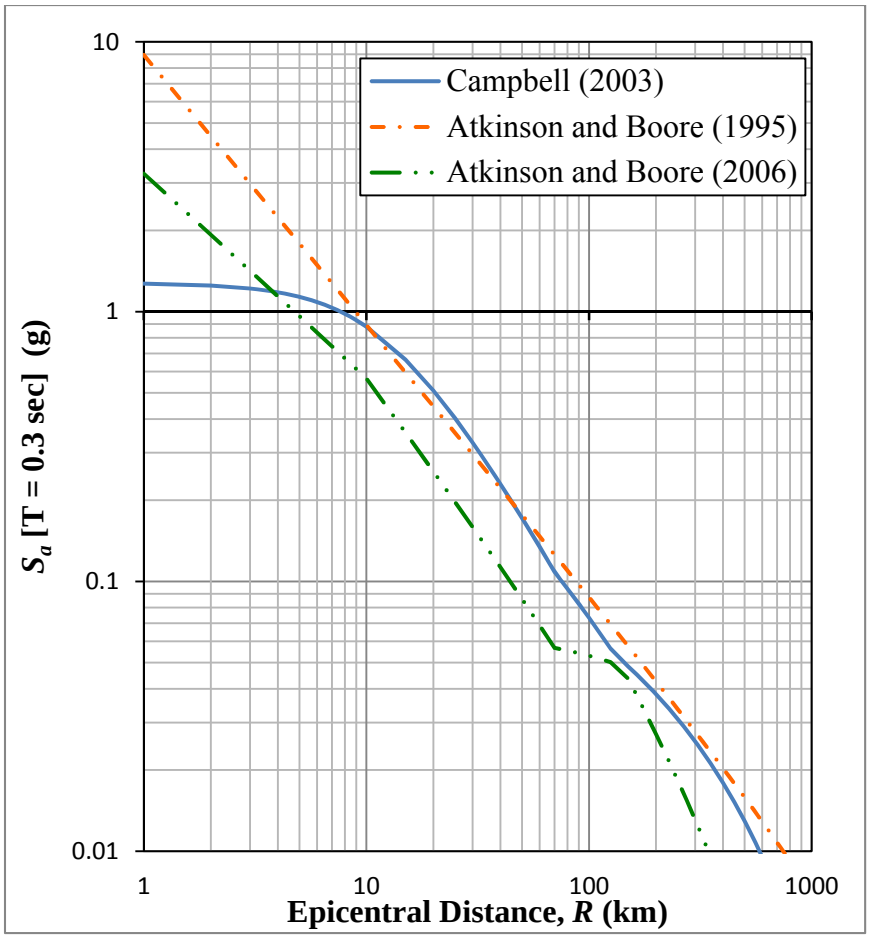

Figure 3-1 Comparison of median attenuation relations for S_a (T_1 = 0.3 sec) when M_w 7.0

3.1.3 Local Soil Amplification

The ground motion attenuation relations in Section 3.1.2 are for hard-rock sites [referred to as Site Class A in *ASCE Standard 7-10* (ASCE, 2010)]. The local soil amplification at a facility site depends on the properties of soil profile within a 100-foot (30 m) depth beneath a site, which may dampen or amplify the ground motion intensity. Soil profiles typically are classified into six categories, as shown in Table 3-1 (ASCE, 2010). The local soil amplification factors are function of seismic intensity, such as

spectral acceleration (S_a), peak ground acceleration (PGA), or peak ground velocity (PGV).

Table 3-1 Site class definition [Table 20-3.1, (ASCE, 2010)]

Site Class	Soil Profile Name	Average Properties in Top 100 feet		
		Soil shear wave velocity, $\overline{v_s}$, ft/s	Standard penetration resistance, $\overline{N}$	Soil undrained shear strength, $\overline{s_u}$, (psf)
A	Hard rock	$\overline{v_s} > 5{,}000$	N/A	N/A
B	Rock	$2{,}500 < \overline{v_s} \leq 5{,}000$	N/A	N/A
C	Very dense soil and soft rock	$1{,}200 < \overline{v_s} \leq 2{,}500$	$\overline{N} > 50$	$\overline{s_u} \geq 2{,}000$
D	Stiff soil profile	$600 \leq \overline{v_s} \leq 1{,}200$	$15 \leq \overline{N} \leq 50$	$1{,}000 \leq \overline{s_u} \leq 2{,}000$
E	Soft soil profile	$\overline{v_s} < 600$	$\overline{N} < 15$	$\overline{s_u} < 1{,}000$
E	-	Any profile with more than 10 feet of soil have the following characteristics: 1. Plasticity index $PI > 20$, 2. Moisture content w ≥ 40%, and 3. Undrained shear strength $\overline{s_u} < 500$ psf		
F	-	Any profile containing soils having one or more of the following characteristics 1. Soils vulnerable to potential failure or collapse under seismic loading such as liquefiable soils, quick and highly sensitive clays, collapsible weakly cemented soils. 2. Peats and/or highly organic clays ($H > 10$ feet of peat and/or highly organic clay where H = thickness of soil) 3. Very high plasticity clays ($H > 25$ feet with plasticity index $PI > 25$) 4. Very thick soft/medium stiff clays ($H > 120$ feet)		

For SI: 1 foot = 304.8 mm, 1 foot = 0.00929 m^2, 1 pound per $foot^2$ = 0.0479 kPa. N/A = Not applicable.

Table 3-2 Values of site coefficient F_a [a] [Table 11.4-1, (ASCE, 2010)]

Site Class	Mapped Spectral Response Acceleration at 1-second Period				
	$S_1 \leq 0.25$	$S_1 = 0.50$	$S_1 = 0.75$	$S_1 = 1.00$	$S_1 \geq 1.25$
A	0.8	0.8	0.8	0.8	0.8
B	1.0	1.0	1.0	1.0	1.0
C	1.2	1.2	1.1	1.0	1.0
D	1.6	1.4	1.2	1.1	1.0
E	2.5	1.7	1.2	0.9	0.9
F	Note b	Note b	Note b	Note b	Note b

a. Use straight-line interpolation for intermediate values of mapped spectral response acceleration at short period, S_s.
b. Values shall be determined in accordance with Section 11.4.7 of ASCE 7.

Table 3-3 Values of site coefficient F_v [a] [Table 11.4-2, (ASCE, 2010)]

Site Class	Mapped Spectral Response Acceleration at 1-second Period				
	$S_1 \leq 0.1$	$S_1 = 0.2$	$S_1 = 0.3$	$S_1 = 0.4$	$S_1 \geq 0.5$
A	0.8	0.8	0.8	0.8	0.8
B	1.0	1.0	1.0	1.0	1.0
C	1.2	1.4	1.2	1.1	1.0
D	2.5	1.7	1.2	0.9	0.9
E	3.5	3.2	2.8	2.4	2.4
F	Note b	Note b	Note b	Note b	Note b

a. Use straight-line interpolation for intermediate values of mapped spectral response acceleration at short period, S_s.

b. Values shall be determined in accordance with Section 11.4.7 of ASCE 7.

The maximum considered earthquake spectral response acceleration for short period, S_{MS}, and at 1-second period, S_{ML}, is computed by *ASCE Standard 7-10*:

$$S_{MS} = F_a \cdot Sa_s \tag{3-9}$$

$$S_{M1} = F_v \cdot Sa_1 \tag{3-10}$$

where F_a and F_v are site coefficients defined in Table 3-2 and Table 3-3, respectively, and Sa_s and Sa_1 are spectral acceleration for short periods and at 1-second period on rock site (Site Class B), respectively. These tables will be used to determine the seismic demand using the Capacity Spectrum Method in Section 3.3.1.

3.1.4 Spatial Correlation in Ground Motion

Seismic intensities resulting from a single earthquake over its affected area are stochastically dependent to some degree due to common source-generating mechanisms, attenuation, and local soil conditions. Ground motion intensity measure of sites *i* and *j* resulting from earthquake event *e* ($Y_{e,i}$ and $Y_{e,j}$) are (Park *et al.*, 2007):

$$\ln Y_{e,i} = \overline{\ln Y_{e,i}} + \sigma \cdot \eta_e + \tau \cdot \varepsilon_{e,i} \tag{3-11}$$

$$\ln Y_{e,j} = \overline{\ln Y_{e,j}} + \sigma \cdot \eta_e + \tau \cdot \varepsilon_{e,j} \tag{3-12}$$

where $\overline{\ln Y_{e,i}}$ and $\overline{\ln Y_{e,j}}$ are the expected values of ground motion intensity measure (logarithmic scale) of sites *i* and *j*, which are computed from Section 3.1.2, respectively; η_e is the inter-event error term of earthquake event *e,* described by a standard normal distribution; σ and τ are the corresponding standard deviation of inter-event and intra-event error terms; and $\varepsilon_{e,i}$, and $\varepsilon_{e,j}$ are the intra-event error terms for sites *i* and *j*, described by a bi-variate standard normal distribution with correlation $\rho_{i,j}$. Note that the total standard deviation in the (log) ground motion intensity, σ_T , is:

$$\sigma_T = \sqrt{\sigma^2 + \tau^2} \tag{3-13}$$

The stochastic dependence of the seismic intensities at sites of nearby buildings, $\rho_{i,j}$, depends on the spatial correlation of the ground motion intensities (Boore *et al.*, 2003; Wang and Takada, 2005; Park *et al.*, 2007; Goda and Hong, 2008; Jayaram and Baker, 2009). Many models of this spatial correlation have been developed over last decade. Boore *et al.* (2003) suggested the following spatial correlation of peak horizontal accelerations based on regression analysis of peak ground motions from the 1994 Northridge, California, earthquake for earthquakes:

$$\rho_{ij} = 1 - \left[1 - \exp\left(-\sqrt{0.6 \cdot r_{ij}}\right)\right]^2 \tag{3-14}$$

where ρ_{ij} is the correlation in intensity between site *i* and site *j*; and r_{ij} is the distance between sites *i* and site *j*, and asserted that Eq (3-14) was applicable to earthquakes with magnitude between 6.0 and 6.9. Wang and Takada (2005) developed exponential spatial correlation models for both PGA and for PGV, based on normalized auto-covariance functions for earthquakes in Japan and Taiwan. Their model is:

$$\rho_{ij} = \exp\left(-\frac{r_{ij}}{r_0}\right) \tag{3-15}$$

where r_0 is a correlation distance, which represents the strength of the spatial correlation. Wang and Takada's study concluded that the correlation distance ranges from 20 to 40 km, based on an analysis of five earthquakes in Japan and the 1999 Chi-Chi earthquake in Taiwan. Lee and Kiremidjian (2007) utilized a covariance model to estimate the spatial correlation of ground motion intensities at bridges in the San Francisco bay area:

$$\rho_{ij} = \exp\left[-\left(\frac{r_{ij}}{r_0}\right)^2\right] \tag{3-16}$$

Figure 3-2 illustrates the three spatial correlation models of ground motion intensities. The correlation models differ substantially because they were estimated from different earthquakes and for areas with different attenuation features. Clearly, using a spatial correlation model developed in one region to predict ground motion in a different region may be questionable. Unfortunately, no spatial correlation models exist for strong ground motion intensities in the EUS due to a lack of seismological data. Thus, the nature of the correlation must be assumed from fundamental seismological considerations.

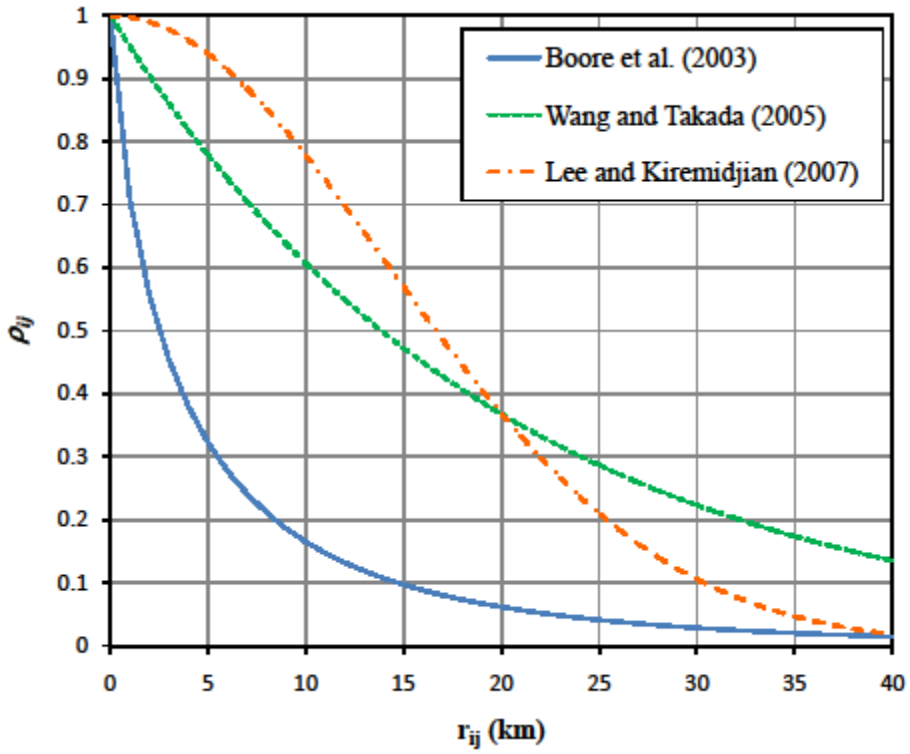

Figure 3-2 Comparison of the spatial correlation models, assuming that r_0 = 20 km for all models

Wang and Takada (2005) found that the correlation distance for both PGA and for PGV was between 20 – 40 km in Taiwan and Japan. A later study by Jayaram and Baker (2009) showed that correlation for the Chi-Chi earthquake in Taiwan and several earthquakes in California (e.g., Northdrige, Parkfield, etc.), decreased exponentially as spectral acceleration period increases. That ground motion correlation distance for sites in the EUS is expected to be larger than that in California and Taiwan, which are seismically active regions, Furthermore, Figure 3-3 shows the felt areas for shaking and damage due to earthquakes of given magnitudes in the EUS and WUS. Earthquakes with comparable magnitude affect a far larger area in the EUS than in the WUS. The seismic waves from earthquakes travel much further in the EUS than in the WUS because the

crust beneath the EUS is more stable and less fractured than in the WUS[1]. Therefore, while the exponential spatial correlation models in Figure 3-2 might be appropriate for the EUS, the correlation distance will be much larger than in the WUS. Unfortunately, no data exist by which this correlation distance can be determined in the EUS. Accordingly, it is assumed that the correlation distance for sites in the EUS is 50 km, rather than the 20 – 40 km distance found for high-seismic areas. The sensitivity analysis in Chapter 7 will consider the impact of this assumption on estimated damage and loss to the building inventories considered.

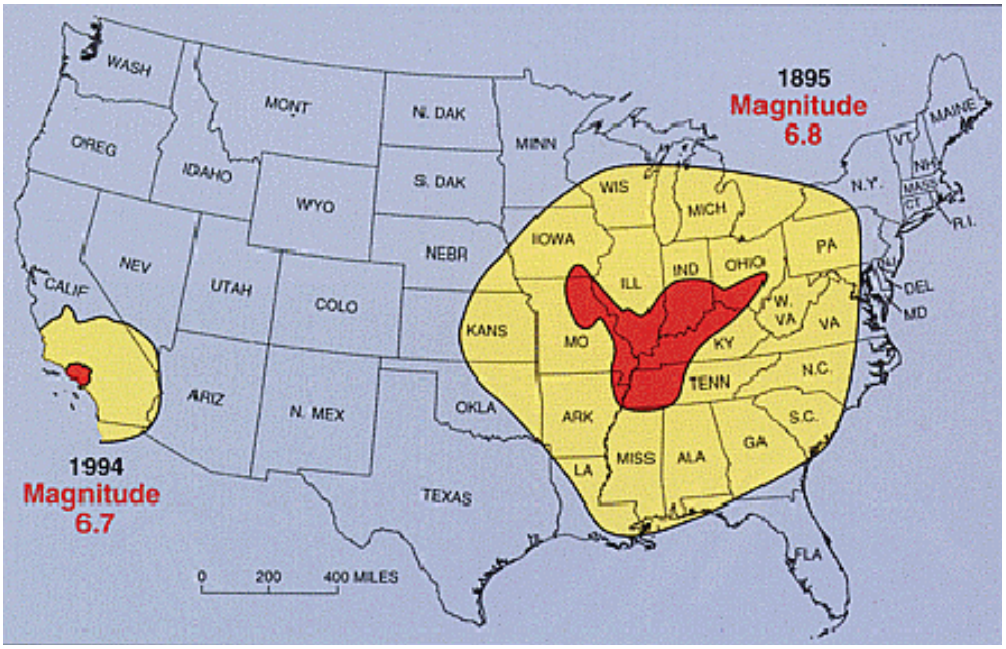

Figure 3-3 Comparison of damage area and shaking felt between WES and EUS (Schweig. E. *et al.*, 1995)

3.2 Characterization of Seismic Hazard for Risk Analysis

Earthquake hazards for purposes of risk analysis can be estimating by: 1) scenario earthquake analysis (SEA), and 2) probabilistic seismic hazard analysis (PSHA). A SEA

[1]http://www.conservativerefocus.com/blog5.php/2011/08/23/the-science-behind-the-east-coast-quake-eastern-crust-colder-denser-than-western-crust

considers only one scenario earthquake, and the site-dependent intensities caused by that earthquake. In contrast, a PSHA considers a broad range of possible earthquakes affecting a study region, and each earthquake is weighted by its probability of occurrence in determining the probability that the ground motion intensity of interest is exceeded at sites of interest. Because it considers only one event, the SEA captures the spatial variability of demand intensities over a region, information that is lost in the necessary process of aggregating the relative contributions of different earthquakes in the PSHA (Adachi, 2007; Lee, 2007). On the other hand, one cannot associate an annual probability with a scenario earthquake because the seismic hazard usually represents the aggregation of numerous earthquakes. Thus, the seismic hazard analysis and the associated risk are conditioned on the occurrence of the specific scenario earthquake.

3.2.1 Scenario Earthquake Analysis (SEA)

For assessment of risk to spatially distributed systems such as transportation networks or building facilities, a scenario earthquake analysis (SEA) has the advantage that it can capture the spatial variability of earthquake intensities over a region in a straightforward fashion. Furthermore, the potential consequences of a SEA are easier to explain to non-specialist decision makers, such as city planners and stakeholders, than a PSHA, especially at the low annual probabilities of interest in civil infrastructure risk analysis and mitigation.

A scenario earthquake may be selected from historic events or it may be determined by a de-aggregation process, which is a methodology to determine earthquakes with given moment magnitude, epicentral distance, and epicenter that contributes to a particular ground motion intensity (PGA, S_a, etc) with a specified return

period (Bazzurro and Cornell, 1999). An illustration of the de-aggregation of an earthquake in Memphis, TN at a probability of 2%/50 years (mean recurrence interval of 2,475 years) is provided in Figure 3-4. Note that the de-aggregation is performed for a specific site, and provides no information on the spatial variation in ground motion intensity or on what the intensity at other sites in close proximity to the site considered.

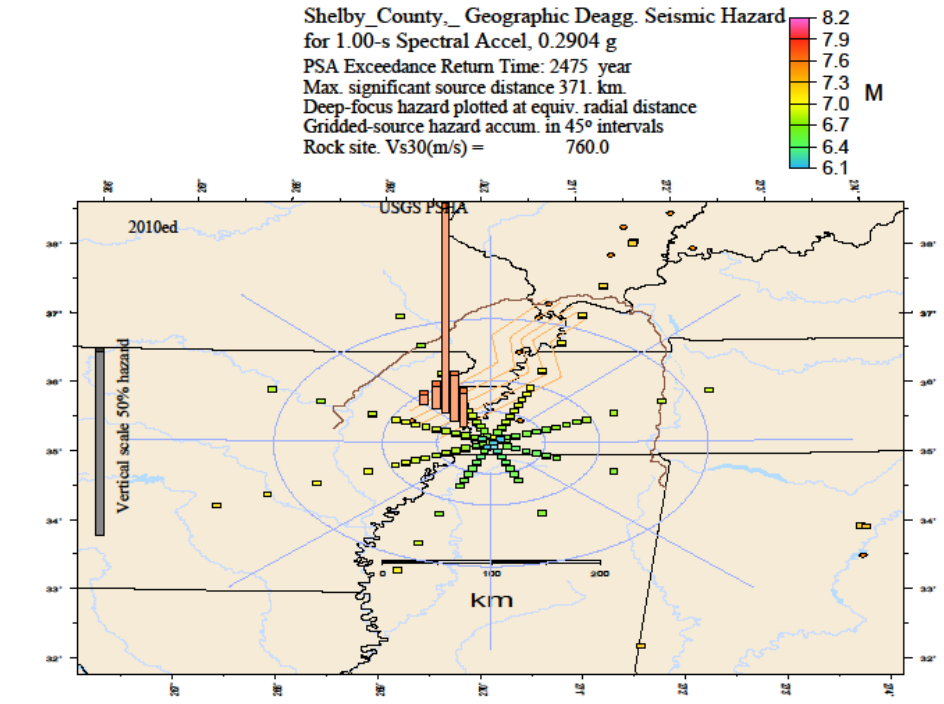

Site cords: -89.8956 35.1837 (yellow disk) Max annual ExcdRate 0.2268E-3 (Column high prop. to ExRate).
Diamonds: historical earthquakes. Orange M>5.CEUS

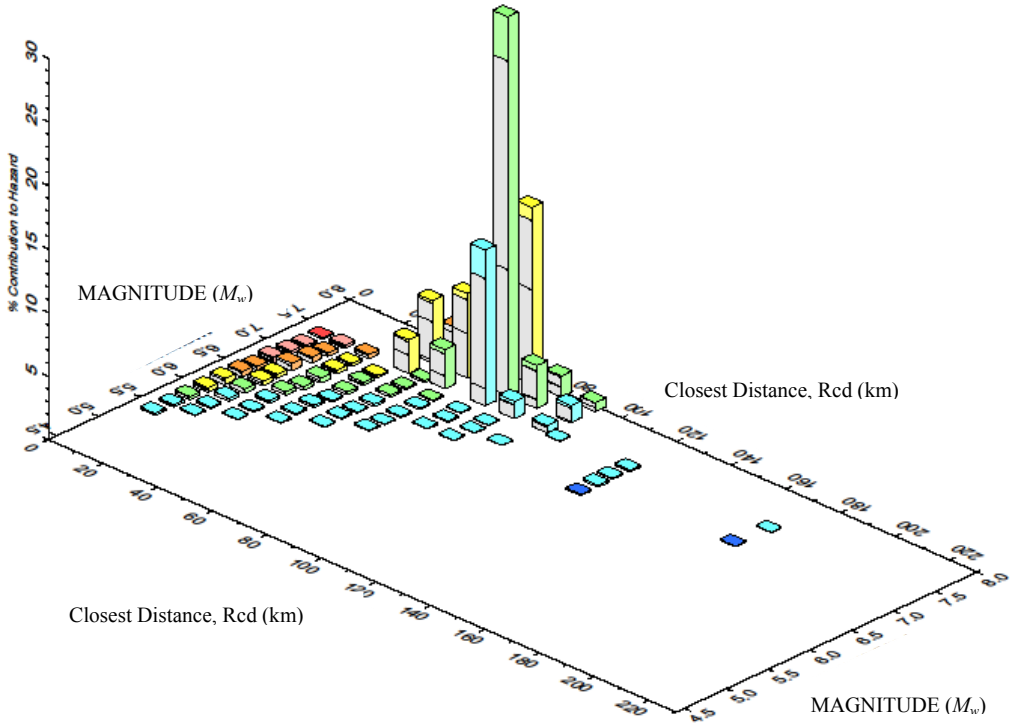

Figure 3-4 Deaggreation of S_a (T= 1.0 s) for 2475-year return period (2% probability of exceedence in 50 years) (from USGS website)

3.2.2 Probabilistic Seismic Hazard Analysis (PSHA)

In contrast with the scenario earthquake analysis, a probabilistic seismic hazard analysis considers the contribution of all possible earthquakes occurring in a region to the mean annual frequency that (random) seismic intensity, *Y*, exceeds a specific parameter, *y* at a specific facility site affected by those earthquakes (McGuire, 1995; Bazzurro and Cornell, 1999). The PSHA represents the reality that a given site may be affected by a number of earthquakes with different magnitudes and epicenters during its service life, and that seismic intensities of different levels at a site may arise from more than one earthquake. The mean annual frequency of exceedence at a site of a specified level, *y*, of seismic intensities, $\lambda_{Y>y}$, is computed as follows (Kramer, 1996):

$$\lambda_{Y>y} = \sum_{i=1}^{N} \nu_i \int_M \int_R P\left[Y > y \mid m, r\right] \cdot f_{M_i}(m) \cdot f_{R_i}(r) dm dr \tag{3-17}$$

where N is the number of earthquake sources, ν_i is the mean annual rate of occurrence of earthquakes generated from source *i* which is evaluated by Eq (3-2), $P\left[Y > y \mid m, r\right]$ is the probability that the seismic intensity generated from source *i* of magnitude *m* and epicentral distance *r* exceeds *y*, $f_{M_i}(m)$ is the probability density function of magnitude of earthquake occurring at source *i*, and $f_{R_i}(r)$ is the probability density function of epicentral distance of the earthquake occurring at source *i*. The result of such an analysis is a "seismic hazard curves," depicting the mean annual frequency of exceedence *vs* intensity, y. Such curves can be obtained from a website maintained by the U.S. Geological Survey, and are the basic for the seismic hazard maps in ASCE Standard 7-10 and building codes.

3.3 Building Response to Seismic Ground Motion

When an earthquake occurs, damage to structural systems is of primary concern because structural damage affects damage to nonstructural systems, occupant casualties, and indirect losses due to unsafe conditions and loss of prior building functions (Kircher *et al.*, 2006). Thus, we begin with a study of the response of building structural systems to seismic demands. Subsequently, damage to nonstructural components also will be consistent.

3.3.1 Individual Buildings

The performance of a building subjected to earthquake ground motion is described for risk assessment purposes by a set of fragility curves, which define the probability of being in or exceeding specific building damage states, conditioned on seismic intensity, such as PGA, PGV, S_a, or S_d.

In this study, the seismic intensity, computed from ground motion attenuation and local soil amplification, is defined by the spectral displacement, S_d, while seismic demand is computed from the Capacity Spectrum Method (CSM) (Chopra and Goel, 1999; Fajfar, 1999), which is based on the use of the inelastic strength and displacement spectra. The acceleration-displacement response spectrum is determined from the seismic intensity, while the strength of a building is represented by the capacity spectrum. The demand spectrum is computed from the reduction of the intensity that depends on the inelastic behavior of the building, described by a ductility factor. The procedure can be described as follows:

1) The seismic demand spectrum (red line in Figure 3-5) from the seismic intensity has initial ductility factor, μ, equal to 1;
2) The intersection of the capacity of building (blue line in Figure 3-5) and the seismic demand is Sd_o and the actual ductility factor, μ_o, is computed by Sd_o/D_y. Note that D_y is the yield displacement of the building;
3) If μ_o equals μ, the spectral displacement demand equals Sd_o and the procedure is finished;
4) If the factors are not equal, the seismic demand is reduced by a ductility factor, μ_R, which is greater than 1. Note that the method to compute the reduced seismic demand (green line in Figure 3-5) follows an approach proposed by Fajfar (1999);
5) Repeat steps 1 to 4 until the initial and actual ductility factors are equal.

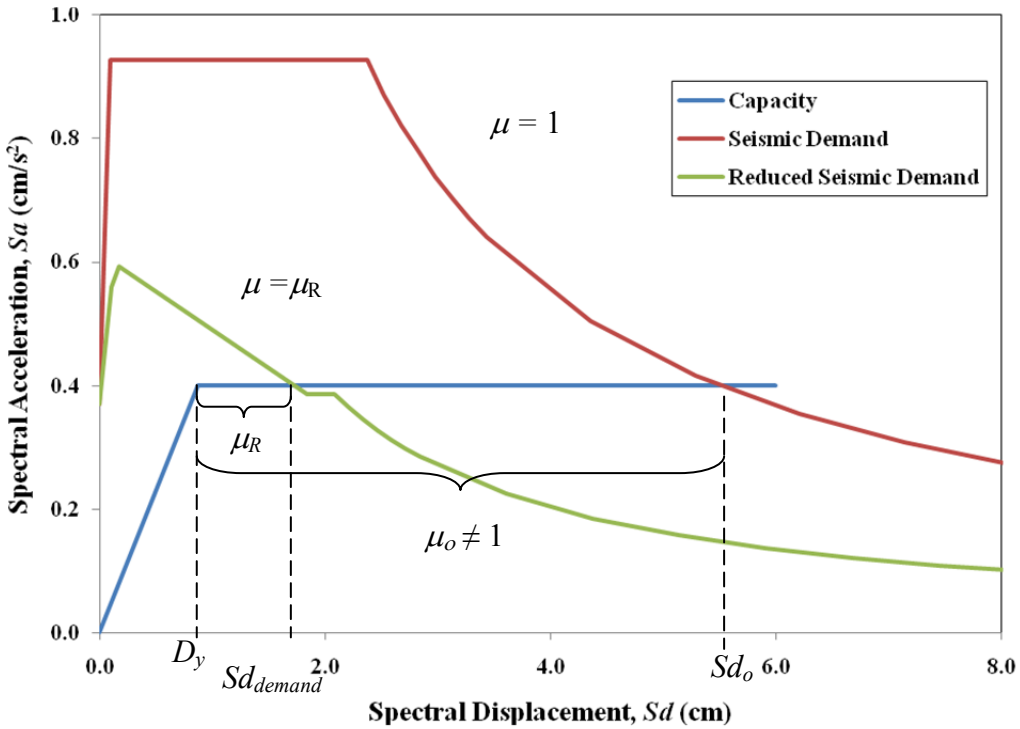

Figure 3-5 Example of demand and capacity spectra.

The fragility often is represented by a lognormal cumulative distribution function (Hwang *et al.*, 1997; Kircher *et al.*, 1997; Celik, 2007; Ellingwood *et al.*, 2007):

$$P\left[DS_i \geq ds_i^{(k)} \mid U_i = u_i \right] = \Phi\left[\frac{1}{\beta_{ds(k)}} \ln\left(\frac{u_i}{m_{ds(k)}} \right) \right] \tag{3-18}$$

where DS_i is a discrete random variable represented by the different damage state of building i given by $ds_i^{(k)}$; $ds^{(k)}$ is the threshold of damage state k, defined subsequently; U_i is the seismic intensity at a location of building i; and $m_{ds}^{(k)}$ and $\beta_{ds}^{(k)}$are the median and logarithmic standard deviation of capacity (in term of seismic intensity) at which the building reaches the threshold of damage state, $ds^{(k)}$, respectively. The probability of being in damage state (k) thus is:

$$\begin{aligned} P\left[DS_i = ds_i^{(k)} \mid U_i = u_i \right] = \quad & \Phi\left[\frac{1}{\beta_{ds(k)}} \ln\left(\frac{u_i}{m_{ds(k)}} \right) \right]_k \\ & -\Phi\left[\frac{1}{\beta_{ds(k+1)}} \ln\left(\frac{u_i}{m_{ds(k+1)}} \right) \right]_{k+1} \end{aligned} \tag{3-19}$$

Many studies have developed fragilities for buildings and other structures for the CEUS (Hwang *et al.*, 1997; FEMA/NIBS, 2003; Ellingwood *et al.*, 2007; Park *et al.*, 2009). However, with the exception of HAZUS-MH (FEMA/NIBS, 2003), most of these studies did not provide repair and replacement costs corresponding to their damage functions. For this reason, then, the seismic fragilities from HAZUS-MH are used to determine the building performance in this study, despite recent evidence that the logarithmic standard deviations in the HAZUS fragilities are conservative when applied to individual buildings (Kinali and Ellingwood, 2007; Celik and Ellingwood, 2009).

HAZUS-MH classifies buildings into 36 types based on their structural system for computing damage states, as shown in Table 3-4. Figure 3-6 shows the example of fragility functions of being at each damage state. Furthermore, damage functions for these structural systems are subcategorized in HAZUS-MH into four levels of earthquake-resistant design: high-code, moderate-code, low-code, and pre-code. Building damage from seismic ground motion is classified by one of four discrete damage states: slight, moderate, extensive, and complete (FEMA/NIBS, 2003; Kircher *et al.*, 2006). The damage state "none" is added herein in order to describe an undamaged building. A description of each damage state for a concrete moment frame is summarized in Table 3-5. Descriptions for other types of building construction are similar (FEMA/NIBS, 2003).

Table 3-4 Building Structure Type [Table 3.1, (FEMA/NIBS, 2003)]

No.	Label	Description	Height			
			Range		Typical	
			Name	Stories	Stories	Feet
1	W1	Wood, Light Frame (≤5,000 sq.ft.)		1 - 2	1	14
2	W2	Wood, Commercial and Industrial (> 5,000 sq. ft.)		All	2	24
3	S1L	Steel Moment Frame	Low-Rise	1 – 3	2	24
4	S1M		Mid-Rise	4 – 7	5	60
5	S1H		High-Rise	8+	13	156
6	S2L	Steel Braced Frame	Low-Rise	1 – 3	2	24
7	S2M		Mid-Rise	4 – 7	5	60
8	S2H		High-Rise	8+	13	156
9	S3	Steel Light Frame		All	1	15
10	S4L	Steel Frame with Cast-in-Place Concrete Shear Walls	Low-Rise	1 – 3	2	24
11	S4M		Mid-Rise	4 – 7	5	60
12	S4H		High-Rise	8+	13	156
13	S5L	Steel Frame with Unreinforced Masonry Infill Walls	Low-Rise	1 – 3	2	24
14	S6M		Mid-Rise	4 – 7	5	60
15	S6H		High-Rise	8+	13	156
16	C1L	Concrete Moment Frame	Low-Rise	1 – 3	2	20
17	C1M		Mid-Rise	4 – 7	5	50
18	C1H		High-Rise	8+	12	120
19	C2L	Concrete Shear Walls	Low-Rise	1 – 3	2	20
20	C2M		Mid-Rise	4 – 7	5	50
21	C2H		High-Rise	8+	12	120
22	C3L	Concrete Frame with Unreinforced Masonry Infill Walls	Low-Rise	1 – 3	2	20
23	C3M		Mid-Rise	4 – 7	5	50
24	C3H		High-Rise	8+	12	120
25	PC1	Precast Concrete Tilt-Up Walls		All	1	15
26	PC2L	Precast Concrete Frames with Concrete Shear Walls	Low-Rise	1 – 3	2	20
27	PC2M		Mid-Rise	4 – 7	5	50
28	PC2H		High-Rise	8+	12	120
29	RM1L	Reinforced Masonry Bearing Walls with Wood or Metal Deck Diaphragms	Low-Rise	1 – 3	2	20
30	RM1M		Mid-Rise	4 – 7	5	50
31	RM2L	Reinforced Masonry Bearing Walls with Precast Concrete Diaphragms	Low-Rise	1 – 3	2	20
32	RM2M		Mid-Rise	4 – 7	5	50
33	RM2H		High-Rise	8+	12	120
34	URML	Unreinforced Masonry Bearing Walls	Low-Rise	1 – 2	1	15
35	URMM		Mid-Rise	3+	3	35
36	MH	Mobile Homes		All	1	10

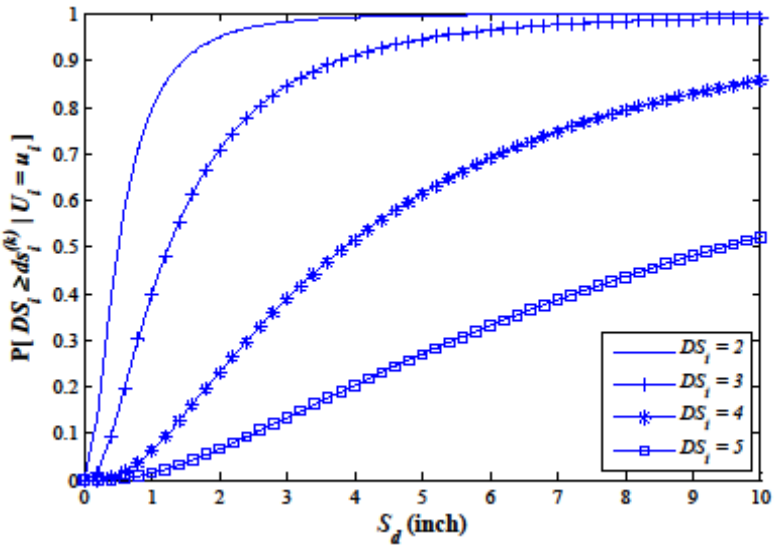

Figure 3-6 Fragility functions of being at each damage state for building type W1

Table 3-5 Example of structural damage states of concrete moment frame (C2) (FEMA/NIBS, 2003)

Damage State	Description
Slight	Flexural or shear type hairline cracks in some beams and columns near joints or within joints.
Moderate	Most beams and columns exhibit hairline cracks. In ductile frames some of the frame elements have reached yield capacity indicated by larger flexural cracks and some concrete spalling. Nonductile frames may exhibit larger shear cracks and spalling.
Extensive	Some of the frame elements have reached their ultimate capacity indicated in ductile frames by large flexural cracks, spalled concrete and buckled main reinforcement; nonductile frame elements may have suffered shear failures or bond failures at reinforcement splices, or broken ties or buckled main reinforcement in columns which may result in partial collapse.
Complete	Structure is collapsed or in imminent danger of collapse due to brittle failure of nonductile frame elements or loss of frame stability. Approximately 13% (low-rise), 10%(mid-rise) or 5%(high-rise) of the total area of C1buildings with complete damage is expected to be collapsed.

3.3.2 Structure-to-structure Correlation

Structure-to-structure correlations in the performance of spatially distributed buildings arise from one of several causes: building design using a common building code, common regulatory practices, common construction material or construction technologies, use of local contractors with similar practices. Together with the

correlation in seismic demand, the performance and damage to buildings sited within an affected area are likely to be highly correlated.

A simple probabilistic model can reveal insight on how the correlation introduced by these factors might affect building response, damage, and loss, a probabilistic model of damage correlation has been developed. Suppose seismic damage of building *i* and *j*, (DM_i and DM_j), are described by the simple model:

$$\begin{aligned} DM_i &= M_i + T_i + C_i + \varepsilon_i \\ &= Y_i + \varepsilon_i \end{aligned} \tag{3-20}$$

$$\begin{aligned} DM_j &= M_j + T_j + C_j + \varepsilon_j \\ &= Y_j + \varepsilon_j \end{aligned} \tag{3-21}$$

where M_i, M_j, T_i, T_j, C_i and C_j are factors denoting the material, structural type, and building code of buildings *i* and *j*; and ε_i and ε_j represent noise terms that account for remaining factors that are not specifically modeled, such as workmanship in construction, quality of building materials, etc. Terms ε_i and ε_j are assumed to be normally distributed, with zero mean and standard deviation, σ_ε. Furthermore, it is assumed that Y and ε are statistically independent. The standard deviations of Y_i and Y_j (σ_{Y_i} and σ_{Y_j}) are computed as the root mean square of the logarithmic standard deviations of all damage states (slight, moderate, extensive, and complete) for specified building type *i* (i = 1,2,…,36) and building code *c*, as shown in Appendix A, Table A-1 to Table A-4. The variance, σ_ε^2, is assumed to be 15 percent of $\sigma_{Y_i} \cdot \sigma_{Y_j}$ for model illustration purpose. A sensitivity analysis examining the role of σ_ε^2 in damage and loss assessment will be performed in Chapter 7.

The covariance of DM_i and DM_j is:

$$\begin{aligned}\mathrm{Covar}\left[DM_i, DM_j\right] &= \mathrm{E}\left[DM_i DM_j\right] - \mathrm{E}\left[DM_i\right]\cdot\mathrm{E}\left[DM_j\right] \\ &= \mathrm{E}\left[\left(Y_i+\varepsilon_i\right)\cdot\left(Y_j+\varepsilon_j\right)\right] - \mathrm{E}\left[Y_i\right]\cdot\mathrm{E}\left[Y_j\right] \\ &= \mathrm{E}\left[Y_i\cdot Y_j + Y_i\cdot\varepsilon_j + Y_j\cdot\varepsilon_i + \varepsilon_i\cdot\varepsilon_j\right] - \mathrm{E}\left[Y_i\right]\cdot\mathrm{E}\left[Y_j\right] \\ &= \mathrm{Covar}\left[Y_i, Y_j\right] + \mathrm{Covar}\left[\varepsilon_i, \varepsilon_j\right]\end{aligned} \tag{3-22}$$

Let

$$\mathrm{Covar}\left[Y_i, Y_j\right] = \rho_{Y_i,Y_j}\cdot\sigma_{Y_i}\cdot\sigma_{Y_j} \tag{3-23}$$

$$\mathrm{Covar}\left[\varepsilon_i, \varepsilon_j\right] = \sigma_\varepsilon^2\cdot\exp\left[-\left(\frac{r_{ij}}{\beta_\varepsilon}\right)\right] \tag{3-24}$$

$$\rho_{Y_i,Y_j} = \beta_{BT_i,BT_j}\cdot\beta_{C_i,C_j} \tag{3-25}$$

where ρ_{Y_i,Y_j} is the correlation of Y_i and Y_j; β_ε defines the scale of correlation of the noise; β_{BT_i,BT_j} describes the correlation of building response *i* and *j* introduced by differences in building material and type; and β_{C_i,C_j} describes the correlation of building response *i* and *j* introduced by the use of different generations of building codes.

Since data to estimate the coefficients β_ε, β_{BT_i,BT_j}, and β_{C_i,C_j} is unavailable, these coefficients are selected using judgement to complete the risk analysis; the sensitivity of the loss assessment to these factors is examined further in Chapter 7. The scale of correlation in the noise term, β_ε, is likely to be affected by common construction practices in an area within an urban region that is developed at approximately the same time. Herein, β_ε is assumed to equal the average dimension of all census tracts in the

study area (i.e. the average census tracts width in Shelby County, TN, is 3 km). The coefficient β_{BT_i,BT_j} is assumed to equal to 0.9 for buildings *i* and *j* in Table 3-4 having similar construction materials, building structural type (frame, shear wall), and story range (low-rise, mid-rise, and high-rise); 0.8 for buildings *i* and *j* having similar construction materials and structural type but different story range; 0.7 for buildings *i* and *j* having similar materials but different structural types; and 0.5 for buildings *i* and *j* having different construction materials and different structural types. Note that the correlation coefficient for identical building material and type is not 1.0, reflecting the fact that not all buildings will suffer the same damage when they are subjected to the same scenario earthquake. Furthermore, although two buildings may be constructed with the same construction material and design capacity, their performance may not be identical because of uncertainties in material quality or capacity. The coefficient β_{C_i,C_j} is assumed to equal to 1.0 for buildings *i* and *j* designed using the same building code; and 0.7 for buildings *i* and *j* designed using different building codes.

Using the above results, the correlation of DM_i and DM_j is:

$$\rho_{DM_i,DM_j} = \frac{\rho_{Y_i,Y_j}\cdot\sigma_{Y_i}\cdot\sigma_{Y_j}+\sigma_\varepsilon^2\cdot\exp\left[-\left(r_{ij}/\beta_\varepsilon\right)\right]}{\sqrt{\left(\sigma_{Y_i}^2+\sigma_\varepsilon^2\right)\cdot\left(\sigma_{Y_j}^2+\sigma_\varepsilon^2\right)}} \tag{3-26}$$

The lower and upper bounds of damage correlation calculated from Eq (3-26) are assumed to equal 0.0 and 0.9, respectively. The probabilistic model shows that the lower bound of damage correlation is greater than zero. However, because many of the terms in Eq (3-26) have little data to support them, the lower bound has been taken equal to 0.0

to provide the most severe test of the methodology. Similarly, the upper bound 0.9 is set from the fact that the performance of two buildings constructed with same construction material, design capacity, and building code and with same code enforcement may not be identical because of uncertainties in material quality or capacity.

3.3.3 Analysis of Correlation in Damage States for Spatially Distributed Buildings

Two (or more) buildings which are separated at some distance but are subjected to the same seismic event will be subjected to correlated seismic demands. As a results, damage functions of these buildings will be stochastically dependent to some degree. If essentially no damage correlation exists between such buildings, the joint probability mass function (PMF) for their damage states would be expressed approximately by:

$$P\left[DS_i = ds_i, DS_j = ds_j \mid U_i, U_j\right] = P\left[DS_i = ds_i \mid U_i\right] \times P\left[DS_j = ds_j \mid U_j\right] \quad (3\text{-}27)$$

where DS_i and DS_j are the damage states of buildings i and j when $i \neq j$, and U_i and U_j are the seismic intensities at the locations of buildings i and j. If the damage states are correlated, however, the joint PMF for their damage states cannot be determined in closed-form, and approximations must be sought.

One such approximation involves the use of copulas. A copula is a technique to approximate a multivariate distribution function when only the marginal distributions of the variables and their correlation are known (Cherubini, 2004; Nelsen, 2006). Copula techniques were first used in financial applications (e.g. asset pricing and risk evaluation techniques). The word "copula" was first employed by Sklar in 1959 (Nelsen, 2006), but statisticians did not refer to it as such until quite recently. A two-dimensional copula,

C(u,v), is a real function defined on $I \times I$, where $I \in [0,1]$, which satisfies the following properties:

(i) $C(u,0) = C(0,v) = 0$

(ii) $C(u,1) = u$ and $C(1,v) = v \quad \forall (u,v) \in (I,I)$

(iii) $C(u_2,v_2) - C(u_1,v_2) - C(u_2,v_1) + C(u_1,v_1) \geq 0 \quad \forall (u,v) \in (I,I)$, such that $u_1 \leq u_2$ and $v_1 \leq v_2$

Many copula families (i.e. Gaussian, Student- t, Archimedean, and dispersion copula) have been developed (Cherubini, 2004; Nelsen, 2006). The simplest copula is the Gaussian copula, defined as;

$$C(\bar{u}) = \Phi^n\left(\Phi^{-1}(u_1), \Phi^{-1}(u_2), ..., \Phi^{-1}(u_n)\right) \tag{3-28}$$

where $\bar{u}$ is a vector of uniform independent *n* random variables; $\Phi^n(\ )$ is an n-variate normal cumulative distribution function with correlation matrix, Σ; and $\Phi^{-1}(\ )$ is the inverse of the cumulative normal distribution.

Lee (2007) adapted a copula technique to determine the joint PMF of earthquake damage states of bridges in transportation networks in the San Francisco, CA Bay Area. The correlation matrix accounts for structure-to-structure correlation in damage. The Gaussian copula is utilized in the current study to model correlated building damage realizations. While the joint distribution of the damage states is discrete, the Gaussian copula is continuous. To solve this different representation, the correlated realizations that are generated from the Gaussian copula must be transformed to correlated discrete

realizations by utilizing an inverse transformation, described in the third step of the following procedure. The algorithm for sampling from this joint distribution is to:

1) Generate n-variate standard normal vector ($x_1, x_2, \ldots, x_n$) with correlation matrix, Σ.
2) Transform x_i into standard uniform random variable, u_i, defined on (0,1), by $u_i = \Phi(x_i)$
3) For a given ground motion intensity, transform the standard uniform variables (from step 2) from the probability of exceedence space to the discrete damage state space, $ds_i^{(k)}$, where k = 1, …, 5, using an inverse transformation.

Figure 3-7 shows the marginal PMFs describing damage probabilities for buildings *i* and *j* that are the starting point for determining the joint probability distribution of damage for these two buildings. The joint probabilities of damage with specific correlations, ρ_D = 0.0, 0.5 and 0.9, are illustrated in Figure 3-8. Note that when ρ_D equals 0.0 (Figure 3-8a), no damage correlation exists between the two buildings.

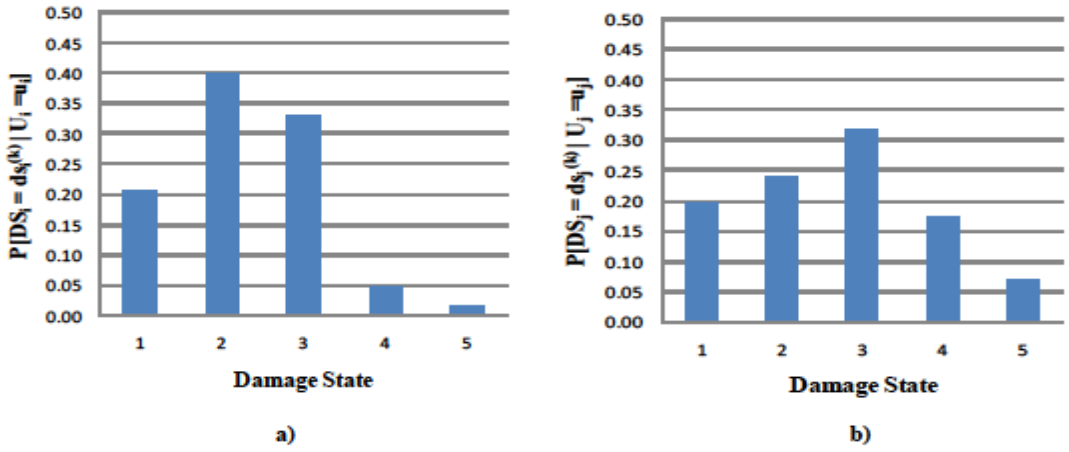

Figure 3-7 Example of building damage function: a) building *i* b) building *j*

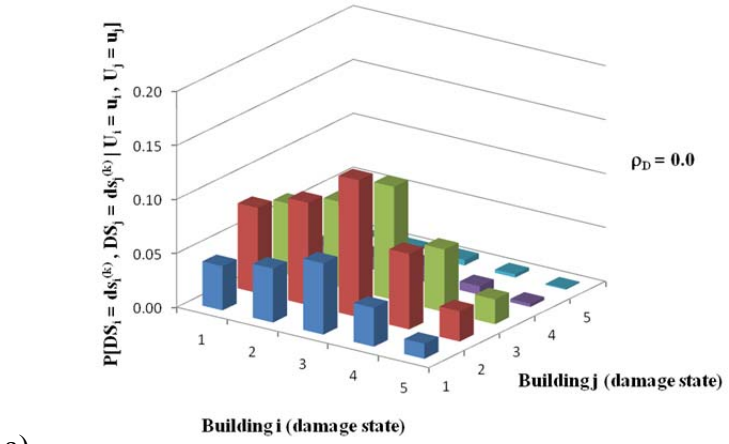

a)

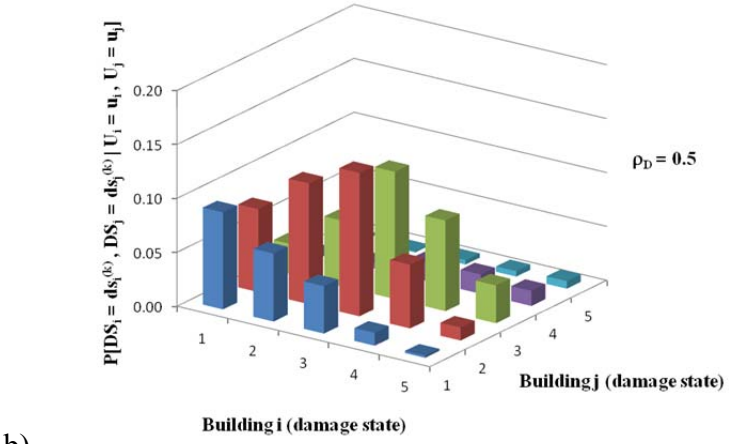

b)

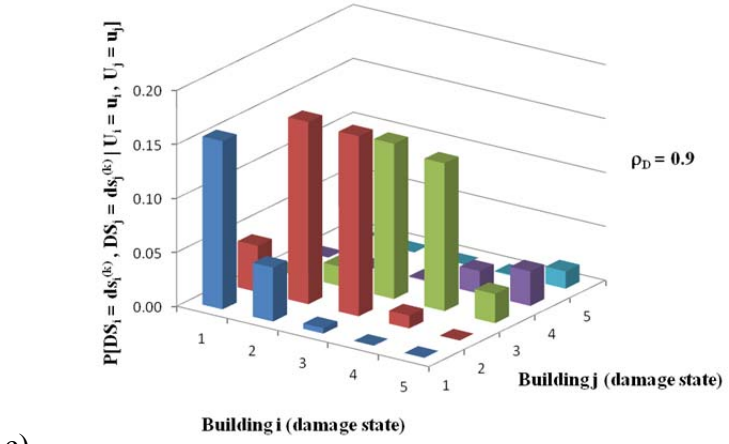

c)

Figure 3-8 Joint probability of damage for building *i* and *j* a) damage correlation (ρ_D) = 0.0, b) damage correlation (ρ_D) = 0.5, and c) damage correlation (ρ_D) = 0.9.

3.4 Summary

This chapter has summarized fundamental concepts used in the following chapters to predict seismic demand, including seismic source zone, ground motion attenuation relationship for S_a (T = 0.3 sec), amplification of seismic intensity due to local soil conditions, and spatial correlation in ground motion intensity. Furthermore, differences between scenario earthquake and probabilistic seismic hazard analyses were summarized. Finally, building response to seismic demand considering single buildings, spatially distributed buildings, and damage correlations between pairs of buildings was illustrated. These fundamental tools will be utilized to assess structural loss to building inventories due to ground shaking in the following chapters.

CHAPTER 4

MODELS OF STRUCTURAL LOSS TO BUILDING INVENTORIES

This chapter builds upon the analytical framework presented in Chapters 2 and 3 to determine structural loss to building inventories from a seismic event. The loss metric is represented in term of a monetary loss ratio, which is the ratio of structural repair cost to full structural replacement cost. Because of the complexity of the analysis and the aggregation of individual losses, which are mutually correlated, the numerical results are obtained by Monte Carlo methods.

Section 4.1 illustrates a methodology to calculate the direct economic (structural) loss ratio of a single building based on its occupancy class as function of epicentral distance. In Section 4.2, an approach to estimate correlation in structural losses of two buildings subjected to the same seismic event is described. Section 4.3 integrates the losses in Section 4.1, taking into account the correlation in losses, to estimate the total structural loss ratio for a building inventory. A random sampling technique is developed to improve the efficiency of the estimation procedure. In Section 4.4, the model methodology is applied to buildings in Shelby County, TN.

4.1 Direct Economic (Structural) Loss Ratios of a Single Building

The loss to a single structure is a function of occupancy class and damage state. These, in turn, depend on epicentral distance, moment magnitude and the level of earthquake-resistant code provisions used in the design of the structural system.

The expected value of structural loss ratio to a single building from a scenario earthquake with moment magnitude M_w and epicentral distance R is computed by the theorem of total probability:

$$\begin{aligned} \mathrm{E}[LR_i \mid M_w, R, OC_a] \;=\; & \sum_k \sum_t \int_{u_i} \mathrm{E}[LR_i \mid DS_i^{(k)} = ds_i^{(k)}, OC_a = oc_a] \cdot \\ & \mathrm{P}\left[DS_i^{(k)} = ds_i^{(k)} \mid BT_i^{(t)} = bt_i^{(t)}, U_i = u_i \right] \cdot \\ & \mathrm{P}[BT_i^{(t)} = bt_i^{(t)} \mid OC_a = oc_a] \cdot f_{U_i} du_i \end{aligned} \tag{4-1}$$

where LR_i is the structural loss ratio of building i; $BT_i^{(t)}$ is the building type t of a building i; OC_a is the occupancy class a; $\mathrm{P}[BT_i^{(t)} = bt_i^{(t)} \mid OC_a = oc_a]$ is the probability mass function defining the frequency of building types bt in each occupancy class a, which is the same relative frequency as used in HAZUS-MH (MR4), as shown in Table 4-1 for building occupancy RES4; and f_{U_i} is the probability density function of ground motion intensity at building/site i. The expected values of structural repair ratio of building i given damage state k and occupancy class a, $\mathrm{E}[LR_{ij} | DS_i^{(k)} = ds_i^{(k)}, OC_a = OC_a]$, are given in Table 4-2. Since $\mathrm{E}[LR_{ij} | DS_i^{(k)} = ds_i^{(k)}, OC_a = OC_a]$ in Table 4-2 is discrete, the distribution of LR_i is also discrete. It is convenient to use average repair ratios of all occupancies in a strong ground motion event because the repair ratios of all occupancies are quite similar for all damage states except the "extensive" damage state of RES2.

Table 4-1 Example of probability mass function defining the frequency of building type in RES4 in Tennessee

Building Type	Code			
	Pre	**Low**	**Moderate**	**High**
W1	-	-	0.50	-
RM1L	-	-	0.03	-
RM2L	-	-	0.02	-
URML	0.12	-	0.33	-

Table 4-2 Occupancy class and structural repair cost ratios [modified from Table 15.1 and 15.2 in FEMA (2003)]

No.	Occupancy Class	Description	Sub-Category	Structural Damage State				
				None	Slight	Moderate	Extensive	Complete
1	RES1	Single Family Dwelling	Single Family Dwelling	0.000	0.021	0.098	0.500	1.000
2	RES2	Manuf. Housing	Manuf. Housing	0.000	0.016	0.098	0.299	1.000
3	RES3A	Duplex	Duplex	0.000	0.022	0.101	0.500	1.000
4	RES3B	Triplex / Quads	Triplex / Quads	0.000	0.022	0.101	0.500	1.000
5	RES3C	Multi-dwellings (5 to 9 units)	Multi-dwellings (5 to 9 units)	0.000	0.022	0.101	0.500	1.000
6	RES3D	Multi-dwellings (10 to 19 units)	Multi-dwellings (10 to 19 units)	0.000	0.022	0.101	0.500	1.000
7	RES3E	Multi-dwellings (20 to 49 units)	Multi-dwellings (20 to 49 units)	0.000	0.022	0.101	0.500	1.000
8	RES3F	Multi-dwellings (50+ units)	Multi-dwellings (50+ units)	0.000	0.022	0.101	0.500	1.000
9	RES4	Temporary Lodging	Hotel, medium	0.000	0.015	0.103	0.500	1.000
10	RES5	Institutional Dormitory	Dorm, small	0.000	0.021	0.101	0.500	1.000
11	RES6	Nursing Home	Nursing home	0.000	0.022	0.098	0.500	1.000
12	COM1	Retail Trade	Dept Store, 1st	0.000	0.020	0.099	0.500	1.000
13	COM2	Wholesale Trade	Warehouse, medium	0.000	0.019	0.099	0.500	1.000
14	COM3	Personal and Repair Services	Garage, Service sta.	0.000	0.019	0.099	0.500	1.000
15	COM4	Professional/Technical Services	Office, Small	0.000	0.021	0.099	0.500	1.000
16	COM5	Banks	Bank	0.000	0.022	0.101	0.500	1.000
17	COM6	Hospital	Hospital, medium	0.000	0.014	0.100	0.500	1.000
18	COM7	Medical Office/Clinic	Med Office, small	0.000	0.021	0.097	0.500	1.000
19	COM8	Entertainment & Recreation	Restaurant	0.000	0.020	0.100	0.500	1.000
20	COM9	Theaters	Movie Theatre	0.000	0.025	0.098	0.500	1.000
21	COM10	Parking	Parking Garage	0.000	0.021	0.100	0.499	1.000
22	IND1	Heavy	Factory, small	0.000	0.025	0.102	0.497	1.000
23	IND2	Light	Warehouse, medium	0.000	0.025	0.102	0.497	1.000
24	IND3	Food/Drugs/Chemicals	Factory, small	0.000	0.025	0.102	0.497	1.000
25	IND4	Metals/Minerals Processing	Factory, small	0.000	0.025	0.102	0.497	1.000
26	IND5	High Technology	Factory, small	0.000	0.025	0.102	0.497	1.000
27	IND6	Construction	Warehouse, small	0.000	0.025	0.102	0.497	1.000
28	AGR1	Agriculture	Warehouse, medium	0.000	0.017	0.100	0.500	1.000
29	REL1	Churches and Other Non-profit Org.	Church	0.000	0.015	0.101	0.500	1.000
30	GOV1	General Services	Post Office	0.000	0.017	0.101	0.503	1.000
31	GOV2	Emergency Response	Police Station	0.000	0.020	0.098	0.503	1.000
32	EDU1	Grade Schools	High School	0.000	0.021	0.101	0.503	1.000
33	EDU2	Colleges/Universities	College Classroom	0.000	0.018	0.100	0.500	1.000

The variance in loss ratio for building *i* is expressed by:

$$\begin{aligned}
\mathrm{Var}[LR_i \mid M_w, R, OC_a] &= \mathrm{E}[LR_i^2 \mid M_w, R, OC_a] - \mathrm{E}\left[LR_i \mid M_w, R, OC_a\right]^2 \\
&= \sum_k \sum_t \int_{u_i} \mathrm{E}[LR_i^2 \mid DS_i^{(k)} = ds_i^{(k)}, OC_a = oc_a] \cdot \\
&\quad \mathrm{P}\left[DS_i^{(k)} = ds_i^{(k)} \mid BT_i^{(t)} = bt_i^{(t)}, U_i = u_i\right] \cdot \\
&\quad \mathrm{P}[BT_i^{(t)} = bt_i^{(t)} \mid OC_a = oc_a] \cdot f_{U_i} du_i \\
&\quad - \left\{ \sum_k \sum_t \int_{u_i} E[LR_i \mid DS_i^{(k)} = ds_i^{(k)}, OC_a = oc_a] \cdot \right. \\
&\quad \mathrm{P}\left[DS_i^{(k)} = ds_i^{(k)} \mid BT_i^{(t)} = bt_i^{(t)}, U_i = u_i\right] \cdot \\
&\quad \left. \mathrm{P}[BT_i^{(t)} = bt_i^{(t)} \mid OC_a] \cdot f_{U_i} du_i \right\}^2
\end{aligned} \tag{4-2}$$

where

$$\begin{aligned}
\mathrm{E}[LR_i^2 \mid DS_i^{(k)} = ds_i^{(k)}, OC_a = oc_a] &= \mathrm{Var}\left[LR_i \mid DS_i^{(k)} = ds_i^{(k)}, OC_a = oc_a\right] \\
&\quad + \left\{\mathrm{E}[LR_i \mid DS_i^{(k)} = ds_i^{(k)}, OC_a = oc_a]\right\}^2
\end{aligned} \tag{4-3}$$

The structural loss ratio conditioned on damage state *i* and occupancy class *a* is assumed to be constant because HAZUS-MH (MR4) only provides a constant value of the structural repair ratio for a given damage state, as illustrated in Table 4-2. Under this assumption, the first term of Eq (4-3) vanishes.

4.2 Structural Loss Correlation of Two Buildings

When two buildings are subjected to the same seismic event, the seismic demand, structural response to that demand, damage and structural loss are correlated. The correlation coefficient for the loss ratio between pairs of buildings is:

$$\rho_{LR_i,LR_j|M_w,OC_a,OC_b} = \frac{\mathrm{COV}\left[LR_i, LR_j \mid M_w, OC_a, OC_b\right]}{\sqrt{\mathrm{Var}\left[LR_i \mid M_w, OC_a\right] \cdot \mathrm{Var}\left[LR_j \mid M_w, OC_b\right]}} \tag{4-4}$$

where

$$\begin{aligned}\mathrm{COV}\left[LR_i, LR_j \mid OC_a, OC_b\right] = \Bigg\{ & \sum_{k_i}\sum_{k_j}\sum_{t_i}\sum_{t_j}\int\int_{u_i\,u_j} \mathrm{E}[LR_i \mid DS_i^{(k_i)} = ds_i^{(k_j)}, OC_a = oc_a] \cdot \\ & \mathrm{E}[LR_j \mid DS_j^{(k_j)} = ds_j^{(k_j)}, OC_b = oc_b] \cdot \\ & \mathrm{P}\Big[DS_i^{(k_i)} = ds_i^{(k_i)}, DS_j^{(k_j)} = ds_j^{(k_j)} \mid \\ & BT_i^{(t)} = bt_i^{(t)}, U_i = u_i, BT_j^{(t_j)} = bt_j^{(t_j)}, U_j = u_j\Big] \cdot \\ & \mathrm{P}[BT_i^{(t_i)} = bt_i^{(t_i)} \mid OC_a = oc_a] \cdot \\ & \mathrm{P}[BT_j^{(t_j)} = bt_j^{(t_j)} \mid OC_b = oc_b] \cdot f_{U_i,U_j} du_i u_j \Bigg\} \\ & -\mathrm{E}\left[LR_i \mid OC_a\right] \cdot \mathrm{E}\left[LR_j \mid OC_b\right]\end{aligned} \tag{4-5}$$

$$f_{U_i,U_j}\left(u_i, u_j\right) = \Phi\left(\frac{\ln\left(u_i\right) - \mu_{\ln(U_i)}}{\sigma_{\ln(U_i)}}, \frac{\ln\left(u_j\right) - \mu_{\ln\left(U_j\right)}}{\sigma_{\ln\left(U_j\right)}}, \rho_{g_{ij}}\right) \tag{4-6}$$

OC_a and OC_b are the occupancy classes of buildings *i* and *j*, respectively; $\mathrm{Var}\left[LR_i \mid M_w, OC_a\right]$ and $\mathrm{Var}\left[LR_j \mid M_w, OC_a\right]$ are computed from Eq (4-2); $DS_i^{(k_i)}$ and $DS_j^{(k_j)}$ are the damage states k_i and k_j of building *i* and *j*, respectively.

If there is no correlation in damage between building *i* and *j*, the term P[$DS_i^{(k)}$ = $ds_i^{(k)}$, $DS_j^{(k)} = ds_j^{(k)} \mid BT_i^{(ti)} = bt_i^{(ti)}$, $U_i = u_i$, $BT_j^{(tj)} = bt_j^{(tj)}$, $U_j = u_j$] in Eq (4-5) can be evaluated by Eq (3-27). Otherwise, it is determined by the copula technique, described in Section 3.3.3.

Figure 4-1 illustrates the correlation in loss ratio, computed using simulation from Eq (4-4), as a function of the distance between buildings *i* and *j*. These curves show that even if two buildings are close to each other, the correlation in loss ratio is substantially less than 1.0. This is caused by the differences in adjacent building construction and code enforcement. Correlation of structural losses is stronger at increasing distances as the magnitude of the earthquake increases because of the increase in the felt area of the larger events. These correlation curves were obtained numerically, and have been smoothed by least-squares fitting, as follows:

$$\rho_{LR_i,LR_j|M_w,OC_a,OC_b}\left(r_{ij}\right) = \begin{cases} \alpha \cdot \exp\left(-\dfrac{r_{ij}}{d_{l0}}\right) & ; \quad r_{ij} \geq w_m \\ 1.0 & ; \quad r_{ij} < w_m \end{cases} \tag{4-7}$$

where r_{ij} is the separation distance between the centroids of buildings *i* and *j*; w_m is the minimum dimension of all buildings; and the coefficients α and d_{l0} are determined by least-squares fitting from structural loss correlation curves between pairs of buildings, as shown in Figure 4-1. The minimum dimension of all buildings is assumed to equal 0.02 km in this study.

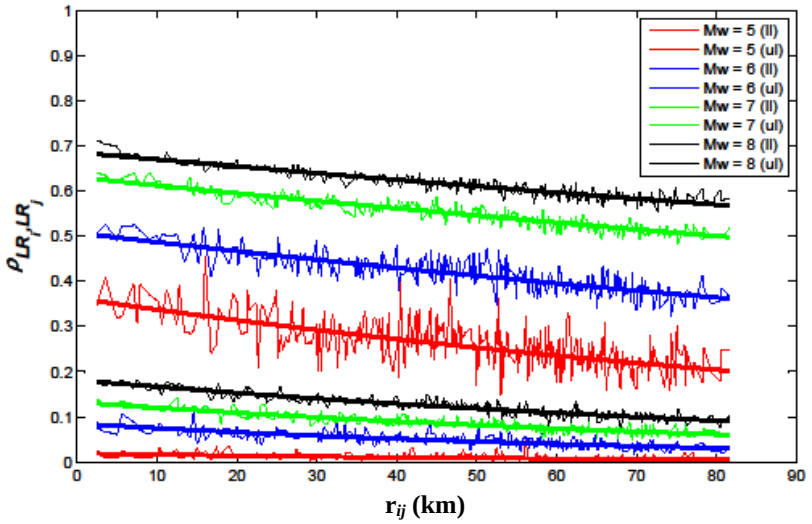

Figure 4-1 The correlation of structural loss ratio between pairs of buildings in class RES4. [ll = lower line ($\rho_D = 0.0$), ul = upper line ($\rho_D = 0.9$). The bold solid lines represent the correlation from regression analysis].

4.3 Structural Loss Correlation for Building Inventory

The structural loss ratio for the building inventory is the summation of losses to all buildings (repair/replacement) divided by the total replacement cost of the building inventory:

$$LR_T = \frac{\sum_{i=1}^{N} LR_i \cdot RPC_i}{\sum_{i=1}^{N} RPC_i} \tag{4-8}$$

where LR_i is the structural loss ratio of building i; and RPC_i is the full structural replacement cost of building i. If losses to buildings with the same occupancy classes are aggregated first, Eq (4-8) can be rewritten as:

$$LR_T = \frac{\sum_{a=1}^{M} L_{T,a}}{\sum_{a=1}^{M}\sum_{i=1}^{N_a} RPC_{i,a}} = \frac{\sum_{a=1}^{M}\left(\sum_{i=1}^{N_a} LR_{i,a}\cdot RPC_{i,a}\right)}{\sum_{a=1}^{M}\sum_{i=1}^{N_a} RPC_{i,a}} \quad (4\text{-}9)$$

where $N = N_1+N_2+\ldots+N_M$; M is the number of building classes; N_a is the number of buildings in occupancy class a; $L_{T,a}$ is the total structural loss assigned to building occupancy a; $LR_{i,a}$ is the structural loss ratio of building i and occupancy class a; and $RPC_{i,a}$ is the full structural replacement cost of building i and occupancy class a. Since the seismic demand on each building is random, as is building performance under a given demand (fragility), the individual building losses are random, as is $LR_{i,a}$. The full structural replacement cost will be treated as a random variable because the cost data may not be available for all building inventories.

Considering one occupancy class (e.g., commercial), the total loss ratio and its expected value and variance are:

$$LR_{T,a} = \frac{\sum_{i=1}^{N_a} LR_{i,a}\cdot RPC_{i,a}}{\sum_{i=1}^{N_a} RPC_{i,a}} \quad (4\text{-}10)$$

$$\mathrm{E}\left[LR_{T,a}\right] = \sum_{i=1}^{N_a}\mathrm{E}\left[\frac{LR_{i,a}\cdot RPC_{i,a}}{\sum_{i=1}^{N_a} RPC_{i,a}}\right] \quad (4\text{-}11)$$

$$\begin{aligned}\mathrm{Var}\left[LR_{T,a}\right] &= \mathrm{Var}\left[\frac{\sum_{i=1}^{N_a} LR_{i,a}\cdot RPC_{i,a}}{\sum_{i=1}^{N_a} RPC_{i,a}}\right] \\ &= \sum_{i=1}^{N_a}\sum_{j=1}^{N_a}\mathrm{Covar}\left[\frac{LR_{i,a}\cdot RPC_{i,a}}{\sum_{k=1}^{N_a} RPC_{k,a}}, \frac{LR_{j,a}\cdot RPC_{j,a}}{\sum_{k=1}^{N_a} RPC_{k,a}}\right]\end{aligned} \tag{4-12}$$

When two or more occupancy classes are considered, the expected value and variance of the total loss ratio are:

$$\begin{aligned}E\left[LR_T\right] &= \mathrm{E}\left[\frac{\sum_{a=1}^{M}\left(\sum_{i=1}^{N_a} LR_{i,a}\cdot RPC_{i,a}\right)}{\sum_{a=1}^{M}\sum_{i=1}^{N_a} RPC_{i,a}}\right] \\ &= \sum_{a=1}^{M}\left\{\sum_{i=1}^{N_a}\mathrm{E}\left[\frac{LR_{i,a}\cdot RPC_{i,a}}{\sum_{b=1}^{M}\sum_{k=1}^{N_b} RPC_{k,b}}\right]\right\}\end{aligned} \tag{4-13}$$

$$\begin{aligned}\mathrm{Var}\left[LR_T\right] &= \mathrm{Var}\left[\frac{\sum_{a=1}^{M}\left(\sum_{i=1}^{N_a} LR_{i,a}\cdot RPC_{i,a}\right)}{\sum_{a=1}^{M}\sum_{i=1}^{N_a} RPC_{i,a}}\right] \\ &= \sum_{a=1}^{M}\sum_{b=1}^{M}\left\{\sum_{i=1}^{N_a}\sum_{j=1}^{N_b}\mathrm{Covar}\left[\frac{LR_{i,a}\cdot RPC_{i,a}}{\sum_{c=1}^{M}\sum_{k=1}^{N_c} RPC_{k,c}}, \frac{LR_{j,b}\cdot RPC_{j,b}}{\sum_{d=1}^{M}\sum_{k=1}^{N_d} RPC_{k,d}}\right]\right\}\end{aligned} \tag{4-14}$$

The evaluation of Eqs (4-11) - (4-14) is laborious if large building inventories are considered in the risk assessment. Thus, a sampling technique has been developed to

estimate the expected value and variance of the structural loss ratio efficiently. Sampling methods are often used in surveys to reduce cost and increase speed. Many techniques have been developed, such as simple random sampling, stratified random sampling, and systematic sampling. In this study, simple random sampling without replacement is utilized because the sampled buildings are selected from different sites. The estimator of total loss ratio for building occupancy class *a* can be computed as:

$$\begin{aligned} \widehat{LR}_{T,a} &= \frac{N_a \cdot \left(\frac{1}{n_a} \cdot \sum_{i=1}^{n_a} LR_{i,a} \cdot RPC_{i,a} \right)}{N_a \cdot \mathrm{E}\left[RPC_a \right]} \\ &= \frac{\sum_{i=1}^{n_a} LR_{i,a} \cdot RPC_{i,a}}{n_a \cdot \mathrm{E}\left[RPC_a \right]} \end{aligned} \tag{4-15}$$

where n_a is the number of buildings sampled in occupancy class *a*, where $n_a<N_a$. The expected value and variance of the estimator are evaluated by MCS. Finally, the estimate of the total loss ratio is:

$$\widehat{LR}_T = \frac{\sum_{a=1}^{M} \left\{ N_a \cdot \left(\frac{1}{n_a} \cdot \sum_{i=1}^{n_a} LR_{i,a} \cdot RPC_{i,a} \right) \right\}}{\sum_{a=1}^{M} N_a \cdot \mathrm{E}\left[RPC_a \right]} \tag{4-16}$$

The expected value and variance of the estimator are computed from MCS. The sampling error involved in this approximation will be evaluated next section.

4.4 Illustration of Building Inventory Loss Assessment

We consider an example consisting of 184 buildings in occupancy RES4 and 681 buildings in occupancy IND1, which are distributed over 216 census tracts in Shelby

County, TN. The buildings are subjected to a M_w 7 event on the Reelfoot Fault in the New Madrid Seismic Zone, with an epicenter approximately 41.5 km from downtown Memphis, and are assumed to be situated on Site Class D[1]. The numbers of RES4 and IND1 buildings in each census tract are shown in Figure 4-2 and Figure 4-3. Since information on the location of these buildings is not available, they are assumed to be randomly distributed in each tract.

The Atkinson and Boore (1995) attenuation relationship with aleatory uncertainty SD[$\log_{10}(S_a)$] equal to 0.3 is used to determine the ground motion intensity (in terms of spectral acceleration, S_a) at the location of each building. The results estimated from this approach are compared to the results computed from HAZUS-MH (MR4) in which this attenuation relationship is also available. The inter- and intra-event variabilities are equal to 34 and 66 percent, respectively, of the total variance, defined in Eq (3-13) (Lee *et al.*, 2000). The spatial correlation in ground motion intensity is defined by Eq (3-15), with the correlation distance equal to 50 km, as in the example presented in Section 4.2.

The lower and upper bound damage correlations (ρ_D = 0.0, 0.9) and the damage correlations computed from the model developed in the previous chapter are used in this analysis. The probability mass functions of structural and nonstructural replacement costs per RES4 building and per IND1 building in Figure 4-5 and Figure 4-6 are estimated from the histogram of the dollar exposure of the average single building, which is computed from the dollar exposure of all buildings in each tract divided by the number of buildings in each tract provided in HAZUS-MH (MR4). The structural repair costs for RES4 and IND1 occupancy classes are 13.6 and 15.7 percent of the structural and

[1]http://earthquake.usgs.gov/regional/ceus/products/download/docs/OFR_MemphisMaps.pdf

nonstructural replacement cost, respectively; these percentages are used in the structural loss assessment.

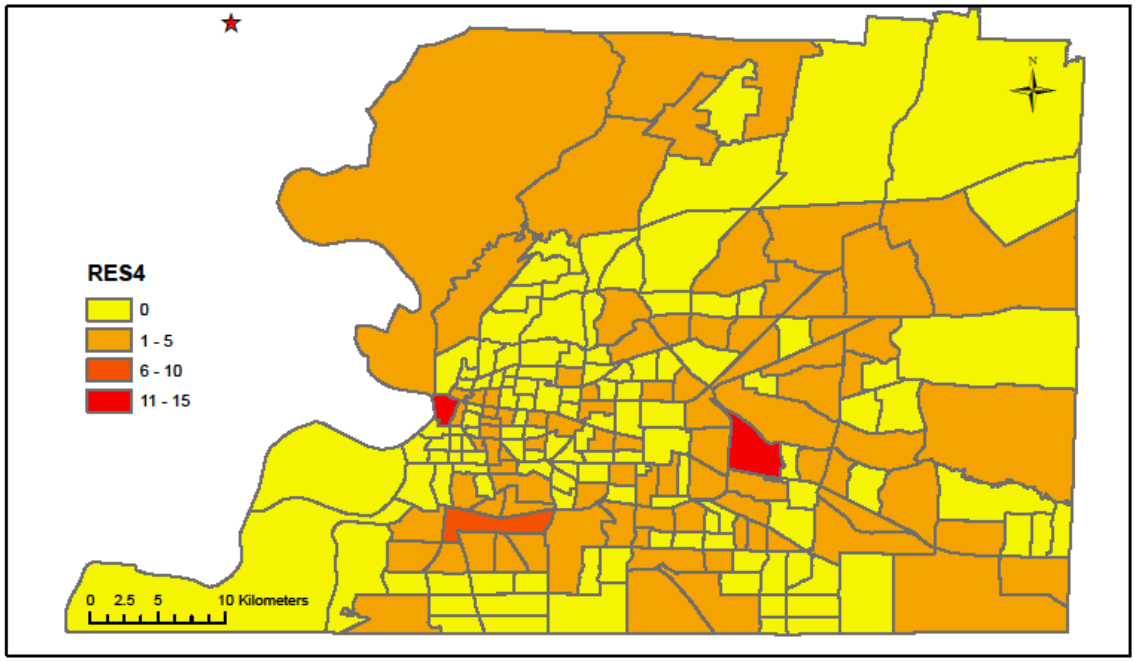

Figure 4-2 Location of 184 buildings with RES4 occupancy class in Shelby County, TN and the M_w 7 epicenter (star).

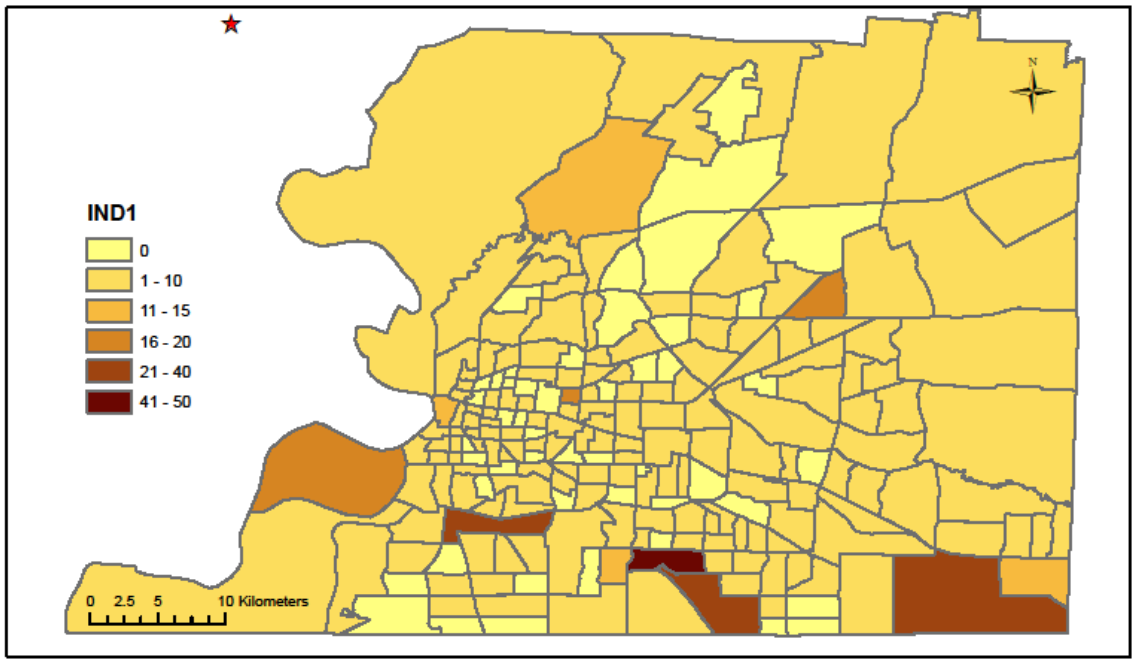

Figure 4-3 Location of 681 buildings with IND1 occupancy class in Shelby County, TN and the M_w 7 epicenter (star).

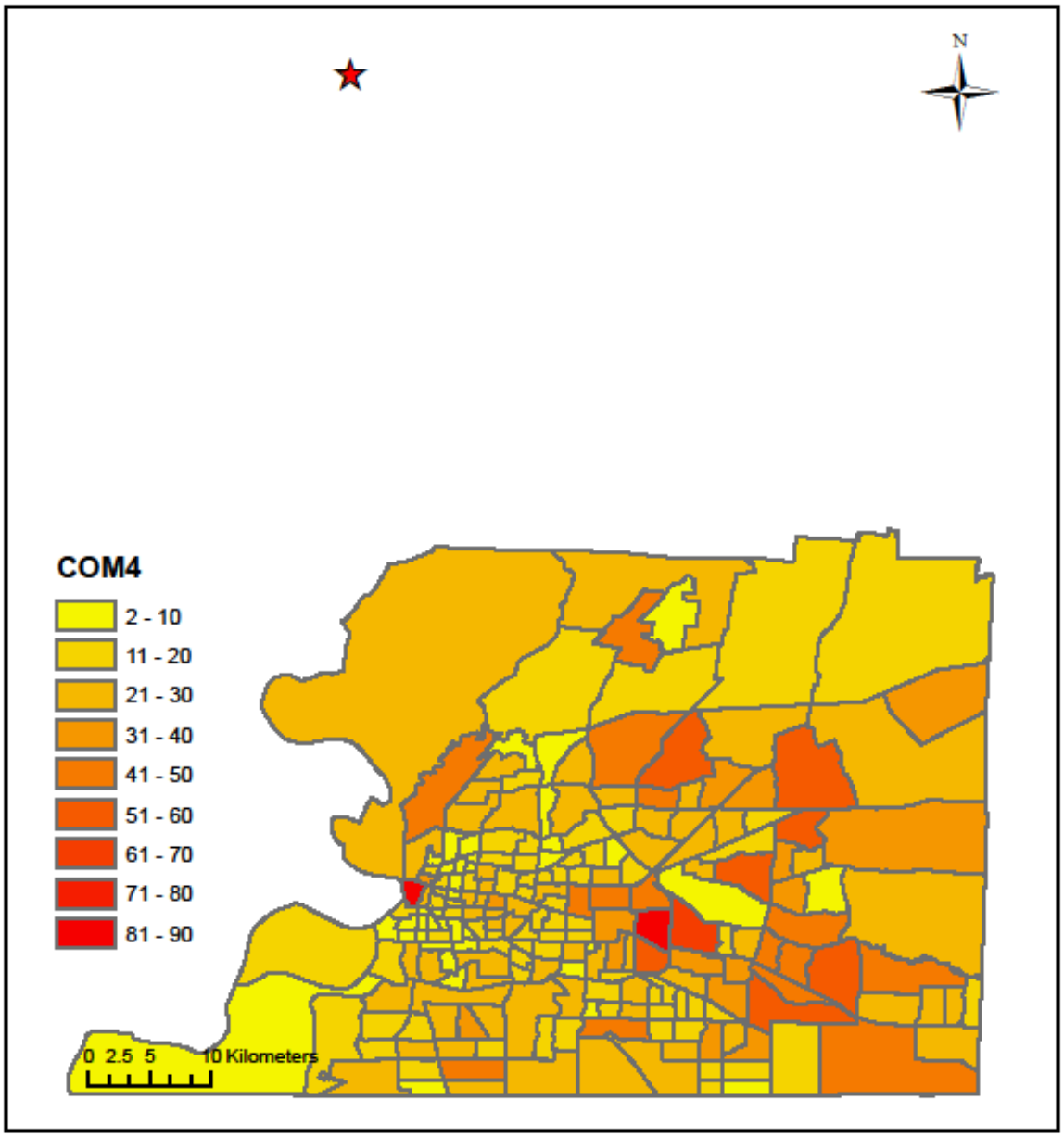

Figure 4-4 Location of 4,793 buildings with COM4 occupancy class in Shelby County, TN and the epicenter of M_w 7.7 event (star)[1].

[1] This particular figure will be used in Section 5.1.

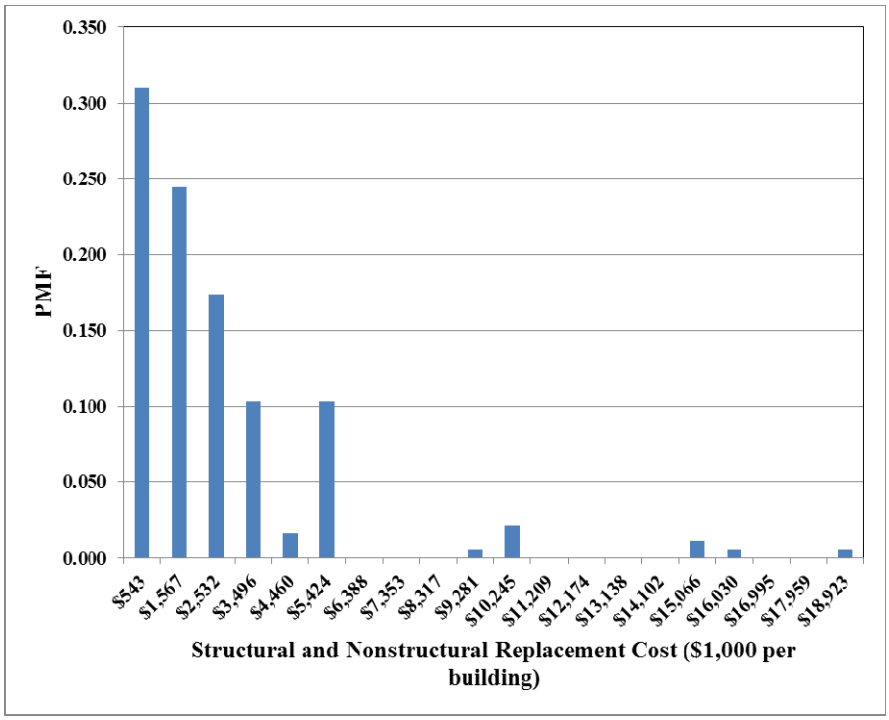

Figure 4-5 Probability mass function of the structural and nonstructural replacement cost for occupancy class RES4

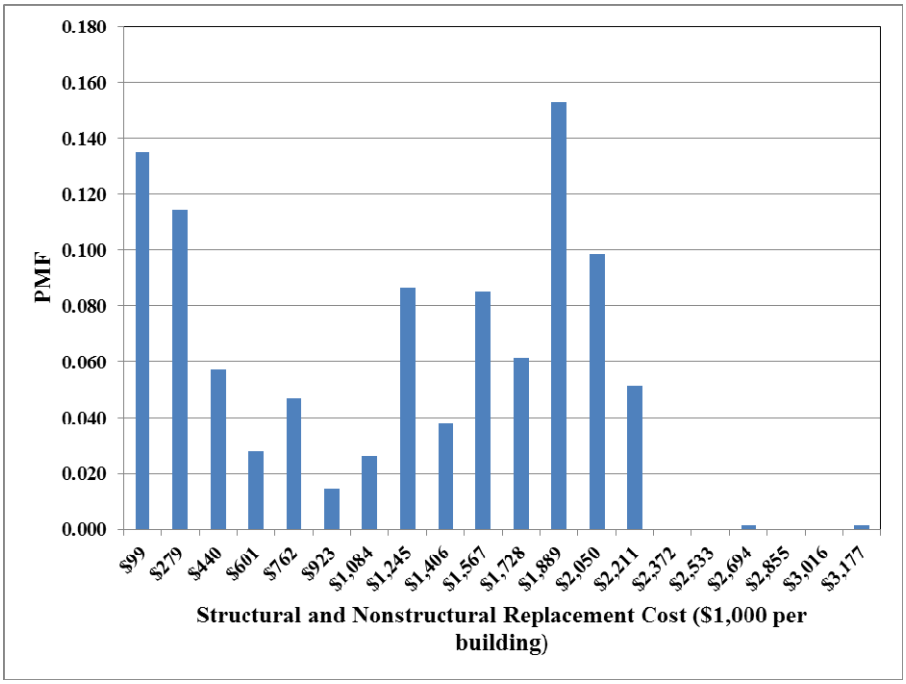

Figure 4-6 Probability mass function of the structural and nonstructural replacement cost for occupancy class IND1

Figure 4-7 shows the estimated structural loss ratio statistics of a single building in occupancy classes RES4 and IND1 as a function of epicentral distance. While the mean and standard deviation in building structural loss ratio decreases as the epicentral distance increases, as would be expected, the coefficient of variation increases with distance. This behavior is directly related to the different rates of decay of expectation and standard deviation of spectral displacement, on which damage depends, as a function of epicentral distance in Figure 4-8.

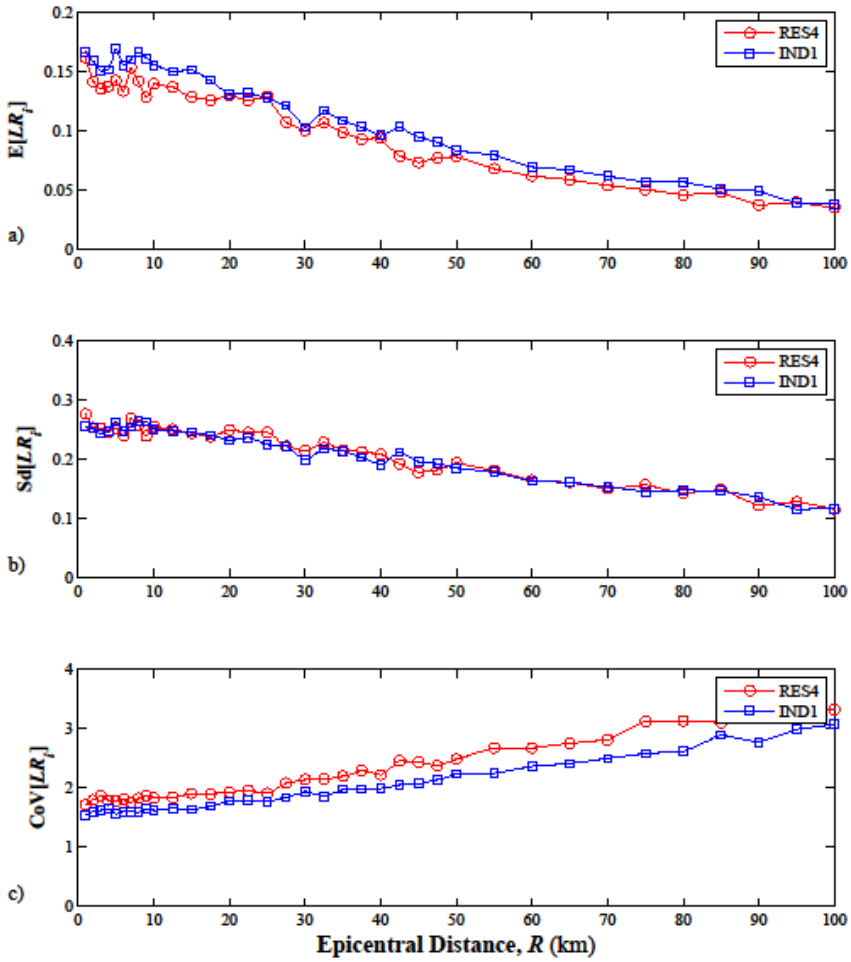

Figure 4-7 a) Expectation, b) standard deviation, and c) coefficient of variation of structural loss ratio of one RES4 building and one IND1 building

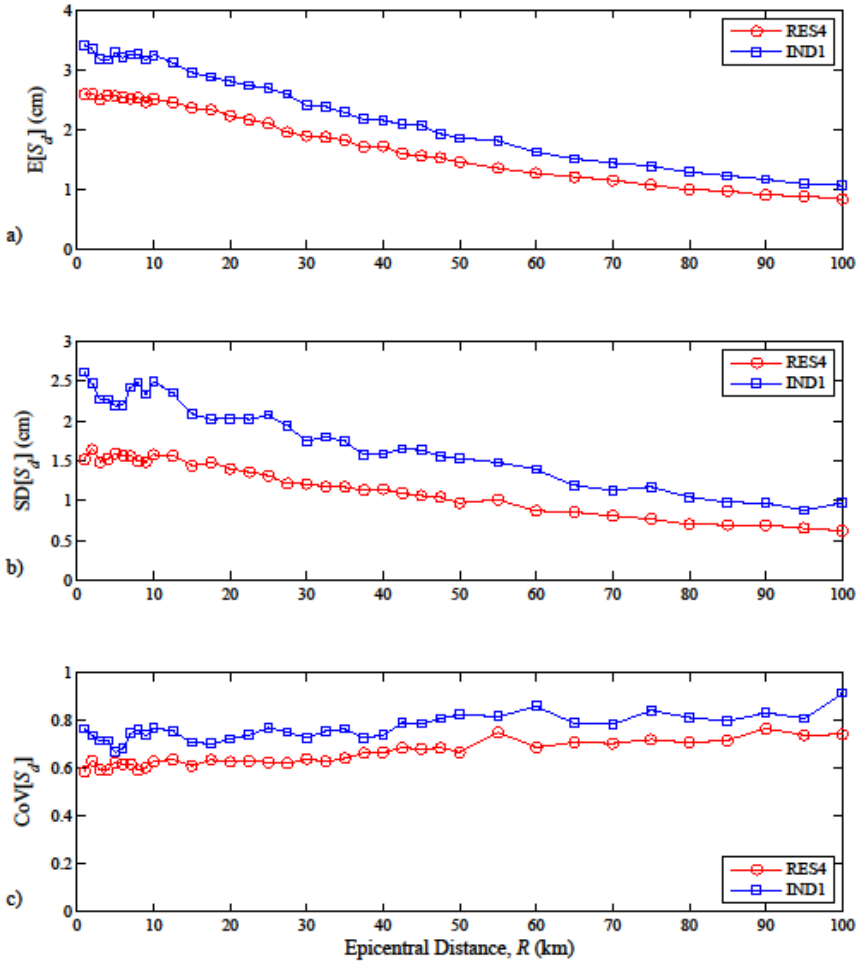

Figure 4-8 a) Expectation, b) standard deviation, and c) coefficient of variation of spectral displacement of one RES4 building and one IND1 building

The correlation in structural loss ratio due to the M_w 7 event on the Reelfoot Fault as a function of building separation, r_{ij}, is shown in Figure 4-9, Figure 4-10, and Figure 4-11 for occupancy RES4, IND1 and between RES4 and IND1, respectively. The estimated correlations in damage between pairs determined from Eq (3-26) lies between the lower and upper bound damage correlations. The structural loss ratio correlations are virtually parallel for the three damage correlations considered.

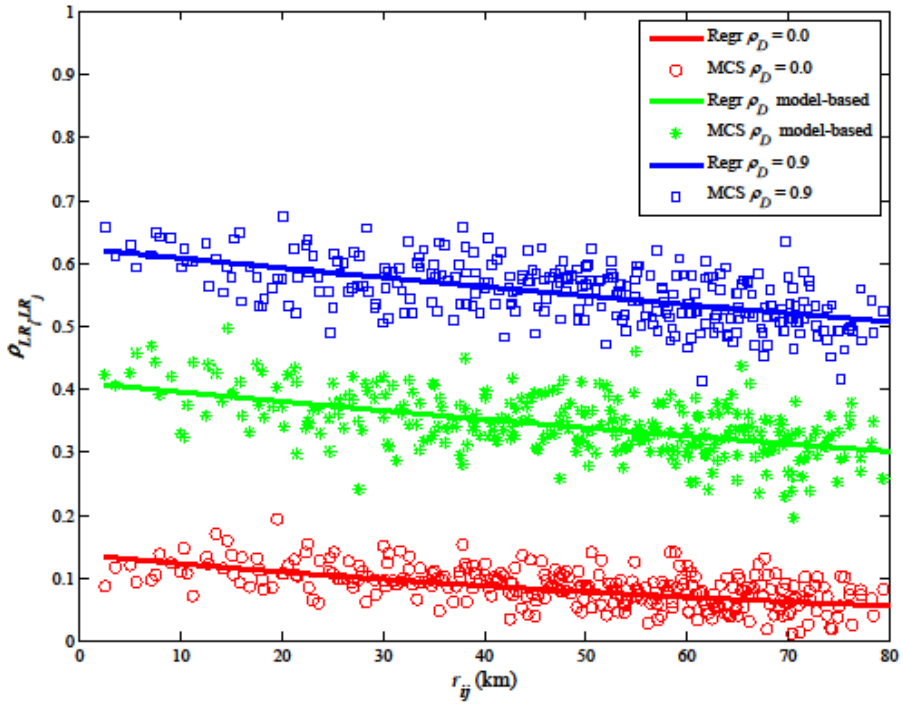

Figure 4-9 The correlation of structural loss ratio between pairs of buildings in class RES4 subjected to M_w 7 event.

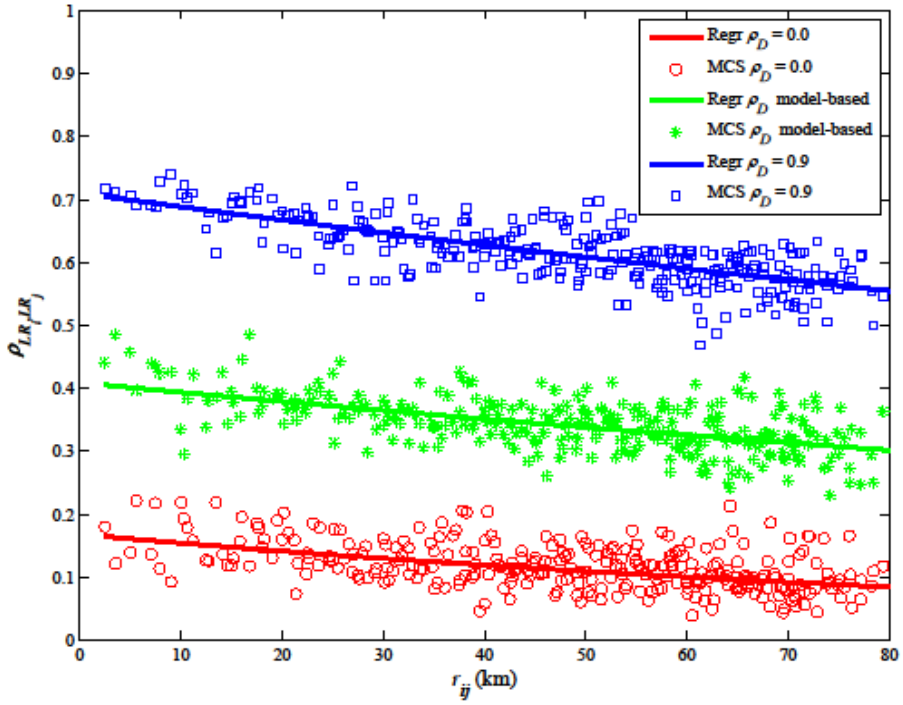

Figure 4-10 The correlation of structural loss ratio between pairs of buildings in class IND1 subjected to M_w 7 event.

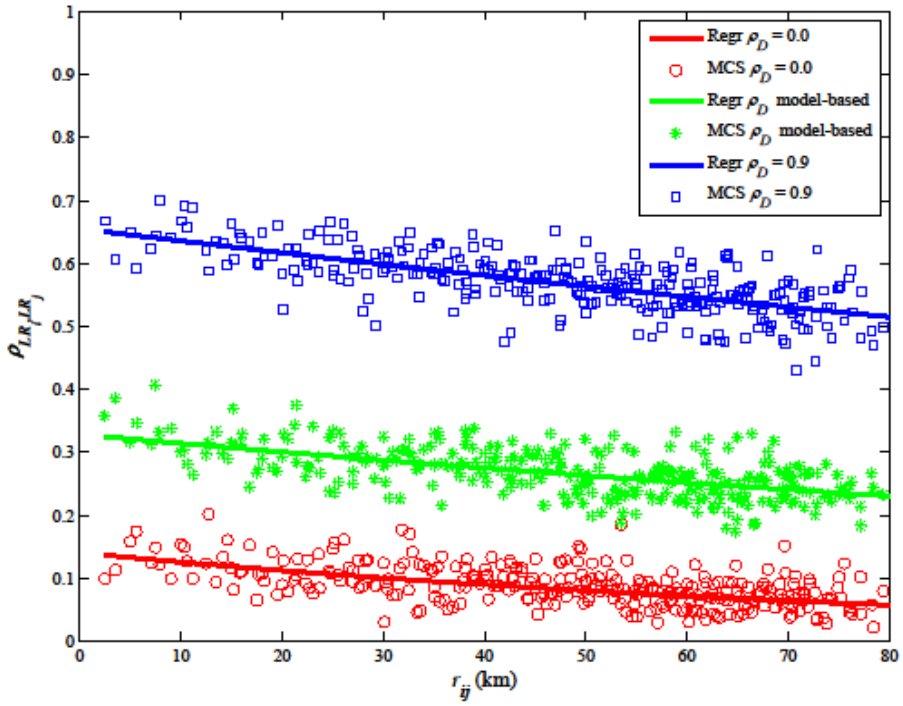

Figure 4-11 The correlation of structural loss ratio between pairs of buildings in classes RES4 and IND1 subjected to M_w 7 event.

Table 4-3, Table 4-4, and Table 4-5 illustrate the dependence of the loss ratio statistics estimated for occupancy classes RES4 and IND1 and damage correlations equal to 0.0, 0.9, and based on Eq (3-26), respectively, for various sample sizes. These estimates were obtained using the sampling procedure described in Section 4.3. The results show that a sample of 100 buildings is sufficiently accurate for estimating losses to populations of 184 RES4 and 681 IND1 buildings for all damage correlation cases because the estimates of the coefficients of variation are different from those for the full population by less than 10%. Note that 100 buildings for occupancy class RES4 are large number of the sample size, approximately 55 percent of the RES4 population. The necessary sample size depends on the level of damage correlation between buildings, and smaller samples may be sufficient if the damage correlation is weak. All subsequent

analyses in this study will be based on a 100-building sample size for each building occupancy class.

Table 4-3 Sample size of RES4 and IND1 occupancy class with damage correlation equal to 0.0

Sample Size (n_a)	RES4 (N_a = 184)			IND1 (N_a = 681)		
	ρ_D	0.0		ρ_D	0.0	
	$E[LR_{T,a}]$	$SD[LR_{T,a}]$	$CoV[LR_{T,a}]$	$E[LR_{T,a}]$	$SD[LR_{T,a}]$	$CoV[LR_{T,a}]$
20	0.0856	0.0788	0.9198	0.0926	0.0740	0.7990
50	0.0827	0.0608	0.7354	0.0895	0.0621	0.6939
100	0.0844	0.0530	0.6276	0.0899	0.0555	0.6181
200	0.0827*	0.0504*	0.6097*	0.0890	0.0550	0.6173
300	0.0855*	0.0523*	0.6124*	0.0945	0.0584	0.6176
700	0.0863*	0.0531*	0.6153*	0.0943$^+$	0.0564$^+$	0.5983$^+$

*Number of samples equal to number of population (184 buildings).
$^+$Number of samples equal to number of population (681 buildings).

Table 4-4 Sample size of RES4 and IND1 occupancy class with damage correlation equals 0.9

Sample Size (n_a)	RES4 (N_a = 184)			IND1 (N_a = 681)		
	ρ_D	0.9		ρ_D	0.9	
	$E[LR_{T,a}]$	$SD[LR_{T,a}]$	$CoV[LR_{T,a}]$	$E[LR_{T,a}]$	$SD[LR_{T,a}]$	$CoV[LR_{T,a}]$
20	0.0847	0.1293	1.5264	0.0957	0.1437	1.5017
50	0.0827	0.1278	1.5466	0.0879	0.1314	1.4956
100	0.0906	0.1405	1.5507	0.0987	0.1542	1.5620
200	0.0810*	0.1186*	1.4638*	0.0872	0.1267	1.4528
300	0.0758*	0.1125*	1.4845*	0.0827	0.1244	1.5038
700	0.0857*	0.1299*	1.5161*	0.0923$^+$	0.1367$^+$	1.4817$^+$

*Number of samples equal to number of population (184 buildings).
$^+$Number of samples equal to number of population (681 buildings).

Table 4-5 Sample size of RES4 and IND1 occupancy class with model-based damage correlation (Eq (3-26))

Sample Size (n_a)	RES4 (N_a = 184)			IND1 (N_a = 681)		
	ρ_D	Model-Based		ρ_D	Model-Based	
	$E[LR_{T,a}]$	$SD[LR_{T,a}]$	$CoV[LR_{T,a}]$	$E[LR_{T,a}]$	$SD[LR_{T,a}]$	$CoV[LR_{T,a}]$
20	0.0802	0.1016	1.2670	0.0881	0.1011	1.1473
50	0.0834	0.1017	1.2199	0.0884	0.0976	1.1042
100	0.0791	0.0913	1.1541	0.0892	0.0962	1.0789
200	0.0865*	0.0994*	1.1480*	0.0926	0.1012	1.0929
300	0.0824*	0.0957*	1.1620*	0.0896	0.0932	1.0400
700	0.0805*	0.0985*	1.2229*	0.0886$^+$	0.0973$^+$	1.0975$^+$

*Number of samples equal to number of population (184 buildings).
$^+$Number of samples equal to number of population (681 buildings).

The structural loss ratios for all RES4 buildings, all IND1 buildings and the two classes combined are shown in Table 4-6 and Table 4-7. One would expect that the expected values for these cases would be approximately equal (subject to sampling error in the simulation process leading to these estimates) because the computation of the expected value of the total loss in Eq (4-1) does not require knowledge of the covariance in losses. The coefficient of variation for correlation damage model is consistent with the correlation damage curves in Figure 4-9, Figure 4-10, and Figure 4-11.

When comparing the results of the total losses in Table 4-6 and Table 4-7 to the expected loss to one building, which was presented in Figure 4-7, we find that the total loss ratio to occupancy classes RES4 and IND1 is approximately equal to the individual loss ratio at epicentral distances of 42.5 and 45 km, respectively. The centroids of buildings in RES4 and IND1 classes are at epicentral distances of 42.6 km and 44.6 km, respectively. Thus, one may estimate the expected value of total loss to building inventories from individual building data if the centroids of their locations are known. However, estimating the second order parameters, such as standard deviations or coefficients of variation, is also required to compute the uncertainties in the losses of all building inventories and their probable maximum losses.

When these results are compared to the results computed by HAZUS-MH (MR4), which are presented in Table 4-8, we find that the differences are on the order of 10 percent for RES4 and 25 percent for IND1. Two factors account for these differences: 1) the model presented herein evaluates the individual losses from the random locations of buildings in each tract and aggregates all losses, while HAZUS-MH computes the individual loss at the centroid of each tract and multiplies that loss by the number of

buildings in each tract to estimate the total loss; and 2) the model herein uses the capacity spectrum method (CSM) to determine spectral displacements, from which it estimates the damage state probability, while HAZUS-MH utilizes a method defined in ATC-40 (1996). The main difference between these two methods is that the seismic demand spectrum in the CSM is reduced for building ductility resulting from inelastic behavior of the building (Fajfar, 1999), while the demand spectrum in the ATC-40 method is reduced using effective damping to account for inelastic action.

Table 4-6 The total structural loss ratio considering RES4 and IND1 occupancy classes and subjected to a M_w 7 event in Shelby County, TN (n_a = 100)

Occupancy Class	**RES4**			**IND1**		
Structural Loss Ratio	**Damage Correlation, ρ_D**			**Damage Correlation, ρ_D**		
	0.0	**Model-Based**	**0.9**	**0.0**	**Model-Based**	**0.9**
E[LR_T]	0.0844	0.0791	0.0906	0.0899	0.0892	0.0987
SD[LR_T]	0.0530	0.0913	0.1405	0.0555	0.0962	0.1542
CoV[LR_T]	0.6276	1.1541	1.5507	0.6181	1.0789	1.5620

Table 4-7 The total structural loss ratio considering both occupancy classes and subjected to a M_w7 event in Shelby County, TN (n_a = 100)

Occupancy Class	**RES4 + IND1**		
Structural Loss Ratio	**Damage Correlation, ρ_D**		
	0.0	**Model-Based**	**0.9**
E[LR_T]	0.0861	0.0827	0.0940
SD[LR_T]	0.0498	0.0863	0.1470
C0V[LR_T]	0.5782	1.0435	1.5635

Table 4-8 The total structural loss ratio subjected to a M_w7 event in Shelby County, TN computed from HAZUS-MH (MR4) software

Occupancy Class	RES4	IND1	RES4 + IND1
E[LR_T]	0.0758	0.1175	0.1042

4.5 Summary

Procedures to determine the direct (monetary) structural loss ratios for inventories of buildings were presented. First, an approach to compute mean value and variance of the loss of single building occupancy class was summarized. The equations are complex because one occupancy class can be comprised of many structural types. This variation in building types is included by considering the distribution of structural types in each occupancy class. Second, an approach to determine correlation in structural losses between same-occupancy and different-occupancy building classes, which accounts for correlations in demand (ground motion) and performance, and a method for aggregating these losses within building inventories were presented. Since the computational effort involved in determining pairwise correlations in losses for every building and aggregating those losses in a large inventory is unmanageable, an approximate method aimed at reducing this numerical effort was developed using sampling theory. It was shown that this sampling method yielded results of a sufficient accuracy that they could be used in subsequent loss estimation for building inventories.

An example involving two occupancy classes was presented into two parts: 1) to determine an appropriate sample size so that the losses for a building inventory could be estimated without exhaustive denumeration, and; 2) to compare estimates losses with similar estimates from HAZUS-MH. In the first part, it was found that using samples of one hundred buildings for each occupancy class is sufficient to estimate the mean value and standard deviation of the structural loss ratio for spatially distributed building inventories accurate. In the second part, it was confirmed that correlations in demand and performance do not affect the mean of total structural loss ratio, but strongly influence

the uncertainty (variance) of the loss. Thus, when damage correlation is neglected, the standard deviation in loss may be underestimated by a factor of as much as three, with a corresponding change in the estimation of probable maximum loss, which will be described in the next chapter.

CHAPTER 5

RISK ASSESSMENT OF BUILDINGS AND BUILDING INVENTORIES DUE TO STRUCTURAL DAMAGE

This chapter illustrates risk assessments of buildings and building inventories using the methods introduced in Chapter 4, and the scenario earthquake analysis (SEA) and probabilistic seismic hazard analysis (PSHA) summarized in Chapter 3.

Section 5.1 presents a scenario earthquake risk assessment which utilizes the approach presented in the previous chapter directly. In contrast, the probabilistic seismic risk analysis (PSRA) in Section 5.2 reflects the spectrum of possible earthquakes that can affect a study area. Losses from each seismic hazard approach can be determined from the method developed in Chapter 4. Section 5.3 introduces a decision metric – the Probable Maximum Loss, or PML - that often is used in the insurance industry for determining the premium that insurers and reinsurers should charge policyholders and is affected by the correlation structure of seismic demands, response and damage, and individual losses.

5.1 Scenario Earthquake Risk Assessment

Scenario Earthquake Risk Assessment (SERA) provides a method for estimating the total structural loss ratio for a building inventory exposed to a single seismic event. In contrast to considering an arbitrary event, as in Chapter 4, the scenario earthquake in this section will be chosen based on a seismic de-aggregation analysis.

A building inventory with three occupancy classes consisting of 184 RES4, 681 IND1, and 4793 COM4 buildings in Shelby County, TN is considered. The total number of buildings is 5,658, and their locations are shown in Figure 4-2, Figure 4-3, and Figure 4-4 for occupancies RES4, IND1, and COM4, respectively. Since the estimation of the losses for all 5,658 buildings individually would be excessively time-consuming and would require large computer resources, the sampling technique described in the previous chapter is implemented. One hundred sample buildings from each class are randomly selected. The loss estimates are obtained by Monte Carlo simulation with 10,000 repetitions.

The Atkinson and Boore (1995) attenuation relationship with aleatory uncertainty equal to 0.3 is used to determine the ground motion intensity at the location of each sampled building. (A sensitivity analysis involving other ground motion attenuation relationships [e.g. Atkinson and Boore (2006) and Campbell (2003)] will be performed in Chapter 7.) The inter- and intra-event variability (cf Eq 3-13) is assumed to equal 34 and 66 percent of the total variance (Lee *et al.*, 2000), respectively. All buildings in this study area are on Site Class D[1]. The ground motion correlation distance is assumed to equal 50 km, as in the previous chapter.

The lower and upper bound damage correlations (equi-damage correlation ρ_D = 0.0 or 0.9), and the model-based damage correlation (cf Eq 3-26) are considered in this analysis. The probability mass functions of structural and nonstructural replacement cost for each RES4 building in Figure 4-5, IND1 building in Figure 4-6, and COM4 building are shown in Figure 5-1. These PMFs are estimated from the histogram of the dollar

[1]http://earthquake.usgs.gov/regional/ceus/products/download/docs/OFR_MemphisMaps.pdf

exposure of the average single building, which is computed from the dollar exposure of all buildings in each tract divided by the number of buildings in each tract provided in HAZUS-MH (MR4). The structural repair cost is 13.6, 15.7, and 19.2 percent of structural and nonstructural replacement cost for RES4, IND1, and COM4 occupancy classes, respectively.

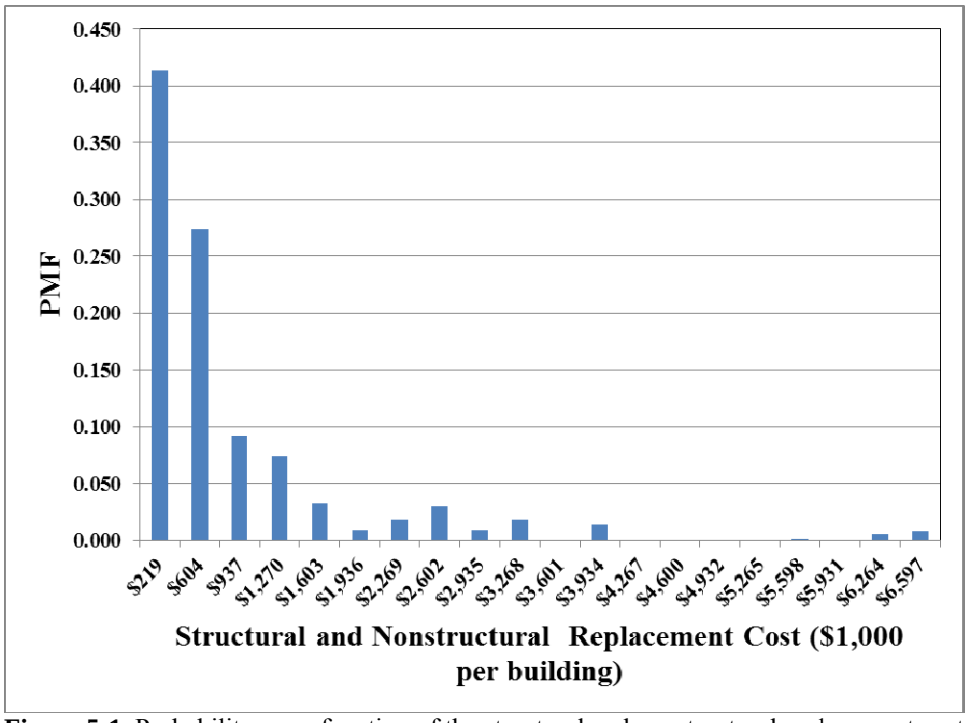

Figure 5-1 Probability mass function of the structural and nonstructural replacement cost for occupancy class COM4

The earthquake scenarios for Shelby County are selected by de-aggregation. Figure 5-2 through Figure 5-5 show the de-aggregation results for S_a (T = 1.0 s) for return periods of 4,975, 2,475, 975, and 72 years from the USGS 2008 Interactive De-aggregations website[1]. The maximum probable earthquakes (MPE) from these return periods are selected as the scenario events. Interestingly, the dominant contributing earthquake at all return periods is from the same moment magnitude 7.7 event, located

[1]https://geohazards.usgs.gov/deaggint/2008/

along the central trace of the Reelfoot faults in Figure 5-2 at latitude 35.74° and longitude -90.10°, as shown in Figure 4-4. Thus, this earthquake event is considered for the scenario earthquake analysis.

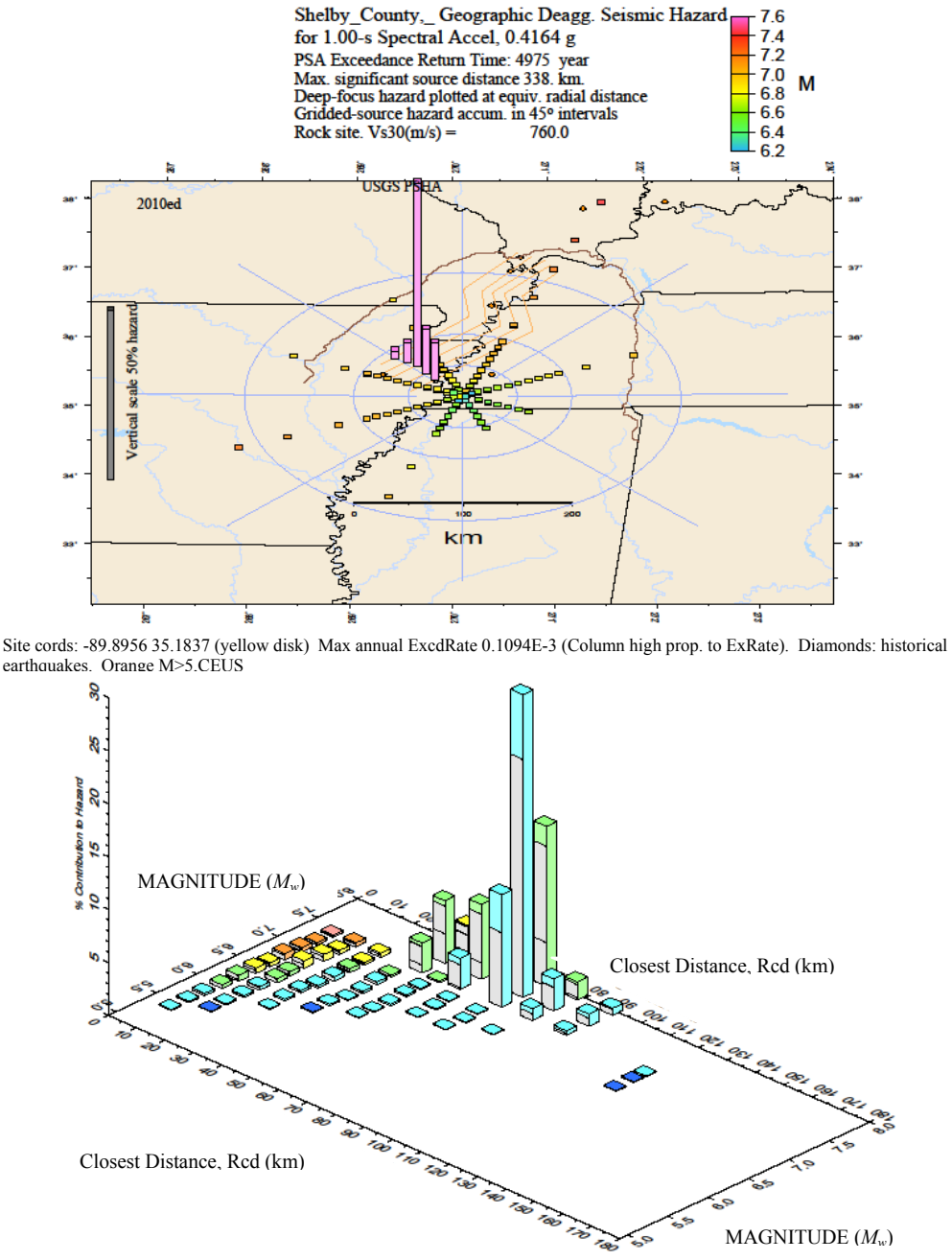

Figure 5-2 Deaggreation of S_a (T= 1.0 s) for 4975-year return period (1% probability of exceedence in 50 years) (from USGS website)

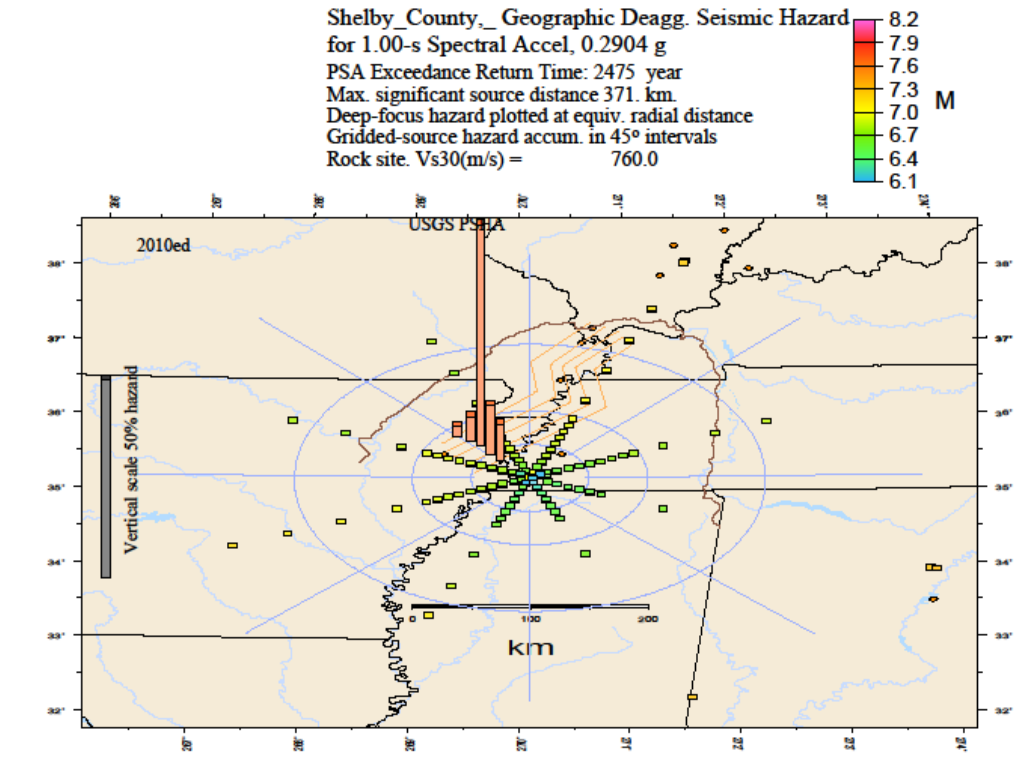

Site cords: -89.8956 35.1837 (yellow disk) Max annual ExcdRate 0.2269E-3 (Column high prop. to ExRate). Diamonds: historical earthquakes. Orange M>5.CEUS

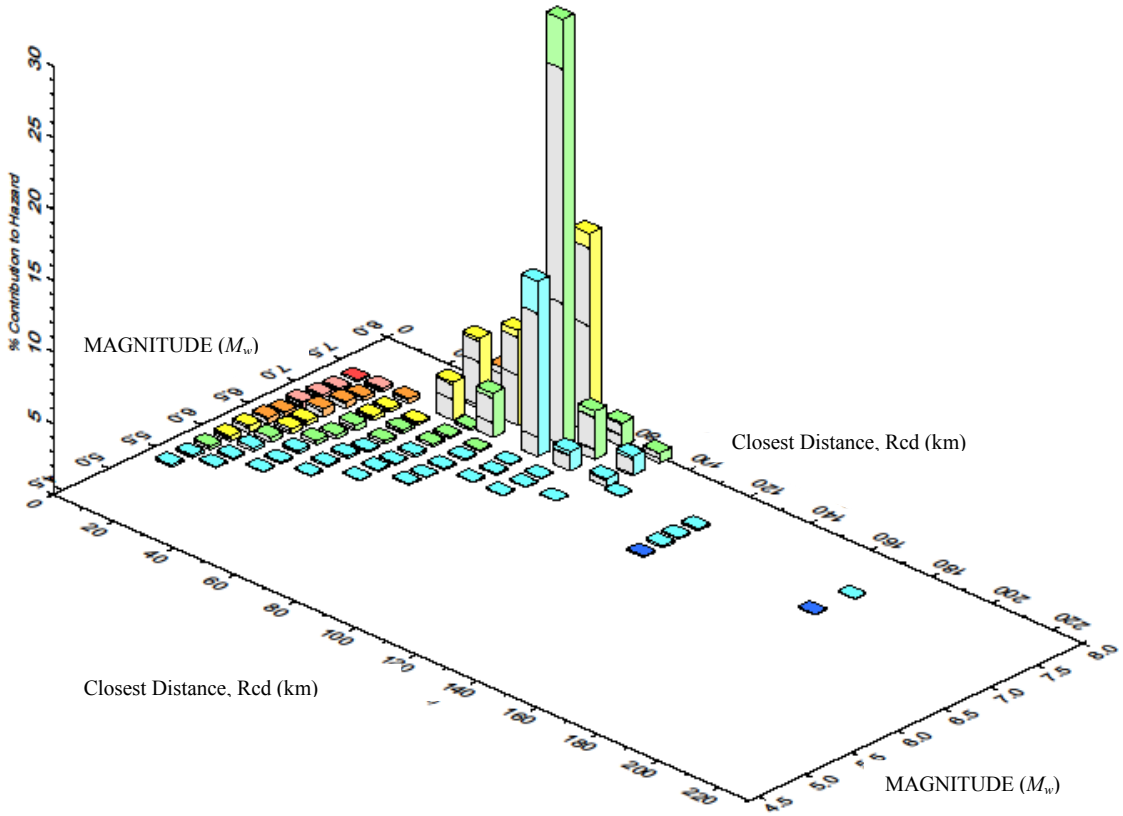

Figure 5-3 Deaggreation of S_a (T= 1.0 s) for 2475-year return period (2% probability of exceedence in 50 years) (from USGS website)

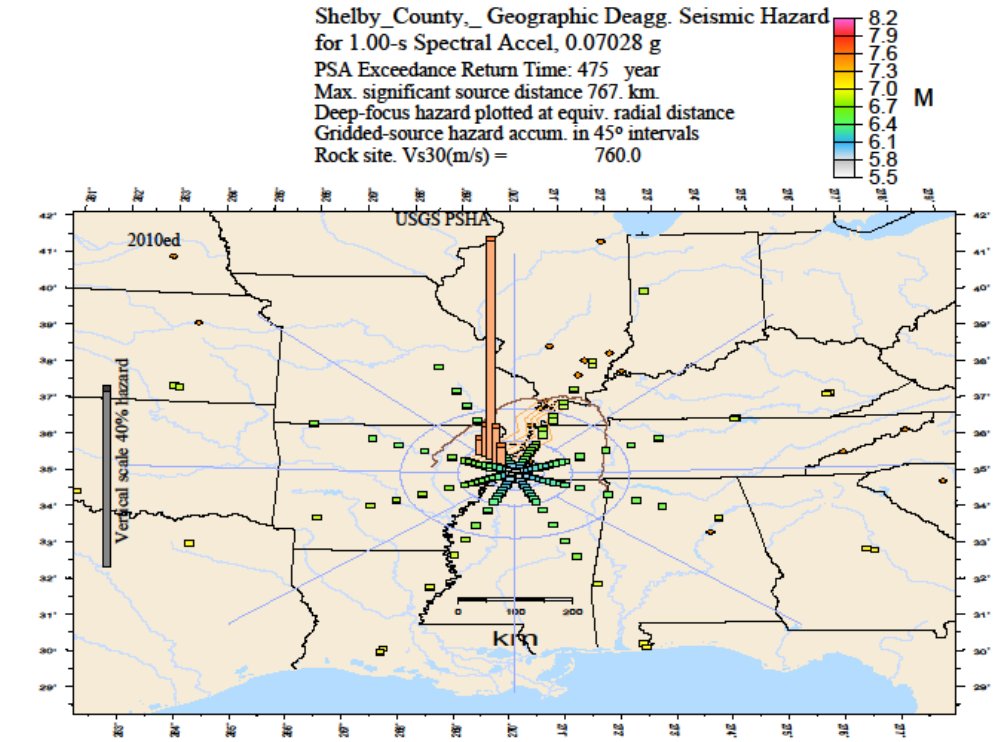

Site cords: -89.8956 35.1837 (yellow disk) Max annual ExcdRate 0.1040e-2 (Column high prop. to ExRate). Diamonds: historical earthquakes. Orange M>5.CEUS

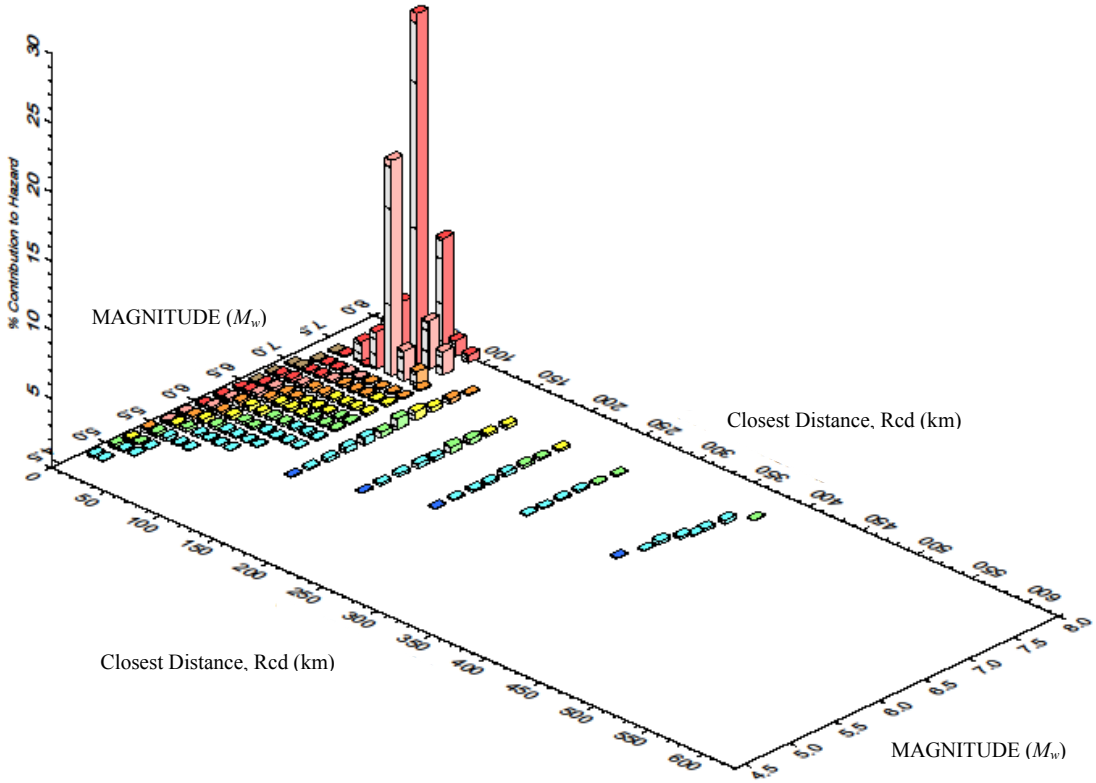

Figure 5-4 Deaggreation of S_a (T= 1.0 s) for 475-year return period (10% probability of exceedence in 50 years) (from USGS website)

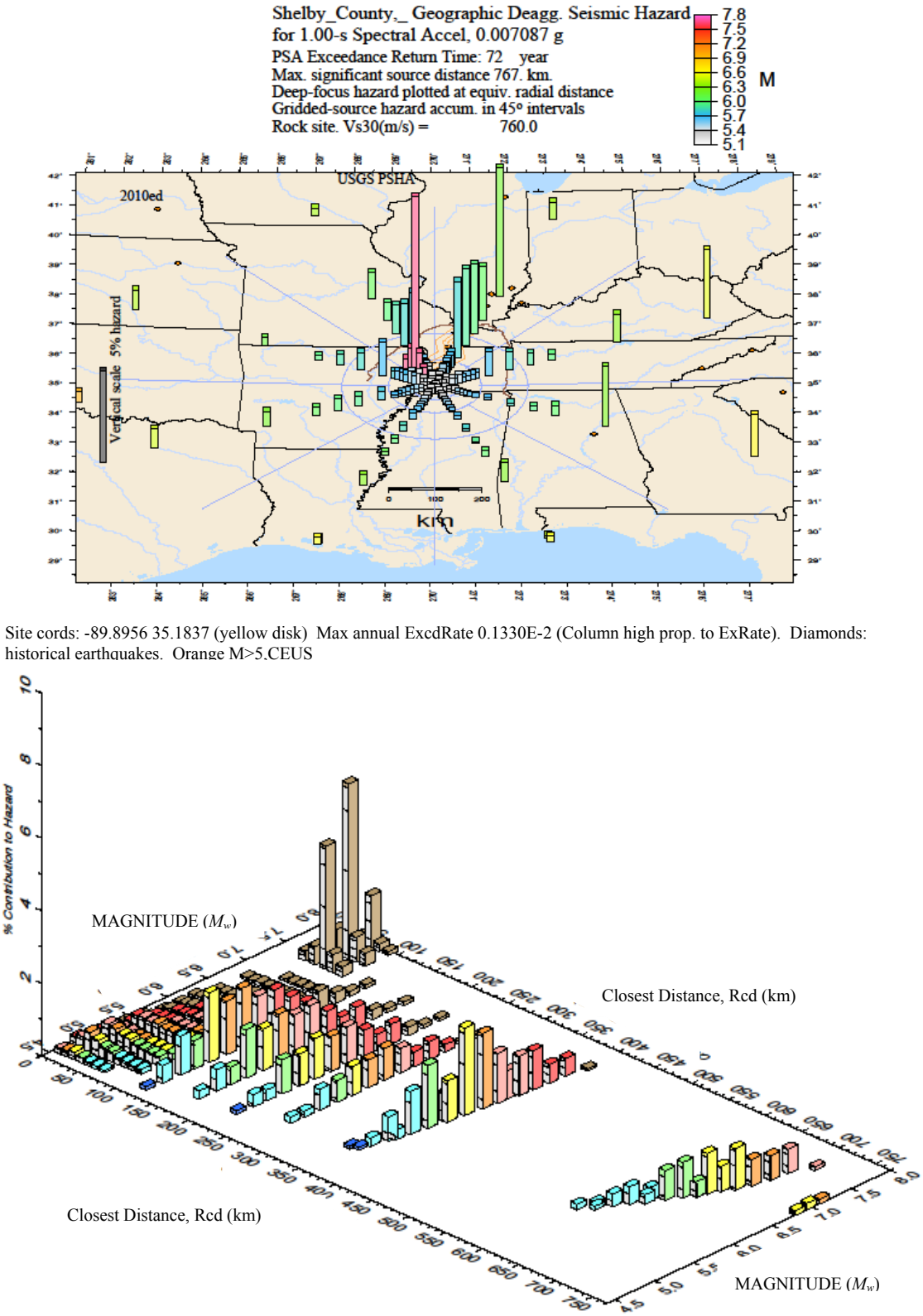

Site cords: -89.8956 35.1837 (yellow disk) Max annual ExcdRate 0.1330E-2 (Column high prop. to ExRate). Diamonds: historical earthquakes. Orange M>5.CEUS

Figure 5-5 Deaggreation of S_a (T= 1.0 s) for 72-year return period (50% probability of exceedence in 50 years) (from USGS website)[1]

[1] This particular figure will be used in Section 5.2.

The total structural loss ratios for each occupancy class separately are shown in Table 5-1 and for all classes combined in Table 5-2. The means and standard deviations of the loss ratio for each occupancy class are slightly different. Since the repair ratios of all occupancies are quite similar for all damage states except the "extensive" damage state of RES2, shown in Table 4-2, this implies that the structural performance of these occupancy classes in this scenario event would be similar for buildings in Shelby County, TN. The coefficients of variation for the cases that include both correlations in demand and damage can be twice as large as those for the cases that consider only correlation in demand. Recall that previous studies that have considered correlation considered only correlation in demand. Table 5-3 illustrates the total loss ratio in which all losses for each occupancy class and all classes are statistically independent. The variance of the loss is caused from uncertainties associated with ground motion attenuation, building response, building type, replacement cost, and buildings location. From the results presented in Table 5-1 through Table 5-3, the contributions of spatial correlation in ground motion and damage for the upper bound case (ρ_D = 0.9) are 15 and 80 percent of the total variance of the total loss ratio, respectively. Interestingly, the coefficient of variation of the losses for the model-based damage correlation is equal to the average of the coefficients of variation of the losses using the upper and lower bound damage correlations. This results from the assumed parameters in the damage correlation models (i.e. coefficients β_{ε}, β_{BT_i,BT_j}, and β_{BT_i,BT_j}, etc.). An examination of those parameters that most affect the variance in the losses will be deferred to the parameter sensitivity analysis in Chapter 7.

Table 5-1 Total structural loss ratio for each occupancy class in Shelby County, TN exposed to M_w 7.7 earthquake event

Occupancy Class	184 RES4			4,793 COM4			681 IND1		
Structural Loss Ratio	Damage Correlation, ρ_D			Damage Correlation, ρ_D			Damage Correlation, ρ_D		
	0.0	Based-Model	0.9	0.0	Based-Model	0.9	0.0	Based-Model	0.9
E[$LR_{T,a}$]	0.1114	0.1147	0.1111	0.1203	0.1227	0.1214	0.1297	0.1306	0.1297
SD[$LR_{T,a}$]	0.0687	0.1260	0.1576	0.0727	0.1202	0.1569	0.0780	0.1303	0.1721
CoV[$LR_{T,a}$]	0.6164	1.0984	1.4189	0.6042	0.9794	1.2928	0.6016	0.9979	1.3267

Table 5-2 Total structural loss ratio for all occupancy classes in Shelby County, TN exposed to M_w 7.7earthquake event

Structural Loss Ratio	Damage Correlation, ρ_D		
	0.0	Based-Model	0.9
E[LR_T]	0.1209	0.1233	0.1213
SD[LR_T]	0.0723	0.1208	0.1583
CoV[LR_T]	0.5984	0.9800	1.3044

Table 5-3 Total structural loss ratio where all losses are statistically independent

Structural Loss Ratio	184 RES4	4,793 COM4	681 IND1	All Classes
E[LR_T]	0.1069	0.1229	0.1325	0.1174
SD[LR_T]	0.0330	0.0362	0.0271	0.0200
CoV[LR_T]	0.3090	0.2949	0.2042	0.1705

The effect of damage correlation on the probability density function of the total structural loss ratio for occupancies RES4, COM4, IND1 and all occupancies combined are illustrated in Figure 5-6, Figure 5-7, Figure 5-8, and Figure 5-9. It is noted that these density functions are computed from histograms of loss ratio in which the bin sizes equal 0.05. Figure 5-6 through 5-9 show that damage correlation affects the upper tail behavior of the loss ratio distribution. As the correlation becomes larger, the probability density

function becomes more strongly skewed in the positive direction. The positive skewness implies that the probability of higher losses is underestimated when the damage correlation is ignored. For instance in Figure 5-9, the likelihood of the total loss ratio exceeding 0.3 when considering damage correlation is 0.09, while the comparable likelihood is 0.01 when damage correlation is neglected.

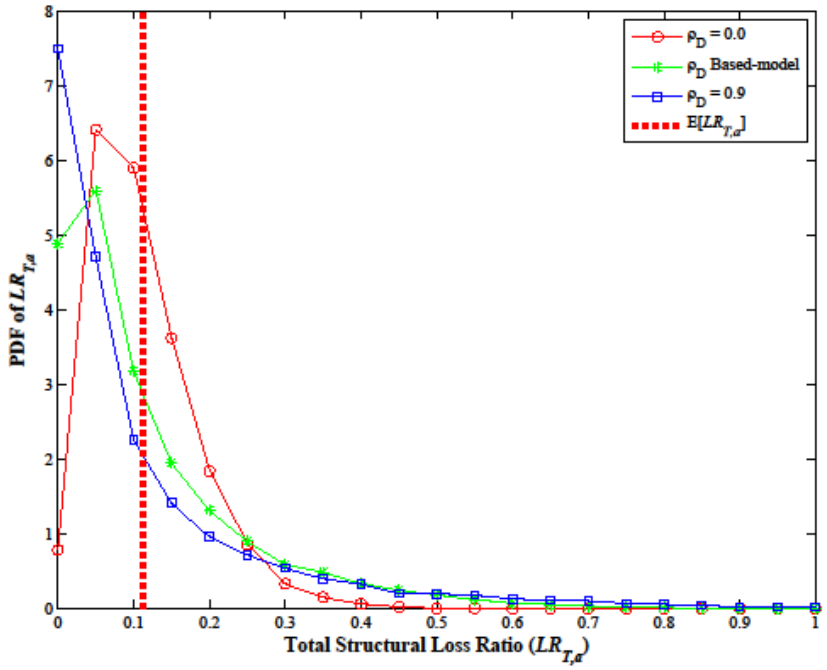

Figure 5-6 Probability density function of total structural loss ratio for RES4 occupancy**.**

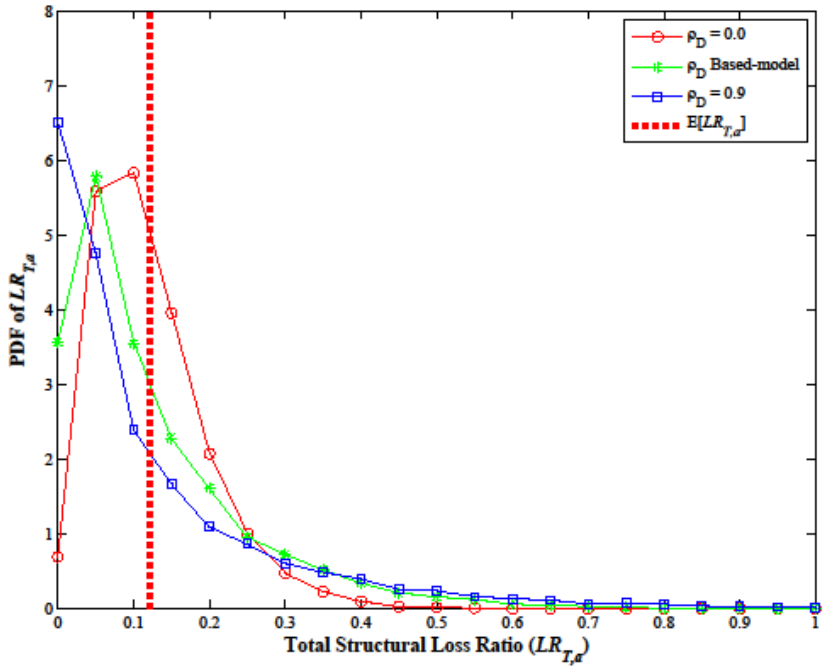

Figure 5-7 Probability density function of total structural loss ratio for COM4 occupancy**.**

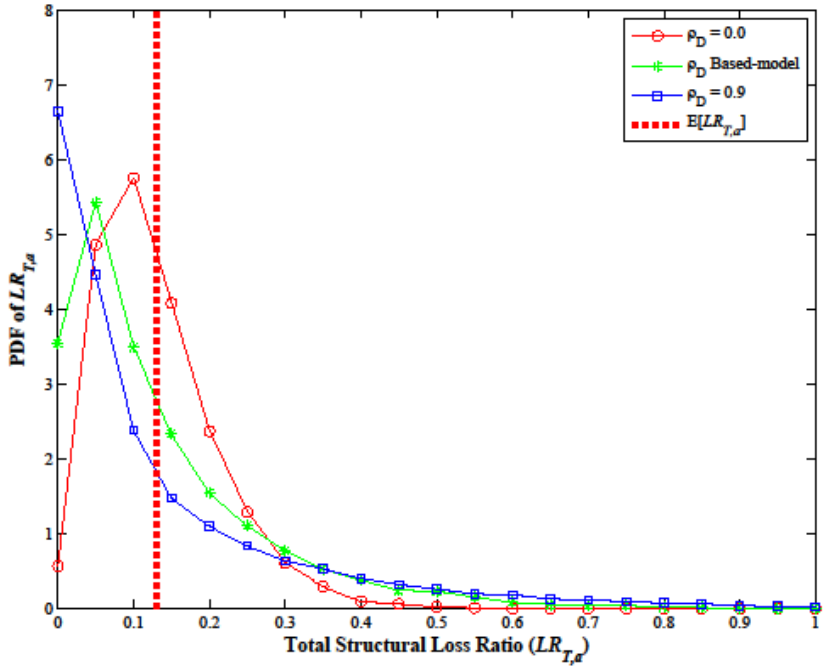

Figure 5-8 Probability density function of total structural loss ratio for IND1 occupancy**.**

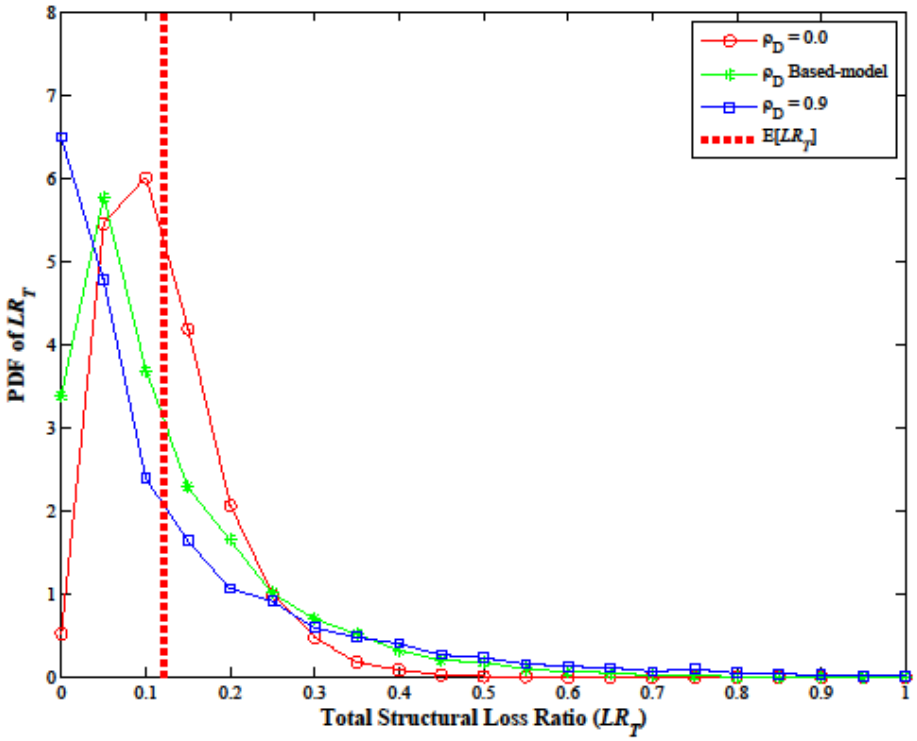

Figure 5-9 Probability density function of total structural loss ratio for all occupancies**.**

5.2 Probabilistic Seismic Risk Assessment

A Probabilistic Seismic Risk Assessment (PSRA) for spatially distributed building inventories estimates the structural loss ratio caused from all possible earthquakes occurring in a region. The loss resulting from each earthquake is computed using a method similar to that used for method to SERA. However, the moment magnitude and epicenter of the earthquake and its resulting intensity are treated as probabilistic instead of deterministic. Since the SERA is a conditional analysis, the method to evaluate the probability density function of the losses in the SERA has to be extended to determine the probability of exceedence of the loss. The seismic intensity from hazard curves provided in USGS website cannot be used to estimate risk to spatially distributed building inventories because of loss of spatial variability of demand intensity

over a region in the procedure of aggregating the relative contributions of different earthquakes in PSHA (Adachi, 2007; Lee, 2007). The mean annual frequency of exceedence of a specified level, *y*, of seismic intensity, $\lambda_{Y>y}$ (cf 3-17) is modified from double integration to double summation, since some of the probability of the moment magnitude and epicenter provided in the *National Seismic-Hazard Maps: Documentation June 1996* and its updated documentation in 2002 (Frankel *et al.*, 1996; Frankel *et al.*, 2002) are discrete functions.

The mean annual frequency of exceeding a specified loss, *l*, of the total structural loss ratio, $\lambda_{LR_T>l}$, (cf Eq 3- 17) is:

$$\lambda_{LR_T>l} = \sum_{i=1}^{N_s} \nu_i \left(M_{w_i} > m_{\min} \right) \cdot \sum_{j=1}^{N_{M_w}} \sum_{s=1}^{N_{Ep}} P\left[LR_T > l \mid m_j, e_s \right] \cdot P\left[M_{w_i} = m_j \right] \cdot P\left[Ep_i = e_s \right] \tag{5-1}$$

where N_s= the number of earthquake sources; $\nu_i \left(M_{w_i} > m_{\min} \right)$ is the mean annual rate of occurrence of earthquake magnitude greater than m_{min} from source *i*; $P\left[LR_T > l \mid m_j, e_s \right]$ is the probability that the total structural loss ratio exceeds *l* given an earthquake with magnitude m_j and epicenter e_s; $P\left[M_{w_i} = m_j \right]$ is the probability mass function of the magnitude of earthquake occurring at source *i*; and $P\left[Ep_i = e_s \right]$ is the probability that the epicenter of the earthquake occurrs at source *i*.

The same distributed building inventory, and parameters used in the previous section are considered to illustrate the PSRA. The de-aggregation results for S_a (T = 1.0 s) for 50% probability of exceedence in 50 years (72-year return period) computed from

USGS 2008 Interactive De-aggregations website[1] in Figure 5-5 shows that the minimum moment magnitude that is considered in the de-aggregation is 4.5, and that the largest epicentral distance of an earthquake that can affect Shelby County, TN is 750 km. The centroid of Shelby County, TN, is latitude 35.18°N and longitude 89.90°W. Thus, the area inside the green rectangle in Figure 5-10 extending from latitude 31°N to 40°N and longitude 83°W to 96°W shown is considered to be the source of seismicity affecting Shelby County in the PSHA. Figure 5-10 also shows the map of various regional zone and special seismic source zones in the Central and Eastern United States (CEUS). The sources considered in this analysis are the New Madrid fault zone (Reelfoot faults), Wabash Valley seismic zone, Eastern Tennessee seismic zone, Craton regional zone, and extended margin regional zone.

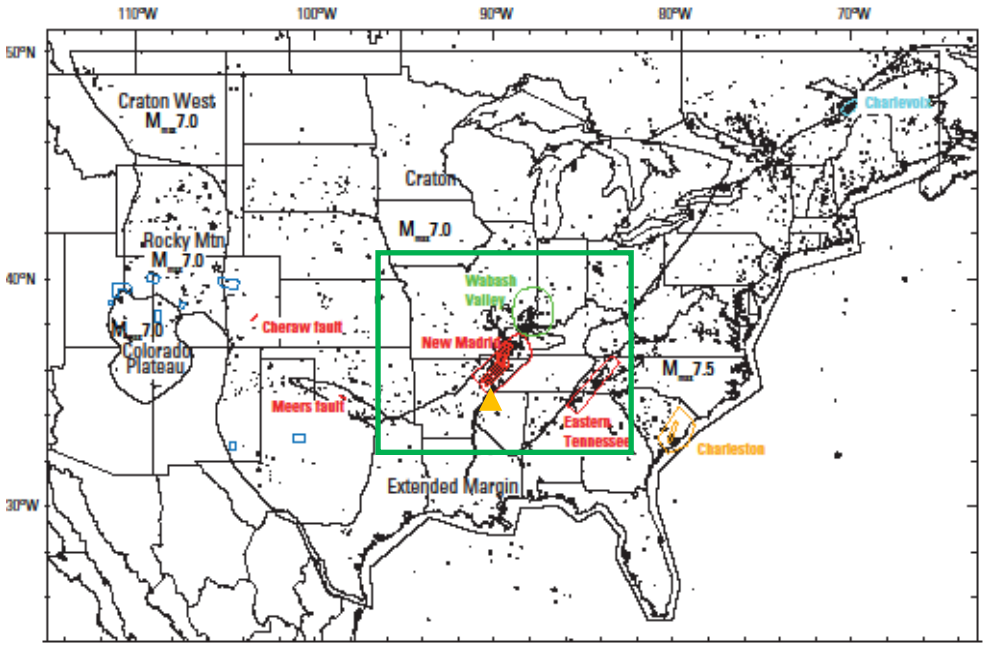

Figure 5-10 Map of special zones (shown by colors), faults and regional $M_{w,max}$ zones in the Central and Eastern United States. Blue polygons west of longitude 100°W denote areas where nontectonic seismic events are removed from the catalog [Figure 4 in Petersen *et al.* (2008)]. The orange triangle represents Shelby County, Tennessee. The dark green rectangle is a seismic source area that is considered in this analysis.

[1]https://geohazards.usgs.gov/deaggint/2008/

The New Madrid fault zone was modeled by three hypothetical faults in the *National Seismic-Hazard Maps: Documentation June 1996* and its updated documentation in 2002 (Frankel *et al.*, 1996; Frankel *et al.*, 2002). In a recent 2008 model, five hypothetical faults rather than three, as shown in Figure 5-11, were used to account for the spatial variability in future earthquakes (Petersen *et al.*, 2008). The central trace is weighted 0.7, the mid west and mid east traces are weighted 0.1, and the west and east traces are weighted 0.05. Petersen *et al.* (2008) applied the distribution of magnitudes (weights) for the northern arm of each hypothetical traces, as follows: M_w 7.1 (0.15), M_w 7.3 (0.2), M_w 7.5 (0.5), and M_w 7.8 (0.15). For the central and southern arms of each hypothetical traces, they applied the following magnitudes (weights): M_w 7.3 (0.15), M_w 7.5 (0.2), M_w 7.7 (0.5), and M_w 8 (0.15). The estimated mean recurrence interval of large New Madrid earthquakes is approximately 500 years (Frankel *et al.*, 2002; Petersen *et al.*, 2008).

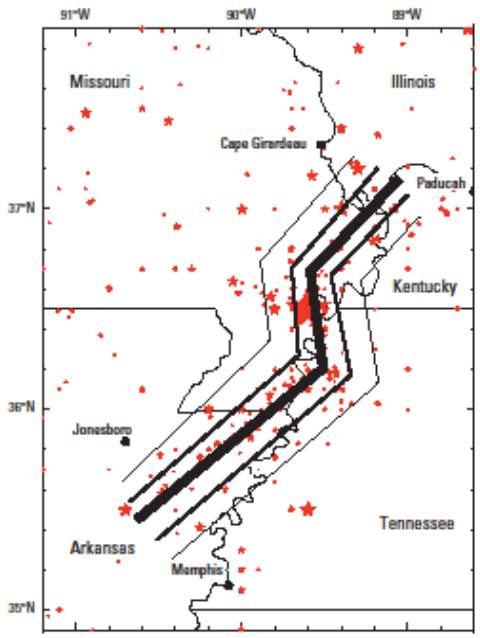

Figure 5-11 Historical seismicity (M_w> 3) and location of the New Madrid hypothetical faults. Relative weights assigned to the hypothetical faults are shown by line width. Size of red stars indicates relative size of earthquake. [Figure 5 in Petersen *et al.* (2008)].

For the other seismicity source zones in Figure 5-10, the distribution of moment magnitude is computed by Eq (3-4) and the mean annual rate of exceedence is evaluated by Eq (3-3). The a-value, b-value, and minimum and maximum moment magnitude for each seismic zone (cf Eq 3-2) are shown in Table 5-4. Since the a-value and b-value for the Eastern Tennessee seismic zone are provided in term of logarithmic body-wave moment, m_{blg}, the magnitude computed from Eq (3-4) is also logarithmic body-wave moment, m_{blg}. The necessary conversion from m_{blg} to M_w is computed by (Frankel *et al.*, 1996):

$$M_w = 3.45 - 0.473 \cdot m_{blg} + 0.145 \cdot m_{blg}^{\,2} \qquad (5\text{-}2)$$

Table 5-4 Minimum and maximum moment magnitude, a-value, and b-value of area seismic zone

	$M_{w,min}$ [+]	$M_{w,max}$	a-value	b-value	Sources
Wabash Valley	4.5	7.5	2.13	0.72	Merino *et al.* (2010)
Eastern Tennessee	4.5	7.0	2.72[*]	0.90[*]	http://www.scdot.org/doing/pdfs/reporttxt.pdf
Craton	4.5	7.0	1.45	0.95	Frankel *et al.* (1996) and Petersen *et al.* (2008)
Extended margin	4.5	7.5	1.45	0.95	Frankel *et al.* (1996) and Petersen *et al.* (2008)

[+] The minimum moment magnitude is used from the de-aggregation results
[*] The a-value and b-value for m_{blg}.

Figure 5-12 compares the hazard curve for spectral acceleration (S_a) at a period of 1 second at the centroid of Shelby County, TN, obtained from the USGS website[1] to the hazard determined from the ground motion attenuation model of Atkinson and Boore (1995) that is used in this study. This difference is caused by differences in the ground motion models (attenuation relationships) that are used by the USGS and in this analysis. The USGS incorporates a weighted average of several ground motion attenuation relationships [e.g. Toro *et al.* (1997), Campbell (2003), Atkinson and Boore (2006), and

[1] http://earthquake.usgs.gov/hazards/products/conterminous/2008/data/#fileformat

Tavakoli and Pezeshk (2005)]. Furthermore, while the USGS considers various minimum moment magnitudes ($M_{w,min}$ = 3, 4, and 5), this study uses $M_{w,min}$ 4.5. Further information relating to the United States National Seismic Hazard Maps can be found in *Documentation for the 2008 Update of the United States National Seismic Hazard Maps.*

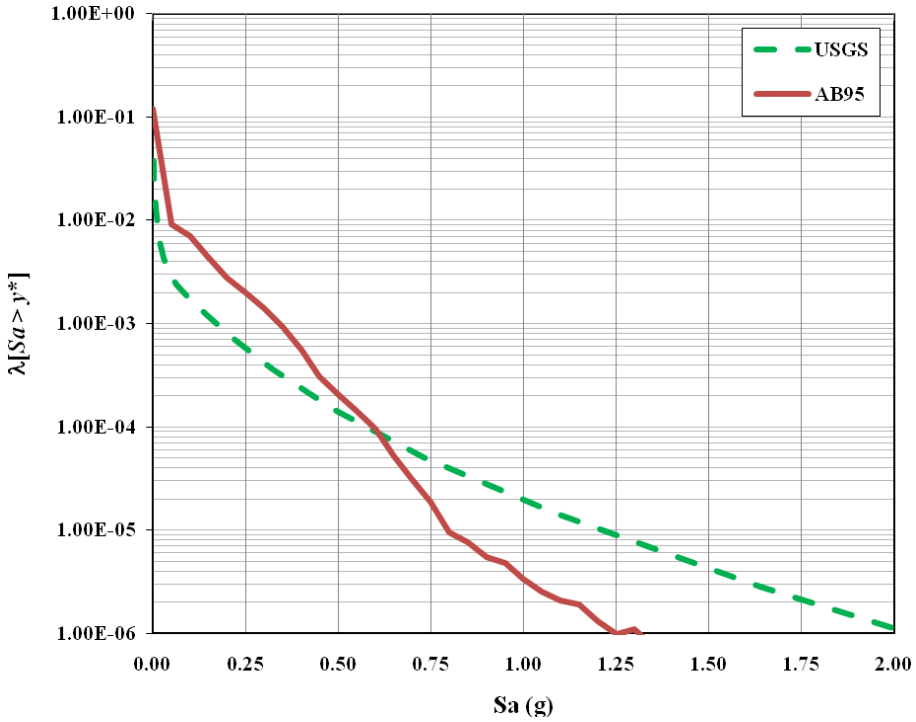

Figure 5-12 Hazard curves for spectral acceleration at period 1 sec at centroid of Shelby County, Tennessee (latitude 38.18°N and longitude -89.90°W).

Risk curves for the aggregated structural loss ratio of all RES4 buildings obtained from the PSHA are illustrated in Figure 5-13. The losses attributed to the Craton and Extended Margin zones cannot be seen in the plot because the losses from these zones are very low. Therefore, neglecting these regional zones will not affect the total occurrence rate. The occurrence rate associated with the New Madrid Seismic Zone is the highest of the three contributing seismic zones. This is caused by the fact that the average moment

magnitude for the New Madrid seismic zone is 7.6, while the average moment magnitudes for the Wabash Valley and Eastern Tennessee seismic zones are only 5.1 and 5, respectively. Furthermore, the average epicentral distances from the Wabash Valley and Eastern Tennessee seismic zones to the centroid of Shelby County, Tennessee, are 440 and 600 km, respectively, which are much greater than the average epicentral distance from the NMSZ (135 km). Although the mean annual rate, $\lambda[M_{w,i}>m_{min}]$, for the NMSZ (0.002 per year) is at least ten times lower than those for the Wabash Valley and Eastern Tennessee seismic zones (0.078 and 0.025 per year, respectively), the large earthquakes associated with the Reelfoot faults in the New Madrid seismic zone have a larger impact on Shelby County than earthquakes in the other seismic zones. The risk curves for the other occupancy classes are consistent with that of occupancy class RES4 in Figure 5-13.

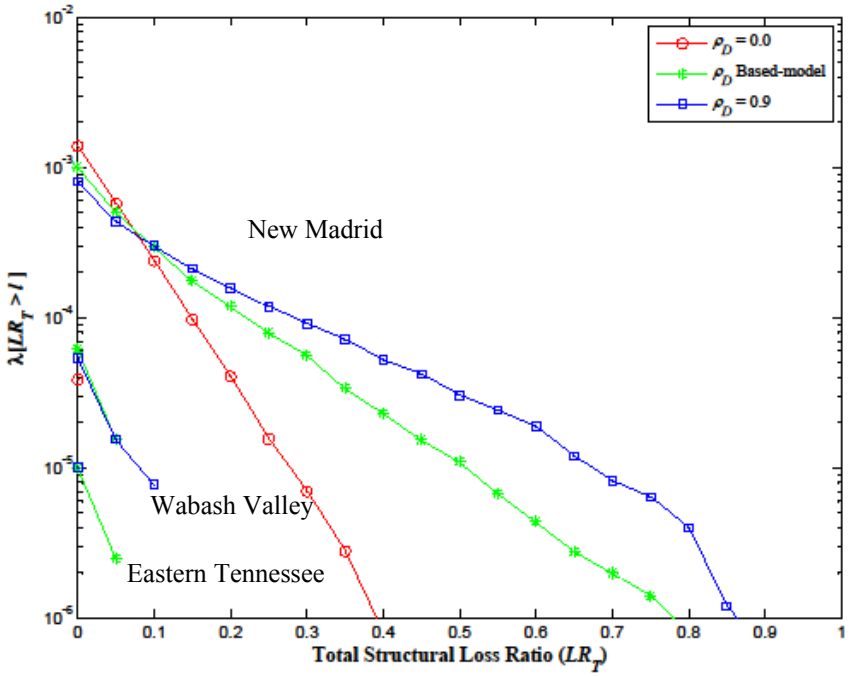

Figure 5-13 Risk curves for total structural loss ratio of 184 RES4 buildings considered each sources separately.

Figure 5-14, Figure 5-15, and Figure 5-16 illustrate mean annual frequencies for total structural loss ratios for 184-RES4, 4,793-COM4, and 681-IND1 buildings, respectively, aggregating all seismic sources. When the occurrence rate is higher than approximately 4×10^{-4}/year for every building occupancy, which is the point at which the risk curves intersect, neglect of correlation in damage is conservative. However, at annual occurrence rates lower than 3×10^{-4}, neglect of damage correlation can cause the loss to be underestimated by up to 90% for the model-based damage correlation and 120% for the upper bound damage correlation. The source for this unconservatism is the variance in total loss, which for the model-based and upper bound damage correlation cases are 1.5 and 2 times that of the case where damage correlation is neglected. Risk curves for aggregated total structural loss ratios of all building occupancies are shown in Figure 5-17. The results are consistent, in a qualitative sense, with the cases where losses to individual occupancy classes were considered separately.

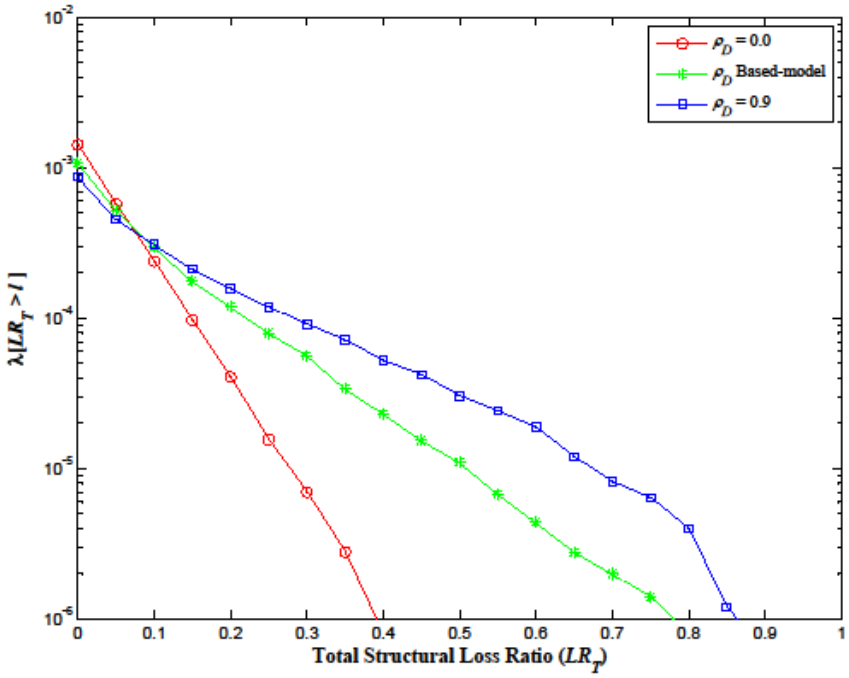

Figure 5-14 Risk curves for total structural loss ratio of 184 RES4 buildings - all earthquake sources aggregated.

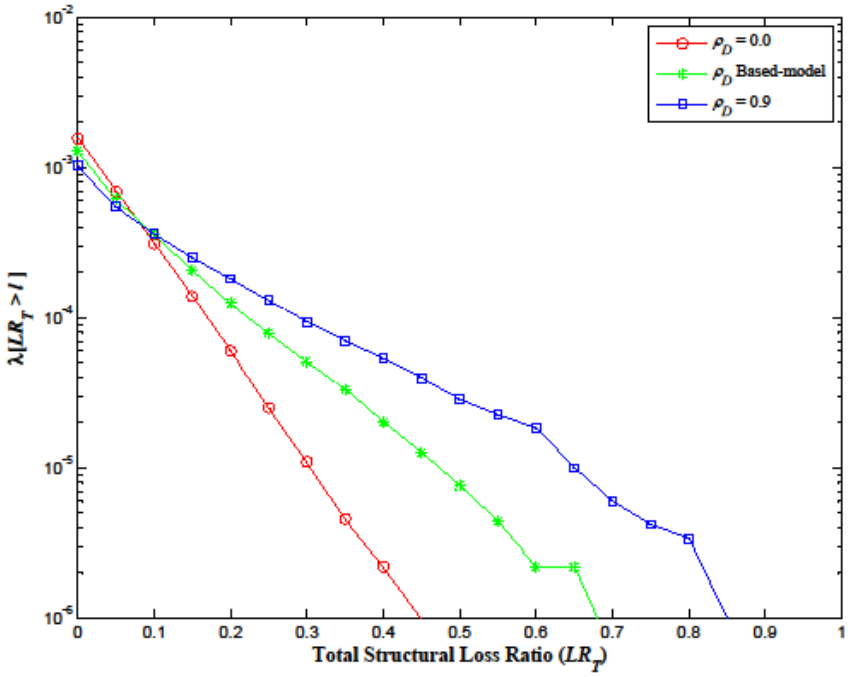

Figure 5-15 Risk curves for total structural loss ratio of 4,793 COM4 buildings - all earthquake sources aggregated.

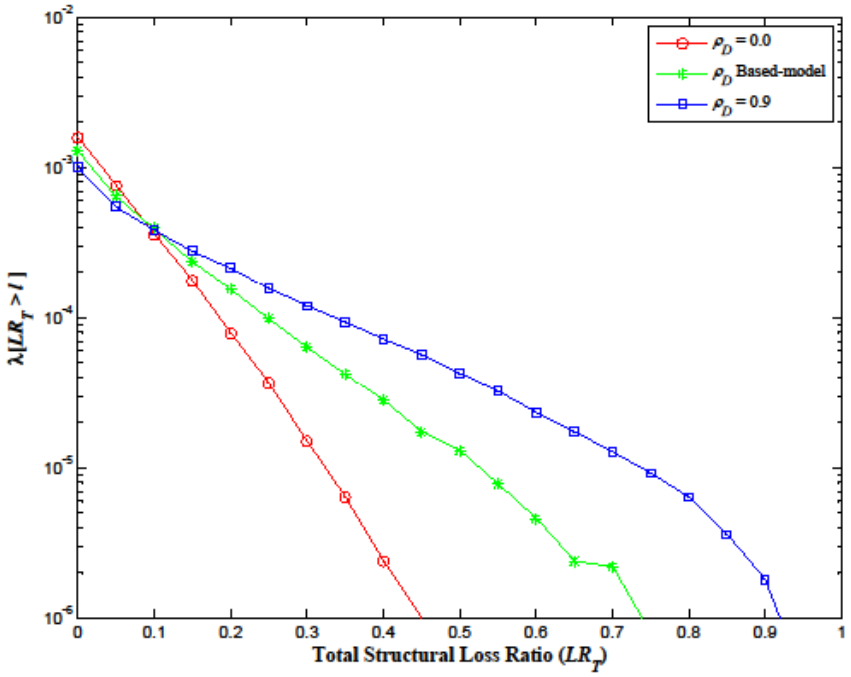

Figure 5-16 Risk curves for total structural loss ratio of 681 IND1 buildings - all earthquake sources aggregated.

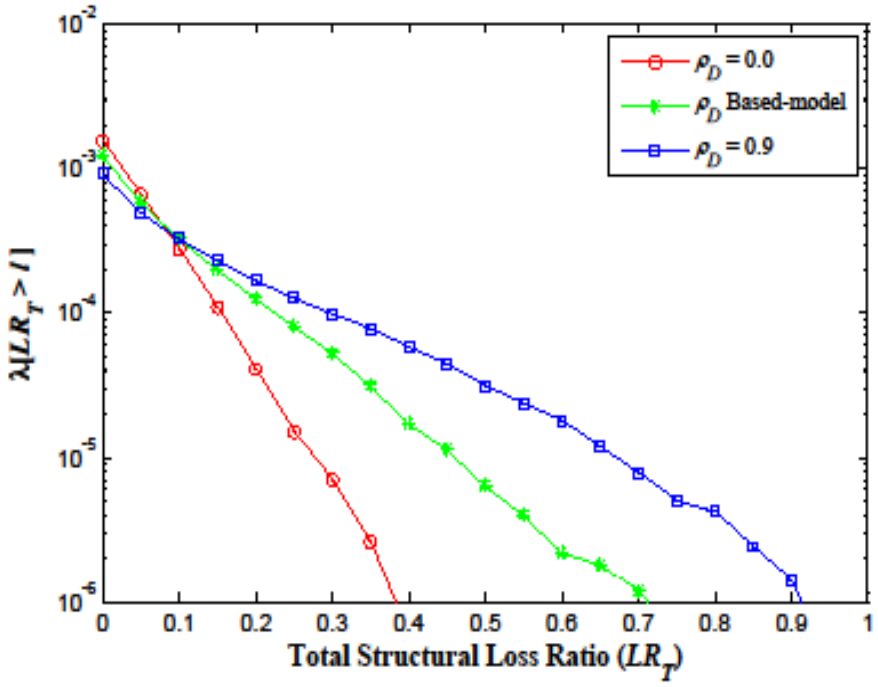

Figure 5-17 Risk curves of total structural loss of all buildings (184 RES4 + 4,973 COM4 + 681 IND1) - all sources aggregated.

5.3 The Probable Maximum Loss

Large scale natural hazards affect not only the building owners and stakeholders, but also insurers and reinsurers who provide natural disaster insurance. Since the losses are usually highly uncertain, insurers and reinsurers must have tools to estimate the losses to calculate the premium that they should charge policyholders. One decision metric that insurers and reinsurers often consider is probable maximum loss (Grossi and Kunreuther, 2005). As shown in previous sections, loss is impacted significantly by spatial correlation in ground motion, seismic demand, and building performance.

The probable maximum loss (PML) is generally taken as that value of the distribution with a small probability of being exceeded in a given year. For this study,

PML at exceedence probabilities 1×10^{-4} and 1×10^{-5} are estimated[1]. Recall that earthquake occurrence are modeled as a Poisson process in basic PSHA, the probability that the total losses exceed a threshold loss, *l*, during a certain interval of time *t* is:

$$P\left[LR_{T,t} > l\right] = 1-\exp\left[-\lambda_{LR_T>l}\cdot t\right] \quad (5\text{-}3)$$

where *t* is time (unit: year) and $\lambda_{LR_T>l}$ is computed from Eq (5-1). The annual probability of exceedence is obtained by setting *t* equal to 1.0.

Figure 5-18, Figure 5-19, Figure 5-20, and Figure 5-21 show the exceedence probabilities of total structural loss ratio of 184-RES4, 4973-COM4, 681-IND1 buildings, and all buildings in the inventory, respectively. The values of the exceedence probability are quite similar to the values of the mean annual occurrence rates in the PSRA in the previous section because the occurrence rates of the total loss are very low. The PML of all buildings for each occupancy class and for aggregate building occupancy classes are summarized in Table 5-5. When considering model-based and upper bound damage correlations, the PML at EP 1×10^{-4}'s are, respectively, approximately 1.5 and 2 times the PML at EP 1×10^{-4} when damage correlation is ignored. The PML at EP 1×10^{-5}'s for model-based and upper bound case are about 1.8 and 2.4 times the PML at EP 1×10^{-5} for the case where damage correlation is neglected. Clearly, neglect of correlation seismic demand and damage can lead to significant underestimation of the PML.

[1]Grossi and Kunreuther (2005) used 0.001-0.004, while Woo (2002) stated that the Natural Disaster Coalition has defined PML at 0.002. However, since the events of interest in the study region have very low occurrence rates, PML at the exceedence probability at 1×10^{-4} and 1×10^{-5} are used.

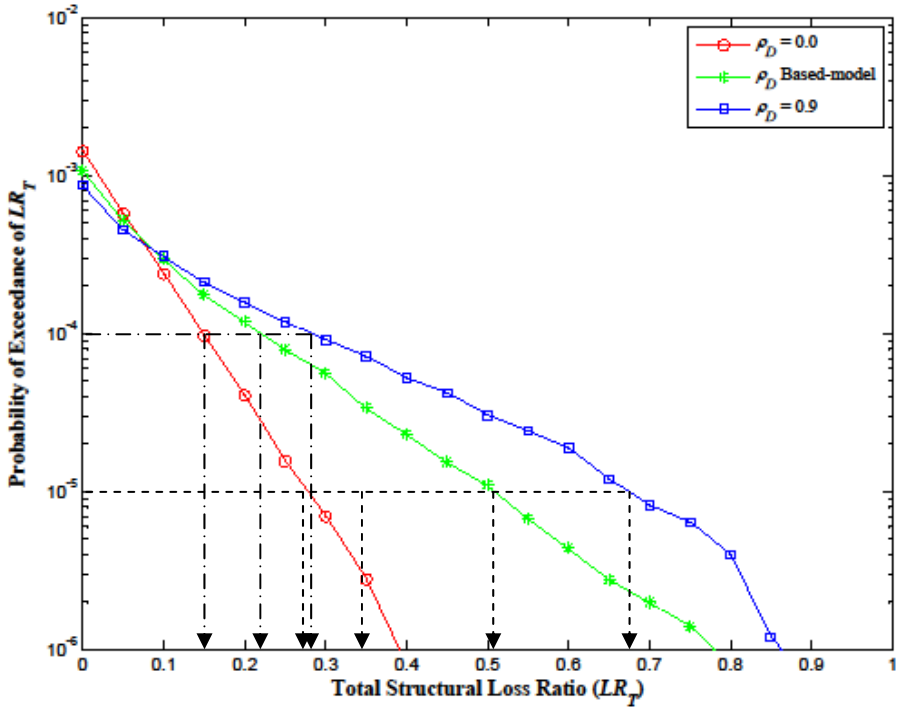

Figure 5-18 Exceedence probability of total structural loss ratio of 184 RES4 buildings. Note that the values of PML at given 10^{-4} and 10^{-5}exceedence probabilities are shown in Table 5-5.

.

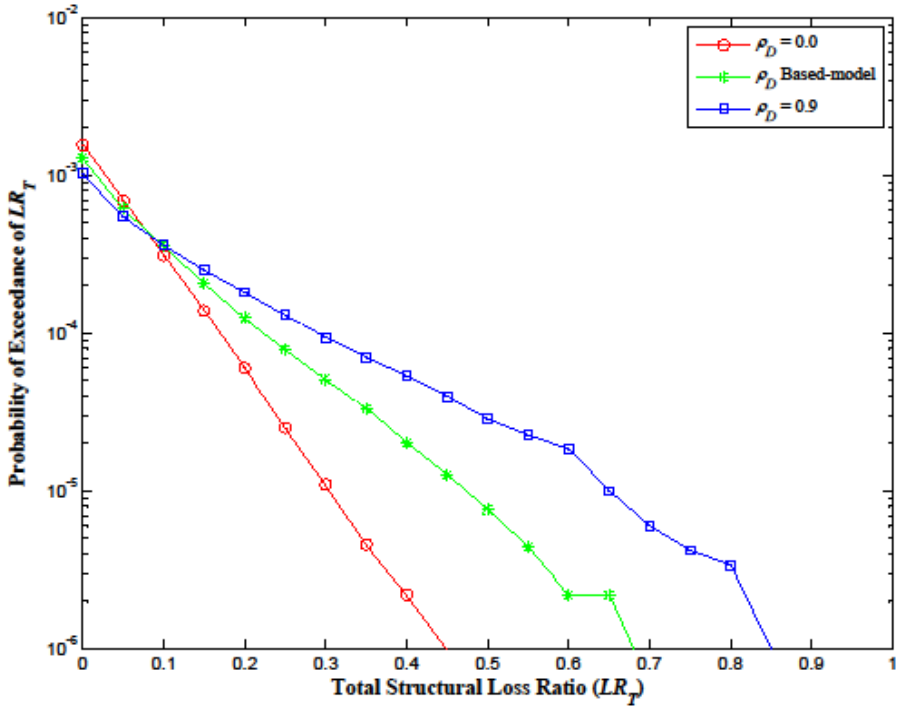

Figure 5-19 Exceedence probability of total structural loss ratio of 4,793 COM4 buildings.

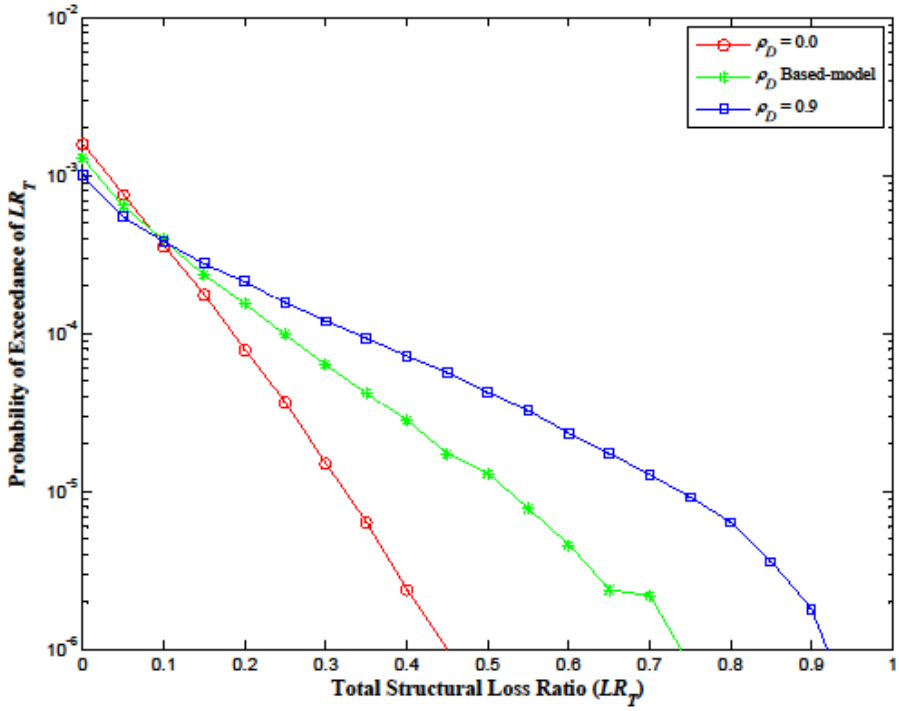

Figure 5-20 Exceedence probability of total structural loss ratio of 681 IND1 buildings.

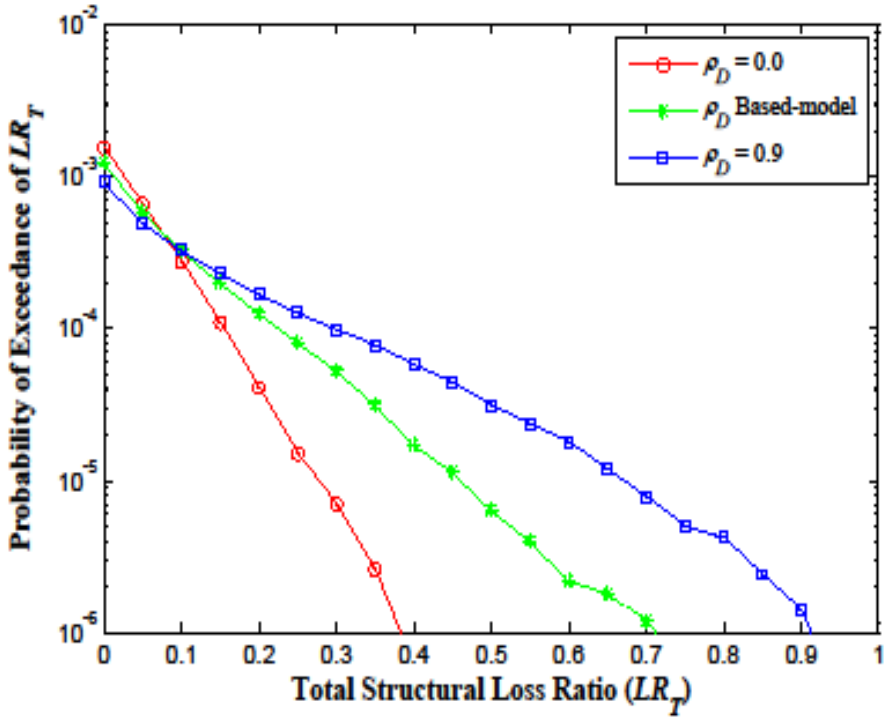

Figure 5-21 Exceedence probability of total structural loss ratio of all buildings in portfolio.

Table 5-5 Probable maximum loss at a specific exceedence probability of aggregate structural loss ratio

Portfolio	PML at EP = 10^{-4}			PML at EP = 10^{-5}		
	Damage Correlation, ρ_D			Damage Correlation, ρ_D		
	0.0	Based-Model	0.9	0.0	Based-Model	0.9
184 RES4	0.149	0.224	0.285	0.283	0.512	0.676
4,793 COM4	0.175	0.227	0.292	0.308	0.476	0.650
681 IND1	0.189	0.250	0.338	0.329	0.529	0.739
All buildings	0.171	0.225	0.294	0.298	0.471	0.655

5.4 Summary

Two approaches to estimate earthquake risk, which utilized the loss estimation model in Chapter 4, were presented. A scenario earthquake risk assessment of spatially distributed buildings in Shelby County, TN, was presented first. The de-aggregation of S_a (T = 1 sec) at various return periods was considered to select a scenario event. The dominant contributing earthquake for de-aggregations at return periods ranging from 72 to 4,975 years is an earthquake occurring on hypothetical Reelfoot faults in New Madrid seismic zone. The probability density functions of the total structural loss ratio for spatially distributed buildings were determined, and it was found that their upper tail behavior is affected significantly by the correlation in damage. When damage correlation is neglected, the standard deviation of the losses is undervalued as much as 50%, and the likelihood of aggregated loss ratio higher than 30% of total replacement cost is underestimated.

Second, a probabilistic seismic risk assessment of aggregated structural loss ratios of building inventories in Shelby County, TN, was described. The seismic sources that affect the study area are New Madrid Seismic Zone (Reelfoot faults), Wabash Valley Seismic Zone, Eastern Tennessee Seismic Zone, Craton Regional Zone, and Extended

Margin Regional Zone. The major contribution to the annual occurrence rate comes from the NMSZ because it is the closest to Shelby County and only large earthquakes ($M_w > 7$), compared to earthquakes in the other source zones in which minimum moment magnitude is 4.5, are considered. When the mean annual earthquake occurrence rate is lower than 4×10^{-4}/yr, neglect of damage correlation may underestimate loss as much as 120%. Finally, the probable maximum loss (PML) was determined from the PSRA; this decision metric is affected by the uncertainty (variance) of individual losses as well as correlation in damage. If correlation in damage is neglected, the estimated PML may increase by as much as 240%.

In this chapter, the standard deviation and PML resulting from the use of the model-based damage correlation are approximately equal to the average values of lower and upper bound and computed from the assumed parameters. However, the effect of each parameter on the uncertainty in the estimate of the aggregated structural losses is still unknown. The sensitivity analysis in Chapter 7 is designed to answer this question.

CHAPTER 6

ESTIMATION OF TOTAL LOSSES TO BUILDING INVENTORIES

Direct economic losses to building inventories exposed to natural hazards include losses from damage to structural systems, to nonstructural components and systems, and to building contents. The building repair/replacement costs from structural damage were analyzed in the previous chapter, while the losses from the damage of nonstructural components and building contents have yet to be determined. The nonstructural loss is usually a large portion of the total seismic losses, since it includes losses due to damage to architectural, mechanical and electrical components. For example, the full replacement cost of nonstructural components in HAZUS-MH is approximately 85 of total replacement cost for residential and industrial occupancy classes. Shinozuka *et al.* (1997), FEMA/NIBS (2003) , and Goda and Hong (2008) separated nonstructural losses by nonstructural components and from building contents, while Aslani and Miranda (2005) considered only loss from damage of nonstructural components.

In the present study, nonstructural loss is separated into nonstructural component and building content losses. Table 6-1 summarizes typical nonstructural components and building contents and relates damage to nonstructural components to the level of either interstory drift ratio (drift-sensitive) or peak floor acceleration (acceleration-sensitive), while damage to building contents usually is related to the level of peak floor acceleration. Similar to the fragility functions for structural components, the fragility functions for nonstructural drift-sensitive (NDSC) and acceleration-sensitive (NASC) components are assumed to follow a lognormal distribution. Since the damage of

building contents depends on the level of peak floor acceleration, the fragility functions for building contents are similar to those for NASC. Several examples of NDSC and NASC fragility functions are illustrated in Figure 6-1.

The remainder of Chapter will introduce an approach to estimate the total losses, aggregating all other losses with structural losses. In Section 6.1, a method to estimate nonstructural losses is developed that includes damage correlations of nonstructural components among buildings. Section 6.2 proposes a method to aggregate structural and nonstructural losses that considers correlation between these components. In Section 6.3, that method is applied to the building inventories defined in Chapter 5 to analyze losses from a scenario event, assess seismic risk, and determine the Probable Maximum Loss, or PML to demonstrate the methodology.

Table 6-1 List of typical nonstructural components and contents of buildings(FEMA/NIBS, 2003)

Type	Item	Drift-Sensitive*	Acceleration-Sensitive*
Architectural	Nonbearing Walls/Partitions	x	o
	Cantilever Elements and Parapets		x
	Exterior Wall Panels	x	o
	Veneer and Finishes	x	o
	Penthouses	x	
	Racks and Cabinets		x
	Access Floors		x
	Appendages and Ornaments		x
Mechanical and Electrical	General Mechanical (boilers, etc.)		x
	Manufacturing and Process Machinery		x
	Piping Systems	o	x
	Storage Tanks and Spheres		x
	HVAC Systems (chillers, ductwork, etc.)	o	x
	Elevators	o	x
	Trussed Towers		x
	General Electrical (switchgear, ducts, etc.)	o	x
	Lighting Fixtures		x
Contents	File Cabinets, Bookcases, etc.		x
	Office Equipment and Furnishings		x
	Computer/Communication Equipment		x
	Nonpermanent Manufacturing Equipment		x
	Manufacturing/Storage Inventory		x
	Art and other Valuable Objects		x

* "x" indicates primary cause of damage; "o" indicates secondary cause of damage.

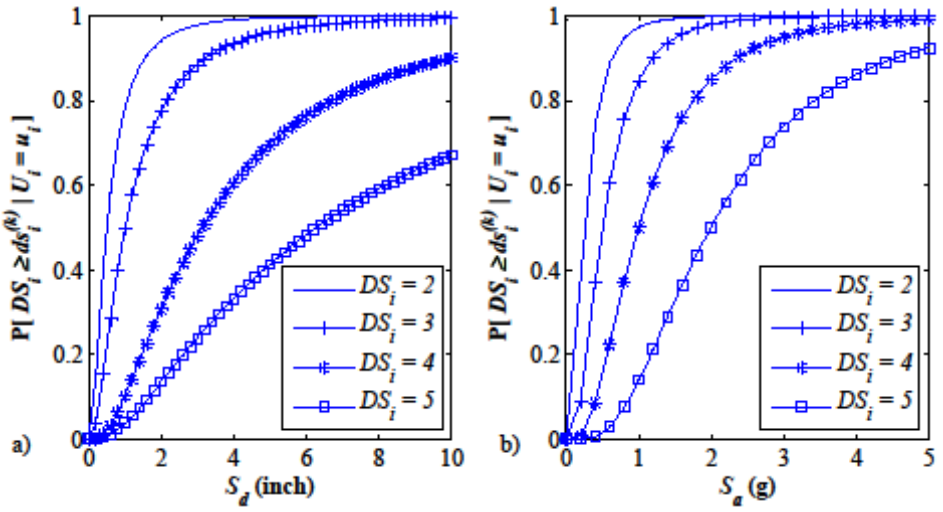

Figure 6-1 a) Nonstructural drift-sensitive component fragility functions for each damage state for building type W1; b) nonstructural acceleration-sensitive component fragility functions for each damage state for building type W1 (DS_i's equal 2,3,4, and 5 refer to slight, moderate, extensive, and complete damage states, respectively)

6.1 Nonstructural and Building Contents Losses

The model for determining nonstructural and building content losses is similar to that used for estimating structural loss in Chapter 4. The correlation in seismic demand (spatial ground motion) is also similar to that used in estimating structural losses (cf Eq 3-14). However, the correlations in performance and damage are different for nonstructural items because different factors are significant in the degree of damage that occurs. Pairwise correlations in non-structural performance and damage of buildings may arise from common building design practices and construction materials because damage of nonstructural items is caused from the level of interstory drift and peak floor acceleration, both of which depend on the response of the structural system. However, the correlation generally would be considerably weaker because the selection of interior finishes and furnishings by the building occupants depends on the nature of the building occupancy and generally is independent of the structural system. Since the correlation

arising from the seismic demand accounts for a major part of the overall correlation in performance and damage, it is assumed that only ground motion correlation need be considered in estimating nonstructural losses.

Figure 6-2 through Figure 6-7 illustrate the correlation in nonstructural loss ratios computed using simulation from Eq (4-4), with nonstructural losses substituted for structural losses, as a function of the distance between buildings *i* and *j*. It is noted that that NDSC loss ratio is defined by the NDSC repair cost normalized with respect to its replacement cost; the NASC loss ratio is defined similarly. Since the fragilities for building contents in HAZUS-MH are included in the fragilities for NASC, the correlation in contents loss is similar to the correlation in NASC loss. These curves show that even if two buildings are in close proximity, the correlation in losses is substantially less than 1.0. This is caused by the differences in construction type that may exist for adjacent buildings. As with structural losses, correlation of nonstructural losses is stronger at increasing distances as the magnitude of the earthquake increases because of the increase in the felt area of the larger events. These correlation curves were obtained numerically and have been smoothed by least-squares fitting using Eq (4-7).

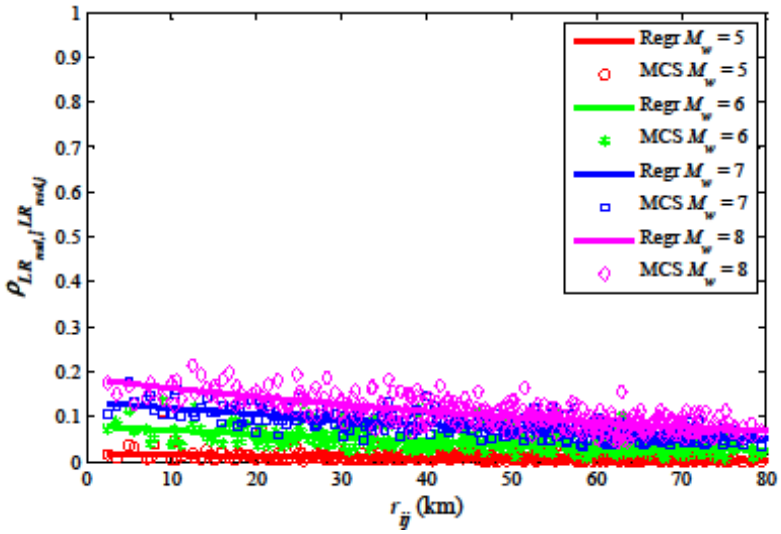

Figure 6-2 Correlation of nonstructural drift-sensitive loss ratio between buildings in class RES4. (Regr = regression analysis)

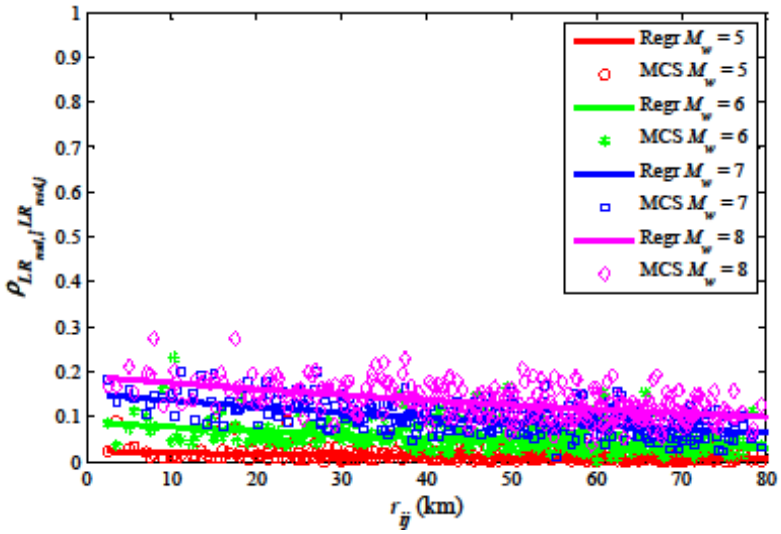

Figure 6-3 Correlation of nonstructural drift-sensitive loss ratio between buildings in class COM4. (Regr = regression analysis)

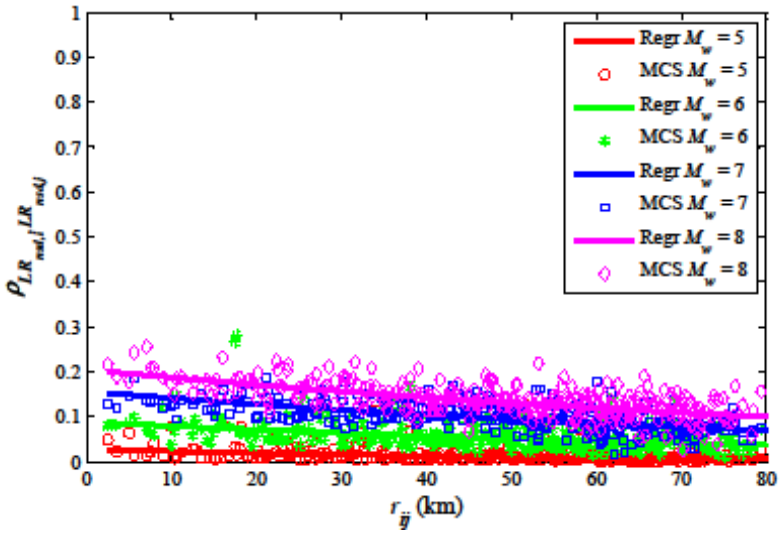

Figure 6-4 Correlation of nonstructural drift-sensitive loss ratio between buildings in class IND1. (Regr = regression analysis)

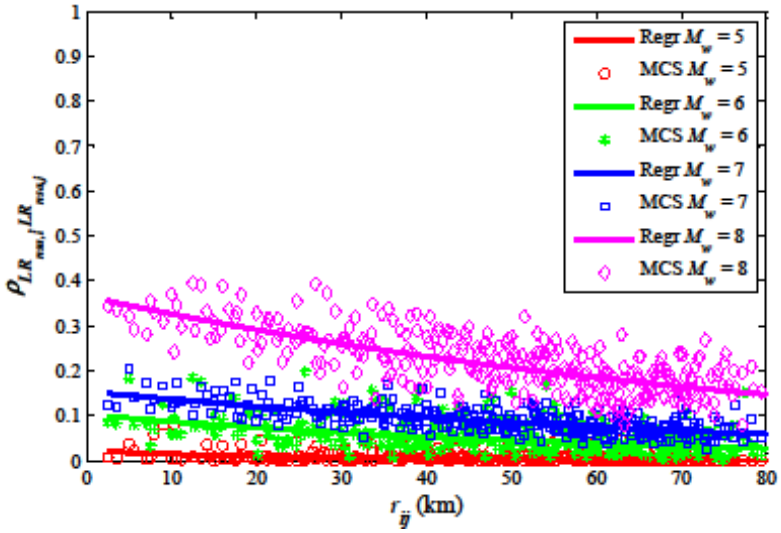

Figure 6-5 Correlation of nonstructural acceleration-sensitive loss ratio between buildings in class RES4. (Regr = regression analysis)

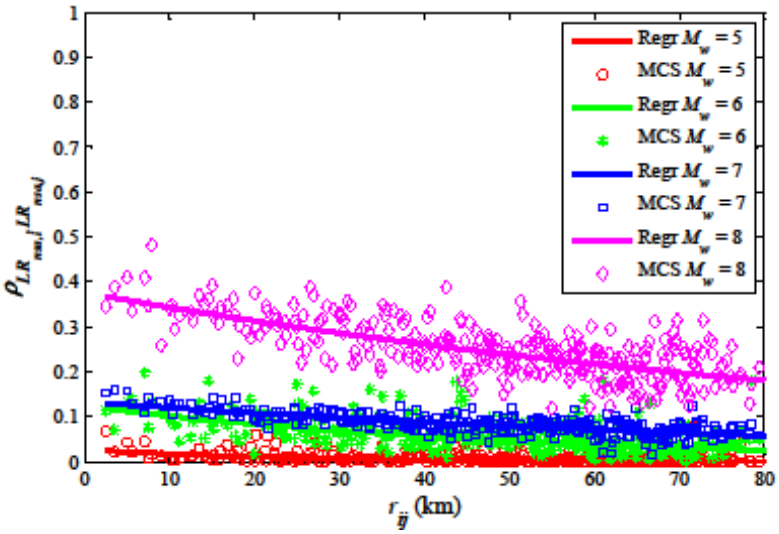

Figure 6-6 Correlation of nonstructural acceleration-sensitive loss ratio between buildings in class COM4. (Regr = regression analysis)

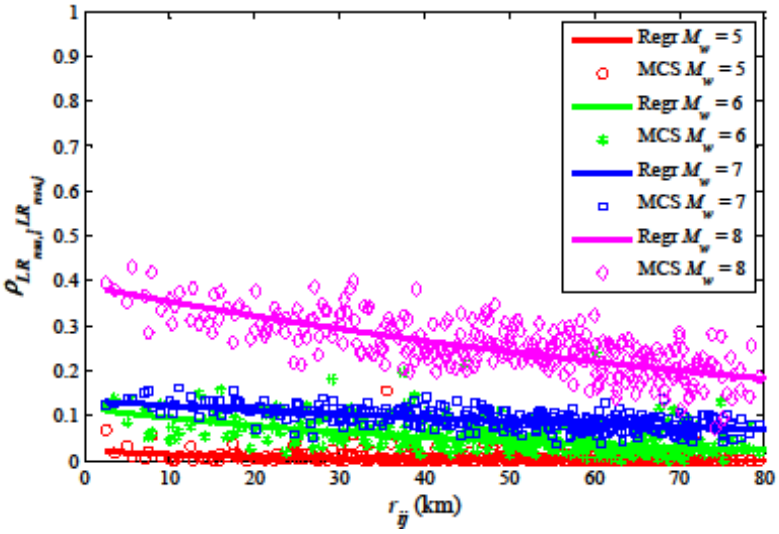

Figure 6-7 Correlation of nonstructural acceleration-sensitive loss ratio between buildings in class IND1. (Regr = regression analysis)

6.2 Aggregation of Nonstructural and Structural Losses

Total losses are estimated by combining the structural losses that were computed in Chapter 5 with the nonstructural losses (drift-sensitive, acceleration-sensitive, and building contents) described in the previous section. The mean of the total loss is computed by summing the means of the structural and nonstructural losses. The variance

in the total loss may be determined simply by summing the variances of structural and nonstructural losses if those losses are statistically independent. However, in practice the structural and nonstructural losses of individual buildings are partially correlated by that fact that their seismic demands are similar but their damage states represented by their fragility functions may be different.

To develop an approach to compute the variance of the total loss to an inventory of buildings, we begin by considering the total loss of two buildings:

$$L_T = L_1 + L_2 \tag{6-1}$$

where $L_1 = L_{s,1} + L_{ns,1}$ and $L_2 = L_{s,2} + L_{ns,2}$; terms $L_{s,i}$, and $L_{ns,i}$ are the structural and nonstructural losses to building *i*, respectively. The total loss ratio is computed by divided Eq (6-1) by the sum of the full replacement costs of buildings *1* and *2* (RPC_1+RPC_2). Note that the full replacement cost is the sum of structural, nonstructural, and building contents costs. The nonstructural loss in Eq (6-1) is not separated into losses due to NDSC, NASC, and building contents in order to simplify the illustration. NDSC, NASC, and contents losses will be added subsequently. The mean and variance of the total loss are:

$$\begin{aligned} \mathrm{E}[L_T] &= \mathrm{E}[L_1] + \mathrm{E}[L_2] \\ &= \mathrm{E}[L_{s,1}] + \mathrm{E}[L_{ns,1}] + \mathrm{E}[L_{s,2}] + \mathrm{E}[L_{ns,2}] \end{aligned} \tag{6-2}$$

$$
\begin{aligned}
\mathrm{Var}\left[L_T\right] &= \mathrm{Var}\left[L_1\right]+\mathrm{Var}\left[L_2\right]+2\cdot\left\{\mathrm{COV}\left[L_1,L_2\right]\right\} \\
&= \mathrm{Var}\left[L_{s,1}+L_{ns,1}\right]+\mathrm{Var}\left[L_{s,2}+L_{ns,2}\right] \\
&\quad +2\cdot\left\{\mathrm{COV}\left[L_{s,1}+L_{ns,1},L_{s,2}+L_{ns,2}\right]\right\} \\
&= \mathrm{Var}\left[L_{s,1}\right]+\mathrm{Var}\left[L_{ns,1}\right]+2\cdot\left\{\mathrm{COV}\left[L_{s,1},L_{ns,1}\right]\right\} \\
&\quad +\mathrm{Var}\left[L_{s,2}\right]+\mathrm{Var}\left[L_{ns,2}\right]+2\cdot\left\{\mathrm{COV}\left[L_{s,2},L_{ns,2}\right]\right\} \\
&\quad +2\cdot\left\{\begin{array}{l}\mathrm{COV}\left[L_{s,1},L_{s,2}\right]+\mathrm{COV}\left[L_{s,1},L_{ns,2}\right] \\ +\mathrm{COV}\left[L_{ns,1},L_{s,2}\right]+\mathrm{COV}\left[L_{ns,1},L_{ns,2}\right]\end{array}\right\} \\
&= \mathrm{Var}\left[L_{s,T}\right]+\mathrm{Var}\left[L_{ns,T}\right]+2\cdot\left\{\mathrm{COV}\left[L_{s,1},L_{ns,1}\right]+\mathrm{COV}\left[L_{s,2},L_{ns,2}\right]\right\}
\end{aligned}
\tag{6-3}
$$

where $\mathrm{Var}[L_{s,T}] = \mathrm{Var}[L_{s,1}] + \mathrm{Var}[L_{s,2}] + 2\mathrm{COV}[L_{s,1},L_{s,2}]$ and $\mathrm{Var}[L_{ns,T}] = \mathrm{Var}[L_{ns,1}] + \mathrm{Var}[L_{ns,2}] + 2\mathrm{COV}[L_{ns,1},L_{ns,2}]$. The term $\mathrm{COV}[L_{s,i},L_{ns,j}]$ is equal to zero if we assume no correlation between structural loss to buildings i and j, where $i \neq j$. The mean and variance of the total loss ratio are computed by divided Eqs (6-2) and (6-3) by $(RPC_1 + RPC_2)$ and $(RPC_1 + RPC_2)^2$, respectively. The covariance of $L_{s,i}$ and $L_{ns,i}$ is expressed by:

$$
\mathrm{COV}\left[L_{s,i},L_{ns,i}\right] = \rho_{L_{s,i},L_{ns,i}}\cdot\sqrt{\mathrm{Var}\left[L_{s,i}\right]\cdot\mathrm{Var}\left[L_{ns,i}\right]} \tag{6-4}
$$

where $\rho_{L_{s,i},L_{ns,i}}$ is the correlation coefficient of structural and nonstructural losses to building i.

Extending the above formulation to consider M occupancy classes and a_M buildings per occupancy class and aggregating structural losses with NDSC, NASC, and building content (BC) losses, Eqs (6-2), (6-3), and (6-4) become:

$$
\mathrm{E}\left[L_T\right] = \sum_{m=1}^{M}\sum_{i=1}^{a_M}\mathrm{E}\left[L_{s,i,m}\right]+\mathrm{E}\left[L_{ndsc,i,m}\right]+\mathrm{E}\left[L_{nasc,i,m}\right]+\mathrm{E}\left[L_{bc,i,m}\right] \tag{6-5}
$$

$$\begin{aligned}\mathrm{Var}\left[L_T\right] &= \sum_{m=1}^{M}\sum_{i=1}^{a_M}\Big\{\mathrm{Var}\left[L_{s,i,m}\right]+\mathrm{Var}\left[L_{ndsc,i,m}\right]+\mathrm{Var}\left[L_{nasc,i,m}\right]+\mathrm{Var}\left[L_{bc,i,m}\right] \\ &\quad +2\cdot\begin{bmatrix}\mathrm{COV}\left[L_{s,i,m},L_{ndsc,i,m}\right]+\mathrm{COV}\left[L_{s,i,m},L_{nasc,i,m}\right] \\ +\mathrm{COV}\left[L_{s,i,m},L_{bc,i,m}\right]+\mathrm{COV}\left[L_{ndsc,i,m},L_{nasc,i,m}\right] \\ +\mathrm{COV}\left[L_{ndsc,i,m},L_{bc,i,m}\right]+\mathrm{COV}\left[L_{nasc,i,m},L_{bc,i,m}\right]\end{bmatrix}\Big\}\end{aligned} \tag{6-6}$$

$$\begin{aligned}\mathrm{COV}\left[L_{s,i,m},L_{ndsc,i,m}\right] &= \rho_{L_{s,i,m},L_{ndsc,i,m}}\cdot\sqrt{\mathrm{Var}\left[L_{s,i,m}\right]\cdot\mathrm{Var}\left[L_{ndsc,i,m}\right]} \\ \mathrm{COV}\left[L_{s,i,m},L_{nasc,i,m}\right] &= \rho_{L_{s,i,m},L_{nasc,i,m}}\cdot\sqrt{\mathrm{Var}\left[L_{s,i,m}\right]\cdot\mathrm{Var}\left[L_{nasc,i,m}\right]} \\ \mathrm{COV}\left[L_{s,i,m},L_{bc,i,m}\right] &= \rho_{L_{s,i,m},L_{bc,i,m}}\cdot\sqrt{\mathrm{Var}\left[L_{s,i,m}\right]\cdot\mathrm{Var}\left[L_{bc,i,m}\right]} \\ \mathrm{COV}\left[L_{ndsc,i,m},L_{nasc,i,m}\right] &= \rho_{L_{ndsc,i,m},L_{nasc,i,m}}\cdot\sqrt{\mathrm{Var}\left[L_{ndsc,i,m}\right]\cdot\mathrm{Var}\left[L_{nasc,i,m}\right]} \\ \mathrm{COV}\left[L_{ndsc,i,m},L_{bc,i,m}\right] &= \rho_{L_{ndsc,i,m},L_{bc,i,m}}\cdot\sqrt{\mathrm{Var}\left[L_{ndsc,i,m}\right]\cdot\mathrm{Var}\left[L_{bc,i,m}\right]} \\ \mathrm{COV}\left[L_{nasc,i,m},L_{bc,i,m}\right] &= \rho_{L_{nasc,i,m},L_{bc,i,m}}\cdot\sqrt{\mathrm{Var}\left[L_{nasc,i,m}\right]\cdot\mathrm{Var}\left[L_{bc,i,m}\right]}\end{aligned} \tag{6-7}$$

Since structural damage and NDSC, NASC, and BC damages result from similar seismic demands but have different fragility functions, the loss correlations in Eq (6-7) depend on both demand and damage correlations. In contrast with the NASC and building content losses, their damage is perfectly correlated because the damage to BC is determined from the fragility functions for NASC components. To gain insight into the correlation between structural and NDSC loss, a simple model of the structural and NDSC losses for building *i* is assumed:

$$L_{s,i} = h_s\left(f_s\left(g\left(M_w,R_i\right)\right)\right) = h_s\left(f_s\left(Y_i\right)\right) = \alpha_s\cdot f_s\left(Y_i\right) \tag{6-8}$$

$$L_{ndsc,i} = h_{ndsc}\left(f_{ndsc}\left(g\left(M_w,R_i\right)\right)\right) = h_{ndsc}\left(f_{ndsc}\left(Y_i\right)\right) = \alpha_{ndsc}\cdot f_{ndsc}\left(Y_i\right) \tag{6-9}$$

where $g(M_w,R_i)$ is the ground motion attenuation that defines function to determine seismic demand at site *i* from an earthquake with an epicentral distance R_i and exposed to an earthquake moment magnitude M_w; $f_s(.)$ and $f_{ndsc}(.)$ are functions that determine the

damage state, as described in Section 3.3.1; $h_s(.)$ and $h_{ndsc}(.)$ are structural and NDSC losses as functions of structural and NDSC damage, and parameters α_s and α_{ndsc} define loss as a function of structural and NDSC damage.

The covariance and correlation coefficient of structural and NDSC losses are

$$\begin{aligned} \mathrm{COV}\left[L_{s,i}, L_{ndsc,i}\right] &= \mathrm{COV}\left[h_s\left(f_s\left(g\left(M_w, R_i\right)\right)\right), h_{ndsc}\left(f_{ndsc}\left(g\left(M_w, R_i\right)\right)\right)\right] \\ &= \mathrm{COV}\left[\alpha_s \cdot f_s\left(Y_i\right), \alpha_{ndsc} \cdot f_{ndsc}\left(Y_i\right)\right] \\ &= \alpha_s \cdot \alpha_{ndsc} \cdot \mathrm{COV}\left[f_s\left(Y_i\right), f_{ndsc}\left(Y_i\right)\right] \\ &= \alpha_s \cdot \alpha_{ndsc} \cdot \rho_{f_s, f_{ndsc}} \cdot \sqrt{\mathrm{Var}\left[f_s\left(Y_i\right)\right] \cdot \mathrm{Var}\left[f_{ndsc}\left(Y_i\right)\right]} \end{aligned} \tag{6-10}$$

$$\begin{aligned} \rho_{L_{s,i}, L_{ndsc,i}} &= \frac{\mathrm{COV}\left[L_{s,i}, L_{ndsc,i}\right]}{\sqrt{\mathrm{Var}\left[L_{s,i}\right] \cdot \mathrm{Var}\left[L_{ndsc,i}\right]}} \\ &= \frac{\alpha_s \cdot \alpha_{ndsc} \cdot \rho_{f_s, f_{ndsc}} \cdot \sqrt{\mathrm{Var}\left[f_s\left(Y_i\right)\right] \cdot \mathrm{Var}\left[f_{ndsc}\left(Y_i\right)\right]}}{\sqrt{\alpha_s{}^2 \cdot \mathrm{Var}\left[f_s\left(Y_i\right)\right] \cdot \alpha_{ndsc}{}^2 \cdot \mathrm{Var}\left[f_{ndsc}\left(Y_i\right)\right]}} \\ &= \rho_{f_s, f_{ndsc}} \end{aligned} \tag{6-11}$$

where $\rho_{f_s, f_{ndsc}}$ is the correlation coefficient of structural and NDSC damage. Similarly, the correlations between structural and NASC losses are $\rho_{L_{s,i}, L_{nasc,i}}$, between structural and contents loss, $\rho_{L_{s,i}, L_{bc,i}}$, between NDSC and NASC, $\rho_{L_{ndsc,i}, L_{nasc,i}}$, and between NDSC and contents, $\rho_{L_{ndsc,i}, L_{bc,i}}$. Since NASC and contents damage share the same fragility function, the correlations between contents and the others are equal to those between NASC and building contents, while the correlation between contents damage and NASC-related damage is assumed to equal 1.

To develop the correlation model between structural, NDSC, NASC, and BC damage, we first consider the model between structural and NDSC damage. The model-

based correlation of $DM_{s,i}$ and $DM_{s,j}$ in Eq (3-26) is modified by substituting $DM_{ndsc,i}$ for $DM_{s,j}$, as follows:

$$\rho_{DMs_i,DMndsc_i} = \frac{\rho_{Ys_i,Yndsc_j} \cdot \sigma_{Ys_i} \cdot \sigma_{Yndsc_i}}{\sqrt{\left(\sigma^2_{Ys_i} + \sigma^2_{\varepsilon_s}\right)\left(\sigma^2_{Yndsc_i} + \sigma^2_{\varepsilon_{ndsc}}\right)}} \tag{6-12}$$

where $\rho_{Ys_i,Yndsc_j}$ is the correlation between structural and NDSC fragility functions. Similar to $\rho_{Ys_i,Yndsc_j}$, the correlations $\rho_{Ys_i,Ynasc_j}$, ρ_{Ys_i,Ybc_j}, $\rho_{Yndsc_i,Ynasc_j}$, and ρ_{Yndsc_i,Ybc_j} are computed from Eq (6-12) by modifying their subscripts. The values of σ_{Yndsc_i} are illustrated in Appendix A, Tables A-5 through A-8 for four damage states and four levels of seismic design: high, moderate, low, and pre-code, respectively. Similarly, the values of σ_{Ynasc_i} are illustrated in Appendix A, Tables A-9 through A-12 for the same four damage states and four levels of seismic design.

6.3 Illustration of Total Building Inventory Loss Assessment

To illustrate the application of the model that was developed in Section 6.2, the same building inventories that were considered in Chapter 5, namely 184 RES4, 4,793 COM4, and 681 IND1 buildings in Shelby County, TN, are examined using both a scenario earthquake risk analysis (SERA) and a probabilistic seismic risk analysis (PSRA). The probable maximum loss (PML) to the assumed building inventory also is estimated. Since the evaluation of Eq (6-6) including structural, nonstructural drift-sensitive, nonstructural acceleration-sensitive, and contents damages for each 100-

building sample[1] which was used in Chapter 5 is laborious, various sampling sizes will be tested for the SERA and will guide the selection of the sample size used for the PSRA.

The drift-sensitive (NDSC) and acceleration-sensitive (NASC) fragility curves for nonstructural elements that are used in this analysis are provided in Table 5.11 and 5.12 in (FEMA/NIBS, 2003). The correlations between $Y_{s,i}$ and $Y_{ndsc,i}$, between $Y_{ndsc,i}$ and $Y_{nasc,i}$, and between $Y_{ndsc,i}$, and $Y_{nasc,i}$ (cf Eq 6-12) are assumed to equal 0.6, 0.5 and 0.5, respectively. The noise terms $\sigma^2_{\varepsilon_s}$, $\sigma^2_{\varepsilon_{ndsc}}$, and $\sigma^2_{\varepsilon_{nasc}}$ are assumed to be 15, 200, and 200 percent of $\sigma^2_{Ys_i}$, $\sigma^2_{Yndsc_i}$, and $\sigma^2_{Ynasc_i}$, respectively. The noise terms for the nonstructural components are as much as twice $\sigma^2_{Yns_i}$ to reflect the diversity of nonstructural components in each building. The sensitivity of the estimated total loss to these assumptions and to correlation between $Y_{s,i}$ and $Y_{ns,i}$ will be examined in Chapter 7.

The probability mass functions of structural and nonstructural replacement cost for each RES4, IND1, and COM4 buildings are presented in Figures 4-5, 4-6, and 5-1, respectively. The NDSC repair costs for occupancy classes RES4, IND1, and COM4 are 43.2, 11.8, and 32.9 percent of full replacement costs, respectively, while the NASC repair costs for those classes are 43.2, 72.5, and 47.9 percent of full replacement cost (FEMA/NIBS, 2003). The NDSC repair cost ratios are 2, 10, 50, and 100 percent of total NDSC replacement cost for slight, moderate, extensive, complete damage states, respectively; while the NASC repair cost ratios are 2, 10, 30, and 100 percent of total NASC replacement cost for the same damage states.

[1] Recall that the structural loss to the entire inventory was estimated from a sample of 100 buildings of each category taken from that inventory. When nonstructural losses are included, however, even this reduction is insufficient, and the sample size must be reduced further. As will be shown, 25 buildings yield a reasonably accurate estimate of total loss.

The probability mass functions of building contents loss are shown for individual RES4 buildings in Figure 6-8, IND1 buildings in Figure 6-9, and COM4 buildings in Figure 6-10. These PMFs are estimated from the histogram of the building contents dollar exposure of the average single building, which is computed by dividing the building contents dollar exposure of all buildings in each tract by the number of buildings in each tract provided in HAZUS-MH (MR4). The building contents repair cost ratios are 1, 5, 25, and 50 percent of total content cost for slight, moderate, extensive, and complete damage states (FEMA/NIBS, 2003). At the complete damage state, it is assumed that there is some salvage value of the building contents (FEMA/NIBS, 2003).

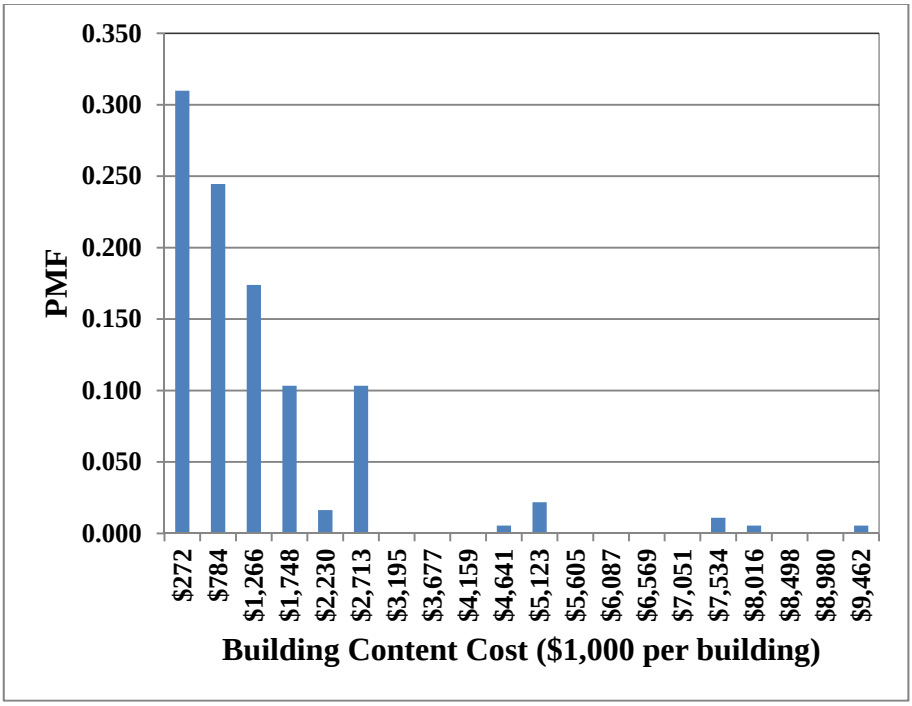

Figure 6-8 Probability mass function of the building contents cost for occupancy class RES4

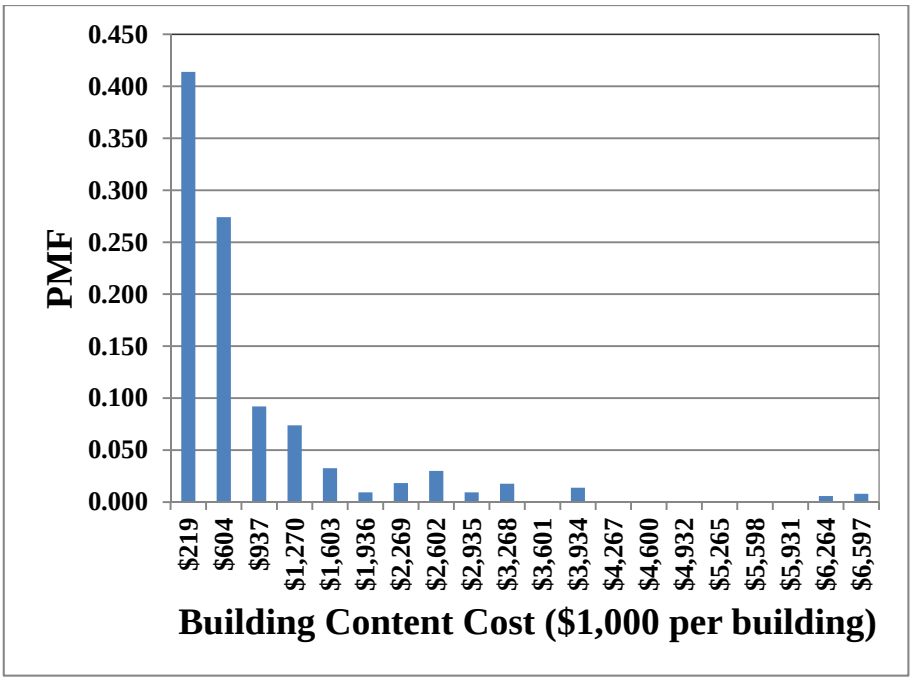

Figure 6-9 Probability mass function of the building contents cost for occupancy class COM4

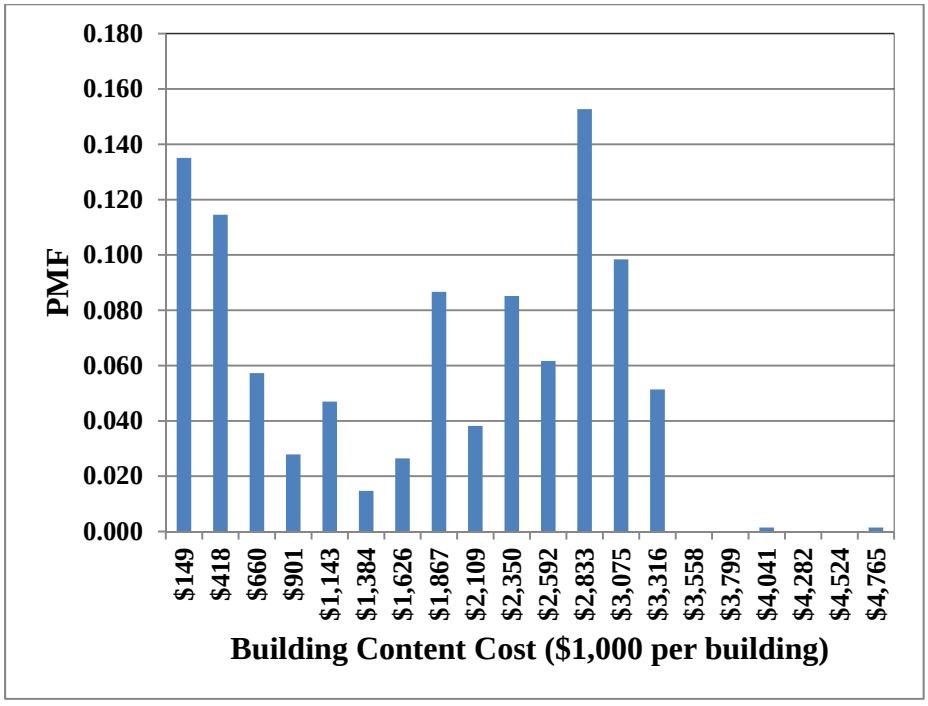

Figure 6-10 Probability mass function of the building contents cost for occupancy class IND1

6.3.1 Scenario Earthquake Risk Assessment (SERA)

Assume that the building inventories are exposed to a scenario earthquake with moment magnitude M_w 7.7 at latitude 35.74° and longitude -90.10°, as shown in Figure 4-4. The combined total loss ratios are estimated for five cases, as shown in Table 6-2. In Case 1 represent losses of all buildings are statistically independent. The results of case 2 can be computed by summation of nonstructural losses with structural losses that were already determined in Chapter 5.

Table 6-2 Five cases of damage correlation in aggregating total loss ratio

	Damage Correlation within Single Building	**Structural Damage Correlation between Buildings**	**Ground Motion Correlation between Buildings**
Case 1	0.0	0.0	0.0
Case 2	0.0	0.0	SGM model[c]
Case 3	S-NDSC-NASC model-based[a]	0.0	SGM model[c]
Case 4	S-NDSC-NASC model-based[a]	Model-based[b]	SGM model[c]
Case 5	S-NDSC-NASC model-based[a]	0.9	SGM model[c]

[a] S-NDSC-NASC model-based developed in Section 6.3
[b] Model-based developed in Chapter 3
[c] SGM model abbreviated from a spatial ground motion correlation model presented in Chapter 3

The means and coefficients of variation of total loss ratio for 184 RES4, 4,793 COM4, 681 IND1 buildings, and all buildings combined are summarized in Table 6-3, Table 6-4, Table 6-5, and Table 6-6. Under this scenario earthquake, the means of the combined nonstructural and structural loss ratios for all occupancy classes in Table 6-6 are approximately 8 percent of the full building replacement cost, while the mean of the total structural loss (cf Tables 5-2) is 12 percent of the full structural replacement cost. From the structural and nonstructural repair cost ratios (cf Table 4-2), these results imply that, on average, the nonstructural components are "slightly" damaged, while the structural components are "moderately" damaged. However, in the comparison of

structural and nonstructural losses shown in Table 6-7, nonstructural losses are 90 percent of the total losses. Table 6-8 shows the examples of the median spectral displacements for each damage state for structural and NDSC components designed at a moderate code level from HAZUS-MH (FEMA/NIBS, 2003) that are used in this study. Building types in which the median spectral displacement of the structural fragility is less than that of nonstructural fragility are shown by italics in Table 6-8. This explains why, on average, the nonstructural components appear to be less damaged at a particular ground motion intensity than the structural components.

The coefficients of variation of the total loss ratio for cases 2 to 5, where correlations are considered, are significantly greater than those for case 1, where correlations are neglected. However, the coefficients of variation of the total loss ratio for Case 3 are only slightly greater than those for Case 2 (cf Table 6-2), in which correlations between structural and nonstructural losses are neglected. These results imply that the effect of correlation in ground motion intensity between buildings on total loss is more significant than that of correlation between structural and nonstructural damage. Of course, this finding depends on the assumptions regarding structural and nonstructural damage correlations within a building in Eq (6-12), an assumption that will be examined further in the sensitivity analysis performed in Chapter 7. The coefficients of variation in the total loss of 184 RES4 buildings for cases 4 and 5 are only 2 and 6 percent greater than those for case 3, in which correlations between structural and nonstructural losses within one building are considered but pairwise correlation in structural damage between two buildings is neglected. Nonstructural loss estimates which do not consider pairwise damage correlation between buildings are 85 percent of

the aggregated total loss, while the structural losses, which are significantly affected by the damage correlation as illustrated in Chapter 5, are only 15 percent of the aggregated total loss, as shown in Table 6-7. The coefficients of variation of the total losses to 4,793 COM4, 681 IND1 buildings, and all building combined for cases 4 and 5 are slightly less than those of case 3.

Tables 6-3 through 6-6 also show the total loss ratios estimated for various sample sizes, and indicate that the estimates of coefficients of variation of small sample sizes are larger than those of larger sample size by as much as 25 percent. Examples of the exceedence probability of the total loss ratio from different sample sizes representing 184 RES4 buildings for cases 2 to 5 are illustrated in Figure 6-11 to Figure 6-15. The exceedence probabilities of these three sample sizes are quite similar except for cases 1 and 4, which the sample size of 25 buildings yields a conservative loss estimate. Hence, in order to determine risk curves and probable maximum loss, sample sizes of 25 buildings will be used to reduce computer resources and calculation times. Given that an earthquake with M_w 7.7 effects Shelby County, TN, there is 10% probability that losses to the building inventory would exceed 15 percent when correlations are considered, and 1% probability that the losses would exceed 25 percent. These losses decrease to 9 and 15 percent when all sources of correlations are neglected. Thus, neglect of correlations may cause the loss ratios at the probability levels to be underestimated by a factor of 1.7.

Table 6-3 Total loss ratio for 184 RES4 buildings in Shelby County, TN exposed to M_w 7.7 earthquake

Sample Size (n_a)	Case 1		Case 2		Case 3		Case 4		Case 5	
	μ^*	V^+	μ^*	V^+	μ^*	V^+	μ^*	V^+	μ^*	V^+
25	0.075	0.363	0.072	0.615	0.072	0.631	0.072	0.654	0.071	0.649
50	0.075	0.288	0.072	0.558	0.072	0.561	0.071	0.576	0.072	0.581
100	0.075	0.206	0.072	0.520	0.072	0.531	0.072	0.542	0.072	0.564

*μ is E[$LR_{T,a}$]
+V is CoV[$LR_{T,a}$]

Table 6-4 Total loss ratio for 4,793 COM4 buildings in Shelby County, TN exposed to M_w 7.7 earthquake

Sample Size (n_a)	Case 1		Case 2		Case 3		Case 4		Case 5	
	μ^*	V^+	μ^*	V^+	μ^*	V^+	μ^*	V^+	μ^*	V^+
25	0.084	0.417	0.080	0.760	0.081	0.760	0.081	0.782	0.080	0.781
50	0.083	0.319	0.080	0.702	0.080	0.700	0.079	0.715	0.080	0.717
100	0.084	0.223	0.080	0.672	0.080	0.684	0.081	0.686	0.080	0.690

$^*\mu$ is E[$LR_{T,a}$]
^+V is CoV[$LR_{T,a}$]

Table 6-5 Total loss ratio for 681 IND1 buildings in Shelby County, TN exposed to M_w 7.7 earthquake

Sample Size (n_a)	Case 1		Case 2		Case 3		Case 4		Case 5	
	μ^*	V^+	μ^*	V^+	μ^*	V^+	μ^*	V^+	μ^*	V^+
25	0.080	0.387	0.076	0.854	0.077	0.838	0.077	0.868	0.076	0.851
50	0.080	0.285	0.076	0.817	0.077	0.802	0.075	0.818	0.075	0.826
100	0.080	0.200	0.076	0.789	0.076	0.801	0.077	0.790	0.076	0.797

$^*\mu$ is E[$LR_{T,a}$]
^+V is CoV[$LR_{T,a}$]

Table 6-6 Total loss ratio for all buildings in Shelby County, TN exposed to M_w 7.7 earthquake

Sample Size (n_a)	Case 1		Case 2		Case 3		Case 4		Case 5	
	μ^*	V^+	μ^*	V^+	μ^*	V^+	μ^*	V^+	μ^*	V^+
25	0.075	0.227	0.075	0.641	0.076	0.635	0.075	0.661	0.075	0.652
50	0.078	0.176	0.075	0.623	0.075	0.614	0.074	0.629	0.074	0.635
100	0.078	0.123	0.075	0.608	0.075	0.619	0.075	0.617	0.075	0.631

$^*\mu$ is E[LR_T]
^+V is CoV[LR_T]

Table 6-7 Comparison of total loss for all buildings in Shelby County, TN exposed to M_w 7.7 earthquake event

Loss	E[L_T]					
	Structural Loss ($1,000)	Nonstructural Loss ($1,000)				Total Loss ($1,000)
		NDSC	NASC	BC	All Nonstructural	
184 RES4	3,616	10,524	5,826	8,245	24,595	28,211
4,793 COM4	1,834	2,651	2,610	6,661	11,923	13,757
681 IND1	2,224	1,386	5,293	13,523	20,202	22,427
Total	7,675	14,561	13,729	28,429	56,720	64,395

Table 6-8 Examples of median spectral displacements for structural and nonstructural drift-sensitive damage – Moderate code (The complete table is in Appendix B, Table B-1)

Building Type	Median of Spectral Displacement (inches)							
	Slight		Moderate		Extensive		Complete	
	S	NDSC	S	NDSC	S	NDSC	S	NDSC
W1	0.50	0.50	1.25	1.01	3.86	3.15	9.45	6.30
W2	0.86	0.86	2.14	1.73	6.62	5.40	16.20	10.80
S1L	1.30	0.86	2.24	1.73	*5.08*	*5.40*	12.96	10.80
.	.	.	.	.	.	.	.	.
.	.	.	.	.	.	.	.	.
.	.	.	.	.	.	.	.	.
URMM	*0.63*	*1.26*	*1.26*	*2.52*	*3.15*	*7.88*	*7.35*	*15.75*
MH	0.48	0.48	0.96	0.96	*2.88*	*3.00*	8.40	6.00

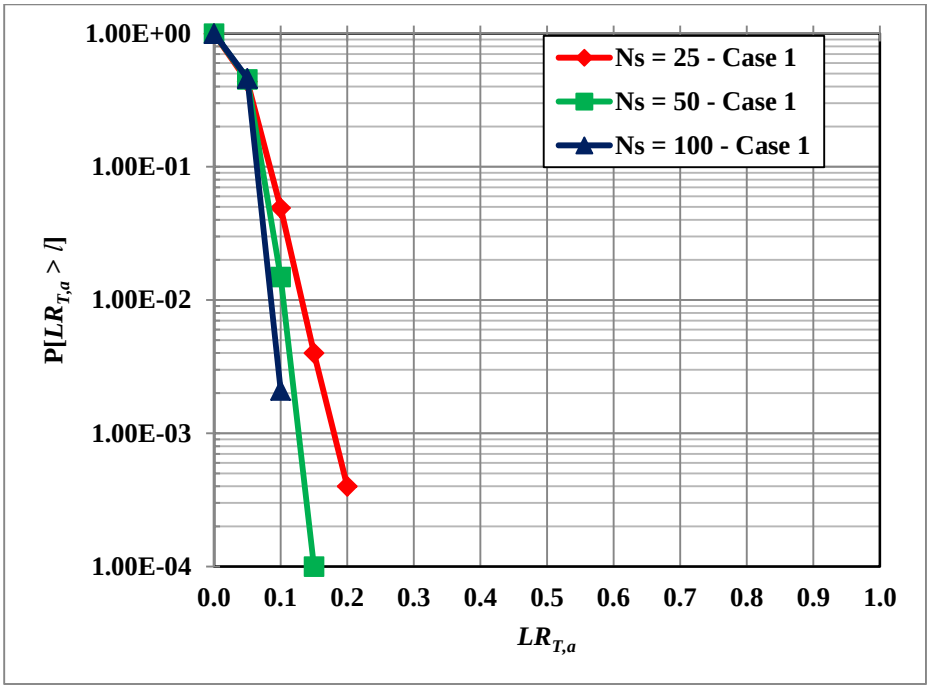

Figure 6-11 Case 1 exceedence probabilities of total loss ratio for 184-RES4 buildings in Shelby County, TN exposed to M_w 7.7 earthquake event

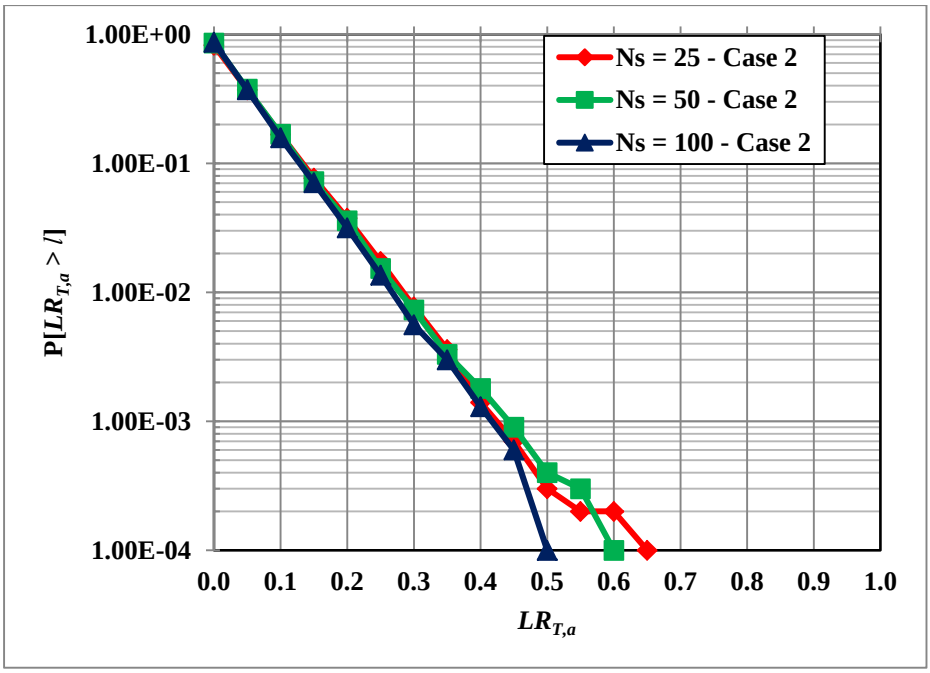

Figure 6-12 Case 2 exceedence probabilities of total loss ratio for 184-RES4 buildings in Shelby County, TN exposed to M_w 7.7 earthquake event

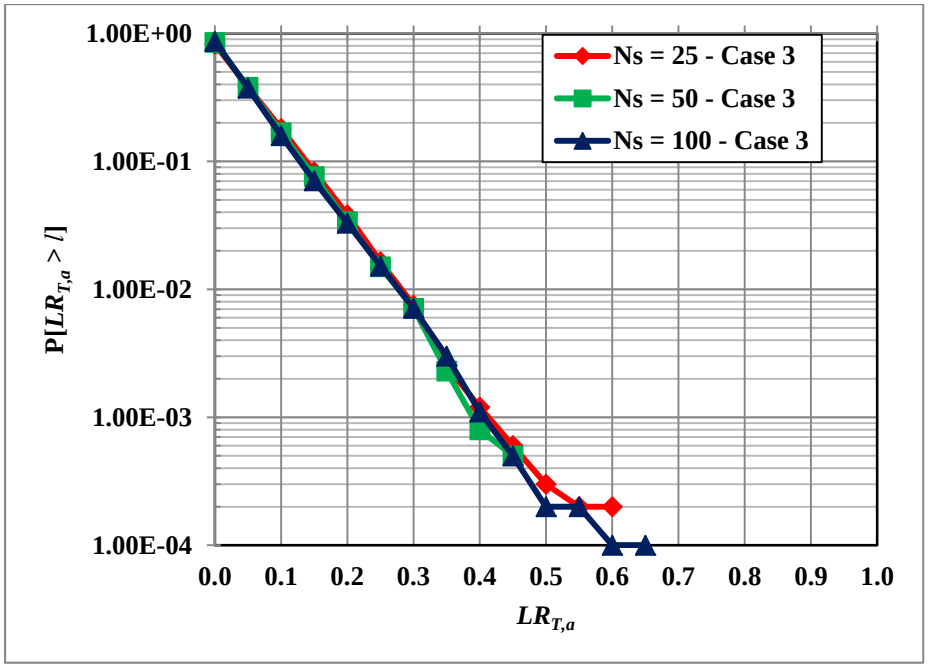

Figure 6-13 Case 3exceedence probabilities of total loss ratio for 184-RES4 buildings in Shelby County, TN exposed to M_w 7.7 earthquake event

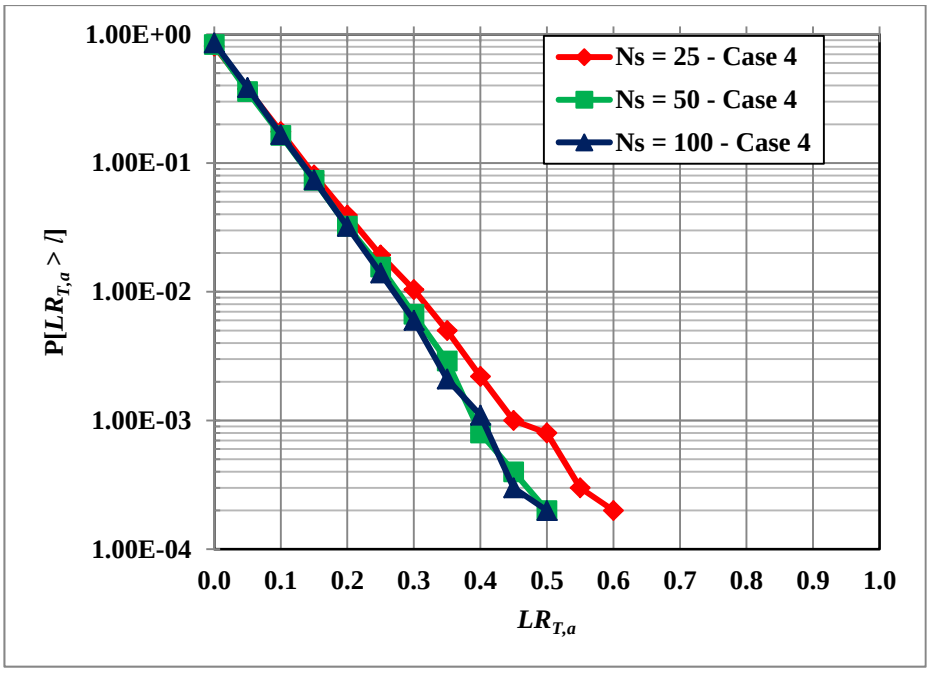

Figure 6-14 Case 4 exceedence probabilities of total loss ratio for 184-RES4 buildings in Shelby County, TN exposed to M_w 7.7 earthquake event

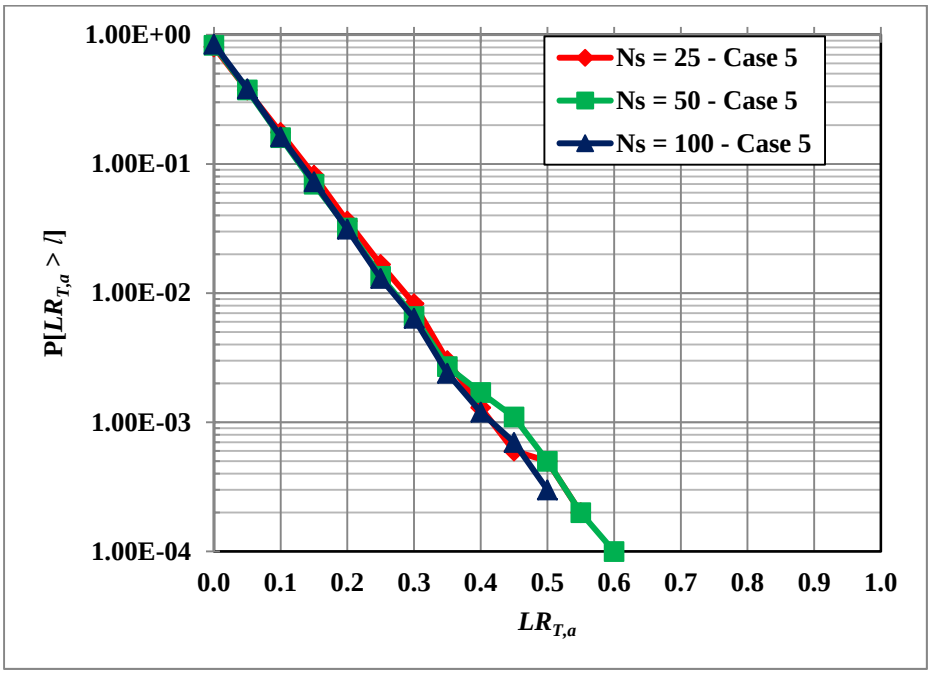

Figure 6-15 Case 5 exceedence probabilities of total loss ratio for 184-RES4 buildings in Shelby County, TN exposed to M_w 7.7 earthquake event

6.3.2 Probabilistic Seismic Risk Assessment (PSRA)

In PSRA, the five seismic zones and their parameters, which are described in Chapter 5 (cf Table 5-4), are considered. The risk curves describing the mean annual frequency for the aggregated nonstructural and structural losses to 184 RES4, 4,793-COM4, 681-IND1 buildings, and all buildings combined, are illustrated in Figure 6-16, Figure 6-17, Figure 6-18, and Figure 6-19, for the five cases listed in Table 6-2. When the mean annual frequency is higher than 2×10^{-4}/year, the total loss ratios for every case are quite similar. When the mean annual frequency is lower than 2×10^{-4}/year, the total loss ratio for case 1, in which all building losses are statistically independent, is less than those for the other cases, where correlations are considered, implying that neglecting correlation in demand and damage at such annual frequencies leads to an unconservative estimate risk. The risk curves for cases 2 to 5 confirm that correlation in seismic demand dominates the variance of the total loss ratios. Furthermore, damage correlations appear to become more significant to the risk estimates when losses with low probability but high consequence are estimated.

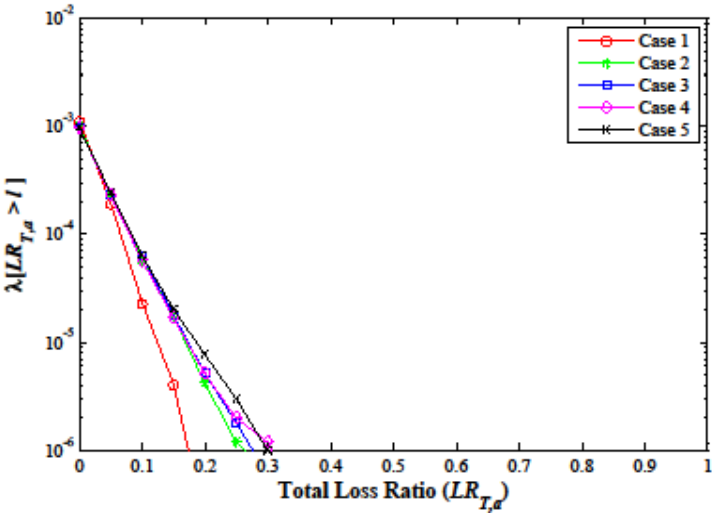

Figure 6-16 Annual frequency of total loss ratio of 184 RES4 buildings - all earthquake sources aggregated.

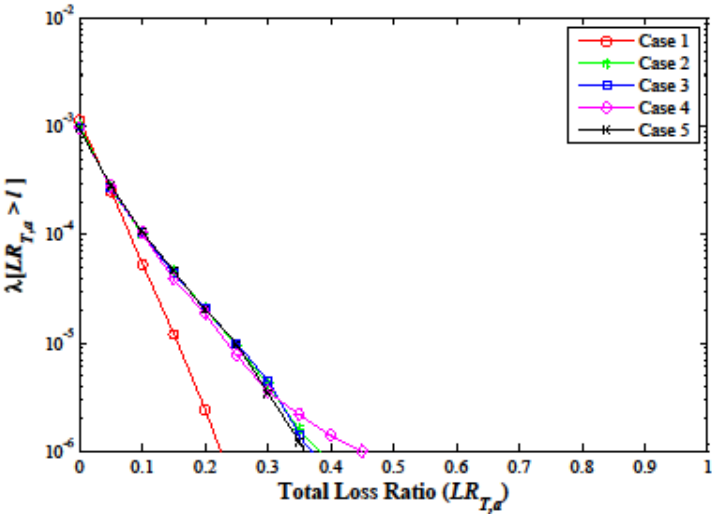

Figure 6-17 Annual frequency of total loss ratio of 4,793 COM4 buildings - all earthquake sources aggregated.

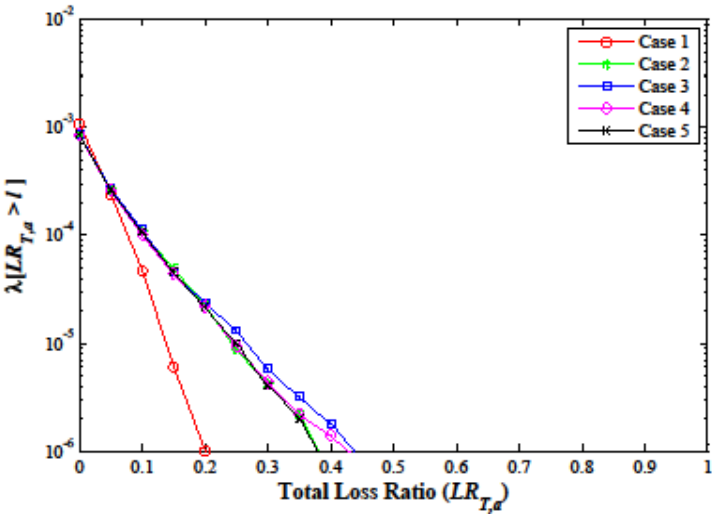

Figure 6-18 Annual frequency of total loss ratio of 681 IND1 buildings - all earthquake sources aggregated.

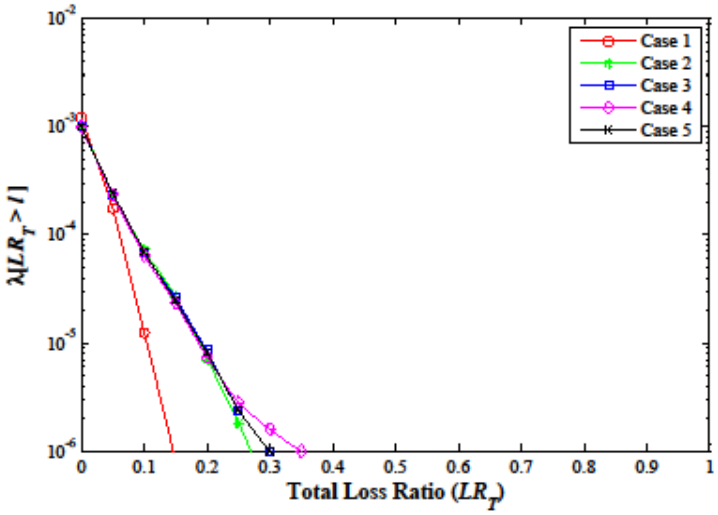

Figure 6-19 Annual frequency of total loss ratio of all buildings in portfolios - all earthquake sources aggregated.

6.3.3 Probable Maximum Loss

Figure 6-16, Figure 6-17, Figure 6-18, and Figure 6-19 represent the exceedence probabilities of the aggregation of nonstructural and structural losses for 184-RES4, 4973-COM4, 681-IND1 buildings, and all buildings in the inventory. The PML of all buildings for each occupancy class and for the aggregated building occupancies are summarized in Table 6-9. The PML at EPs of $1\times10^{-4}$and 1×10^{-5}'s are 25 and 70 percent higher when considering demand and damage correlations than PMLs when these correlations are neglected. The PML at both exceedence probabilities for cases 2 to 5 (cf Table 6-2) are about the same, implying that seismic demand correlation has more influence than damage correlation at EPs of 1×10^{-4} or 1×10^{-5}. This is caused by the assumption that there are no damage correlations between nonstructural components in pairs of buildings and that the correlation of structural and nonstructural damage in Eq (6-12) within a building is relatively low.

Table 6-9 Probable maximum loss at a specific exceedence probability of aggregate loss ratio

Portfolio	PML at EP = 10^{-4}					PML at EP = 10^{-5}				
	Case					Case				
	1	2	3	4	5	1	2	3	4	5
184 RES4	0.077	0.088	0.089	0.088	0.090	0.134	0.180	0.186	0.180	0.187
4,793 COM4	0.089	0.102	0.105	0.102	0.105	0.158	0.242	0.250	0.243	0.237
681 IND1	0.085	0.108	0.105	0.105	0.106	0.145	0.245	0.267	0.255	0.248
All buildings	0.073	0.092	0.091	0.091	0.091	0.115	0.187	0.198	0.191	0.199

6.4 Summary

This chapter presented a method to aggregate nonstructural and structural losses to building inventories. Nonstructural losses result from damages to nonstructural drift-sensitive (NDSC) components, nonstructural acceleration-sensitive (NASC) components, and building contents (BC). The damage to NDSC is measured by NDSC fragility functions, while the damage to both NASC and BC is computed from NASC fragility functions. These fragility functions are taken from HAZUS-MH (MR4). Only correlation in ground motion intensities between pairwise buildings was considered in estimating nonstructural losses, in contrast to the estimation of structural loss, which included both ground motion and damage correlations.

A scenario earthquake risk assessment and a probabilistic risk seismic assessment were performed, the latter assessment leading to an estimate of probable maximum loss (PML), to building inventories in Shelby County, TN. The mean of the combined nonstructural and structural losses to the building inventory estimated from the SERA was 8 percent of the total replacement cost. The coefficients of variation of the total loss for the cases where correlations in demand and damage were considered were at least 80 percent higher than the corresponding coefficients of variation when both correlations

were neglected. However, the coefficients of variation of the total loss ratio for the cases where correlations in demand and damage were considered only were slightly greater than those for the case in which only demand correlation was included. These results indicate that damage correlation has an insignificant effect on the uncertainty of building inventory losses in which nonstructural loss dominates. However, it has a significant impact on the uncertainty in loss to spatially distributed structures in which structural losses are a large portion of the total loss (i.e. bridges and certain nonbuilding civil infrastructure) (Lee and Kiremidjian, 2007). Similarly, the results of the PSRA and PML for the cases where demand and damage correlations were included were quite similar to when only demand correlation was considered. Finally, the PMLs at annual exceedence probabilities of 1×10^{-4} and 1×10^{-5} where losses of all buildings are statistically independent are, respectively, 9 and 15 percent of the total replacement cost, while the corresponding PMLs where losses to all building are partially correlated are, respectively, 11 and 25 percent of the total replacement cost. Thus, neglect of spatial correlation in ground motion intensity and correlation in damage may caused the PML to be underestimated by as much as 70 percent.

The variances in the total losses were evaluated from models of damage correlation between structural and nonstructural components that involved a number of plausible but nonetheless assumed parameters. The sensitivity of the total losses to these assumptions will be examined in the next chapter.

CHAPTER 7

UNCERTAINTY AND SENSITIVITY ANALYSIS

The risk assessments of buildings and building inventories presented in Chapters 4 through 6 are based on numerous modeling assumptions and parameters, including ground motion attenuation models and correlations in seismic demand and building performance. The selection of ground motion attenuation model affects the expected value of total structural loss because the mean (or median) seismic demands are determined by the ground motion model selected. Correlations in seismic demand and building damage have a significant impact on the variance in total structural loss.

This chapter examines the sensitivity of the loss estimates presented in Chapters 4 through 6 to some of the assumptions that were made necessary by modeling or limiting in available data sources. Section 7.1 will consider the sensitivity of the estimated risk to building inventories caused by the selection of ground motion attenuation model under a scenario earthquake. The sensitivity of the uncertainty (variance) of the total structural losses to those parameters assumed in the demand and damage correlation models also will be examined. Section 7.2 will examine the sensitivity of the variance of the total loss to the presumed parameters in the model of damage correlation between structural and nonstructural components. In Section 7.3, an analysis of epistemic uncertainty in total structural loss ratio and probable maximum loss will be presented.

7.1 Dependence of Total Structural Loss Ratio to Choice of Attenuation Model and Damage Correlation Models under a Scenario Earthquake

In this section the sensitivity of the estimated risk (loss) to the selection of ground motion attenuation prediction equation and to assumed correlations in demand and damage that were presented in Chapter 3 are examined to test which parameters have the most significant effect on loss estimates. For this purpose, the risk to 184 RES4 and 681 IND1 buildings under a scenario earthquake event with M_w 7 and an epicenter at latitude 35.4° and longitude -90.2°, which is similar to the event illustrated in Chapter 4, is investigated. The number of buildings in each census tract and the epicenter were illustrated in Figure 4-2 and Figure 4-3, respectively.

7.1.1 Sensitivity of Total Structural Loss Ratio to Ground Motion Attenuation Model

The ground motion attenuation prediction equation is one of the most important ingredients for estimating loss to a building inventory because it determines the mean seismic intensity at each site. The losses estimated in previous chapters were based on the Atkinson and Boore (1995) attenuation model. Other attenuation models are considered in the following paragraphs.

Table 7-1, Table 7-2, and Table 7-3 shows how the choice of attenuation relationship affects the mean value, standard deviation, and coefficient of variation of the total structural loss ratio for 184-RES4 buildings, 681-IND1 buildings, and the two occupancy classes combined. The expected losses using the Atkinson and Boore 1995 (AB95) attenuation are approximate 20% less than those due to the Campbell 2003 (C03)

attenuation, while the results from the Atkinson and Boore 2006 (AB06) attenuation relation are only 50% of the losses estimated using attenuation C03. These differences reflect the fact that the expected loss to a single building in occupancy classes RES4 and IND1 due to attenuation C03 are 1.2 and 1.5 times of those due to attenuations AB95 and AB06, respectively, as illustrated in Figure 7-1 and Figure 7-2. Plots of seismic demands as a function of epicentral distance from the three ground motion attenuation models for RES4 and IND1 are presented in Figure 7-3 and Figure 7-4, respectively[1]. Seismic demands computed from the AB06 and AB95 attenuations are 50% and 80% of those from the C03 attenuation model. The differences in seismic demand arise from the fact that the parameters of the new equations (Eq 3-8) are estimated from a stochastic ground-motion model (Eq 3-1) that used lower average stress drop parameters and a steeper near-source attenuation (Atkinson and Boore, 2006).

Table 7-1 Sensitivity of structural loss ratio to ground motion attenuation model for 184-RES4 buildings in Shelby County, TN exposed to a M_w7 earthquake

Structural Loss Ratio	**Occupancy Class: 184 RES4**								
	Damage Correlation (ρ_D = 0.0)			**Damage Correlation (Based-Model)**			**Damage Correlation (ρ_D = 0.9)**		
	Ground Motion Attenuation			**Ground Motion Attenuation**			**Ground Motion Attenuation**		
	AB95$^+$	**AB06$^+$**	**C03$^+$**	**AB95$^+$**	**AB06$^+$**	**C03$^+$**	**AB95$^+$**	**AB06$^+$**	**C03$^+$**
E[LR_T]	0.0844	0.0461	0.0940	0.0791	0.0466	0.0935	0.0906	0.0462	0.0934
SD[LR_T]	0.0530	0.0355	0.0533	0.0913	0.0651	0.1028	0.1405	0.0836	0.1352
CoV[LR_T]	0.6276	0.7689	0.5670	1.1541	1.3986	1.0991	1.5507	1.8096	1.4478

$^+$AB95 = Atkinson and Boore (1995), AB06 = Atkinson and Boore (2006), and C03 = Campbell (2003)

[1] Recall that the alternative ground motion attenuation model defines the seismic intensity at the building site, while the seismic demand is defined by the capacity spectrum method.

Table 7-2 Sensitivity of structural loss ratio to ground motion attenuation model for 681-IND1 buildings in Shelby County, TN exposed to a M_w7 earthquake

Structural Loss Ratio	Occupancy Class: 681 IND1								
	Damage Correlation (ρ_D = 0.0)			Damage Correlation (Based-Model)			Damage Correlation (ρ_D = 0.9)		
	Ground Motion Attenuation			Ground Motion Attenuation			Ground Motion Attenuation		
	AB95[+]	AB06[+]	C03[+]	AB95[+]	AB06[+]	C03[+]	AB95[+]	AB06[+]	C03[+]
E[LR_T]	0.0899	0.0553	0.1164	0.0892	0.0565	0.1155	0.0987	0.0566	0.1154
SD[LR_T]	0.0555	0.0434	0.0646	0.0962	0.0729	0.1104	0.1542	0.0987	0.1541
CoV[LR_T]	0.6181	0.7850	0.5545	1.0789	1.2909	0.9561	1.5620	1.7421	1.3349

[+]AB95 = Atkinson and Boore (1995), AB06 = Atkinson and Boore (2006), and C03 = Campbell (2003)

Table 7-3 Sensitivity of structural loss ratio to ground motion attenuation model for 184-RES4 and 681-IND1 buildings in Shelby County, TN exposed to a M_w7 earthquake

Structural Loss Ratio	Occupancy Class: 184 RES4 + 681 IND1								
	Damage Correlation (ρ_D = 0.0)			Damage Correlation (Based-Model)			Damage Correlation (ρ_D = 0.9)		
	Ground Motion Attenuation			Ground Motion Attenuation			Ground Motion Attenuation		
	AB95[+]	AB06[+]	C03[+]	AB95[+]	AB06[+]	C03[+]	AB95[+]	AB06[+]	C03[+]
E[LR_T]	0.0861	0.0493	0.1017	0.0827	0.0500	0.1011	0.0940	0.0498	0.1009
SD[LR_T]	0.0498	0.0348	0.0526	0.0863	0.0629	0.0973	0.1470	0.0873	0.1397
CoV[LR_T]	0.5782	0.7074	0.5169	1.0435	1.2579	0.9628	1.5635	1.7540	1.3842

[+]AB95 = Atkinson and Boore (1995), AB06 = Atkinson and Boore (2006), and C03 = Campbell (2003)

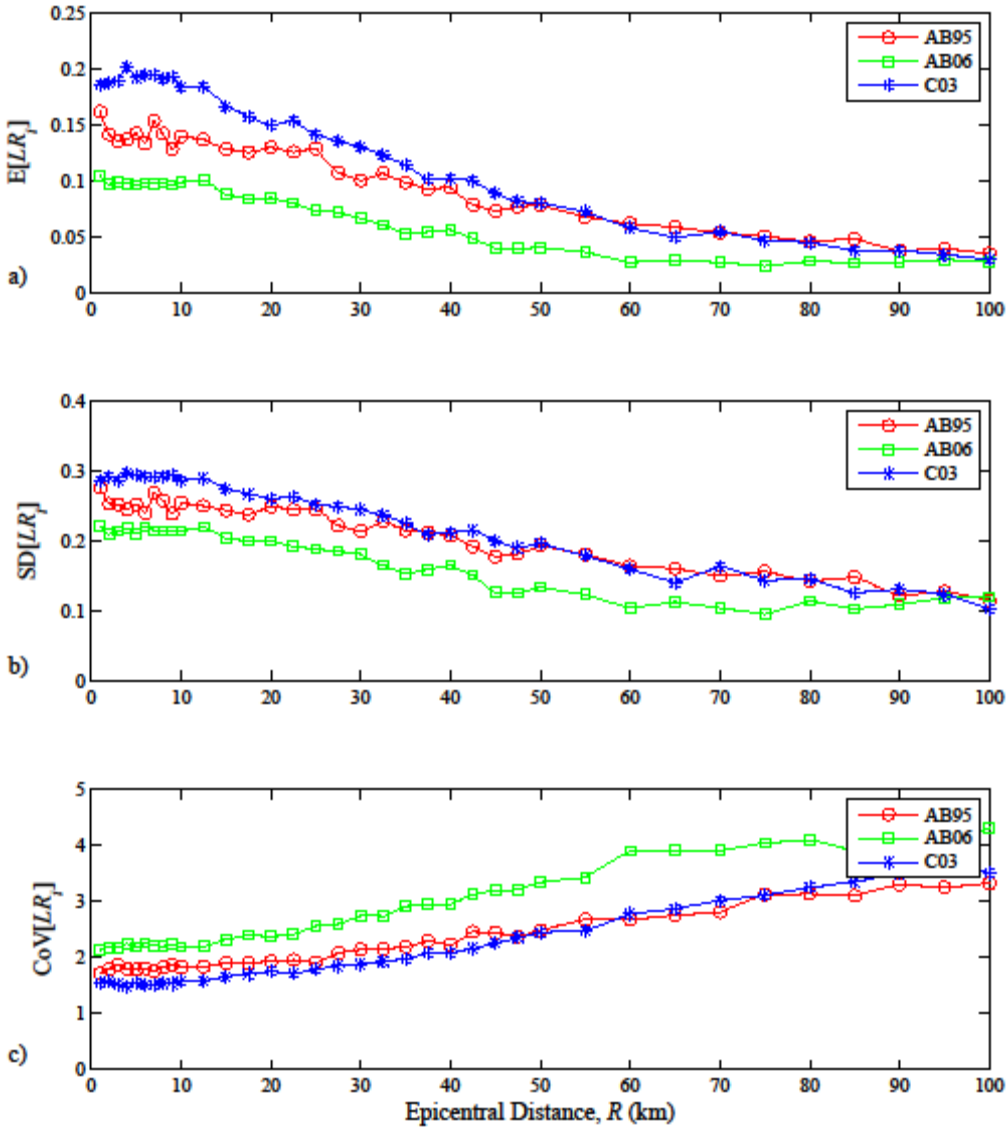

Figure 7-1 a) Mean, b) standard deviation, and c) coefficient of variation of structural loss ratio for single RES4 building computed from different ground motion attenuation relationships

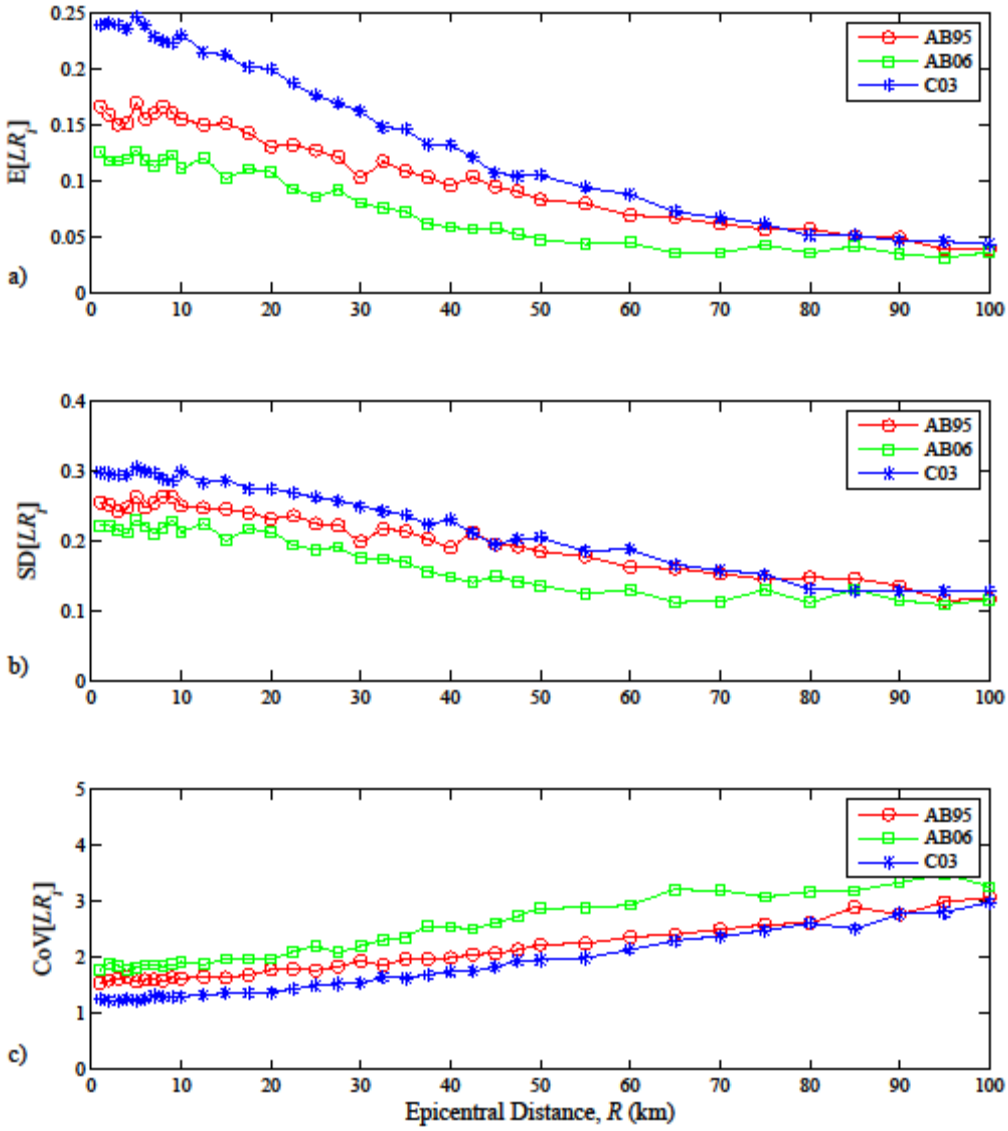

Figure 7-2 a) Mean, b) standard deviation, and c) coefficient of variation of structural loss ratio for single IND1 building computed from different ground motion attenuation relationships

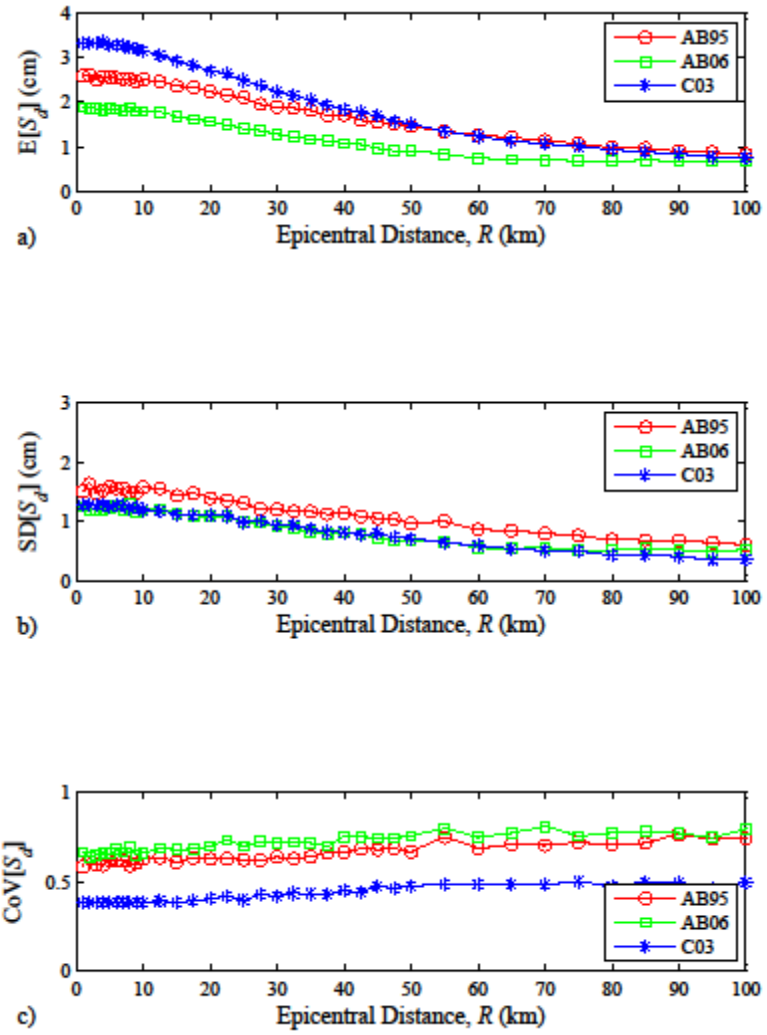

Figure 7-3 a) Mean, b) standard deviation, and c) coefficient of variation of spectral displacement for single RES4 building computed from different ground motion attenuation relationships

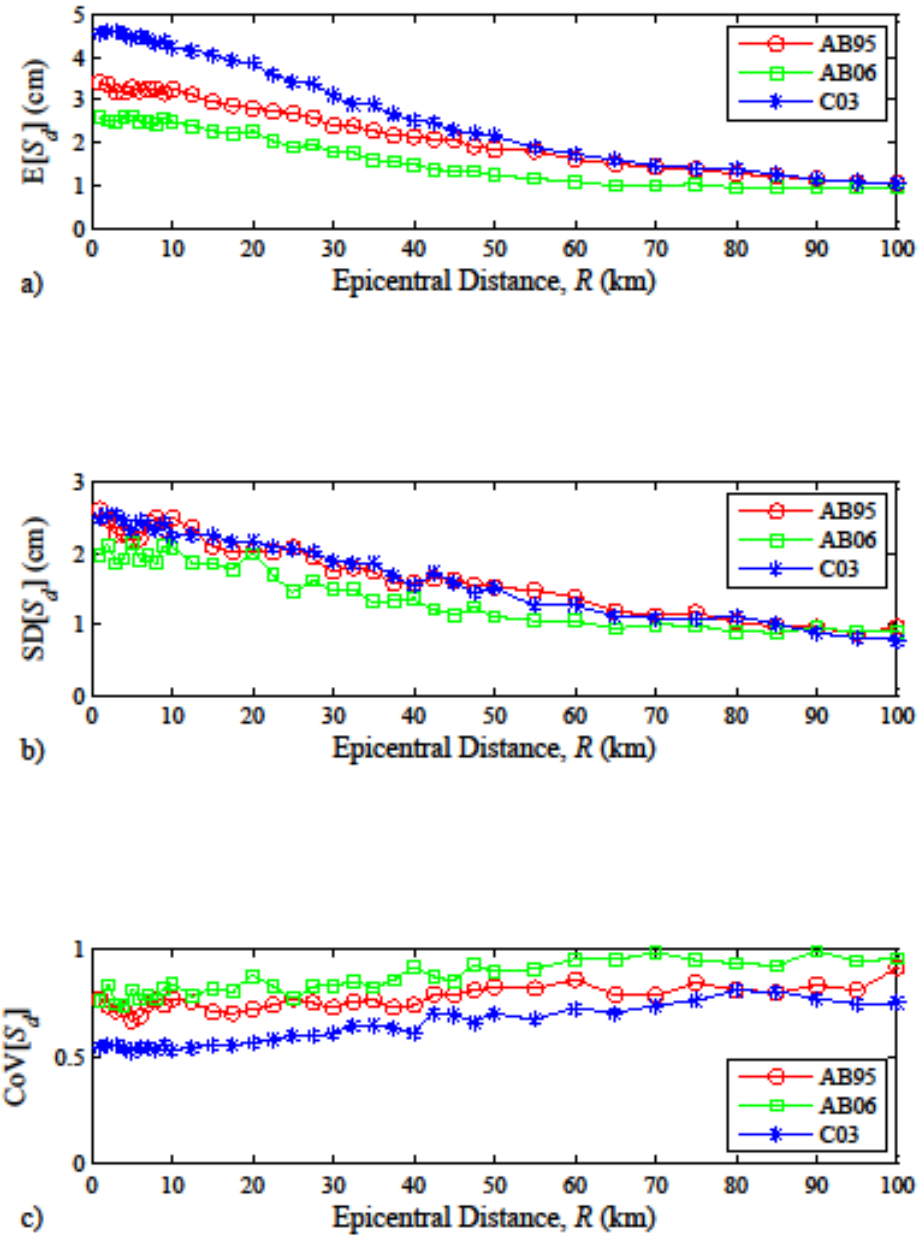

Figure 7-4 a) Mean, b) standard deviation, and c) coefficient of variation of spectral displacement for single IND1 building computed from different ground motion attenuation relationships

7.1.2 Sensitivity of Total Structural Loss Ratio to Spatial Ground Motion Correlation Distance

Spatial ground motion correlation distance (Eq 3-14) plays an important role in estimating the uncertainty (variance) in the total structural loss ratio because the variance is influenced by pairwise correlations of the individual losses in the building inventory. At the present time, there are no data with which to estimate this correlation distance between sites in the Eastern United States, and the correlation distance was assumed to equal 50 km for reasons described in Chapter 3. Therefore, the impact of this assumption on the loss to the building inventories must be considered.

The dependence of the uncertainty (measured by standard deviations and coefficients of variation) in the total structural loss ratio on correlation distance of spatial ground motion for 184 RES4, 681 IND1 buildings, and both occupancy classes is summarized in Table 7-4, Table 7-5, and Table 7-6. Since the spatial correlation in ground motion for a given scenario earthquake clearly is non-negative, the standard deviation in the total loss might be expected to increase as the ground motion correlation distance is increased and the seismic demands become more coherent over a larger area. When the correlation distance is increased from 2 to 10 times over the baseline assumption, the coefficients of variation in estimated losses are increased by up to 10 to 15 percent if either lower or upper bound damage correlations are assumed. However, increasing the ground motion correlation distance by a factor of 2 or 10 when the model-based damage correlation is considered only increases the coefficients of variation in estimated total loss by 3 to 6 percent. Thus, it can be concluded that the assumption

regarding the ground motion correlation distance has a relatively minor effect on the uncertainty in the total structural loss.

Table 7-4 Sensitivity of the total structural loss ratio to ground motion correlation distance for 184-RES4 buildings in Shelby County, TN, exposed to a M_w 7 earthquake.

Structural Loss Ratio	Occupancy Class: 184 RES4								
	Damage Correlation (ρ_D = 0.0)			Damage Correlation (Based-Model)			Damage Correlation (ρ_D = 0.9)		
	Ground Motion Correlation Distance			Ground Motion Correlation Distance			Ground Motion Correlation Distance		
	50 km	100 km	500 km	50 km	100 km	500 km	50 km	100 km	500 km
E[LR_T]	0.0844	0.0830	0.0827	0.0791	0.0835	0.0834	0.0906	0.0840	0.0831
SD[LR_T]	0.0530	0.0559	0.0575	0.0913	0.0985	0.1013	0.1405	0.1304	0.1456
CoV[LR_T]	0.6276	0.6740	0.6962	1.1541	1.1796	1.2148	1.5507	1.5523	1.7525

Table 7-5 Sensitivity of the total structural loss ratio to ground motion correlation distance for 681-IND1 buildings in Shelby County, TN, exposed to a M_w 7 earthquake.

Structural Loss Ratio	Occupancy Class: 681 IND1								
	Damage Correlation (ρ_D = 0.0)			Damage Correlation (Based-Model)			Damage Correlation (ρ_D = 0.9)		
	Ground Motion Correlation Distance			Ground Motion Correlation Distance			Ground Motion Correlation Distance		
	50 km	100 km	500 km	50 km	100 km	500 km	50 km	100 km	500 km
E[LR_T]	0.0899	0.0919	0.0908	0.0892	0.0916	0.0923	0.0987	0.0933	0.0921
SD[LR_T]	0.0555	0.0614	0.0638	0.0962	0.0996	0.1012	0.1542	0.1418	0.1510
CoV[LR_T]	0.6181	0.6673	0.7030	1.0789	1.0866	1.0968	1.5620	1.5206	1.6393

Table 7-6 Sensitivity of the total structural loss ratio to ground motion correlation distance for both occupancy classes in Shelby County, TN, exposed to a M_w 7 earthquake.

Structural Loss Ratio	Occupancy Class: 184 RES4 + 681 IND1								
	Damage Correlation (ρ_D = 0.0)			Damage Correlation (Based-Model)			Damage Correlation (ρ_D = 0.9)		
	Ground Motion Correlation Distance			Ground Motion Correlation Distance			Ground Motion Correlation Distance		
	50 km	100 km	500 km	50 km	100 km	500 km	50 km	100 km	500 km
E[LR_T]	0.0861	0.0861	0.0855	0.0827	0.0863	0.0864	0.0940	0.0872	0.0862
SD[LR_T]	0.0498	0.0538	0.0559	0.0863	0.0928	0.0948	0.1470	0.1332	0.1459
CoV[LR_T]	0.5782	0.6249	0.6547	1.0435	1.0747	1.0972	1.5635	1.5272	1.6934

7.1.3 Sensitivity of Total Structural Loss Ratio to Damage Correlation Model

The impact of the assumed damage parameters in the building damage correlation model in Chapter 3 (Eq 3-26) is investigated by considering variations in the aggregated losses due to parameters σ_ε^2, β_ε, $\beta_{BTi,BTj}$, and $\beta_{Ci,Cj}$.

Table 7-7 shows the dependence of the standard deviations and the coefficients of variation in the aggregated structural loss ratio on the assumed noise variance (σ_ε^2) for three building inventories. Three values of σ_ε^2 are considered: 15, 30, and 50 percent of $\sigma_{Yi} \cdot \sigma_{Yj}$ for cases 1, 2, and 3, respectively. Case 1 is the value of σ_ε^2 that was used in Chapters 4 and 5. The change in σ_ε^2 has an insignificant effect on the uncertainty of the total losses. When σ_ε^2 is increased from 15 percent to 30 and 50 percent of $\sigma_{Yi} \cdot \sigma_{Yj}$, the coefficients of variation of the total loss of cases 2 and 3 are decreased to 93 and 87 percent of that of case 1. This decrease may be contrary to intuition, and one might think that the increase in σ_ε^2 should increase the variance of the aggregate losses. To verify the results presented in Table 6-7, recall Eq (3-26):

$$\rho_{DM_i,DM_j} = \frac{\rho_{Y_i,Y_j} \cdot \sigma_{Y_i} \cdot \sigma_{Y_j} + \sigma_\varepsilon^2 \cdot \exp\left[-\left(r_{ij} \middle/ \beta_\varepsilon\right)\right]}{\sqrt{\left(\sigma_{Y_i}^2 + \sigma_\varepsilon^2\right) \cdot \left(\sigma_{Y_j}^2 + \sigma_\varepsilon^2\right)}} \tag{3-26}$$

and differentiate Eq (3-26) with respect to σ_ε^2:

$$\begin{aligned} \frac{d}{d\sigma_\varepsilon^2} \rho_{DM_i,DM_j} = & \left[\left(\sigma_{Y_i}^2 + \sigma_\varepsilon^2\right) \cdot \left(\sigma_{Y_j}^2 + \sigma_\varepsilon^2\right)\right]^{-3/2} \cdot \\ & \left[\Delta \cdot \sigma_{Y_i}^2 \cdot \sigma_{Y_j}^2 - 0.5 \cdot \rho_{Y_i,Y_j} \cdot \sigma_{Y_i}^3 \cdot \sigma_{Y_j} - 0.5 \cdot \rho_{Y_i,Y_j} \cdot \sigma_{Y_i} \cdot \sigma_{Y_j}^3 + \right. \\ & \left. \left(0.5 \cdot \Delta \cdot \sigma_{Y_i}^2 - \rho_{Y_i,Y_j} \cdot \sigma_{Y_i} \cdot \sigma_{Y_j} + 0.5 \cdot \Delta \cdot \sigma_{Y_j}^2\right) \cdot \sigma_\varepsilon^2 \right] \end{aligned} \tag{7-1}$$

where $\Delta = \exp\left[-\left(r_{ij}/\beta_{\varepsilon}\right)\right]$. If Eq (7-1) is less than 0, Eq (3-26) will be a decreasing function of σ_{ε}^2. Assume that

$$\frac{d}{d\sigma_{\varepsilon}^2}\rho_{DM_i,DM_j} > 0 \tag{7-2}$$

After Eq (7-1) is rearranged, it becomes

$$\begin{aligned} &2\cdot\Delta\cdot\sigma_{Y_i}\cdot\sigma_{Y_j} - \rho_{Y_i,Y_j}\cdot\sigma_{Y_i}^2 - \rho_{Y_i,Y_j}\cdot\sigma_{Y_j}^2 \\ &+\left(\Delta\cdot\sigma_{Y_i}^2 + \Delta\cdot\sigma_{Y_j}^2 - 2\cdot\rho_{Y_i,Y_j}\cdot\sigma_{Y_i}\cdot\sigma_{Y_j}\right)\cdot p > 0 \end{aligned} \tag{7-3}$$

where p is a fraction of $\sigma_{Yi}\cdot\sigma_{Yj}$. Depending on values of $\sigma_{Yi}, \sigma_{Yji}$, $\rho_{Yi,Yj}$, and Δ, the left hand side of Eq (7-3) may be either positive or negative. Thus, Eq (3-26) cannot be assumed to be a strictly increasing (or decreasing) function of σ_{ε}^2.

Table 7-7 Sensitivity of the total structural loss ratio to σ_{ε}^2 for buildings exposed to a M_w 7 earthquake

Structural Loss Ratio	184 RES4			681 IND1			184 RES4 + 681 IND1		
	p			*P*			*p*		
	0.15	**0.30**	**0.50**	**0.15**	**0.30**	**0.50**	**0.15**	**0.30**	**0.50**
E[LR_T]	0.0791	0.0848	0.0783	0.0880	0.0932	0.0900	0.0818	0.0874	0.0820
SD[LR_T]	0.0952	0.0904	0.0816	0.0932	0.0902	0.0886	0.0887	0.0843	0.0778
CoV[LR_T]	1.2040	1.0661	1.0420	1.0592	0.9671	0.9837	1.0841	0.9638	0.9491

The dependence of the standard deviations and the coefficients of variation of the aggregated structural loss ratio to the scale of correlation of the noise, β_{ε}, is presented in Table 7-8. The case in which β_{ε} = 3 km is the baseline case considered in Chapters 4 and 5. The coefficient of variation of the total losses generally increases in all cases as the scale of correlation of the noise is increased. The correlation in damage between buildings *i* and *j* (cf Eq 3-26) is an increasing function of β_{ε}. On the other hand, when

β_ε increases to 30 km from 3 km, the coefficient of variation is only increased by 10 percent. Thus, scale of correlation β_ε is insignificant effect on uncertainty of the total losses.

Table 7-8 Sensitivity of the total structural loss ratio to β_ε for buildings exposed to a M_w 7 earthquake

Structural Loss Ratio	184 RES4			681 IND1			184 RES4 + 681 IND1		
	β_ε			β_ε			β_ε		
	3 km	6 km	30 km	3 km	6 km	30 km	3 km	6 km	30 km
E[LR_T]	0.0791	0.0845	0.0839	0.0892	0.0934	0.0907	0.0827	0.0875	0.0862
SD[LR_T]	0.0913	0.0999	0.1064	0.0962	0.0985	0.1029	0.0863	0.0929	0.0984
CoV[LR_T]	1.1541	1.1815	1.2687	1.0789	1.0553	1.1340	1.0435	1.0608	1.1416

Table 7-9 defines three cases used to examine the sensitivity of the standard deviations and the coefficients of variation of the total structural loss ratio to $\beta_{BTi,BTj}$. Case 1 represents the baseline considered in Chapters 4 and 5. The results of this sensitivity analysis are shown in Table 7-10. As $\beta_{BTi,BTj}$ is decreased to 25 and 50 percent of case 1, the coefficients of variation of the total losses for case 2 and case 3 are decreased to 15 and 25 percent of that of case 1, respectively. When the variances of the total loss are considered, those for case 2 and case 3 are decreased up to 30 and 40 percent of that of case 1, respectively. It is clear that changes in $\beta_{BTi,BTj}$ have a significant effect on the uncertainty in the total structural losses.

Table 7-9 Three cases of $\beta_{BTi,BTj}$ that are considered in the sensitivity analysis of the variance of the total structural loss ratio.

$\beta_{BTi,BTj}$	Case 1	Case 2 (75% of Case 1)	Case 3 (50% of Case 1)
- Similar construction material, structural type, and height rage	0.900	0.675	0.450
- Similar construction material and structural type, but different height rage	0.800	0.600	0.400
- Similar construction material, but different structural type	0.700	0.525	0.350
- Different construction materials and different structural type	0.500	0.375	0.250

Table 7-10 Sensitivity of the total structural loss ratio to $\beta_{BTi,BTj}$ for buildings exposed to a M_w 7 earthquake

Structural Loss Ratio	184 RES4			681 IND1			184 RES4 + 681 IND1		
	$\beta_{BTi,BTj}$			$\beta_{BTi,BTj}$			$\beta_{BTi,BTj}$		
	Case 1	**Case 2**	**Case 3**	**Case 1**	**Case 2**	**Case 3**	**Case 1**	**Case 2**	**Case 3**
E[LR_T]	0.0791	0.0827	0.0836	0.0892	0.0918	0.0933	0.0827	0.0858	0.0869
SD[LR_T]	0.0913	0.0837	0.0753	0.0962	0.0868	0.0780	0.0863	0.0791	0.0713
CoV[LR_T]	1.1541	1.0122	0.9003	1.0789	0.9453	0.8363	1.0435	0.9222	0.8197

Table 7-11 defines three cases used to consider the sensitivity of the standard deviations and the coefficients of variation in the aggregated structural loss ratio due to $\beta_{Ci,Cj}$. Case 1 represents values that were used in Chapters 3 and 4. Table 7-12 shows that when $\beta_{Ci,Cj}$ is decreased to 25 and 50 percent of case 1, the coefficients of variation of the total losses for case 2 and case 3 are decreased 15 and 25 percent of case 1, respectively. Thus, changes in $\beta_{Ci,Cj}$ have a significant effect on the uncertainty of the total structural losses. Intuitively, the sensitivity of the variance in total loss to $\beta_{Ci,Cj}$ and $\beta_{BTi,BTj}$ would be expected to be similar because both parameters are multipliers of $\sigma_{Yi} \cdot \sigma_{Yj}$ in Eq (3-23).

Table 7-11 Three cases of $\beta_{Ci,Cj}$ that are considered in sensitivity analysis

$\beta_{Ci,Cj}$	**Case 1**	**Case 2 (75% of Case 1)**	**Case 3 (50% of Case 1)**
- Similar Building Code	1.000	0.750	0.500
- Different Building Code	0.500	0.375	0.250

Table 7-12 Sensitivity of variance of the total structural loss ratio to $\beta_{Ci,Cj}$ for buildings exposed to a M_w 7 earthquake

Structural Loss Ratio	184 RES4			681 IND1			184 RES4 + 681 IND1		
	$\beta_{Ci,Cj}$			$\beta_{Ci,Cj}$			$\beta_{Ci,Cj}$		
	Case 1	**Case 2**	**Case 3**	**Case 1**	**Case 2**	**Case 3**	**Case 1**	**Case 2**	**Case 3**
E[LR_T]	0.0791	0.0847	0.0838	0.0892	0.0926	0.0928	0.0827	0.0874	0.0869
SD[LR_T]	0.0913	0.0856	0.0765	0.0962	0.0869	0.0792	0.0863	0.0805	0.0723
CoV[LR_T]	1.1541	1.0102	0.9130	1.0789	0.9386	0.8532	1.0435	0.9207	0.8313

7.2 Dependence of Total Losses on Damage Correlation Model between Structural and Nonstructural Losses under a Scenario Earthquake

In this section the sensitivity of total losses to assumed correlations between structural and nonstructural losses in Chapter 6 are examined by considering variations in the aggregated losses due to parameters ρ_{Ys_i,Yns_j} and $\sigma^2_{Yns_i}$ (Eq 6-12). For this purpose, the same building inventories and scenario earthquake event in the previous section are considered.

Table 7-13 defines three cases that are used to examine the dependence of the standard deviations and the coefficients of variation of the total loss ratio on ρ_{Ys_i,Yns_j}. Case 1 represents the values that were used in Chapter 6. The results of this analysis of the total loss for the cases where only correlation in spatial ground motion are considered are shown in Table 7-14. As ρ_{Ys_i,Yns_j} for cases 2 and 3 by increases 10 and 20 percent over the values used in case 1, the coefficients of variation of the total losses for cases 2 and 3 increase by only 0.5 and 1.5 percent. Thus, changes in ρ_{Ys_i,Yns_j} clearly have an insignificant effect on the uncertainty in the total losses.

Table 7-13 Three cases of ρ_{Ys_i,Yns_j} that are considered in sensitivity analysis

ρ_{Ys_i,Yns_j}	**Case 1**	**Case 2 (Increased 10% of Case 1)**	**Case 3 (Increase 20% of Case 1)**
S-NDSC[a]	0.600	0.660	0.720
S-NASC[b]	0.500	0.550	0.600
NDSC-NASC[c]	0.500	0.550	0.600

[a] Correlation between structural and nonstructural drift-sensitive components
[b] Correlation between structural and nonstructural acceleration-sensitive components
[c] Correlation between nonstructural drift- and acceleration-sensitive components

Table 7-14 Sensitivity of the total loss ratio to ρ_{Ys_i,Yns_j} for buildings exposed to a M_w 7 earthquake

Occupancy Class	RES4			IND1			RES4 + IND1		
Total Loss Ratio	ρ_{Ys_i,Yns_j}			ρ_{Ys_i,Yns_j}			ρ_{Ys_i,Yns_j}		
	Case 1	Case 2	Case 3	Case 1	Case 2	Case 3	Case 1	Case 2	Case 3
E[LR_T]	0.0477	0.0474	0.0475	0.0387	0.0388	0.0388	0.0438	0.0437	0.0438
SD[LR_T]	0.0206	0.0206	0.0208	0.0208	0.0209	0.0211	0.0188	0.0189	0.0191
CoV[LR_T]	0.4315	0.4340	0.4371	0.5379	0.5395	0.5449	0.4298	0.4323	0.4355

Table 7-15 shows the dependence of the standard deviations and the coefficients of variation of the total loss ratio on nonstructural noise variance ($\sigma^2_{Yns_i}$) for three building inventories. Three values of σ_ε^2 are considered: 50, 100, and 200 percent of $\sigma^2_{Yns_i}$ for cases 1, 2, and 3, respectively. Case 3 is the value of $\sigma^2_{Yns_i}$ that was used in Chapter 6. When σ_ε^2 is increased from 50 percent to 100 and 200 percent of $\sigma^2_{Yns_i}$, the coefficients of variation of the total loss of 681 IND1 buildings for cases 2 and 3 are increased 0.6 percent and decreased 0.3 percent of that of case 1, respectively. Accordingly, the impact of $\sigma^2_{Yns_i}$ on the uncertainty (measured by standard deviations and coefficients of variation) in the total losses is insignificant.

Table 7-15 Sensitivity of the total loss ratio to $\sigma^2_{Yns_i}$ for buildings exposed to a M_w 7 earthquake

Occupancy Class	184 RES4			681 IND1			184 RES4 + 681 IND1		
Total Loss Ratio	*p**			*p**			*p**		
	0.5	1	2	0.5	1	2	0.5	1	2
E[LR_T]	0.0469	0.0473	0.0470	0.0383	0.0386	0.0382	0.0432	0.0436	0.0432
SD[LR_T]	0.0205	0.0206	0.0202	0.0209	0.0210	0.0207	0.0187	0.0189	0.0186
CoV[LR_T]	0.4371	0.4351	0.4303	0.5445	0.5447	0.5428	0.4333	0.4340	0.4298

p is a fraction of $\sigma^2_{Yns_i}$.

7.3 Analysis of Epistemic Uncertainty in Estimated Structural Losses

Epistemic uncertainties arises from imperfect representations of the real world and may be reduced with more information, better prediction models, or improved experiments (Ang and Tang, 2007). The epistemic uncertainty can be estimated by comparing observed data to model predictions. However, existing information on low-probability, high-consequence events to compare with the prediction model, such as ground motions caused by large earthquakes in the Central and Eastern United States, is very limited. As an alternative to a comparison between observed data and model prediction, the epistemic uncertainty in seismic hazard analysis may be depicted by an event tree model (Petersen *et al.*, 2008), which represents a sequence of alternative modeling assumptions in each procedure together with a weight assigned to measure the plausibility of each assumption. These weights for all branches extending from each node are assigned by judgment to reflect the relative confidence in each alternative model (in a Bayesian sense), and they must sum to unity.

The event tree model used for estimating the epistemic uncertainty in the total structural loss ratio of a building subjected to the scenario earthquake described in Section 6.1 is illustrated in Figure 7-5. For the purpose of this illustration, three ground motion attenuation relations are selected. The Atkinson and Boore (1995) (AB95), Atkinson and Boore (2006) (AB06), and Campbell (2003) (C03) ground motion prediction equations are given in Eqs (3-7), (3-8), and (3-5), respectively. The weight factors for AB06 and C03 ground motion relations are assumed to equal 0.4, while that for attenuation AB95 is 0.2. The weight for AB95 ground motion model is less than AB06 by the same authors because the later model incorporates new information

obtained from Eastern North America seismographic data (Atkinson and Boore, 2006). However, the AB95 equation is still considered in this illustration, since it was used in the risk estimates in Chapters 4 and 5.

The spatial ground motion correlation distance in Eq (3-15) is assumed to equal either 50 or 500 km. The distance 500 km is selected because the variance of the loss from this case in Section 7.1.2 was found to differ significantly from the case where the correlation distance is 50 km. Furthermore, the correlation distance of 50 km is comparable to what has been found for earthquakaes in high-seismic areas (see Chapter 3), and earthquakes in the CEUS have a larger felt area. These correlation distances are weighted equally. There are seven branches associated with different assumptions regarding damage correlation: lower-bound ($\rho_D = 0.0$), five model-based correlations, and upper-bound ($\rho_D = 0.9$).

The five model-based damage correlations are described in Table 7-16. The weighting factors for each model-based damage correlation assumption are 0.16, while those for lower and upper bound damage correlation are 0.1. These assumed values reflect the fact the model-based damage correlation matrix is believed to be more realistic than the two bounds, which were assumed to equal 0.0 and 0.9 (at the limits of plausibility) for all pairs of buildings. The details of the cases for σ_ε^2, the coefficients $\beta_{BTi,BTj}$, and $\beta_{Ci,Cj}$ are similar to the cases discussed in Section 6.1.3. The coefficient β_ε is not considered in the analysis of epistemic uncertainty since it was found to have an insignificant effect on the variance of the total loss.

Table 7-16 also illustrates sets of parameters and weights of each outcome in Figure 7-5 that will be used in the analysis of epistemic uncertainty. Note that the sum of all total outcome weights must equal unity.

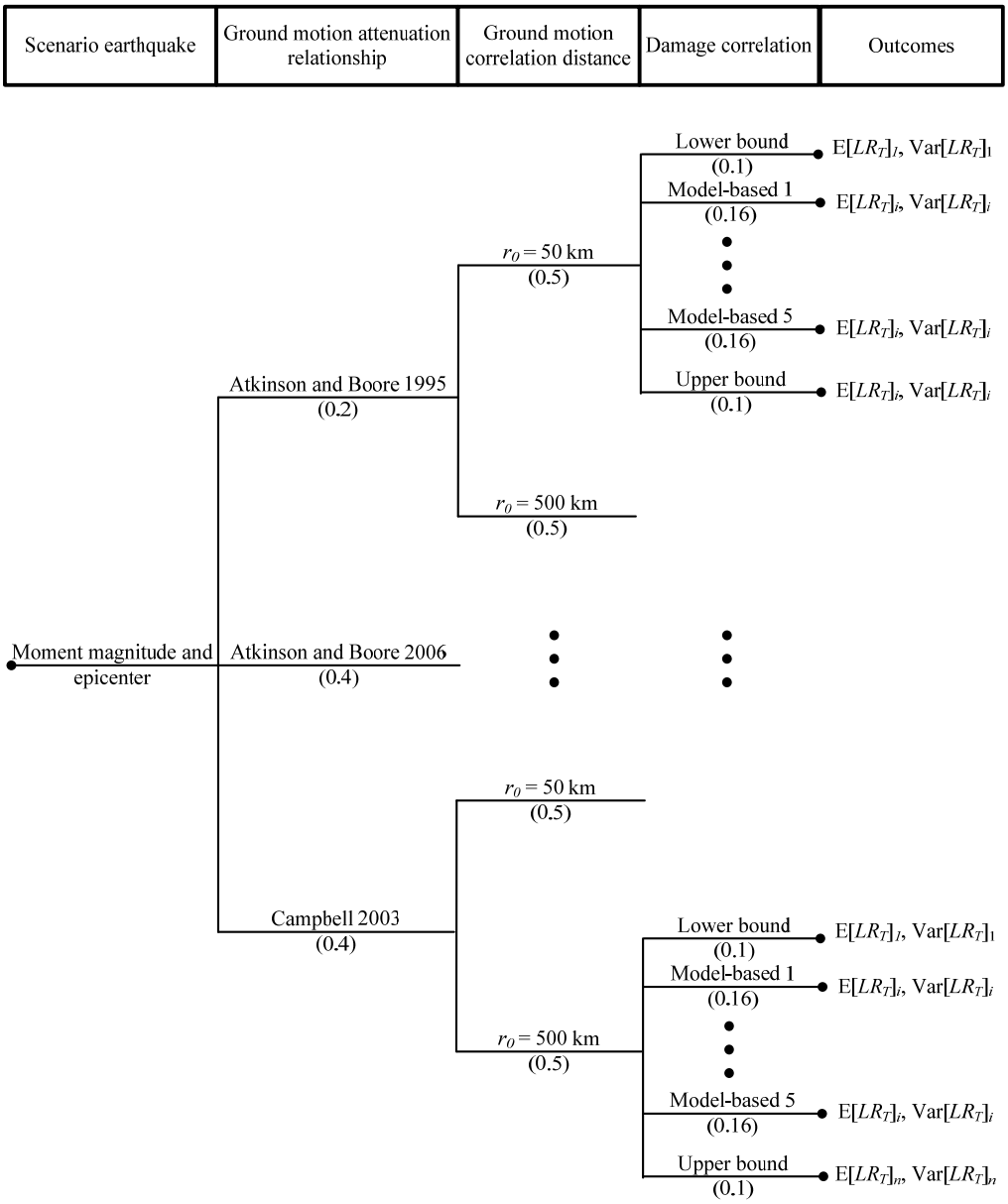

Figure 7-5 Event tree model for analysis of epistemic uncertainty in estimated total structural loss ratio for building inventories in Shelby County, TN. Values in parentheses are weights assigned to each model. The lines that end in circles represent outcomes.

Table 7-16 Parameters and total weights for each branch in Figure 7-5

Outcome No.	Ground Motion Attenuation	Ground Motion Correlation Distance, r_0 (km)	Damage Correlation				Weight, w_i
			Cases	σ_ε^2	$\beta_{BTi,BTj}$	$\beta_{Ci,Cj}$	
1	AB95	50	lower bound	-	-	-	0.010
2	AB95	50	model-based 1	case 1	case 3	case 1	0.016
3	AB95	50	model-based 2	case 1	case 2	case 1	0.016
4	AB95	50	model-based 3	case 3	case 1	case 1	0.016
5	AB95	50	model-based 4	case 2	case 1	case 1	0.016
6	AB95	50	model-based 5	case 1	case 1	case 1	0.016
7	AB95	50	upper bound	-	-	-	0.010
8	AB95	500	lower bound	-	-	-	0.010
9	AB95	500	model-based 1	case 1	case 3	case 1	0.016
10	AB95	500	model-based 2	case 1	case 2	case 1	0.016
11	AB95	500	model-based 3	case 3	case 1	case 1	0.016
12	AB95	500	model-based 4	case 2	case 1	case 1	0.016
13	AB95	500	model-based 5	case 1	case 1	case 1	0.016
14	AB95	500	upper bound	-	-	-	0.010
15	AB06	50	lower bound	-	-	-	0.020
16	AB06	50	model-based 1	case 1	case 3	case 1	0.032
17	AB06	50	model-based 2	case 1	case 2	case 1	0.032
18	AB06	50	model-based 3	case 3	case 1	case 1	0.032
19	AB06	50	model-based 4	case 2	case 1	case 1	0.032
20	AB06	50	model-based 5	case 1	case 1	case 1	0.032
21	AB06	50	upper bound	-	-	-	0.020
22	AB06	500	lower bound	-	-	-	0.020
23	AB06	500	model-based 1	case 1	case 3	case 1	0.032
24	AB06	500	model-based 2	case 1	case 2	case 1	0.032
25	AB06	500	model-based 3	case 3	case 1	case 1	0.032
26	AB06	500	model-based 4	case 2	case 1	case 1	0.032
27	AB06	500	model-based 5	case 1	case 1	case 1	0.032
28	AB06	500	upper bound	-	-	-	0.020
29	C03	50	lower bound	-	-	-	0.020
30	C03	50	model-based 1	case 1	case 3	case 1	0.032
31	C03	50	model-based 2	case 1	case 2	case 1	0.032
32	C03	50	model-based 3	case 3	case 1	case 1	0.032
33	C03	50	model-based 4	case 2	case 1	case 1	0.032
34	C03	50	model-based 5	case 1	case 1	case 1	0.032
35	C03	50	upper bound	-	-	-	0.020
36	C03	500	lower bound	-	-	-	0.020
37	C03	500	model-based 1	case 1	case 3	case 1	0.032
38	C03	500	model-based 2	case 1	case 2	case 1	0.032
39	C03	500	model-based 3	case 3	case 1	case 1	0.032
40	C03	500	model-based 4	case 2	case 1	case 1	0.032
41	C03	500	model-based 5	case 1	case 1	case 1	0.032
42	C03	500	upper bound	-	-	-	0.020

7.3.1 Epistemic Uncertainty in Total Structural Loss Ratio

Risk assessments to determine the total structural loss ratios for 184 RES4 and 681 IND1 buildings using all 42 sets of parameters were conducted in accordance with the event tree in Figure 7-5. A numerical average, probability mass function (PMF), cumulative density function (CDF), and 5th and 95th percentiles of the estimated loss ratios are determined. Figure 7-6, Figure 7-7, and Figure 7-8 show the PMF of the mean total structural loss ratios of all outcomes for 184 RES4, 681 IND1, and both occupancy classes. The PMFs in these figures depict the epistemic uncertainty in the estimated mean loss ratio. The total losses are grouped into three regions, which is consistent with the results of the sensitivity analysis of the total loss due to different ground motion attenuations in Section 6.1.1. The lowest losses are computed when the Atkinson and Boore (2006) attenuation is used, while the highest losses are associated with the Campbell (2003) attenuation. The PMF of the mean total losses depends on the assumed weight factors of the ground motion attenuation models, but is not affected by the assumed weight factors of the correlation in demand and damage. This implies that the weight factors of all ground motion attenuation relations should be selected carefully.

Table 7-17 shows the numerical average, standard deviation and coefficient of variation associated with the estimated mean of the total structural loss ratio. The 5th and 95th percentiles on the total loss for 184 RES4, 681 IND1, and both occupancy classes combined are presented in Table 7-18. The 5th and 95th percentiles are approximately equal to the mean value plus or minus 1.25 times the standard deviations.

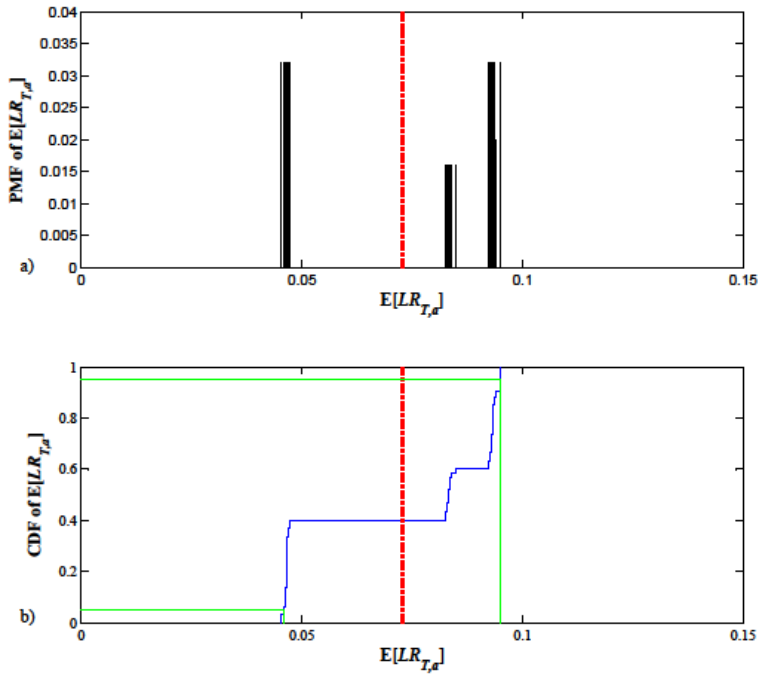

Figure 7-6 a) Probability mass function and b) cumulative density function of estimated mean total structural loss ratio for 184 RES4 buildings in Shelby County, TN exposed to a M_w 7 earthquake. The red dot dash line is the average value. The green lines are 5th and 95th percentiles of the epistemic uncertainty on the total losses and their numerical values are shown in Table 7-18.

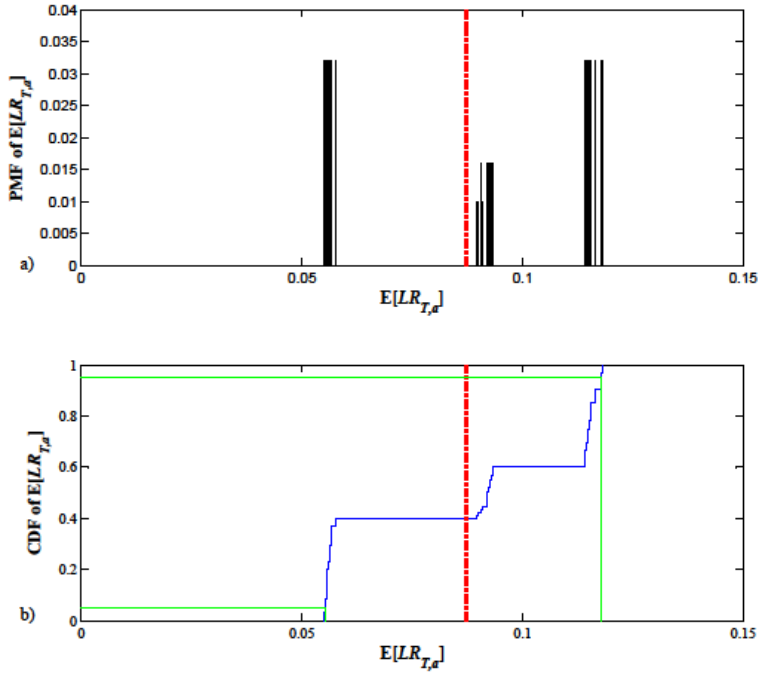

Figure 7-7 a) Probability mass function and b) cumulative density function of estimated mean total structural loss ratio for 681 IND1 buildings in Shelby County, TN exposed to a M_w 7 earthquake. The red dot dash line is the average value. The green lines are 5th and 95th percentiles of the epistemic uncertainty on the total losses and their numerical values are shown in Table 7-18.

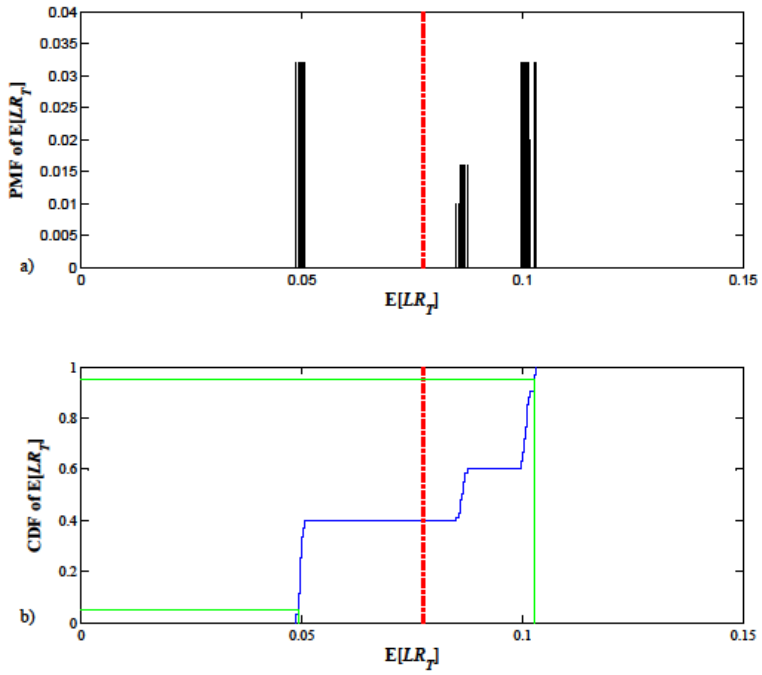

Figure 7-8 a) Probability mass function and b) cumulative density function of estimated mean total structural loss ratio for both occupancy classes in Shelby County, TN exposed to a M_w 7 earthquake. The red dot dash line is the average value. The green lines are 5th and 95th percentiles of the epistemic uncertainty on the total losses and their numerical values are shown in Table 7-18.

Table 7-17 Epistemic uncertainty –- total structural loss ratio for building inventories in Shelby County, TN exposed to a M_w 7 earthquake

	184 RES4	**681 IND1**	**184 RES4 + 681 IND1**
Average of E[LR_T]	0.0726	0.0871	0.0776
SD of E[LR_T]	0.0218	0.0268	0.0235
CoV of E[LR_T]	0.3001	0.3081	0.3023

Table 7-18 The 5th and 95th percentiles of the estimated mean total structural loss ratio for building inventories in Shelby County, TN exposed to a M_w 7 earthquake

	184 RES4		**681 IND1**		**184 RES4 + 681 IND1**	
	Percentile		**Percentile**		**Percentile**	
	5th	**95th**	**5th**	**95th**	**5th**	**95th**
E[LR_T]	0.0458	0.0950	0.0553	0.1177	0.0492	0.1028

7.3.2 Epistemic Uncertainty in Probable Maximum Loss

In order to illustrate the epistemic uncertainty in probable maximum loss (PML), defined at annual probabilities of exceedence of 1×10^{-4} and 1×10^{-5}, three different values

of earthquake occurrence rate of the scenario earthquake M_w 7.0 at the epicenter at latitude 35.4° and longitude -90.2°- 0.004, 0.002, and 0.001 per year - are assumed. Therefore, the PMLs that are computed in the following illustrations are conditioned on this scenario event. Three values of the occurrence rate are considered to study the effect of the occurrence rate on epistemic uncertainty.

Figures 7-9, 7-10, and 7-11 show the annual exceedence probabilities (E.P.) *vs* total structural loss ratios for the 42 outcomes in Table 7-16 for 184 RES4, 681 IND1, and both occupancy classes. The mean value, standard deviation, and coefficient of variation in the PML at exceedence probability (E.P.) 1×10^{-4} and 1×10^{-5} are summarized in Table 7-19 and Table 7-20. The coefficients of variation for every case are approximately 30 percent; recall, however, that only one scenario event was considered. While the scatter in the loss ratios increases for the same occurrence rate as the E.P. decreases, some of the sample exceedence probability curves are lightly weighted (cf Table 7-16). Accordingly, the coefficients of variation in PML in Table 7-19 and Table 7-20 are relatively insensitive to the probability band chosen to estimate the PML.

The PMF and CDF of the probable maximum loss at exceedence probability (E.P.) 1×10^{-4}/yr for 184 RES4, 681 IND1, and both occupancy classes are plotted in Figures 7-12, 7-13, and 7-14; while those at E.P. 1×10^{-5}/yr for 184 RES4, 681 IND1, both occupancy classes are shown in Figures 7-15, 7-16, and 7-17. The 5^{th} and 95^{th} percentiles are also shown in Table 7-21 and Table 7-22. The epistemic uncertainty in PML at the same E.P. is smaller for the low earthquake occurrence rate case than for the high occurrence rate. These plots also illustrate that the PML at the same level of E.P. of the lower occurrence rate case has lower variance.

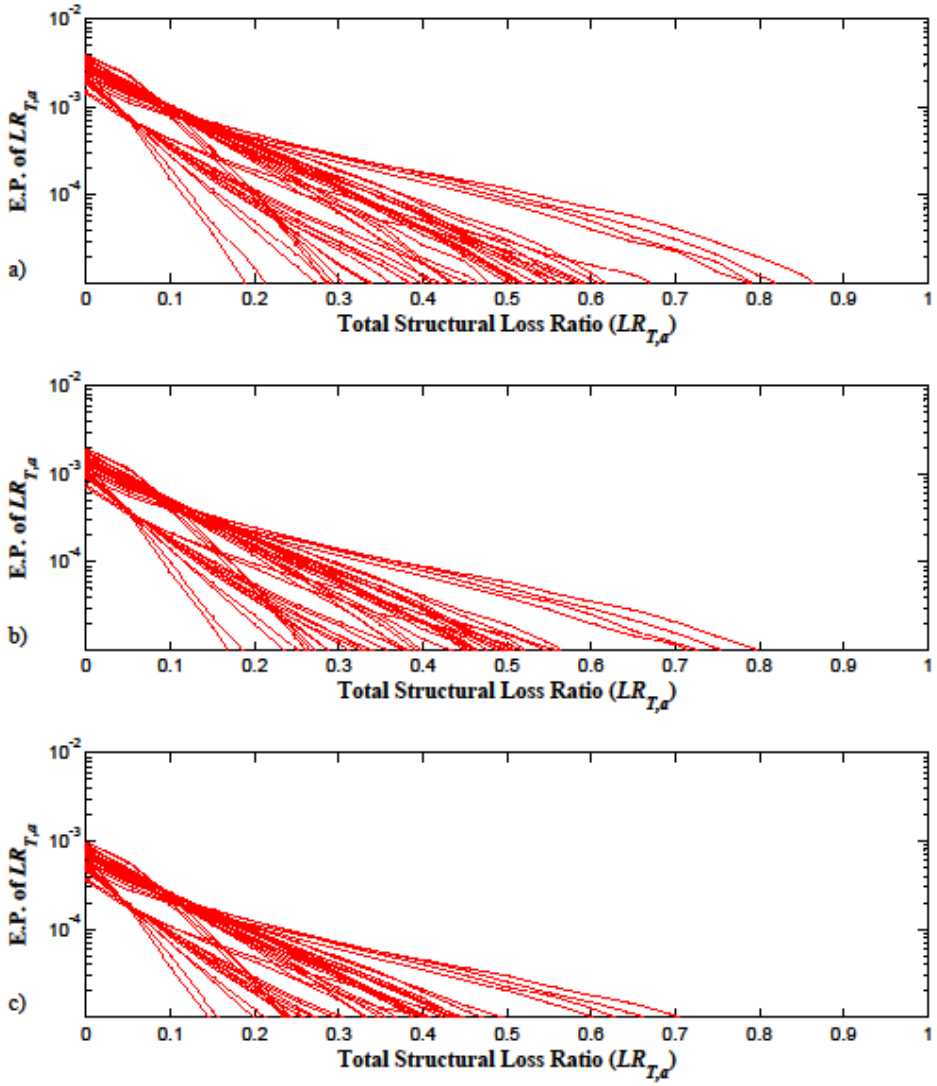

Figure 7-9 a) Exceedence probability (E.P.) of total structural loss ratio for 184 RES4 buildings for earthquake occurrence rates: (a) 1 in 250 years; (b) 1 in 500 years; and (c) 1 in 1000 years. Each red line represents an outcome for a case considered in Table 7-16.

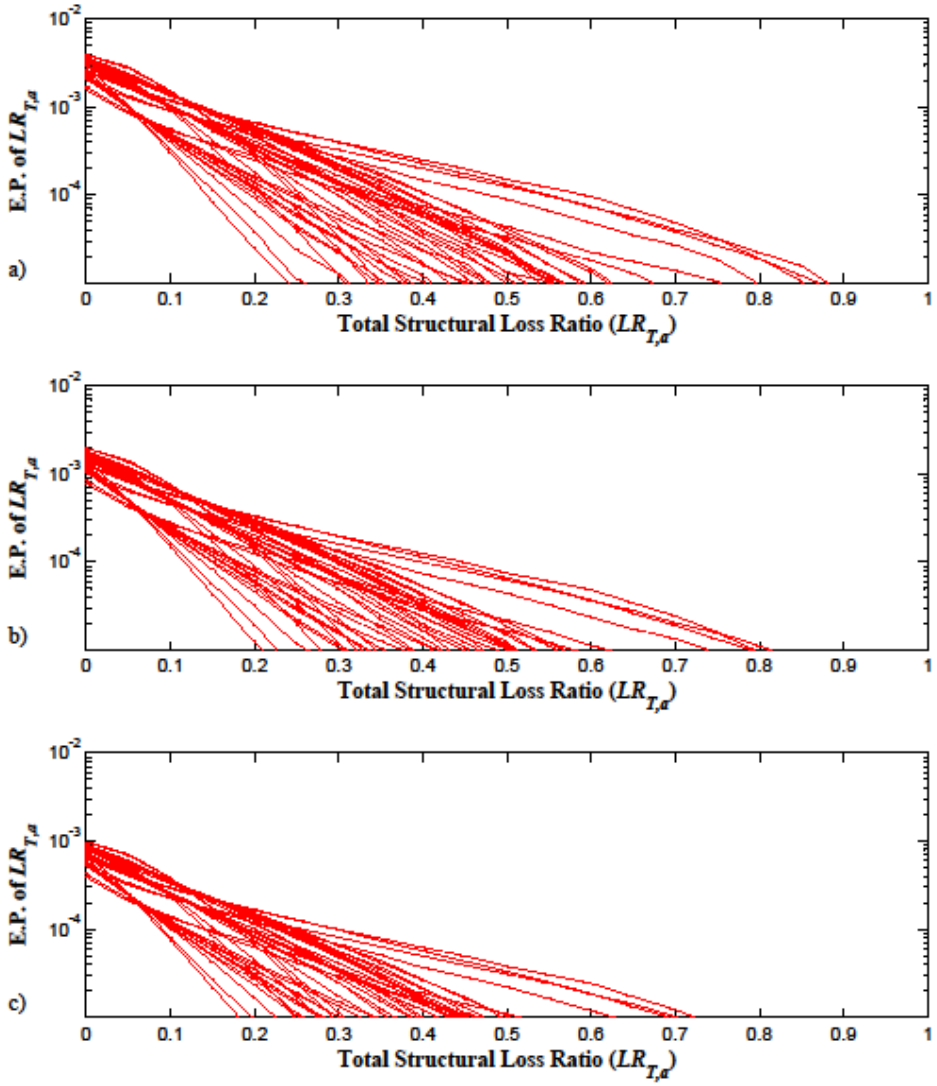

Figure 7-10 Exceedence probability (E.P.) of total structural loss ratio for 681 IND1 buildings for earthquake occurrence rates: (a) 1 in 250 years; (b) 1 in 500 years; and (c) 1 in 1000 years. Each red line represents an outcome for a case considered in Table 7-16.

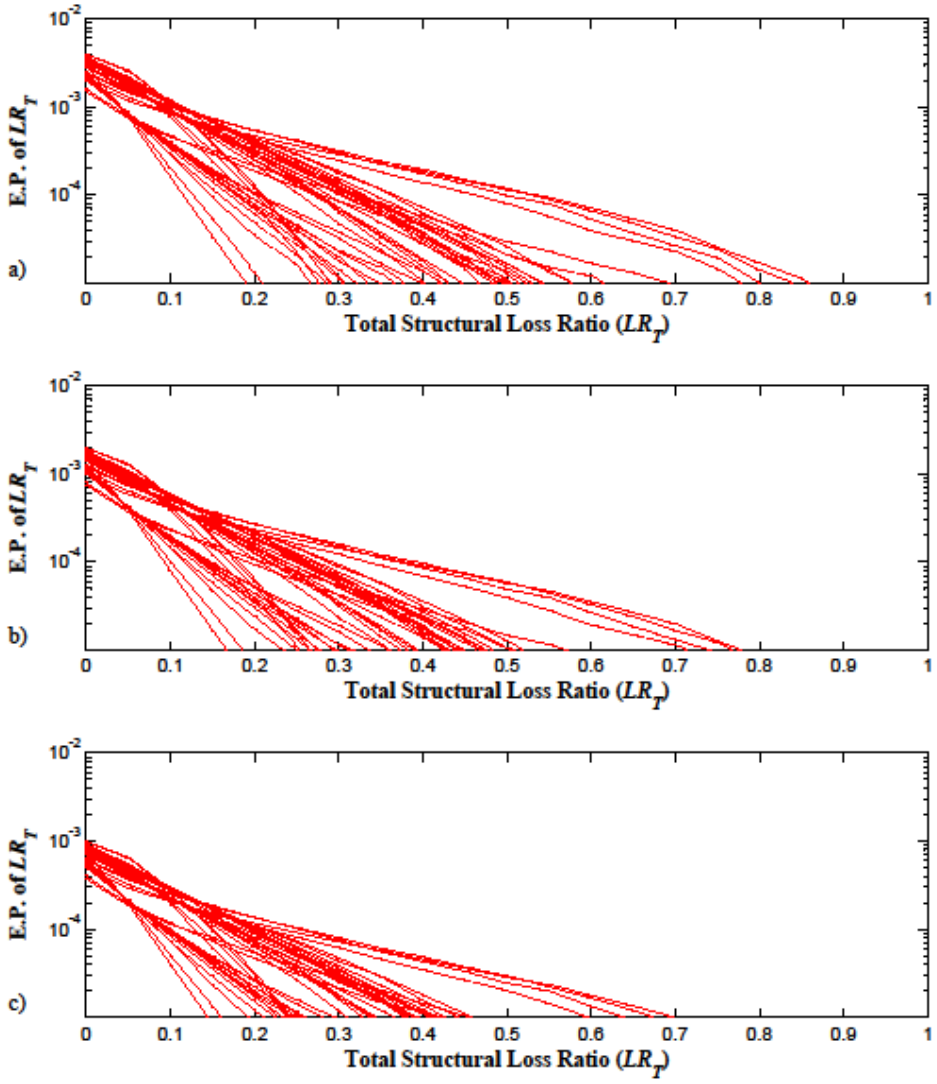

Figure 7-11 Exceedence probability (E.P.) of total structural loss ratio for both occupancy classes for earthquake occurrence rates: (a) 1 in 250 years; (b) 1 in 500 years; and (c) 1 in 1000 years. Each red line represents an outcome for a case considered in Table 7-16.

Table 7-19 Probable maximum loss (PML) at exceedence probability 1×10^{-4} of the total structural loss ratio for building inventories in Shelby County exposed to a M_w 7 earthquake event

E.P. = 1×10^{-4}	**184 RES4**			**681 IND1**			**184 RES4 + 681 IND1**		
	λ			**λ**			**λ**		
	0.004	**0.002**	**0.001**	**0.004**	**0.002**	**0.001**	**0.004**	**0.002**	**0.001**
E[PML]	0.275	0.212	0.150	0.307	0.244	0.178	0.270	0.212	0.154
SD[PML]	0.091	0.070	0.049	0.095	0.076	0.058	0.091	0.070	0.051
CoV[PML]	0.332	0.329	0.329	0.311	0.313	0.325	0.338	0.333	0.332

Table 7-20 Probable maximum loss (PML) at exceedence probability 1×10^{-5} of the total structural loss ratio for building inventories in Shelby County exposed to a M_w 7 event

E.P. = 1×10^{-5}	184 RES4			681 IND1			184 RES4 + 681 IND1		
	λ			λ			λ		
	0.004	**0.002**	**0.001**	**0.004**	**0.002**	**0.001**	**0.004**	**0.002**	**0.001**
E[PML]	0.471	0.417	0.357	0.503	0.449	0.388	0.452	0.400	0.345
SD[PML]	0.142	0.132	0.116	0.141	0.131	0.117	0.142	0.130	0.115
CoV[PML]	0.303	0.316	0.326	0.279	0.292	0.302	0.315	0.325	0.332

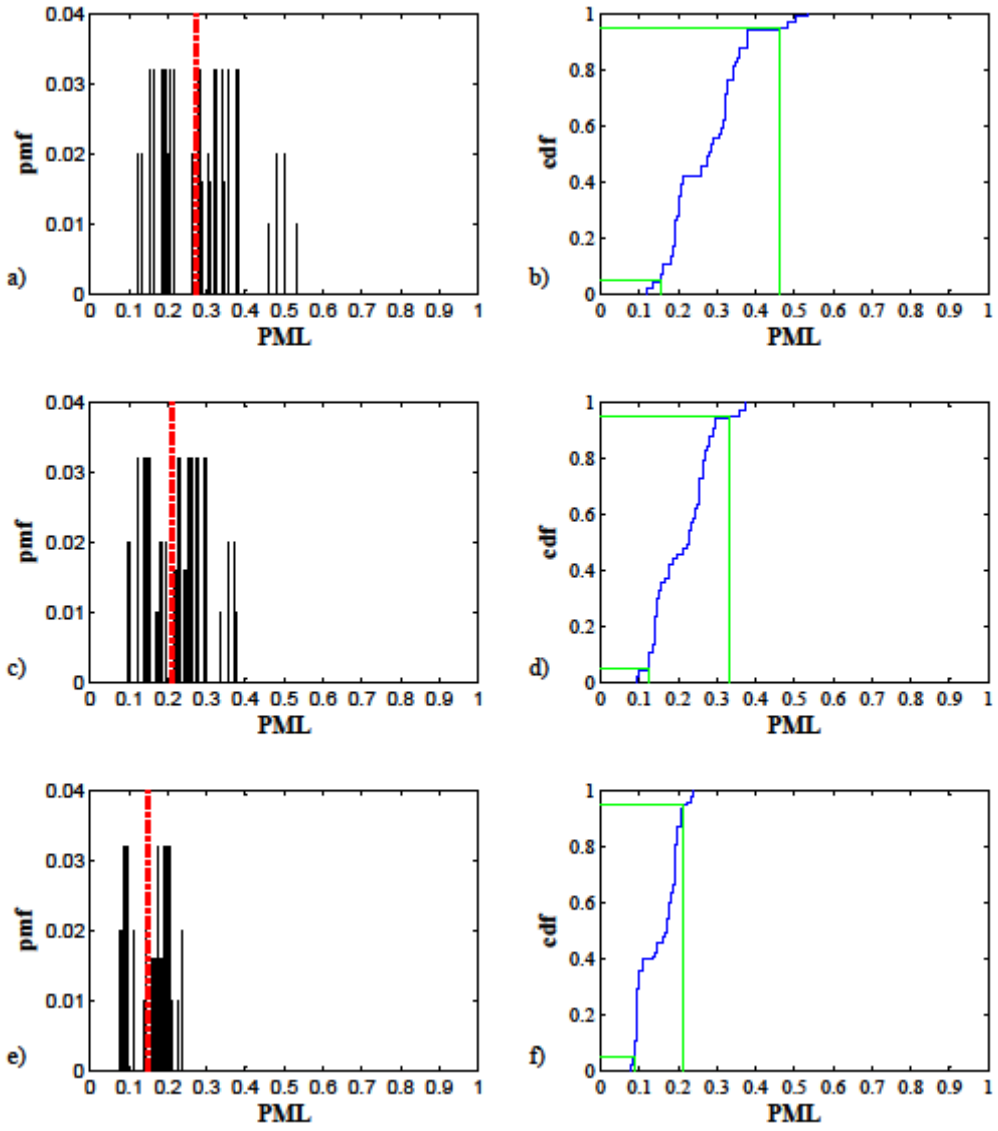

Figure 7-12 a) Probability mass function and cumulative distribution function of the probable maximum loss (PML) at exceedence probability 1×10^{-4} for the total structural loss ratio of 184 RES4 buildings when the M_w 7 scenario earthquake has occurrence rates: (a), (b) 1 in 250 years; (c), (d) 1 in 500 years; (e), (f) 1 in 1000 years. The red dashed-dotted line is the expected value of PML. The green lines are 5th and 95th percentile of PML.

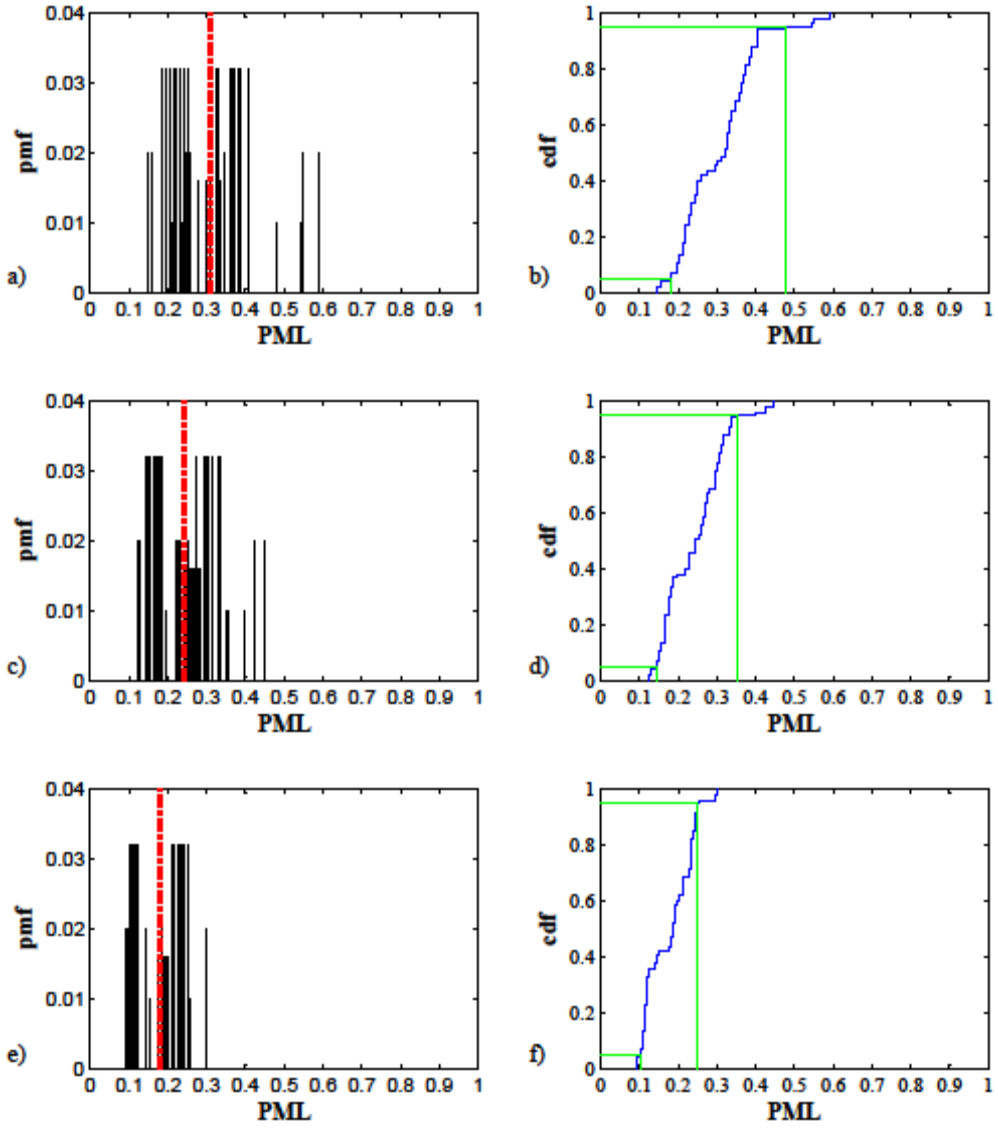

Figure 7-13 a) Probability mass function and cumulative distribution function of the probable maximum loss (PML) at exceedence probability 1×10^{-4} for the total structural loss ratio of 681 RES4 buildings when the M_w 7 scenario earthquake has occurrence rates: (a), (b) 1 in 250 years; (c), (d) 1 in 500 years; (e), (f) 1 in 1000 years. The green lines are 5th and 95th percentile of PML.

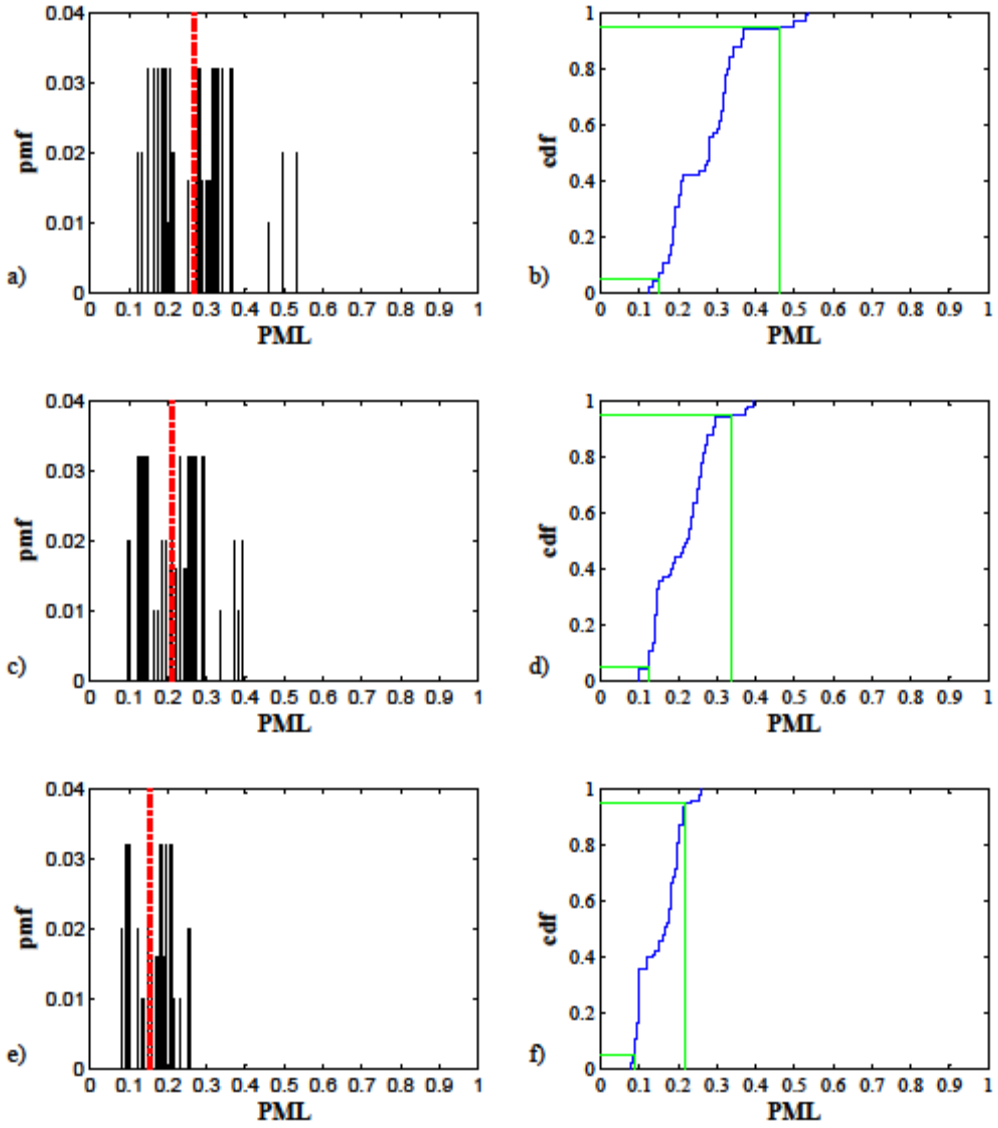

Figure 7-14 a) Probability mass function and cumulative distribution function of the probable maximum loss (PML) at exceedence probability 1×10^{-4} for the total structural loss ratio of both occupancy classes when the M_w 7 scenario earthquake has occurrence rates: (a), (b) 1 in 250 years; (c), (d) 1 in 500 years; (e), (f) 1 in 1000 years. The red dashed-dotted line is the expected value of PML. The green lines are 5th and 95th percentile of PML.

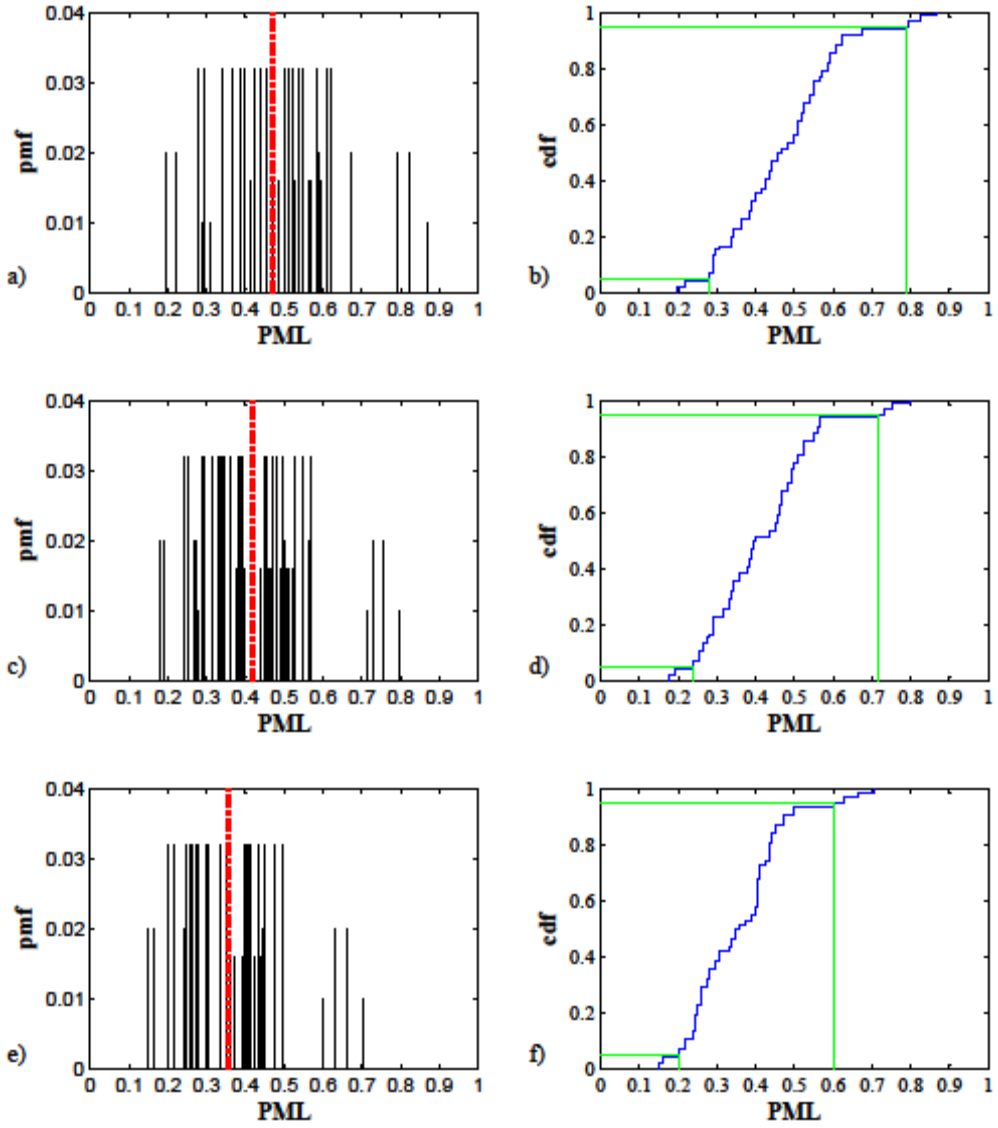

Figure 7-15 a) Probability mass function and cumulative distribution function of the probable maximum loss (PML) at exceedence probability 1×10^{-5} for the total structural loss ratio of 184 RES4 buildings when the M_w 7 scenario earthquake has occurrence rates: (a), (b) 1 in 250 years; (c), (d) 1 in 500 years; (e), (f) 1 in 1000 years. The green lines are 5th and 95th percentile of PML.

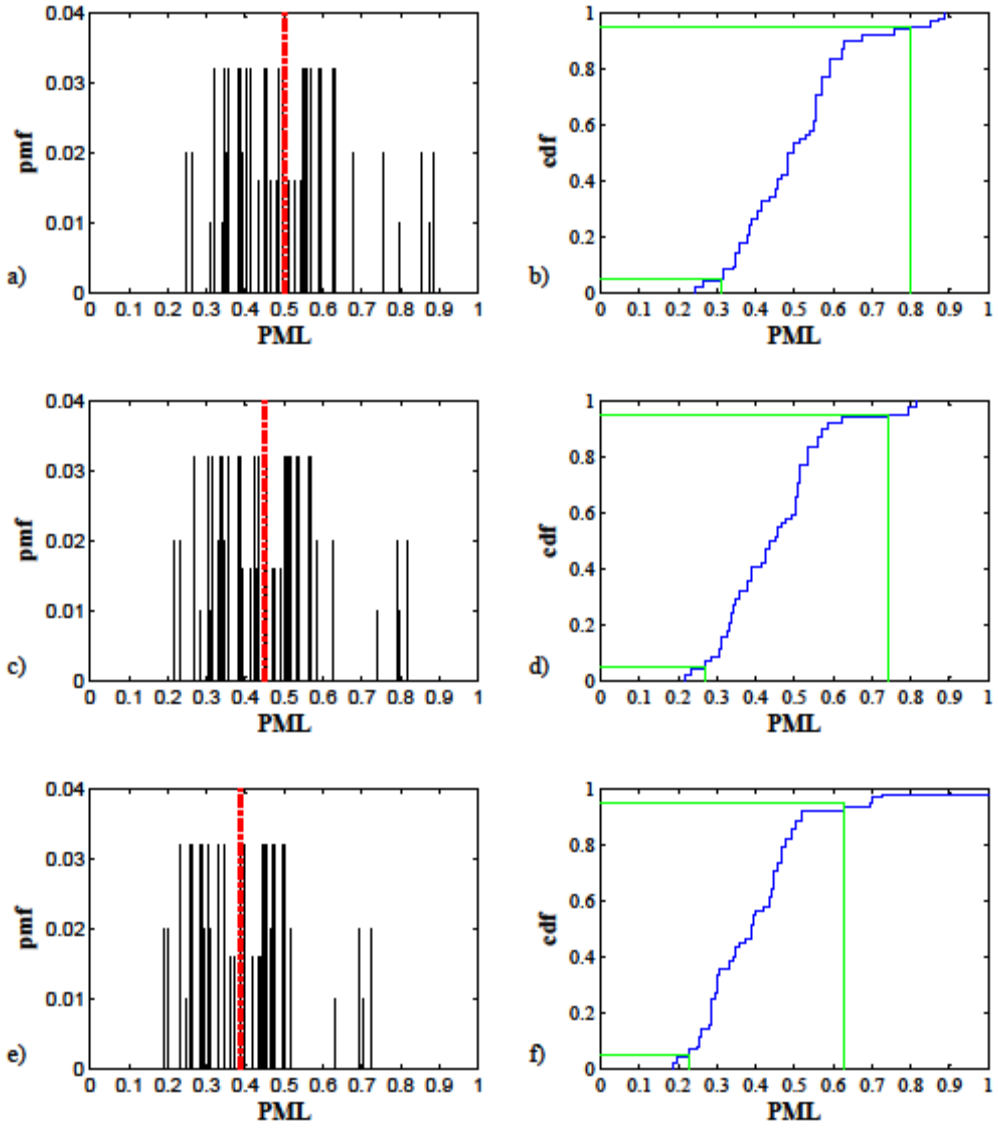

Figure 7-16 a) Probability mass function and cumulative distribution function of the probable maximum loss (PML) at exceedence probability 1×10^{-5} for the total structural loss ratio of 681 IND1 buildings when the M_w 7 scenario earthquake has occurrence rates: (a), (b) 1 in 250 years; (c), (d) 1 in 500 years; (e), (f) 1 in 1000 years. The red dashed-dotted line is the expected value of PML. The green lines are 5th and 95th percentile of PML.

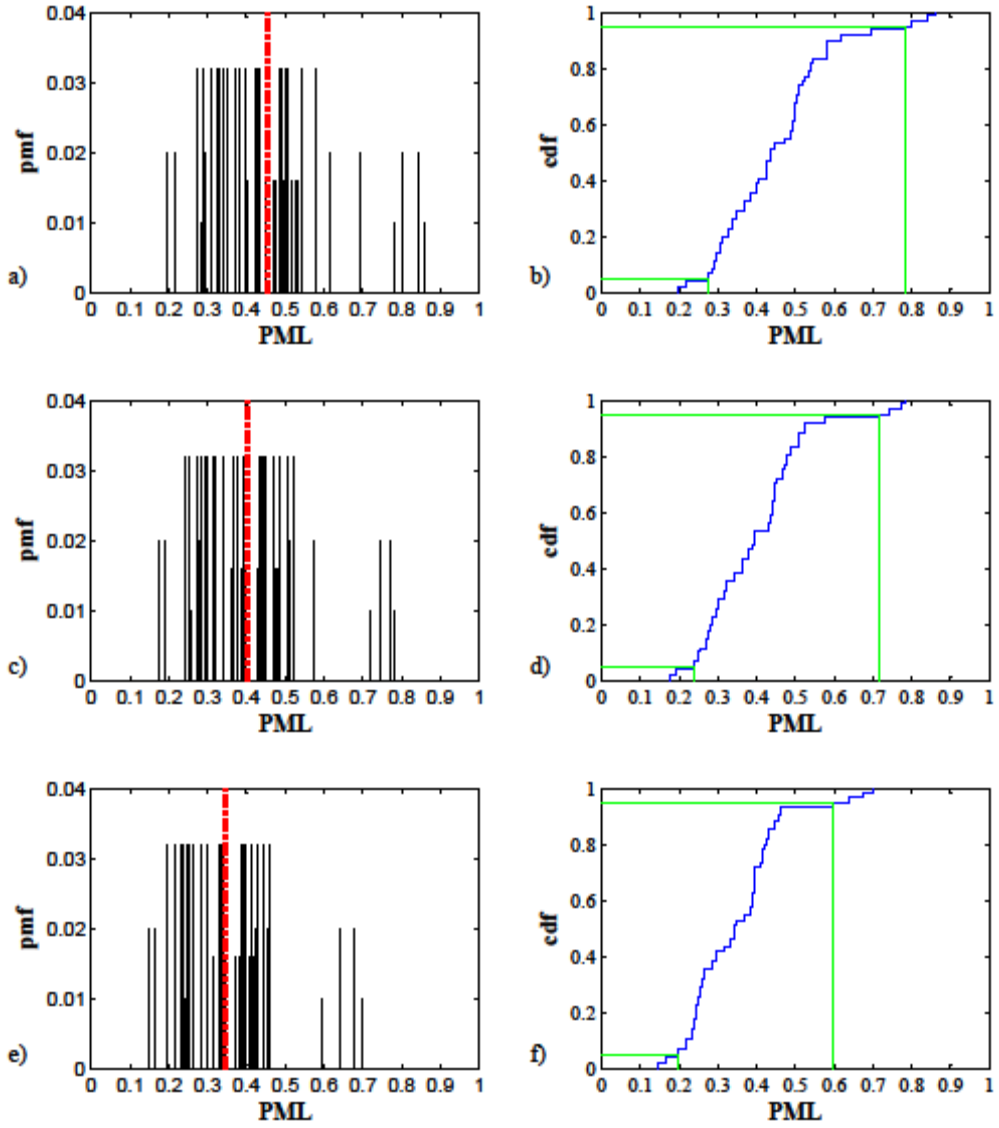

Figure 7-17 a) Probability mass function and cumulative distribution function of the probable maximum loss (PML) at exceedence probability 1×10^{-5} for the total structural loss ratio of both occupancy classes when the M_w 7 scenario earthquake has occurrence rates: (a), (b) 1 in 250 years; (c), (d) 1 in 500 years; (e), (f) 1 in 1000 years. The green lines are 5th and 95th percentile of PML.

Table 7-21 The 5th and 95th percentiles of probable maximum loss (PML) at exceedence probability 1×10^{-4} for building inventories in Shelby County exposed to a M_w 7 earthquake event

E.P. = 1×10^{-4}	**184 RES4**			**681 IND1**			**184 RES4 + 681 IND1**		
	λ			**λ**			**λ**		
	0.004	**0.002**	**0.001**	**0.004**	**0.002**	**0.001**	**0.004**	**0.002**	**0.001**
5th percentile	0.1540	0.1232	0.0874	0.1826	0.1429	0.1012	0.1489	0.1241	0.0903
95th percentile	0.4621	0.3332	0.2113	0.4791	0.3535	0.2505	0.4614	0.3367	0.2171

Table 7-22 The 5th and 95th percentiles of probable maximum loss (PML) at exceedence probability 1×10^{-5} for building inventories in Shelby County exposed to a M_w 7 earthquake event

E.P. = 1×10^{-5}	**184 RES4**			**681 IND1**			**184 RES4 + 681 IND1**		
	λ			**λ**			**λ**		
	0.004	**0.002**	**0.001**	**0.004**	**0.002**	**0.001**	**0.004**	**0.002**	**0.001**
5th percentile	0.2804	0.2410	0.2000	0.3114	0.2679	0.2304	0.2742	0.2396	0.1960
95th percentile	0.7900	0.7160	0.6018	0.7977	0.7405	0.6297	0.7824	0.7167	0.5967

7.4 Summary

This chapter has considered the impact on the estimated total structural loss ratio of various modeling and parameter assumptions under a scenario earthquake. The sensitivity to ground motion attenuation model was examined first. It was found that the expected aggregated structural losses depended strongly on the particular ground motion attenuation model selected. The total structural loss may be underestimated or overestimated if the ground motion attenuation selected for a study area was developed from seismicity in other regions. Second, the sensitivity of the total structural losses to characteristics of spatial ground motion was examined. Increasing the ground motion correlation distance by a factor of 10 increases the coefficient of variation in the total structural loss by 15 percent when damage correlations between pairs of buildings are equal, while it increases the coefficient of variation in the total structural loss by 6 percent for the model-based correlation, in which damage correlations between pairwise of buildings are unequal. Third, the sensitivity of the total structural loss to parameters σ_ε^2, β_ε, $\beta_{BTi,BTj}$, and $\beta_{Ci,Cj}$ in the model-based damage correlation developed in Chapter 3 was investigated. When the variance, σ_ε^2, increased, the variance of the total structural loss decreased. On the other hand, changes in β_ε have an insignificant effect on the variance of the total structural loss because the distance β_ε(< 10 km) is very small when

comparing to the ground motion correlation distance (≥ 50 km). A decrease in $\beta_{BTi,BTj}$ of 50 percent reduces the coefficient of variation of the total structural loss by 25 percent. This result is similar for $\beta_{Ci,Cj}$ because both parameters are multipliers of $\sigma_{Yi} \cdot \sigma_{Yj}$.

The dependence of the combined nonstructural and structural losses on parameters ρ_{Ys_i,Yns_j} and $\sigma^2_{Yns_i}$ was investigated. When ρ_{Ys_i,Yns_j} increased, the standard deviation and the coefficient of variation of the total loss increased insignificantly. An increase in ρ_{Ys_i,Yns_j} also caused an insignificant increase in the standard deviation and the coefficient of variation of the total losses. Comparing these two parameters, ρ_{Ys_i,Yns_j} has more impact on the standard deviation and the coefficient of variation of the total loss than $\sigma^2_{Yns_i}$.

An analysis of epistemic uncertainty in total structural loss ratio and PML under a scenario earthquake event was presented. First, the epistemic uncertainty in the total loss is affected by the ground motion attenuation model and the assumed weight factor for each equation. However, the PML at the same level of exceedence probability (E.P.) depends on the total weight factors of each outcome and earthquake occurrence rate. The range between 5th and 95th percentiles of PML at the same E.P is smaller for the low occurrence rate case than for high occurrence rate case. For PML's at different level of E.P. but in same occurrence rate, their coefficients of variation are similar.

CHAPTER 8

CONCLUSIONS

Estimates of losses to building inventories exposed to large-scale natural hazards such as earthquakes are essential to stakeholders, city planners, governments and insurers. While point estimates of losses are a first step, significant uncertainties arise from spatially distributed earthquake intensities, building vulnerability, and building repair/replacement costs. Understanding the nature of these uncertainties is equally important in mitigating damage arising from large scale natural hazards. This study has explored the assessment of seismic risk to distributed building inventories and the probable maximum loss decision metric. The case studies have highlighted the significant contribution to risk of direct physical damage arising from structure-to-nonstructure correlation within a single building and from pairwise structure-to-structure correlation between buildings.

8.1 Summary and Conclusions

The risk assessment of distributed building inventories in this study advances building loss estimation over the methodologies developed in previous researches in several respects:

i) The methodology incorporates demand and damage correlations and investigates the effect of these correlations on estimates of probable maximum losses to distributed building inventories. The assessment of the impact of spatially ground motion and structural damage correlation on the risk to building inventories

confirms that the means of total structural losses are independent to these correlations, while the uncertainties (measured by variance or coefficient of variation and probable maximum loss) of total structural losses are strongly dependent on correlations in both seismic demand and damage. The contribution of damage correlation to the total structural losses is greater than that of demand correlation. However, the impact of spatial ground motion correlation on the combination of nonstructural and structural losses was greater than that of correlation in damage, which included correlations in structural and nonstructural loss within an individual building as well as pairwise correlations of structural loss between buildings.

ii) It introduces a sampling technique to assess risk to spatially distributed building inventories to reduce the computational and numerical effort involved in determining pairwise correlation in losses for every building and accumulating those losses for a large inventory of buildings. The sampling technique used in this study was shown to provide accurate loss estimates.

iii) Seismic risk was estimated for distributed building inventories in Shelby County, TN, under a scenario earthquake and a probabilistic seismic hazard. The scenario earthquake was selected from a seismic de-aggregation analysis, while the probabilistic seismic hazard included five seismic zones - New Madrid seismic zone, Wabash Valley seismic zone, Eastern Tennessee seismic zone, Craton source zone, and extended margin source zones – that are dominant contributors to seismic hazard to Shelby County, TN. Of those, the New Madrid seismic zone is clearly the most important. The subsequent probabilistic seismic risk analysis

(PSRA) considered earthquake events in these seismic zones, treating their magnitudes and epicenters as probabilistic. The PSRA was extended to estimate the probable maximum loss (PML) decision metric, which is often used for underwriting purposes in the insurance industry. Comparisons of total structural loss ratios computed from these analyses revealed that the uncertainties for the case that included both demand and damage correlations were higher than those for the case that considered only demand correlation. However, the uncertainties in combined nonstructural and structural losses for both aforementioned cases were quite similar.

iv) The sensitivity analysis of uncertainty of inventory losses to modeling parameters suggests potential directions for further experiment, data acquisition, and development. The results of this sensitivity assessment revealed that the means of the total estimated structural loss were strongly dependent on the selection of ground motion attenuation, while the uncertainties (measured by standard deviation or coefficient of variation) were dependent on the parameters that were assumed to model spatial correlation in seismic demand, in damage and loss.

v) The role of epistemic (modeling) uncertainty in estimating total structural losses and probable maximum losses was examined in detail by means of an event tree model. This uncertainty is dependent on the weight for each branch in the decision tree and the choice of modeling parameters. Reduction in epistemic uncertainty is achieved by better modeling or more data.

The methodologies and numerical methods for risk assessment of building inventories developed in this dissertation utilize fundamental concepts and computational

tools. Their applications to other distributed infrastructure would appear to be straightforward, at least conceptually.

Damage correlation models between structural and nonstructural components within a building, and between buildings can be integrated into risk assessments for other structures (i.e. bridges, facilities, or civil infrastructures). For instance, structural-to-nonstructural damage correlation model can be included in loss estimation of any individual building and structure. Furthermore, structure-to-structure damage correlation model might be replaced the assumed damage correlation model for bridge networks in Lee and Kiremidjian (2007).

The probable maximum loss, which is impacted by correlation in demand and damage, is often used in the insurance industry to calculate premiums that insurers and reinsurers charge policyholders. Consideration of correlation between losses from different buildings or policies in their risk portfolios will enhance the accuracy of estimated PML and lead to more accurate rate-setting.

8.2 Recommendations for Future Study

The present work also has identified some issues for additional and future research:

- Spatial correlation in ground motion and seismic demand in this study were based on a simple exponential model and an assumed correlation distance for the Eastern United States (EUS). The model and parameters were adapted from studies of earthquakes in high-seismic areas in the Western United States, Japan, and Taiwan because the required information did not exist for the EUS.
- Although, the simple structure-to-structure damage correlation model between two buildings and structure-to-nonstructure damage correlation model within an

individual building used in this research are believed to be plausible, values of the parameters were based on assumptions rather than empirical data. Hence, additional experimental investigation and validation of these correlation models and their parameters would be desirable.

- Degradation of building materials and in structural components and systems was neglected in the fragility functions used to estimate damage states in the current study. As the age of a building increases, it would tend to become more vulnerable to earthquakes. Although the fragility functions that were used in this study were categorized by generation of seismic code, this categorization included only differences in building codes and regulations, and it did not reflect structural degradation. Fragility functions that take into account the impact of degradation would provide more realistic estimates of potential losses, particularly in areas with older construction.
- The present study focused on direct physical damage to building inventories at a fixed point in time. Future research should examine the effect of time horizon (on the order of decades), depreciation and/or inflation of building repair/replacement cost, damage and losses due to fire, release of hazardous materials, and other events caused by the earthquake, and indirect economic losses (such as fire following earthquake, business interruption, and loss of opportunity) on total building inventory losses.

APPENDIX A

ROOT MEAN SQUARE STANDARD DEVIATION

Table A-1 Root mean square of standard deviation of structural damage state *k* and building type *i* for high code [adjusted from (FEMA/NIBS, 2003)]

No.	Label	Logarithmic Standard Deviation (inches) - High Code					
		Slight	Moderate	Extensive	Complete	Sum	Root Mean
		Beta	Beta	Beta	Beta	Square	Square
1	W1	0.800	0.810	0.850	0.970	2.960	0.860
2	W2	0.810	0.880	0.900	0.830	2.929	0.856
3	S1L	0.800	0.760	0.690	0.720	2.212	0.744
4	S1M	0.650	0.660	0.670	0.740	1.855	0.681
5	S1H	0.640	0.640	0.650	0.670	1.691	0.650
6	S2L	0.810	0.890	0.940	0.830	3.021	0.869
7	S2M	0.670	0.670	0.680	0.790	1.984	0.704
8	S2H	0.630	0.630	0.640	0.710	1.708	0.653
9	S3	0.810	0.820	0.910	0.900	2.967	0.861
10	S4L	0.890	0.890	0.980	0.870	3.302	0.909
11	S4M	0.770	0.720	0.700	0.890	2.393	0.774
12	S4H	0.640	0.660	0.690	0.770	1.914	0.692
13	S5L	1.120	1.040	0.990	0.950	4.219	1.027
14	S5M	0.770	0.790	0.870	0.990	2.954	0.859
15	S5H	0.700	0.730	0.890	0.970	2.756	0.830
16	C1L	0.810	0.840	0.860	0.800	2.741	0.828
17	C1M	0.680	0.670	0.680	0.810	2.030	0.712
18	C1H	0.660	0.640	0.670	0.780	1.903	0.690
19	C2L	0.820	0.840	0.930	0.920	3.089	0.879
20	C2M	0.740	0.770	0.680	0.770	2.196	0.741
21	C2H	0.680	0.650	0.660	0.760	1.898	0.689
22	C3L	1.090	1.070	1.080	0.910	4.328	1.040
23	C3M	0.850	0.830	0.790	0.980	2.996	0.865
24	C3H	0.710	0.740	0.900	0.960	2.783	0.834
25	PC1	0.760	0.860	0.880	1.000	3.092	0.879
26	PC2L	0.840	0.880	0.980	0.940	3.324	0.912
27	PC2M	0.770	0.800	0.700	0.830	2.412	0.776
28	PC2H	0.640	0.660	0.680	0.800	1.948	0.698
29	RM1L	0.840	0.860	0.920	1.010	3.312	0.910
30	RM1M	0.710	0.800	0.770	0.750	2.300	0.758
31	RM2L	0.800	0.820	0.910	0.980	3.101	0.880
32	RM2M	0.710	0.790	0.700	0.730	2.151	0.733
33	RM2H	0.670	0.650	0.660	0.720	1.825	0.676
34	URML	1.000	1.050	1.090	1.080	4.457	1.056
35	URMM	0.910	0.920	0.870	0.910	3.260	0.903
36	MH	0.910	1.000	1.030	0.920	3.735	0.966

Table A-2 Root mean square of standard deviation of structural damage state *k* and building type *i* for moderate code [adjusted from (FEMA/NIBS, 2003)]

No.	Label	Logarithmic Standard Deviation (inches) - Moderate Code					
		Slight Beta	Moderate Beta	Extensive Beta	Complete Beta	Sum Square	Root Mean Square
1	W1	0.840	0.860	0.890	1.040	3.319	0.911
2	W2	0.890	0.950	0.950	0.920	3.444	0.928
3	S1L	0.800	0.750	0.740	0.880	2.525	0.794
4	S1M	0.650	0.680	0.690	0.870	2.118	0.728
5	S1H	0.640	0.640	0.710	0.830	2.012	0.709
6	S2L	0.930	0.920	0.930	0.930	3.441	0.928
7	S2M	0.700	0.690	0.690	0.890	2.234	0.747
8	S2H	0.660	0.640	0.690	0.800	1.961	0.700
9	S3	0.880	0.920	0.970	0.890	3.354	0.916
10	S4L	0.960	1.000	1.030	0.920	3.829	0.978
11	S4M	0.750	0.720	0.720	0.940	2.483	0.788
12	S4H	0.660	0.670	0.700	0.900	2.185	0.739
13	S5L	1.120	1.040	0.990	0.950	4.219	1.027
14	S5M	0.750	0.720	0.720	0.940	2.483	0.788
15	S5H	0.700	0.730	0.890	0.970	2.756	0.830
16	C1L	0.890	0.900	0.900	0.890	3.204	0.895
17	C1M	0.700	0.700	0.700	0.890	2.262	0.752
18	C1H	0.660	0.660	0.760	0.910	2.277	0.754
19	C2L	0.910	0.970	1.030	0.870	3.587	0.947
20	C2M	0.810	0.770	0.730	0.910	2.610	0.808
21	C2H	0.660	0.680	0.700	0.870	2.145	0.732
22	C3L	1.090	1.070	1.080	0.910	4.328	1.040
23	C3M	0.850	0.830	0.790	0.980	2.996	0.865
24	C3H	0.710	0.740	0.900	0.960	2.783	0.834
25	PC1	0.890	0.920	0.970	1.040	3.661	0.957
26	PC2L	0.960	1.000	1.030	0.880	3.757	0.969
27	PC2M	0.820	0.790	0.750	0.930	2.724	0.825
28	PC2H	0.680	0.690	0.770	0.890	2.324	0.762
29	RM1L	0.960	0.990	1.050	0.940	3.888	0.986
30	RM1M	0.810	0.820	0.800	0.890	2.761	0.831
31	RM2L	0.910	0.960	1.020	0.930	3.655	0.956
32	RM2M	0.810	0.800	0.750	0.880	2.633	0.811
33	RM2H	0.670	0.690	0.700	0.860	2.155	0.734
34	URML	1.000	1.050	1.090	1.080	4.457	1.056
35	URMM	0.910	0.920	0.870	0.910	3.260	0.903
36	MH	0.910	1.000	1.030	0.920	3.735	0.966

Table A-3 Root mean square of standard deviation of damage state *k* and building type *i* for low code [adjusted from (FEMA/NIBS, 2003)]

No.	Label	Logarithmic Standard Deviation (inches) - Low Code					
		Slight	Moderate	Extensive	Complete	Sum Square	Root Mean Square
		Beta	Beta	Beta	Beta		
1	W1	0.930	0.980	1.020	0.990	3.846	0.981
2	W2	0.970	0.900	0.890	0.990	3.523	0.938
3	S1L	0.770	0.780	0.780	0.960	2.731	0.826
4	S1M	0.680	0.780	0.850	0.980	2.754	0.830
5	S1H	0.660	0.700	0.760	0.920	2.350	0.766
6	S2L	0.960	0.890	0.860	0.980	3.414	0.924
7	S2M	0.700	0.730	0.850	0.980	2.706	0.822
8	S2H	0.660	0.670	0.740	0.920	2.279	0.755
9	S3	0.980	0.990	1.010	0.900	3.771	0.971
10	S4L	1.050	0.980	0.890	0.980	3.815	0.977
11	S4M	0.760	0.780	0.900	0.990	2.976	0.863
12	S4H	0.700	0.750	0.900	0.980	2.823	0.840
13	S5L	1.110	1.040	0.990	0.950	4.196	1.024
14	S5M	0.770	0.790	0.870	0.980	2.934	0.856
15	S5H	0.700	0.730	0.890	0.970	2.756	0.830
16	C1L	0.950	0.910	0.850	0.970	3.394	0.921
17	C1M	0.700	0.740	0.860	0.980	2.738	0.827
18	C1H	0.700	0.810	0.890	0.980	2.899	0.851
19	C2L	1.040	1.020	0.990	0.950	4.005	1.001
20	C2M	0.820	0.810	0.810	0.990	2.965	0.861
21	C2H	0.680	0.730	0.840	0.950	2.603	0.807
22	C3L	1.090	1.070	1.080	0.910	4.328	1.040
23	C3M	0.850	0.830	0.790	0.980	2.996	0.865
24	C3H	0.710	0.740	0.900	0.970	2.803	0.837
25	PC1	1.000	1.050	1.120	0.890	4.149	1.018
26	PC2L	1.080	1.030	0.980	0.960	4.109	1.014
27	PC2M	0.810	0.790	0.840	0.990	2.966	0.861
28	PC2H	0.710	0.750	0.890	0.980	2.819	0.840
29	RM1L	1.110	1.100	1.100	0.920	4.499	1.060
30	RM1M	0.870	0.840	0.790	0.960	3.008	0.867
31	RM2L	1.050	1.070	1.090	0.910	4.264	1.032
32	RM2M	0.840	0.810	0.770	0.960	2.876	0.848
33	RM2H	0.690	0.720	0.870	0.960	2.673	0.817
34	URML	0.990	1.050	1.100	1.080	4.459	1.056
35	URMM	0.910	0.920	0.870	0.910	3.260	0.903
36	MH	0.910	1.000	1.030	0.920	3.735	0.966

Table A-4 Root mean square of standard deviation of structural damage state *k* and building type *i* for pre code [adjusted from (FEMA/NIBS, 2003)]

No.	Label	Logarithmic Standard Deviation (inches) - Pre Code					
		Slight	Moderate	Extensive	Complete	Sum Square	Root Mean Square
		Beta	Beta	Beta	Beta		
1	W1	1.010	1.050	1.070	1.060	4.391	1.048
2	W2	1.040	0.970	0.900	0.990	3.813	0.976
3	S1L	0.850	0.820	0.800	0.950	2.937	0.857
4	S1M	0.700	0.750	0.810	0.980	2.669	0.817
5	S1H	0.690	0.710	0.850	0.930	2.568	0.801
6	S2L	1.010	0.960	0.880	0.980	3.677	0.959
7	S2M	0.730	0.750	0.800	0.980	2.696	0.821
8	S2H	0.700	0.700	0.840	0.910	2.514	0.793
9	S3	1.060	1.030	1.070	0.890	4.122	1.015
10	S4L	1.110	1.030	0.990	0.980	4.234	1.029
11	S4M	0.810	0.800	0.940	1.000	3.180	0.892
12	S4H	0.730	0.750	0.900	0.970	2.846	0.844
13	S5L	1.200	1.110	1.080	0.950	4.741	1.089
14	S5M	0.850	0.830	0.940	0.990	3.275	0.905
15	S5H	0.720	0.750	0.920	0.960	2.849	0.844
16	C1L	0.980	0.940	0.900	0.970	3.595	0.948
17	C1M	0.730	0.770	0.830	0.980	2.775	0.833
18	C1H	0.710	0.800	0.940	1.010	3.048	0.873
19	C2L	1.110	1.090	1.070	0.930	4.430	1.052
20	C2M	0.860	0.830	0.800	0.980	3.029	0.870
21	C2H	0.730	0.750	0.920	0.970	2.883	0.849
22	C3L	1.190	1.150	1.150	0.920	4.908	1.108
23	C3M	0.900	0.860	0.900	0.960	3.281	0.906
24	C3H	0.730	0.750	0.900	0.950	2.808	0.838
25	PC1	1.140	1.140	1.170	0.980	4.929	1.110
26	PC2L	1.140	1.100	1.100	0.930	4.585	1.071
27	PC2M	0.870	0.830	0.910	1.000	3.274	0.905
28	PC2H	0.740	0.750	0.910	0.960	2.860	0.846
29	RM1L	1.200	1.170	1.170	0.940	5.061	1.125
30	RM1M	0.910	0.890	0.890	0.960	3.334	0.913
31	RM2L	1.140	1.100	1.150	0.920	4.679	1.081
32	RM2M	0.890	0.870	0.870	0.960	3.228	0.898
33	RM2H	0.750	0.750	0.840	0.940	2.714	0.824
34	URML	1.150	1.190	1.200	1.180	5.571	1.180
35	URMM	0.990	0.970	0.900	0.880	3.505	0.936
36	MH	1.110	1.100	0.950	0.970	4.286	1.035

Table A-5 Root mean square of standard deviation of nonstructural drift-sensitive damage state *k* and building type *i* for high code [adjusted from(FEMA/NIBS, 2003)]

No.	Label	Logarithmic Standard Deviation (inches) - High Code					
		Slight Beta	Moderate Beta	Extensive Beta	Complete Beta	Sum Square	Root Mean Square
1	W1	0.72	0.77	0.76	0.88	0.78	0.89
2	W2	0.76	0.79	0.92	0.88	0.84	0.92
3	S1L	0.66	0.72	0.59	0.58	0.64	0.80
4	S1M	0.52	0.52	0.52	0.64	0.55	0.74
5	S1H	0.52	0.50	0.55	0.59	0.54	0.74
6	S2L	0.71	0.81	0.94	0.85	0.83	0.91
7	S2M	0.52	0.55	0.56	0.69	0.58	0.76
8	S2H	0.50	0.50	0.52	0.61	0.53	0.73
9	S3	0.74	0.77	0.96	0.96	0.86	0.93
10	S4L	0.86	0.90	1.02	1.00	0.95	0.97
11	S4M	0.64	0.56	0.58	0.88	0.67	0.82
12	S4H	0.52	0.52	0.62	0.83	0.62	0.79
13	S5L	1.30	1.08	0.96	1.02	1.09	1.04
14	S5M	0.71	0.90	1.06	1.17	0.96	0.98
15	S5H	0.71	0.92	1.06	1.12	0.95	0.98
16	C1L	0.72	0.77	0.81	0.79	0.77	0.88
17	C1M	0.52	0.53	0.56	0.72	0.58	0.76
18	C1H	0.50	0.50	0.61	0.79	0.60	0.78
19	C2L	0.76	0.76	0.94	0.98	0.86	0.93
20	C2M	0.69	0.67	0.55	0.66	0.64	0.80
21	C2H	0.49	0.52	0.55	0.72	0.57	0.75
22	C3L	1.28	1.17	0.90	1.00	1.09	1.04
23	C3M	0.77	0.85	1.02	1.12	0.94	0.97
24	C3H	0.69	0.92	1.04	1.10	0.94	0.97
25	PC1	0.67	0.83	0.90	1.06	0.87	0.93
26	PC2L	0.81	0.86	1.06	1.08	0.95	0.98
27	PC2M	0.76	0.69	0.58	0.81	0.71	0.84
28	PC2H	0.53	0.53	0.59	0.79	0.61	0.78
29	RM1L	0.79	0.83	0.94	1.12	0.92	0.96
30	RM1M	0.67	0.74	0.64	0.66	0.68	0.82
31	RM2L	0.72	0.76	0.90	1.06	0.86	0.93
32	RM2M	0.67	0.71	0.58	0.64	0.65	0.81
33	RM2H	0.50	0.53	0.53	0.72	0.57	0.76
34	URML	1.14	1.25	1.37	1.02	1.20	1.09
35	URMM	0.94	0.83	0.96	1.08	0.95	0.98
36	MH	0.92	1.10	1.17	0.86	1.01	1.01

Table A-6 Root mean square of standard deviation of nonstructural drift-sensitive damage state *k* and building type *i* for moderate code [adjusted from(FEMA/NIBS, 2003)]

No.	Label	Logarithmic Standard Deviation (inches) - Moderate Code					
		Slight Beta	Moderate Beta	Extensive Beta	Complete Beta	Sum Square	Root Mean Square
1	W1	0.79	0.83	0.81	1.08	0.88	0.94
2	W2	0.88	0.96	1.00	0.81	0.91	0.96
3	S1L	0.72	0.69	0.62	0.76	0.70	0.84
4	S1M	0.52	0.55	0.72	0.90	0.67	0.82
5	S1H	0.50	0.53	0.71	0.90	0.66	0.81
6	S2L	0.86	0.96	0.92	0.85	0.90	0.95
7	S2M	0.55	0.55	0.72	0.92	0.68	0.83
8	S2H	0.52	0.53	0.66	0.88	0.65	0.80
9	S3	0.86	0.96	1.02	0.88	0.93	0.97
10	S4L	1.00	1.10	1.00	0.92	1.01	1.00
11	S4M	0.61	0.64	0.90	1.08	0.81	0.90
12	S4H	0.53	0.67	0.86	1.02	0.77	0.88
13	S5L	1.30	1.08	0.96	1.02	1.09	1.04
14	S5M	0.71	0.90	1.06	1.17	0.96	0.98
15	S5H	0.71	0.92	1.06	1.12	0.95	0.98
16	C1L	0.85	0.92	0.90	0.79	0.87	0.93
17	C1M	0.58	0.58	0.76	0.96	0.72	0.85
18	C1H	0.55	0.66	0.90	1.06	0.79	0.89
19	C2L	0.92	1.00	1.12	0.90	0.99	0.99
20	C2M	0.69	0.66	0.69	0.94	0.74	0.86
21	C2H	0.53	0.58	0.79	1.00	0.73	0.85
22	C3L	1.28	1.17	0.90	1.00	1.09	1.04
23	C3M	0.77	0.85	1.02	1.12	0.94	0.97
24	C3H	0.69	0.92	1.04	1.10	0.94	0.97
25	PC1	0.88	0.98	1.10	1.17	1.03	1.02
26	PC2L	1.00	1.12	1.14	0.85	1.03	1.01
27	PC2M	0.74	0.69	0.85	1.00	0.82	0.90
28	PC2H	0.55	0.62	0.86	1.04	0.77	0.88
29	RM1L	1.02	1.12	1.23	1.02	1.10	1.05
30	RM1M	0.79	0.72	0.71	0.96	0.80	0.89
31	RM2L	0.92	1.04	1.21	0.98	1.04	1.02
32	RM2M	0.76	0.69	0.67	0.96	0.77	0.88
33	RM2H	0.53	0.58	0.77	0.98	0.72	0.85
34	URML	1.14	1.25	1.37	1.02	1.20	1.09
35	URMM	0.94	0.83	0.96	1.08	0.95	0.98
36	MH	0.92	1.10	1.17	0.86	1.01	1.01

Table A-7 Root mean square of standard deviation of nonstructural drift-sensitive damage state *k* and building type *i* for low code [adjusted from (FEMA/NIBS, 2003)]

No.	Label	Logarithmic Standard Deviation (inches) - Low Code					
		Slight	Moderate	Extensive	Complete	Sum Square	Root Mean Square
		Beta	Beta	Beta	Beta		
1	W1	0.96	1.00	1.04	1.19	1.05	1.02
2	W2	1.02	0.94	0.86	1.06	0.97	0.99
3	S1L	0.74	0.71	0.77	1.00	0.80	0.90
4	S1M	0.56	0.79	0.98	1.10	0.86	0.93
5	S1H	0.56	0.76	0.94	1.08	0.84	0.91
6	S2L	1.02	0.90	0.88	1.06	0.97	0.98
7	S2M	0.59	0.76	0.98	1.10	0.86	0.93
8	S2H	0.55	0.74	0.94	1.08	0.83	0.91
9	S3	1.06	1.04	0.92	0.98	1.00	1.00
10	S4L	1.19	0.98	0.92	1.06	1.04	1.02
11	S4M	0.67	0.92	1.08	1.17	0.96	0.98
12	S4H	0.71	0.90	1.10	1.14	0.96	0.98
13	S5L	1.30	1.08	0.96	1.02	1.09	1.04
14	S5M	0.71	0.90	1.06	1.17	0.96	0.98
15	S5H	0.71	0.92	1.06	1.12	0.95	0.98
16	C1L	1.00	0.92	0.81	1.04	0.94	0.97
17	C1M	0.62	0.77	0.98	1.12	0.88	0.94
18	C1H	0.76	0.92	1.04	1.14	0.97	0.98
19	C2L	1.17	1.10	0.90	1.00	1.04	1.02
20	C2M	0.69	0.76	1.00	1.12	0.89	0.94
21	C2H	0.62	0.85	1.00	1.14	0.90	0.95
22	C3L	1.28	1.17	0.90	1.00	1.09	1.04
23	C3M	0.77	0.85	1.02	1.12	0.94	0.97
24	C3H	0.69	0.92	1.04	1.10	0.94	0.97
25	PC1	1.08	1.21	1.21	0.88	1.10	1.05
26	PC2L	1.25	1.08	0.86	1.04	1.06	1.03
27	PC2M	0.74	0.88	1.04	1.14	0.95	0.98
28	PC2H	0.69	0.88	1.08	1.14	0.95	0.97
29	RM1L	1.35	1.25	1.06	0.98	1.16	1.08
30	RM1M	0.79	0.79	1.00	1.10	0.92	0.96
31	RM2L	1.19	1.17	1.02	0.98	1.09	1.04
32	RM2M	0.72	0.74	1.00	1.12	0.90	0.95
33	RM2H	0.62	0.85	0.96	1.14	0.89	0.95
34	URML	1.14	1.25	1.37	1.02	1.20	1.09
35	URMM	0.94	0.83	0.96	1.08	0.95	0.98
36	MH	0.92	1.10	1.17	0.86	1.01	1.01

Table A-8 Root mean square of standard deviation of nonstructural drift-sensitive damage state *k* and building type *i* for pre code [adjusted from(FEMA/NIBS, 2003)]

No.	Label	Logarithmic Standard Deviation (inches) - High Code					
		Slight Beta	Moderate Beta	Extensive Beta	Complete Beta	Sum Square	Root Mean Square
1	W1	1.14	1.23	1.23	1.32	1.23	1.11
2	W2	1.12	1.00	0.86	1.02	1.00	1.00
3	S1L	0.81	0.76	0.83	1.04	0.86	0.93
4	S1M	0.64	0.85	1.00	1.12	0.90	0.95
5	S1H	0.62	0.79	1.00	1.14	0.89	0.94
6	S2L	1.10	0.94	0.92	1.08	1.01	1.01
7	S2M	0.62	0.81	1.04	1.14	0.90	0.95
8	S2H	0.62	0.81	0.98	1.10	0.88	0.94
9	S3	1.23	1.10	0.92	1.00	1.06	1.03
10	S4L	1.25	1.02	0.98	1.10	1.09	1.04
11	S4M	0.74	0.96	1.12	1.21	1.01	1.00
12	S4H	0.77	0.98	1.14	1.19	1.02	1.01
13	S5L	1.39	1.12	0.96	1.06	1.13	1.07
14	S5M	0.74	0.98	1.10	1.19	1.00	1.00
15	S5H	0.76	0.83	1.10	1.19	0.97	0.98
16	C1L	1.04	0.96	0.86	1.06	0.98	0.99
17	C1M	0.67	0.83	1.04	1.12	0.92	0.96
18	C1H	0.81	0.98	1.10	1.21	1.03	1.01
19	C2L	1.32	1.17	0.94	1.02	1.11	1.05
20	C2M	0.79	0.81	1.06	1.14	0.95	0.98
21	C2H	0.69	0.92	1.08	1.17	0.96	0.98
22	C3L	1.42	1.23	0.98	1.04	1.17	1.08
23	C3M	0.83	0.90	1.06	1.19	0.99	1.00
24	C3H	0.74	0.81	1.08	1.19	0.95	0.98
25	PC1	1.39	1.35	1.25	0.90	1.22	1.11
26	PC2L	1.35	1.12	0.92	1.04	1.11	1.05
27	PC2M	0.76	0.92	1.08	1.17	0.98	0.99
28	PC2H	0.76	0.96	1.12	1.17	1.00	1.00
29	RM1L	1.49	1.30	1.06	1.00	1.21	1.10
30	RM1M	0.86	0.85	1.04	1.14	0.97	0.99
31	RM2L	1.37	1.25	1.02	0.98	1.16	1.08
32	RM2M	0.81	0.81	1.02	1.14	0.95	0.97
33	RM2H	0.67	0.92	1.08	1.17	0.96	0.98
34	URML	1.46	1.49	1.49	1.06	1.38	1.17
35	URMM	0.98	0.90	1.00	1.10	1.00	1.00
36	MH	1.32	1.19	0.88	0.98	1.09	1.05

Table A-9 Root mean square of standard deviation of nonstructural acceleration-sensitive damage state *k* and building type *i* for high code [adjusted from(FEMA/NIBS, 2003)]

No.	Label	Logarithmic Standard Deviation (inches) - Moderate Code					
		Slight Beta	Moderate Beta	Extensive Beta	Complete Beta	Sum Square	Root Mean Square
1	W1	0.53	0.48	0.46	0.45	0.48	0.69
2	W2	0.50	0.45	0.45	0.46	0.47	0.68
3	S1L	0.45	0.45	0.45	0.44	0.45	0.67
4	S1M	0.45	0.46	0.45	0.45	0.45	0.67
5	S1H	0.48	0.45	0.45	0.45	0.46	0.68
6	S2L	0.45	0.44	0.45	0.45	0.45	0.67
7	S2M	0.48	0.44	0.44	0.44	0.45	0.67
8	S2H	0.46	0.44	0.42	0.42	0.44	0.66
9	S3	0.46	0.45	0.44	0.44	0.45	0.67
10	S4L	0.46	0.46	0.45	0.45	0.46	0.68
11	S4M	0.45	0.42	0.44	0.44	0.44	0.66
12	S4H	0.45	0.44	0.42	0.42	0.43	0.66
13	S5L	0.42	0.46	0.45	0.45	0.45	0.67
14	S5M	0.41	0.45	0.44	0.44	0.43	0.66
15	S5H	0.42	0.46	0.46	0.46	0.45	0.67
16	C1L	0.45	0.46	0.45	0.45	0.45	0.67
17	C1M	0.45	0.45	0.44	0.44	0.44	0.67
18	C1H	0.44	0.44	0.44	0.44	0.44	0.66
19	C2L	0.49	0.45	0.44	0.41	0.45	0.67
20	C2M	0.49	0.44	0.42	0.42	0.44	0.67
21	C2H	0.46	0.44	0.42	0.42	0.44	0.66
22	C3L	0.42	0.45	0.44	0.44	0.44	0.66
23	C3M	0.41	0.45	0.44	0.44	0.43	0.66
24	C3H	0.41	0.45	0.45	0.45	0.44	0.66
25	PC1	0.55	0.45	0.45	0.41	0.46	0.68
26	PC2L	0.48	0.45	0.45	0.45	0.46	0.68
27	PC2M	0.46	0.42	0.44	0.44	0.44	0.66
28	PC2H	0.45	0.42	0.42	0.42	0.43	0.66
29	RM1L	0.50	0.45	0.45	0.40	0.45	0.67
30	RM1M	0.52	0.44	0.42	0.42	0.45	0.67
31	RM2L	0.50	0.44	0.45	0.41	0.45	0.67
32	RM2M	0.52	0.42	0.42	0.42	0.45	0.67
33	RM2H	0.49	0.42	0.42	0.42	0.44	0.66
34	URML	0.48	0.44	0.42	0.42	0.44	0.66
35	URMM	0.41	0.44	0.44	0.44	0.43	0.66
36	MH	0.42	0.45	0.45	0.45	0.44	0.67

Table A-10 Root mean square of standard deviation of nonstructural acceleration-sensitive damage state *k* and building type *i* for moderate code [adjusted from (FEMA/NIBS, 2003)]

No.	Label	Logarithmic Standard Deviation (inches) - Low Code					
		Slight	Moderate	Extensive	Complete	Sum Square	Root Mean Square
		Beta	Beta	Beta	Beta		
1	W1	0.52	0.46	0.45	0.41	0.46	0.68
2	W2	0.46	0.44	0.46	0.46	0.46	0.68
3	S1L	0.45	0.44	0.45	0.45	0.45	0.67
4	S1M	0.44	0.45	0.45	0.45	0.45	0.67
5	S1H	0.44	0.45	0.45	0.45	0.45	0.67
6	S2L	0.44	0.44	0.46	0.46	0.45	0.67
7	S2M	0.44	0.42	0.44	0.44	0.43	0.66
8	S2H	0.44	0.44	0.44	0.44	0.44	0.66
9	S3	0.45	0.44	0.42	0.42	0.43	0.66
10	S4L	0.44	0.44	0.44	0.44	0.44	0.66
11	S4M	0.42	0.44	0.42	0.42	0.43	0.65
12	S4H	0.42	0.44	0.44	0.44	0.43	0.66
13	S5L	0.42	0.46	0.45	0.45	0.45	0.67
14	S5M	0.41	0.45	0.44	0.44	0.43	0.66
15	S5H	0.42	0.46	0.46	0.46	0.45	0.67
16	C1L	0.45	0.44	0.44	0.44	0.44	0.66
17	C1M	0.44	0.44	0.40	0.40	0.42	0.65
18	C1H	0.42	0.45	0.45	0.45	0.44	0.67
19	C2L	0.46	0.44	0.45	0.45	0.45	0.67
20	C2M	0.45	0.41	0.44	0.44	0.43	0.66
21	C2H	0.44	0.42	0.42	0.42	0.43	0.65
22	C3L	0.42	0.45	0.44	0.44	0.44	0.66
23	C3M	0.41	0.45	0.44	0.44	0.43	0.66
24	C3H	0.41	0.45	0.45	0.45	0.44	0.66
25	PC1	0.46	0.45	0.44	0.44	0.45	0.67
26	PC2L	0.44	0.44	0.42	0.42	0.43	0.66
27	PC2M	0.42	0.42	0.42	0.42	0.42	0.65
28	PC2H	0.41	0.42	0.42	0.42	0.42	0.65
29	RM1L	0.48	0.45	0.45	0.45	0.46	0.68
30	RM1M	0.45	0.41	0.45	0.45	0.44	0.66
31	RM2L	0.46	0.44	0.45	0.45	0.45	0.67
32	RM2M	0.45	0.41	0.45	0.45	0.44	0.66
33	RM2H	0.44	0.41	0.41	0.41	0.42	0.65
34	URML	0.48	0.44	0.42	0.42	0.44	0.66
35	URMM	0.41	0.44	0.44	0.44	0.43	0.66
36	MH	0.42	0.45	0.45	0.45	0.44	0.67

Table-A-11 Root mean square of standard deviation of nonstructural acceleration-sensitive damage state *k* and building type *i* for low code [adjusted from (FEMA/NIBS, 2003)]

No.	Label	Logarithmic Standard Deviation (inches) - Pre Code					
		Slight	Moderate	Extensive	Complete	Sum Square	Root Mean Square
		Beta	Beta	Beta	Beta		
1	W1	0.50	0.46	0.44	0.44	0.46	0.68
2	W2	0.45	0.45	0.49	0.49	0.47	0.69
3	S1L	0.42	0.46	0.46	0.46	0.45	0.67
4	S1M	0.44	0.48	0.48	0.48	0.47	0.68
5	S1H	0.45	0.42	0.42	0.42	0.43	0.66
6	S2L	0.42	0.46	0.46	0.46	0.45	0.67
7	S2M	0.41	0.45	0.45	0.45	0.44	0.66
8	S2H	0.42	0.46	0.46	0.46	0.45	0.67
9	S3	0.42	0.46	0.46	0.46	0.45	0.67
10	S4L	0.42	0.46	0.46	0.46	0.45	0.67
11	S4M	0.42	0.46	0.46	0.46	0.45	0.67
12	S4H	0.42	0.46	0.46	0.46	0.45	0.67
13	S5L	0.42	0.46	0.45	0.45	0.45	0.67
14	S5M	0.41	0.45	0.44	0.44	0.43	0.66
15	S5H	0.42	0.46	0.46	0.46	0.45	0.67
16	C1L	0.42	0.46	0.46	0.46	0.45	0.67
17	C1M	0.42	0.46	0.46	0.46	0.45	0.67
18	C1H	0.45	0.45	0.45	0.45	0.45	0.67
19	C2L	0.44	0.45	0.44	0.44	0.44	0.66
20	C2M	0.40	0.44	0.42	0.42	0.42	0.65
21	C2H	0.41	0.44	0.44	0.44	0.43	0.66
22	C3L	0.42	0.45	0.44	0.44	0.44	0.66
23	C3M	0.41	0.45	0.44	0.44	0.43	0.66
24	C3H	0.41	0.45	0.45	0.45	0.44	0.66
25	PC1	0.44	0.44	0.44	0.44	0.44	0.66
26	PC2L	0.42	0.46	0.46	0.46	0.45	0.67
27	PC2M	0.41	0.45	0.45	0.45	0.44	0.66
28	PC2H	0.41	0.45	0.45	0.45	0.44	0.66
29	RM1L	0.44	0.44	0.41	0.41	0.42	0.65
30	RM1M	0.41	0.44	0.41	0.41	0.42	0.65
31	RM2L	0.44	0.44	0.41	0.41	0.42	0.65
32	RM2M	0.41	0.44	0.42	0.42	0.42	0.65
33	RM2H	0.40	0.44	0.44	0.44	0.43	0.65
34	URML	0.48	0.44	0.42	0.42	0.44	0.66
35	URMM	0.41	0.44	0.44	0.44	0.43	0.66
36	MH	0.42	0.45	0.45	0.45	0.44	0.67

Table A-12 Root mean square of standard deviation of nonstructural acceleration-sensitive damage state *k* and building type *i* for pre code [adjusted from (FEMA/NIBS, 2003)]

No.	Label	Logarithmic Standard Deviation (inches) - Pre Code					
		Slight	Moderate	Extensive	Complete	Sum Square	Root Mean Square
		Beta	Beta	Beta	Beta		
1	W1	0.52	0.49	0.44	0.44	0.47	0.69
2	W2	0.44	0.45	0.42	0.42	0.43	0.66
3	S1L	0.44	0.46	0.46	0.46	0.46	0.68
4	S1M	0.44	0.48	0.48	0.48	0.47	0.68
5	S1H	0.45	0.45	0.45	0.45	0.45	0.67
6	S2L	0.42	0.46	0.46	0.46	0.45	0.67
7	S2M	0.42	0.46	0.46	0.46	0.45	0.67
8	S2H	0.44	0.45	0.45	0.45	0.45	0.67
9	S3	0.42	0.46	0.46	0.46	0.45	0.67
10	S4L	0.44	0.46	0.46	0.46	0.46	0.68
11	S4M	0.42	0.46	0.46	0.46	0.45	0.67
12	S4H	0.44	0.45	0.45	0.45	0.45	0.67
13	S5L	0.42	0.46	0.46	0.46	0.45	0.67
14	S5M	0.42	0.46	0.46	0.46	0.45	0.67
15	S5H	0.44	0.46	0.46	0.46	0.46	0.68
16	C1L	0.44	0.46	0.46	0.46	0.46	0.68
17	C1M	0.44	0.46	0.46	0.46	0.46	0.68
18	C1H	0.45	0.45	0.45	0.45	0.45	0.67
19	C2L	0.42	0.45	0.45	0.45	0.44	0.67
20	C2M	0.41	0.45	0.45	0.45	0.44	0.66
21	C2H	0.42	0.45	0.45	0.45	0.44	0.67
22	C3L	0.42	0.46	0.46	0.46	0.45	0.67
23	C3M	0.41	0.45	0.45	0.45	0.44	0.66
24	C3H	0.42	0.45	0.45	0.45	0.44	0.67
25	PC1	0.44	0.44	0.44	0.44	0.44	0.66
26	PC2L	0.42	0.46	0.46	0.46	0.45	0.67
27	PC2M	0.42	0.45	0.45	0.45	0.44	0.67
28	PC2H	0.44	0.44	0.44	0.44	0.44	0.66
29	RM1L	0.44	0.45	0.44	0.44	0.44	0.66
30	RM1M	0.41	0.44	0.42	0.42	0.42	0.65
31	RM2L	0.44	0.45	0.45	0.45	0.45	0.67
32	RM2M	0.41	0.44	0.44	0.44	0.43	0.66
33	RM2H	0.42	0.44	0.44	0.44	0.43	0.66
34	URML	0.48	0.42	0.42	0.42	0.44	0.66
35	URMM	0.41	0.44	0.44	0.44	0.43	0.66
36	MH	0.45	0.42	0.42	0.42	0.43	0.66

APPENDIX B

MEDIAN SPECTRAL DISPLACEMENTS

Table B-1 Median spectral displacements for structural and nonstructural drift-sensitive damage – Moderate code

Building Type	Median of Spectral Displacement (inches)							
	Slight		Moderate		Extensive		Complete	
	S	NDSC	S	NDSC	S	NDSC	S	NDSC
W1	0.50	0.50	1.25	1.01	3.86	3.15	9.45	6.30
W2	0.86	0.86	2.14	1.73	6.62	5.40	16.20	10.80
S1L	1.30	0.86	2.24	1.73	*5.08*	*5.40*	12.96	10.80
S1M	2.16	2.16	*3.74*	*4.32*	*8.46*	*13.50*	*21.60*	*27.00*
S1H	*3.37*	*4.49*	*5.83*	*8.99*	*13.21*	*28.08*	*33.70*	*56.16*
S2L	1.08	0.86	1.87	1.73	5.04	5.40	12.96	10.80
S2M	*1.80*	*2.16*	*3.12*	*4.32*	*8.40*	*13.50*	*21.60*	*27.00*
S2H	*2.81*	*4.49*	*4.87*	*8.99*	*13.10*	*28.08*	*33.70*	*56.16*
S3	0.54	0.54	*0.94*	*1.08*	*2.52*	*3.38*	*7.09*	*6.75*
S4L	0.86	0.86	*1.50*	*1.73*	*4.04*	*5.40*	*11.34*	*10.80*
S4M	*1.44*	*2.16*	*2.50*	*4.32*	*6.73*	*13.50*	*18.90*	*27.00*
S4H	*2.25*	*4.49*	*3.90*	*8.99*	*10.50*	*28.08*	*29.48*	*56.16*
S5L	*0.65*	*0.86*	*1.30*	*1.73*	*3.24*	*5.40*	*7.56*	*10.80*
S5M	*1.44*	*2.16*	*2.50*	*4.32*	*6.73*	*13.50*	*18.90*	*27.00*
S5H	*1.68*	*4.49*	*3.37*	*8.99*	*8.42*	*28.08*	*19.66*	*56.16*
C1L	*0.90*	*0.72*	1.56	1.44	*4.20*	*4.50*	10.80	9.00
C1M	*1.50*	*1.80*	*2.60*	*3.60*	*7.00*	*11.25*	*18.00*	*22.50*
C1H	*2.16*	*3.46*	*3.74*	*6.91*	*10.08*	*21.60*	*25.92*	*43.20*
C2L	0.72	0.72	1.52	1.44	*4.17*	*4.50*	10.80	9.00
C2M	*1.20*	*1.80*	*2.53*	*3.60*	*6.95*	*11.25*	*18.00*	*22.50*
C2H	*1.73*	*3.46*	*3.64*	*6.91*	*10.00*	*21.60*	*25.92*	*43.20*
C3L	*0.54*	*0.72*	*1.08*	*1.44*	*2.70*	*4.50*	*6.30*	*9.00*
C3M	*0.90*	*1.80*	*1.80*	*3.60*	*4.50*	*11.25*	*10.50*	*22.50*
C3H	*1.30*	*3.46*	*2.59*	*6.91*	*6.48*	*21.60*	*15.12*	*43.20*
PC1	0.54	0.54	*0.94*	*1.08*	*2.52*	*3.38*	7.09	6.75
PC2L	0.72	0.72	*1.25*	*1.44*	*3.37*	*4.50*	9.45	9.00
PC2M	*1.20*	*1.80*	*2.08*	*3.60*	*5.61*	*11.25*	*15.75*	*22.50*
PC2H	*1.73*	*3.46*	*3.00*	*6.91*	*8.08*	*21.60*	*22.68*	*43.20*
RM1L	0.72	0.72	*1.25*	*1.44*	*3.37*	*4.50*	9.45	9.00
RM1M	*1.20*	*1.80*	*2.08*	*3.60*	*5.61*	*11.25*	*15.75*	*22.50*
RM2L	0.72	0.72	*1.25*	*1.44*	*3.37*	*4.50*	9.45	9.00
RM2M	*1.20*	*1.80*	*2.08*	*3.60*	*5.61*	*11.25*	*15.75*	*22.50*
RM2H	*1.73*	*3.46*	*3.00*	*6.91*	*8.08*	*21.60*	*22.68*	*43.20*
URML	*0.41*	*0.54*	*0.81*	*1.08*	*2.03*	*3.38*	*4.73*	*6.75*
URMM	*0.63*	*1.26*	*1.26*	*2.52*	*3.15*	*7.88*	*7.35*	*15.75*
MH	0.48	0.48	0.96	0.96	*2.88*	*3.00*	8.40	6.00

REFERENCES

Adachi, T. (2007). *Impact of Cascading failures on Performance Assessment of Civil Infrastructure Systems*, Civil and Environmental Engineering, Georgia Institute of Technology, Atlanta, GA.

Ang, A. H., and Tang, W. H. (2007). *Probability Concepts in Engineering, 2nd Ed.* New York, NY.: John Wiley & Sons.

ASCE. (2010). Minimum Design Loads for Buildings and Other Structures (7-10). Reston, VA: American Society of Civil Engineers.

Aslani, Hesameddin, and Miranda, Eduardo. (2005). Probabilistic Earthquake Loss Estimation and Loss Disaggregation in Buildings. The John A. Blume Earthquake Engineering Center.

ATC-40. (1996). Seismic Evaluation and Retrofit of Concrete Buildings. Redwood City, CA: Applied Technology COncil.

ATC-58. (2011). Seismic Performance Assessment of Buildings Volumne 1 - Methodology (ATC-58-1 75% Draft). Redwood, CA: Applied Technology Council.

Atkinson, Gail M., and Boore, David M. (1995). "Ground-Motion Relation for Eastern North America." *Bulletin of the Seismological Society of America* no. 85 (1):14.

Atkinson, Gail M., and Boore, David M. (2006). "Earthquake Ground-Motion Prediction Equations for Eastern North America." *Bulletin of the Seismological Society of America* no. 96 (6):25.

Bazzurro, Paolo, and Cornell, Allin C. (1999). "Disaggregation of seismic hazard." *Bulletin of the Seismological Society of America* no. 89 (2):501-520.

Bensi, M. T., Straub, D., Friis-Hansen, P., and Der Kiureghian, A. (2009). Modeling Infrastructure System Performance using BN. Paper read at ICOSSAR Conference.

Boore, David. (2003). "Simulation of Ground Motion Using the Stochastic Method." *Pure and Applied Geophysics* no. 160:42.

Boore, David M., Gibbs, J. F., Joyner, W. B., Tinsley, J. C., and Ponti, D. J. (2003). "Estimated ground motion from the 1994 Northridge, California, earthquake at the site of the interstate 10 and La Cienega Boulevard bridge collapse, west Los Angeles, California." *Bulletin of the Seismological Society of America* no. 93 (6):15.

Campbell, Kenneth W. (2003). "Prediction of Strong Ground Motion Using the Hybrid Empirical Method and Its Use in the Development of Ground-Motion (Attenuation) Relations in Eastern North America." *Bulletin of the Seismological Society of America* no. 93 (3):1012-1033. doi: 10.1785/0120020002.

Cardona, Omar D., Ordaz, Mario G., Yamin, Luis E., Marulanda, Mabel C., and Barbat, Alex H. (2008). "Earthquake Loss Assessment for Integrated Disaster Risk Management." *Journal of Earthquake Engineering* no. 12 (sup2):48-59. doi: 10.1080/13632460802013495.

Celik, Ozan Cem. (2007). *Probabilistic Assessment of Non-Ductile Reinforced Concrete Frames Susceptible to Mid-America Ground Motions*, Civil and Environmental Engineering, Georgia Institute of Technology, Atlanta, GA.

Celik, Ozan Cem, and Ellingwood, Bruce R. (2009). "Seismic Risk Assessment of Gravity Load Designed Reinforced Concrete Frames Subjected to Mid-America Ground Motions." *Journal of Structural Engineering* no. 135 (4):414-424.

Cha, Eun Jeong, and Ellingwood, Bruce R. (2011). Decision-Making for Civil Infrastructure Exposed to Low-Probability, High-Consequence Hazards: the Role of Risk-Aversion. In *ICASP11*. Zurich, Switzerland.

Chang, Stephanie E., and Shinozuka, Masanobu. (1996). "Life-Cycle Cost Analysis with Natural Hazard Risk." *Journal of Infrastructure Systems* no. 2 (3):118-126.

Chen, Yong, Li, Ge-Ping, Chen, Qi-Fu, Chen, Ling, and Li, Min-Feng. (1998). "Earthquake damage and loss estimation with Geographic Information System." *Acta Seismologica Sinica* no. 11 (6):751-758.

Cherubini, Umberto. (2004). *Copula methods in finance*. Edited by Elisa Luciano and Walter Vecchiato, *Wiley finance series*. Hoboken, NJ :: John Wiley & Sons.

Chopra, Anil K., and Goel, Rakesh K. (1999). "Capacity-Demand-Diagram Methods Based on Inelastic Design Spectrum." *Earthquake Spectra* no. 15 (4):20.

Corotis, R. B. (2009). "Societal Issues in Adopting Life-Cycle Concepts within the Political System." *Structure and Infrastructure Engineering* no. 5 (1):7.

Duenas-Osorio, L. A. (2005). *Interdependent Response of Networked Systems to Natural Hazards and Intentional Disruptions*, Civil and Environmental Engineering, Georgia Institute of Technology, Atlanta, GA.

Ellingwood, Bruce R., Celik, Ozan Cem, and Kinali, Kursat. (2007). "Fragility assessment of building structural systems in Mid-America." *Earthquake Engineering & Structural Dynamics* no. 36 (13):1935-1952.

Elms, David G. (1997). "Risk balancing in structural problems." *Structural Safety* no. 19 (1):67-77.

Faber, M. H., and Stewart, M. G. (2003). "Risk assessment for civil engineering facilities: critical overview and discussion." *Reliability Engineering & System Safety* no. 80 (2):173-184.

Fajfar, Peter. (1999). "Capacity spectrum method based on inelastic demand spectra." *Earthquake Engineering & Structural Dynamics* no. 28 (9):979-993. doi: 10.1002/(sici)1096-9845(199909)28:9<979::aid-eqe850>3.0.co;2-1.

FEMA/NIBS. (2003). *Multi-hazard Loss Estimation Methodology Earthquake Model (HAZUS-MH MR4): Technical Manual*. Washington, D.C.

Frankel, Arthur D., Mueller, Charles S., Barnhard, Theodore, Perkins, David M., Leyendecker, E.V., Dickman, Nancy, Hanson, Stanley, and Hopper, Margaret. (1996). National Seismic-Hazard Maps: Documentation June 1996. U.S. Geological Survey.

Frankel, Arthur D., Petersen, Mark D., Mueller, Charles S. , Haller, Kathleen M. , Wheeler, Russell L. , Leyendecker, E.V., Wesson, Robert L. , Harmsen, Stephen C. , Cramer, Chris H. , Perkins, David M. , and Rukstales, Kenneth S. . (2002). Documentation for the 2002 Update of the National Seismic Hazard Maps. U.S. Geological Survey.

Goda, Katsuichiro, and Hong, H. P. (2008). "Estimation of Seismic Loss for Spatially Distributed Buildings." *Earthquake Spectra* no. 24 (4):889-910.

Grossi, Patricai, and Kunreuther, Howard. (2005). *Catastrophe Modeling: A New Approach to Managing Risk*. Newyork, NY: Springer.

He, Yuhong. (2006). *Earthquake Loss and Risk Estimattion of Buildings by Monte Carlo Simulation*, Civil Engineering and Engineering Mechanics Department, Columbia University, New Yokr, NY.

Hwang, Howard H. M., Lin, Huijie, and Huo, Jun-Rong. (1997). "Seismic Performance Evaluation of Fire Stations in Shelby County, Tennessee." *Earthquake Spectra* no. 13 (4):759-772.

Jayaram, Nirmal. (2010). *Probabilistic Seismic Lifeline Risk Assessment Using Efficient Sampling and Data Reduction Techniques*. Doctor of Philosophy, Civil and Environmental Engineering, Stanford University, Stanford, CA.

Jayaram, Nirmal , and Baker, Jack W. (2009). "Correlation model for spatially distributed ground-motion intensities." *Earthquake Engineering & Structural Dynamics* no. 38 (15):22.

Jayaram, Nirmal, and Baker, Jack W. (2010). "Efficient sampling and data reduction techniques for probabilistic seismic lifeline risk assessment." *Earthquake Engineering & Structural Dynamics* no. 9999 (9999):n/a.

Kanda, Jun, and Shah, Haresh. (1997). "Engineering role in failure cost evaluation for buildings." *Structural Safety* no. 19 (1):79-90.

Kappos, A., Lekidis, V., Panagopoulos, G., Sous, I., Theodulidis, N., Karakostas, Ch., Anastasiadis, T., Salonikios, T., and Margaris, B. (2007). "Analytical Estimation of Economic Loss for Buildings in the Area Struck by the 1999 Athens Earthquake and Comparison with Statistical Repair Costs." *Earthquake Spectra* no. 23 (2):333-355.

Kinali, Kursat, and Ellingwood, Bruce R. (2007). "Seismic fragility assessment of steel frames for consequence-based engineering: A case study for Memphis, TN." *Engineering Structures* no. 29 (6):1115-1127. doi: 10.1016/j.engstruct.2006.08.017.

Kircher, Charles A., Nassar, Aladdin A., Kustu, Onder, and Holmes, William T. (1997). "Development of Building Damage Functions for Earthquake Loss Estimation." *Earthquake Spectra* no. 13 (4):663-682.

Kircher, Charles A., Whitman, Robert V., and Holmes, William T. (2006). "HAZUS Earthquake Loss Estimation Methods." *Natural Hazards Review* no. 7 (2):45-59.

Kiremidjian, Anne, Moore, James, Yue Yue, Fan, Yazlali, Ozgur, Basoz, Nesrin, and Williams, Meredith. (2007). "Seismic Risk Assessment of Transportation Network Systems." *Journal of Earthquake Engineering* no. 11:371-382.

Kramer, Steven L. (1996). *Geotechnical Earthquake Engineering*. Upper Saddle River, NJ: Prentice Hall.

Lee, Kyung Ho, and Rosowsky, David V. (2006). "Fragility analysis of woodframe buildings considering combined snow and earthquake loading." *Structural Safety* no. 28 (3):289-303.

Lee, Renee. (2007). *Uncertainty and Correlation in Seismic Risk Assessment of Transportation Systems*, Civil and Environmental Engineering, Stanford University, Stanford, CA.

Lee, Renee, and Kiremidjian, Anne S. (2007). "Uncertainty and Correlation for Loss Assessment of Spatially Distributed Systems." *Earthquake Spectra* no. 23 (4):753-770.

Lee, Yajie, Anderson, John G., and Zeng, Yuehua. (2000). "Evaluation of Empirical Ground-Motion Relations in Southern California." *Bulletin of the Seismological Society of America* no. 90 (6B):13.

McGuire, Robin K. (1995). "Probabilistic seismic hazard analysis and design earthquakes: Closing the loop." *Bulletin of the Seismological Society of America* no. 85 (5):1275-1284.

Melchers, R. E. (1999). *Structural Reliability Analysis and Prediction*. 2nd Ed. ed. Chichester, NY.: John Wiley & Sons.

Merino, Miguel, Stein, Seth, Liu, Mian, and Okal, Emile A. (2010). "Comparison of Seismicity Rates in the New Madrid and Wabash Valley Seismic Zones." *Seismological Research Letters* no. 81 (6):951-954. doi: 10.1785/gssrl.81.6.951.

Muthukumar, Subrahmanyam. (2008). *The Application of Advanced Inventory Techiques in Urban Invetory Data Development to Earthquaek Risk Modeling and Mititaion in Mid-America*, College of Architecture, Georgia Institute of Technology, Atlanta, GA.

Nelsen, Roger B. (2006). *An introduction to copulas*. 2nd ed. ed, *Springer series in statistics*. New York :: Springer.

Padgett, Jamie E. (2007). *Seismic Vulnerability Assessment of Retrofitted Bridges Using Probabilistic Methods*, Civil and Environmental Engineering, Georgia Institute of Technology, Atlanta, GA.

Park, J., Bazzurro, P., and Baker, Jack W. (2007). Modeling spatial correlation of ground motion intensity measures for regional seismic hazard and portfolio loss estimation. In *10th International Conference on Application of Statistic and Probability in Civil Engineering (ICASP10)*. Tokyo, Japan.

Park, Joonam, Towashiraporn, Peeranan, Craig, James I., and Goodno, Barry J. (2009). "Seismic fragility analysis of low-rise unreinforced masonry structures." *Engineering Structures* no. 31 (1):125-137.

Petersen, Mark D., Frankel, Arthur D., Harmsen, Stephen C., Mueller, Charles S., Haller, Kathleen M., Wheeler, Russell L., Wesson, Robert L., Zeng, Yuehua, Boyd, Oliver S., Perkins, David M., Luco, Nicolas, Field, Edward H., Wills, Chris J., and Rukstales, Kenneth S. (2008). Documentation for the 2008 Update of the United States National Seismic Hazard Maps. US. Gelological Survey.

Ploeger, S., Atkinson, G., and Samson, C. (2010). "Applying the HAZUS-MH software tool to assess seismic risk in downtown Ottawa, Canada." *Natural Hazards* no. 53 (1):1-20. doi: 10.1007/s11069-009-9408-x.

Schweig. E., Gomberg, J., and Hendly, J. W. (1995). The Mississipi Valley-"Whole Lotta Shakin' Goin' On'. USGS Fact Sheet 168-95.

Shinozuka, Masanobu, Chang, Stephanie E., Eguchi, Ronald T., Abrams, Daniel P., Hwang, Howard H. M., and Rose, Adam. (1997). "Advances in Earthquake Loss

Estimation and Application to Memphis, Tennessee." *Earthquake Spectra* no. 13 (4):739-758.

Srbulov, Milutin. (2008). *Geotechnical Earthquake Engineering: Simplified Analyses with Case Studies and Examples*. Edited by Atilla Ansal. Vol. 9, *Geotechnical, Geological and Earthquake Engineering*: Springer.

Straub, D., Bensi, M. T., and Der Kiureghian, A. (2008). Spatial Modeling of Earthquake Hazard and Infrastructure System Performance through Bayesian Network. Paper read at Proceedings of EM'08 conference.

Tavakoli, Behrooz, and Pezeshk, Shahram. (2005). "Empirical-Stochastic Ground-Motion Prediction for Eastern North America." *Bulletin of the Seismological Society of America* no. 95 (6):2283-2296. doi: 10.1785/0120050030.

Toro, Gabriel R., Abrahamson, Norman A., and Schneider, John, F. (1997). "Model of Strong Ground Motions from Earthquakes in Central and Eastern North America: Best Estimates and Uncertainties." *Seismological Reseach Letter* no. 68 (1):17.

Trendafiloski, Goran, Wyss, Max, Rosset, Philippe, and Marmureanu, Gheorghe. (2009). "Constructing City Models to Estimate Losses Due to Earthquakes Worldwide: Application to Bucharest, Romania." *Earthquake Spectra* no. 25 (3):665-685.

Wang, Min, and Takada, Tsuyoshi. (2005). "Macrospatial Correlation Model of Seismic Ground Motions." *Earthquake Spectra* no. 21 (4):1137-1156.

Wen, Y. K., and Ellingwood, B. R. (2005). "The Role of Fragility Assessment in Consequence-Based Engineering." *Earthquake Spectra* no. 21 (3):861-877.

Wen, Y. K., and Kang, Y. J. (2001). "Minimum Building Life-Cycle Cost Design Criteria. II: Applications." *Journal of Structural Engineering* no. 127 (3):338.

Wesson, Robert L., Perkins, David M., Luco, Nicolas, and Karaca, Erdem. (2009). "Direct Calculation of the Probability Distribution for Earthquake Losses to a Portfolio." *Earthquake Spectra* no. 25 (3):687-706.

Woo, Gordon. (1997). "The Treatment of Earthquake Portfolio Uncertainty: A Focus on Issues of Asset Distribution." *Earthquake Spectra* no. 13 (4):833-849.

Woo, Gordon. (2002). "Natural Catastrophe Probable Maximum Loss." *British Actuarial Journal* no. 8 (5).

Zimmerman, Rae. (2001). "Thoughts on Extreme Events." *Short paper for the Extreme Events Workshop*.